The Dissertation Committee for Susan Amy Garner Certifies that this is the approved version of the following dissertation:

Hydrogen-Mediated Carbon-Carbon Bond Formations:

Applied to Reductive Aldol and Mannich Reactions

Committee:

Michael J. Krische, Supervisor

Christopher W. Bielawski

Philip D. Magnus

Jennifer S. Brodbelt

Hung-wen Liu

Hydrogen-Mediated Carbon-Carbon Bond Formations:

Applied to Reductive Aldol and Mannich Reactions

by

Susan Amy Garner, B. S.

Dissertation

Presented to the Faculty of the Graduate School of

The University of Texas at Austin

in Partial Fulfillment

of the Requirements

for the Degree of

Doctor of Philosophy

The University of Texas at Austin

May 2007

Dedication

To my husband, Terence Garner, whose love and support have made all the difference.

Acknowledgements

I would like to thank Professor Michael J. Krische for allowing me the opportunity to work in his laboratory. During my graduate studies Professor Krische has provided an intellectually simulating environment, within which I have learned a great deal. I am also grateful to the members of the Krische group past and present, for their support and help proofreading this dissertation.

Hydrogen-Mediated Carbon-Carbon Bond Formations: Applied to Reductive Aldol and Mannich Reactions

Publication No._____

Susan Amy Garner, Ph.D.

The University of Texas at Austin, 2007

Supervisor: Michael J. Krische

Hydrogen gas is the cleanest and most cost-effective reductant available to mankind, and the use of hydrogen gas in catalytic hydrogenation reactions is one of the oldest and most utilized organic reactions. Although catalytic hydrogenation has been practiced in industry on enormous scale, the use of hydrogen gas as a terminal reductant in C-C bond forming reactions has been limited to processes involving the migratory insertion of carbon monoxide such as: alkene hydroformylation and the Fischer-Tropsch reaction. A significant advance to the field of synthetic organic chemistry would be the expansion of C-C bond forming reactions beyond reductive coupling *via* carbon monoxide insertion.

Herein, related metal catalyzed reductive couplings to α,β-unsaturated compounds in the presence of reducing agents such as: silane, borane, and hydrogen are reviewed. The following chapters discuss the development of hydrogen-mediated reductive aldol and Mannich reactions. The results from this body of work clearly

demonstrate that hydrogen-mediated C-C bond forming reactions are emerging as a powerful tool for synthetic chemists.

Table of Contents

List of Tables

List of Figures

List of Schemes

CHAPTER 1. METAL CATALYZED REDUCTIVE COUPLINGS TO ENONES

1.1.1 INTRODUCTION – REDUCTIVE GENERATION OF ENOLATES FROM ENONES

Enolate-mediated C-C bond formations rank among the most fundamental and broadly utilized processes in synthetic organic chemistry. Nearly 150 years ago the first aldol addition reaction was accomplished *via* the coupling of an enolate and a ketone.[1] Enolate chemistry has continued to be an important feature in organic chemistry to this very day.

A major advance in the development of enolate chemistry came about in 1951 by Hauser, who was the first person to advent a method of enolate preformation by using lithium amide in ammonia as a base for the stoichiometric deprotonation of esters.[2] With these advances in enolate generation, certain limitations were brought to light, including the challenge of regioselective enolate formation. Regioselective generation of an enolate by deprotonation is possible only when there is a steric differentiation between the protons α to the carbonyl group, as in the case of methylcyclohexanone, regioselective enolate formation may be achieved by conducting the deportonation under kinetic or thermodynamic conditions (Scheme 1.1).[4]

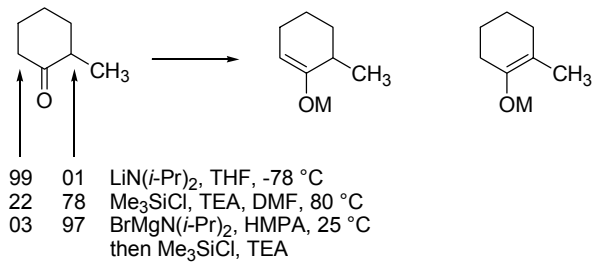

Scheme 1.1: Regioselective generation of enolates *via* kinetic or thermodynamic control.

When there is little steric differentiation between the protons α to the carbonyl group, regioselective generation of the enolate is problematic. The seminal work of Stork in the 1960s established the use of an enone as a latent enolate, which allows for the regioselective enolate formation (Scheme 1.2).[5] A dissolving metal reduction (Li/NH_3) was utilized to regiospecifically generate the enolate from the enone, which is impossible to obtain selectively by other methods, followed by trapping of the enolate *via* alkylation.

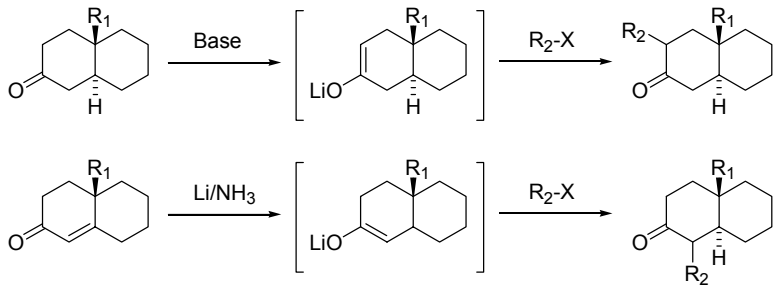

Scheme 1.2: Regiospecific enolization *via* dissolving metal reduction – enones as latent enolates.

Since this time a large number of metal catalyzed enone reductions to generate enolates have been developed. The first catalytic asymmetric conjugate reduction of an

α,β-unsaturated carbonyl compound was developed by Pfaltz using a cobalt catalyst and borohydride as the hydride source.[6] This area of study has had a large amount of interest with the discovery of new chiral ligands, which allows reaction conditions to be tuned in order to achieve maximum yield and selectivity.[7,8] A number of metal catalyst have been utilized for the asymmetric conjugate reduction of α,β-unsaturated carbonyl compounds such as: cobalt,[6] rhodium,[9] copper,[10] palladium,[11] and platinum.[12]

Related processes have emerged, wherein solutions of α,β-unsaturated carbonyl compound are reduced directly in the presence of electrophiles to furnish products of C-C coupling. A challenge inherent to the development of such transformations relates to the design of catalytic systems that exhibit high levels of chemoselectivity for conjugate reduction, thereby mitigating competitive reduction of the electrophile. By meeting this challenge, one dispenses altogether with the requirement of stoichiometric enolate preformation.

For the remainder of this review the enolates that are generated by reduction are trapped by an electrophile in order to make a new C-C bond. This is a very powerful method of C-C bond synthesis, due to the variety of enolate/electrophile combinations. In this review, the metal catalyzed reductive coupling to α,β-unsaturated carbonyl compounds is catalogued. Content is organized on the basis of reaction type, and is categorized further on the basis of the catalyst type.

1.2.1 REACTION OF ENONES WITH ALDEHYDES AND KETONES (ALDOL REACTION)

The aldol reaction is one of the oldest and most utilized organic reactions of all time.[13] The aldol reaction was first discovered in 1869 by Borodin, but Wurtz receives most of the credit for the homodimerization of acetone in 1872.[1] The traditional aldol reaction requires the stoichiometric and regioselctive performation of the enolate with a strong base at low temperature. As discussed previously, regioselective enolate formation is not always a trivial process. After preformation of the enolate then the electrophile can be added to the reaction for the aldol reaction to proceed. Due to the utility of the aldol synthons in natural product synthesis considerable attention has been given to improve this process.

The issues of selectivity posed by the aldol reaction continue to inspire development of increasingly effective protocols for stereocontrolled aldol addition.[13,14] The development of metallic[15] and organic[16] catalysts for direct enantioselective aldol addition of unmodified carbonyl compounds represents an especially significant milestone, as these processes eliminate the necessity to use chiral auxiliaries and preformed enol(ate) derivatives. Regioselective enolization in direct enantioselective aldol additions of nonsymmetric ketones generally favors activation of the less substituted enolizable position. For example, direct aldol couplings of 2-butanone catalyzed by L-proline[17,18] or the heterobimetallic catalyst $LaLi_3$-tris(binaphthoxide) (LLB) furnish linear aldol adducts.[20] Complementary regiochemistry may be achieved through the catalytic reductive coupling of α,β-unsaturated carbonyl compounds and aldehydes to form aldol products. By exploiting enones as regiochemical control

elements, one gains access to the branched aldol adducts relevant to polypropionate synthesis (Scheme 1.3).

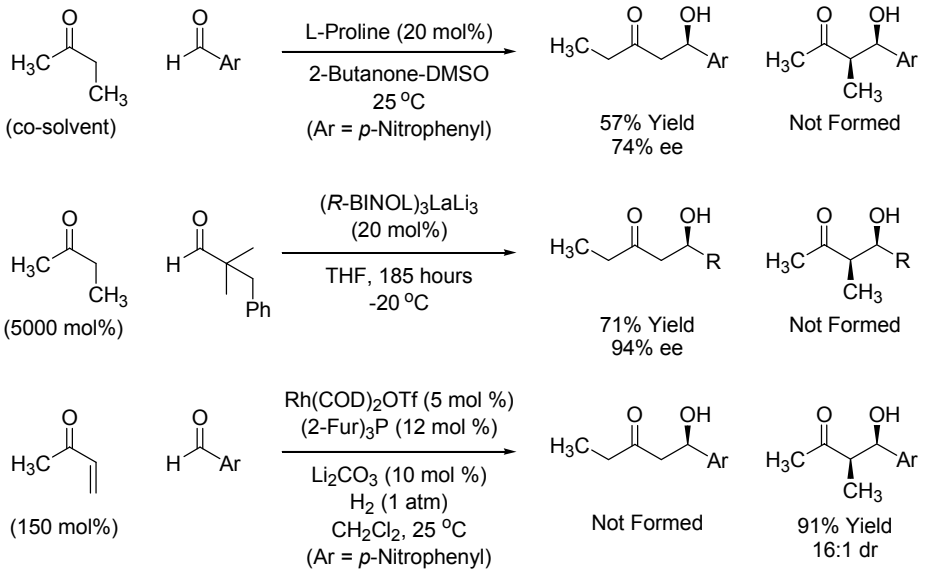

Scheme 1.3: Complementary regiocontrol in direct *vs*. reductive catalytic aldol couplings.

Following seminal studies by Revis (1987),[21a] the reductive aldol reaction has become the topic of intensive investigation.[20] To date, catalysts for reductive aldol coupling based on rhodium,[21,22] cobalt,[23] iridium,[24] ruthenium,[25] palladium,[26] copper,[27,28] nickel,[29] and indium[30,31] have been devised. A survey of these catalytic systems is given below.

1.2.2 RHODIUM

In 1987, Revis reported the first metal catalyzed reductive coupling of α,β-unsaturated esters with carbonyls to form aldol products, termed the "reductive aldol reaction."[21a] In this transformation, $RhCl_3 \bullet 3H_2O$ serves as the precatalyst and trimethylsilane serves as terminal reductant. At ambient temperature, α,β-unsaturated

esters and lactones were found to couple to both aldehydes and ketones. Notably, as demonstrated by the coupling of methyl methacrylate to acetone, two contiguous tetrasubstituted centers may be created in this transformation. The silyl ketene acetal derived from methyl methacrylate does not couple to acetone upon exposure to the reaction conditions, suggesting intervention of a rhodium enolate in the reductive catalytic process (Scheme 1.4).

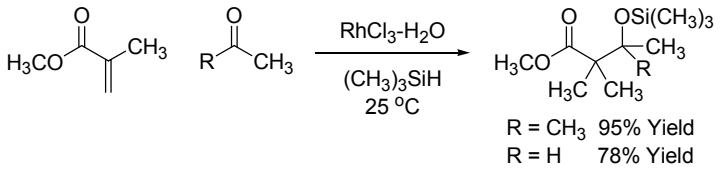

Scheme 1.4: First reported reductive aldol reaction described by Revis in 1987.

Attempted coupling of methyl vinyl ketone to acetone under the conditions reported by Revis does not provide the aldol adduct, but delivers the corresponding enol silane. It is likely that rhodium enolates derived from vinyl ketones are not sufficiently nucleophilic to engage ketone electrophiles in intermolecular aldol coupling. Consistent with this hypothesis, the reductive aldol coupling of vinyl ketones to aldehydes reported by Matsuda in 1990 proceeds readily using $Rh_4(CO)_{12}$ as catalyst precursor and Et_2MeSiH as terminal reductant.[21b] As demonstrated by the coupling of methyl vinyl ketone and mesityl oxide, variable degrees β-substitution are tolerated in the enone partner. Again, control experiments involving introduction of preformed enol silane to the reaction conditions does not provide aldol product, suggesting intermediacy of

rhodium enolates in the reductive catalytic process. This interpretation is supported by the fact that structurally related *O*-bound rhodium enolates have been isolated and are found to react with benzaldehyde to furnish corresponding rhodium aldolates (Scheme 1.5).[32]

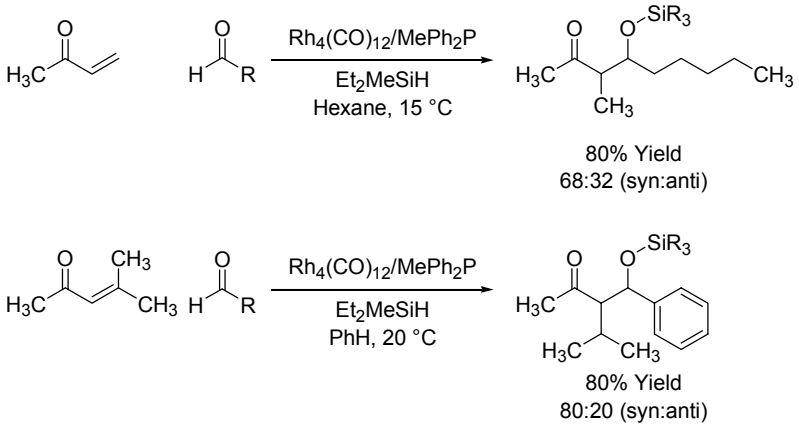

Scheme 1.5: Rhodium catalyzed reductive aldol coupling employing $Rh_4(CO)_{12}$ as catalyst precursor.

In 1999, the first diastereoselective reductive aldol reaction was discovered by Morken using an arrayed catalyst evaluation protocol.[21c] Evaluation of 192 independent catalytic systems revealed a strong interdependence of reaction variables. Optimal conditions identified for the reductive aldol coupling of methyl acrylate and benzaldehyde, which involve use of $[(COD)RhCl]_2$ dimer as the precatalyst, Me-DuPhos as ligand and Cl_2MeSiH as terminal reductant, provide the aldol coupling product in good yield with exceptional *syn*-diastereoselectivity. When these conditions are applied to other substrate combinations, good levels of *syn*-diastereoselectivity persist although

isolated yields are diminished in the case of enolizable aldehyde partners. Despite the use of a chiral ligand, asymmetric induction is not observed. It was later found that reactions employing Cl_2MeSiH as reductant give rise to silyl ketene acetals that spontaneously engage aldehydes in carbonyl addition, thus precluding involvement of the chirally modified catalyst in the enantiodetermining event.[21d] In contrast, using Et_2MeSiH as the terminal reductant, high levels of enantioselection may be achieved.[21e] However, diminished yields again were observed in connection with the use of enolizable aldehyde partners (Scheme 1.6).

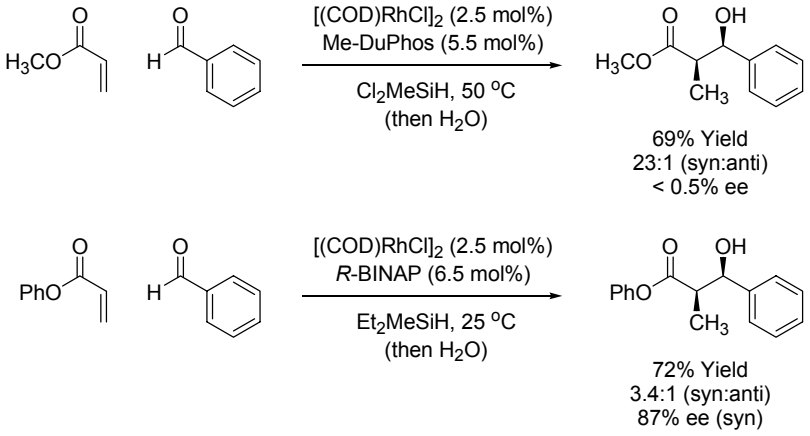

Scheme 1.6: First highly diastereo- and enantioselective reductive aldol couplings.

Two plausible mechanistic pathways for the rhodium catalyzed reductive aldol coupling of acrylates and aldehydes have been proposed. Both mechanism involves initial oxidative addition of hydrosilane to LnRh(I) to form LnRh(H)(SiR_3) **I**. In one possible scenario, catalytic cycle **A**, the aldehyde inserts into the Rh-Si bond to form complex **II**, followed by acrylate insertion into the newly formed Rh-C bond to form intermediate **III**. Finally, C-H reductive elimination delivers the aldol as the silyl ether along with

LnRh(I). A related mechanism has been proposed for the rhodium catalyzed silyformylation of the aldehydes.[33] Alternatively, as depicted in catalytic mechanism **B**, LnRh(H)(SiR_3) **I** may insert the acrylate to furnish rhodium enolate **IV**. Carbonyl addition provides the rhodium aldolate **V**, which upon O-Si reductive elimination delivers the silyl-protected aldol and LnRh(I). This mechanism finds support in the aldol addition of stoichiometrically preformed rhodium enolates.[32] For the enantioselective reductive aldol coupling depicted in Scheme 1.6, use of phenyldimethylsilyldeuteride as terminal reductant results in partial deuteration at the former acrylate β-position, which is consistent with both catalytic cycles **A** and **B**. In another experiment, it was found that after 24 hours in the absence of aldehyde less than 5% of the silylketene acetal was detected. Also, if preformed silyl ketene acetal is used instead of the acrylate less than 5% of the reductive aldol product is formed. These data are consistent with the intermediacy of a rhodium enolate. Intervention of rhodium enolate **IV** is especially attractive, as partial deuterium incorporation at the former enone β-position would arise as a consequence of reversible acrylate hydrometallation. Two additional mechanistic possibilities that were not enumerated by the authors, but that are consistent with the results of deuterium labeling, and which may be operative in other catalytic systems (*vide supra*), are represented by catalytic cycles **C** and **D**. In catalytic cycle **C**, acrylate-aldehyde oxidative coupling mediated by LnRh(I) provides the oxametallacyclic intermediate **VI**. σ-Bond metathesis of **VI** with silane provides intermediate **III**, which upon C-H reductive elimination provides the silyl-protected aldol adduct. Finally, as

shown in catalytic cycle **D**, monohydride based catalytic cycles involving rhodium(I) enolate **VII** and rhodium(I) aldolates **VIII** and **IX** may be envisioned (Scheme 1.7).

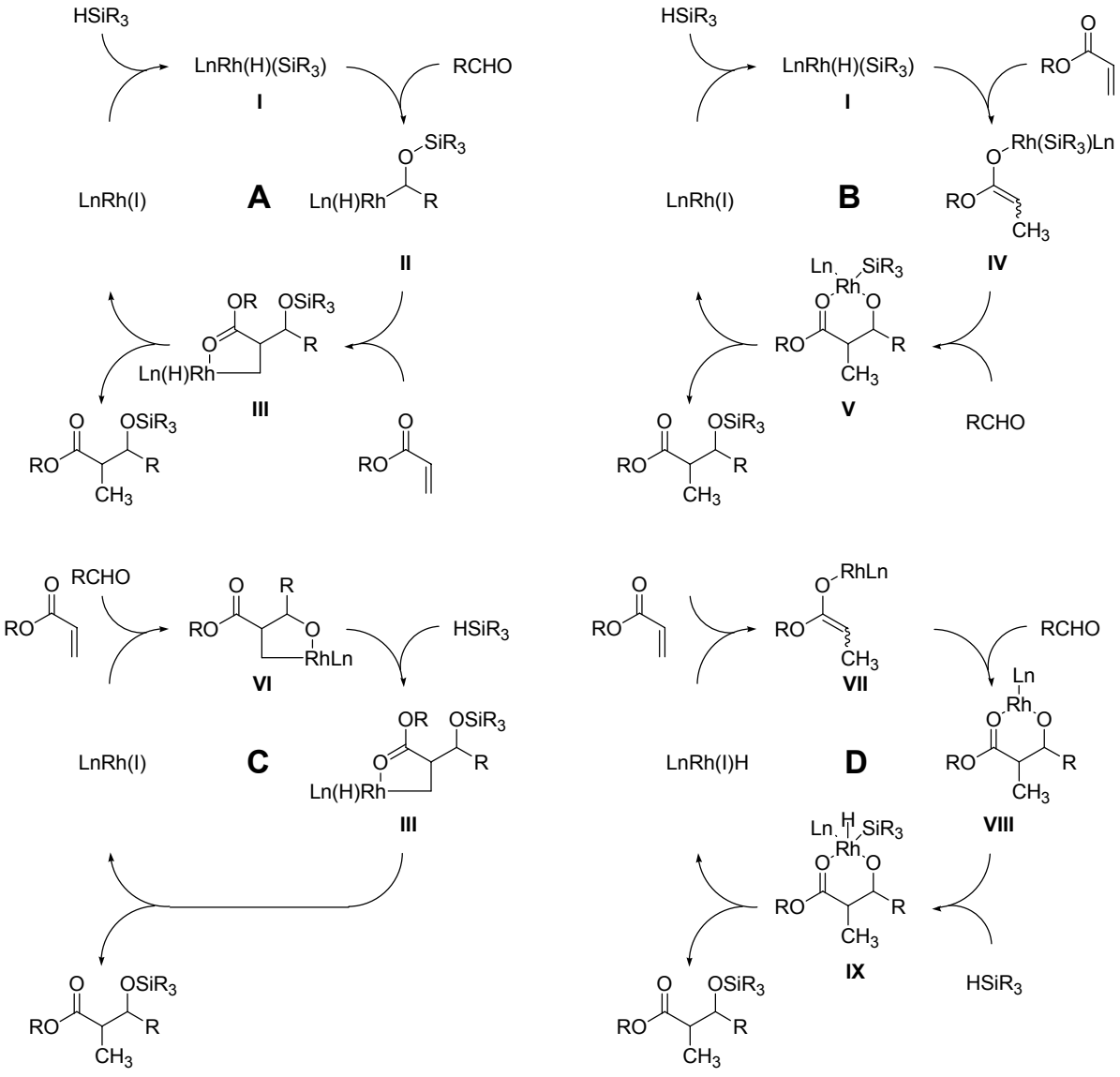

Scheme 1.7: Plausible mechanistic pathways for reductive aldol coupling as corroborated by deuterium labeling.

Silane-mediated reductive aldol cyclizations employing Wilkinson's complex, $RhCl(PPh_3)_3$, or $RhH(PPh_3)_4$ as precatalyst have been described.[21g,h] Although triphenylphosphine is used as ligand in each case, the stereochemical outcome of the reaction was found to be highly dependant upon the choice of precatalyst. Whereas cyclizations employing $RhCl(PPh_3)_3$ provide the *cis*-isomer with modest levels of stereoselection, cyclizations employing $RhH(PPh_3)_4$ as precatalyst deliver the *anti*-isomer with relatively high levels of stereoselectivity. These data suggest a precatalyst-dependant partitioning of alternate catalytic mechanisms. It is possible that Wilkinson's complex, $RhCl(PPh_3)_3$, promotes catalytic cycle **B** involving intermediates **I**, **IV** and **V**, while $RhH(PPh_3)_4$ promotes monohydride catalytic cycle **D** involving intermediates **VII**, **VIII** and **IX** (Scheme 1.7). Notably, attempted cyclization of the corresponding methyl ketone using Wilkinson's complex, $RhCl(PPh_3)_3$, provides an acyclic product that appears to arise by way of olefin isomerization to furnish a conjugated enone that is subject to 1,4-reduction (Scheme 1.8).

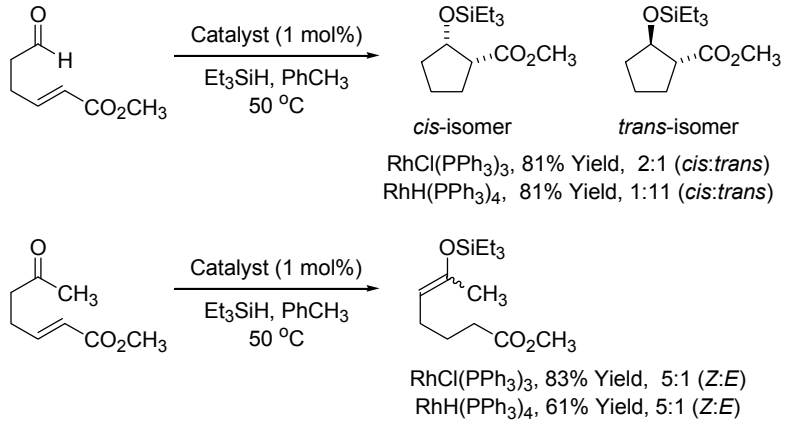

Scheme 1.8: Rhodium catalyzed reductive aldol cyclization.

Using a Rh(Phebox) catalyst, silane-mediated intermolecular reductive aldol coupling is achieved with excellent levels of *anti*-diastereoselectivity accompanied by exceptional levels of asymmetric induction across a range of substrates.[21i] The coupling reactions are conducted at 50 °C with dropwise addition of the hydrosilane to a solution of *tert*-butyl acrylate, aldehyde, and the rhodium complex. The reaction is believed to involve initial reduction of the Rh^{III}(Phebox) complex to provide Rh^{I}(Phebox), which promotes catalytic cycle **B** involving intermediates **I**, **IV** and **V** (Scheme 1.7). Intervention of a chair-like transition state and an (*E*)-rhodium enolate are invoked in the stereodetermining step. The reaction is applicable to both aromatic and aliphatic aldehydes, as well as β-substituted pronucleophiles such as *tert*-butyl crotonate. Further studies of the Rh(Phebox) catalyst demonstrate that appropriate substitution of the ligand phenyl moiety confers heightened levels of reactivity and selectivity (Scheme 1.9).[21j,k]

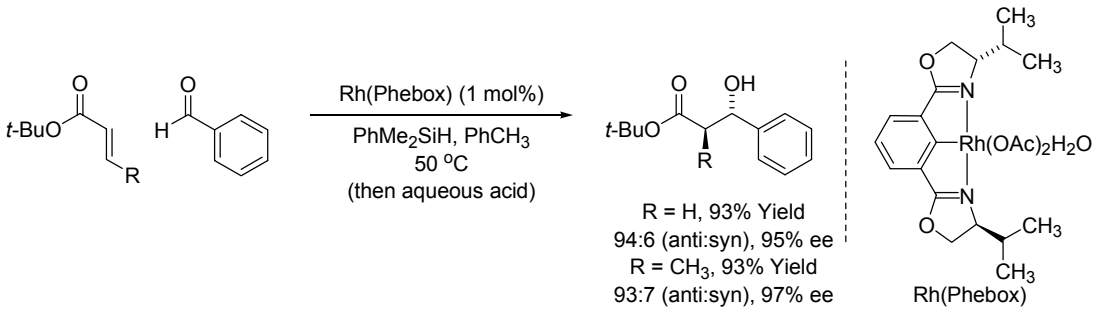

Scheme 1.9: Highly *anti*-diastereo- and enantioselective reductive aldol coupling catalyzed by Rh(Phebox).

Another addition to the reductive aldol literature involves use of β-sulfido-aldehydes as the stoichiometic reductant.[21l] The β-sulfido moiety promotes formation of

chelated acyl rhodium hydrides, which engage in enone hydrometallation *en route* to rhodium enolates. Carbonyl addition to a second molecule of aldehyde followed by C-O reductive elimination from the resulting aldolate delivers the *O*-acylated aldol adduct with concomitant regeneration of the active catalyst. This first generation catalytic system provides aldol adducts in good yields with diastereoselectivities ranging from 1:1 to 3.3:1 (Scheme 1.10).

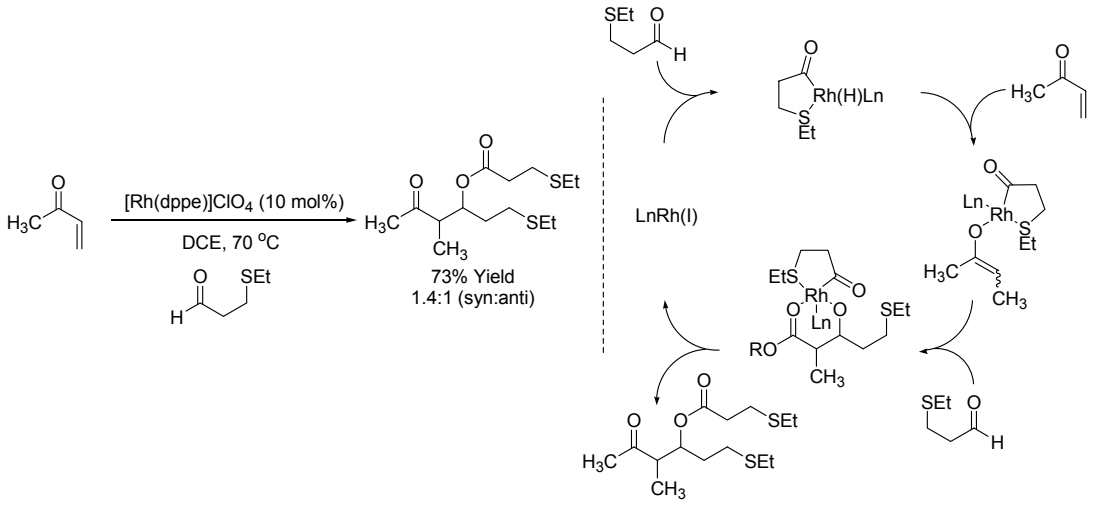

Scheme 1.10: Rhodium catalyzed reductive aldol coupling of β-sulfido-aldehydes and proposed catalytic mechanism.

In 2002, it was found that reductive aldol coupling could be achieved by simply hydrogenating enones in the presence of aldehydes.[22] Through the use of tri-2-furylphosphine as ligand,[34] the observed levels of *syn*-diastereoselection, which are obtained at ambient temperature, exceed those observed in reactions of lithium enolates conducted at -78 °C.[22e] High *syn*-diastereoselectivity suggests a kinetically controlled process,[13] and may be rationalized on the basis of a mechanism involving stereospecific formation of the *Z*(*O*)-enolate, as determined by internal hydride delivery to the enone *s*-

cis conformer through a 6-centered transition structure, and subsequent addition of the *Z*(*O*)-enolate to the aldehyde through a Zimmerman-Traxler type transition state.[35] By virtue of the facile kinetic pathway for enone reduction, competitive conventional hydrogenation of "hydrogen-labile" functional groups (alkynes, alkenes, benzylic ethers and nitroarenes) is not observed under the conditions of hydrogen-mediated coupling, thus enabling chemoselective activation of vinyl ketones and even divinyl ketones.[22f] Because hydrogen-mediated aldol coupling occurs under essentially neutral conditions in low dielectric media at ambient temperature, sensitive *N*-Boc-α-aminoaldehydes may react through hydrogen-bonded chelates without epimerization to furnish aldol adducts that embody that embody exceptional levels of *syn*-aldol diastereoselectivity and *anti*-Felkin-Anh control (Scheme 1.11).[22g]

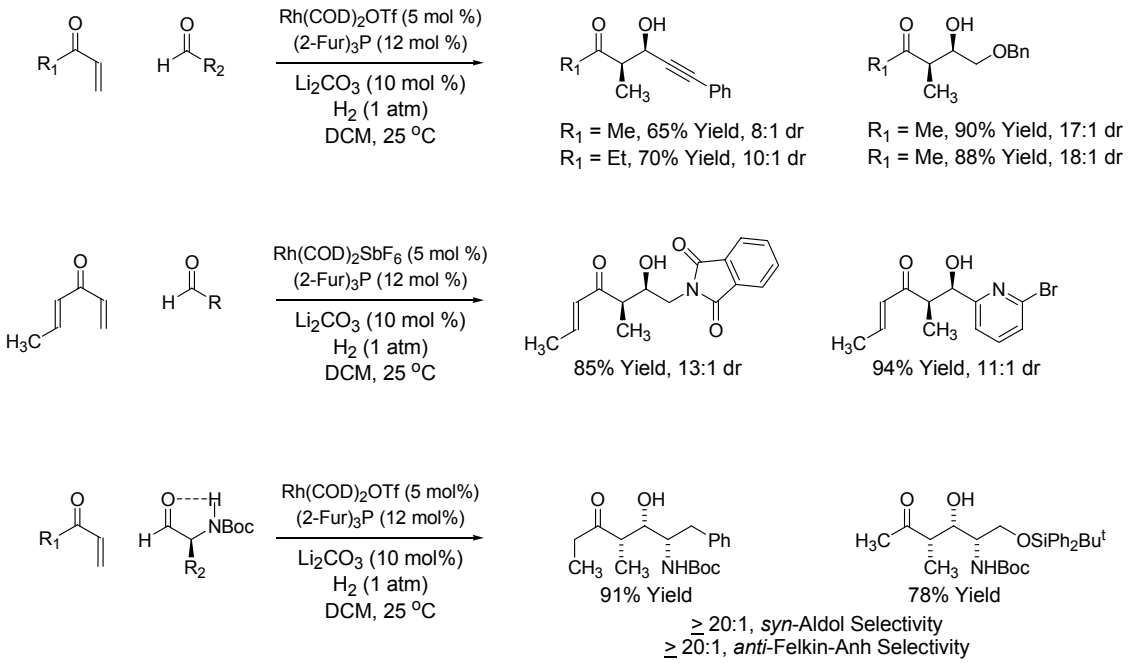

Scheme 1.11: Highly *syn*-diastereoselective rhodium catalyzed reductive aldol couplings mediated by hydrogen.

For the hydrogen-mediated reductive aldol additions, cationic rhodium precatalysts along with substoichiometric quantities of mild basic additives are found to suppress competitive conventional hydrogenation pathways. Whereas neutral rhodium(I)-catalysts induce homolytic hydrogen activation,[36] corresponding cationic complexes used in the presence of basic additives are known to promote heterolytic hydrogen activation (H_2 + M-X $\rightarrow$ M-H + HX).[37] This behavior derives from the enhanced acidity of the cationic dihydrides.[38] Hence, basic additives may disable direct enolate-hydrogen reductive elimination manifolds by deprotonation of the (hydrido)rhodium intermediates $LnRh^{III}X(H)_2$ or (enolato)$Rh^{III}X(H)Ln$, thereby promoting entry into a monohydride based catalytic cycle. The results of isotopic labeling studies involving reductive coupling

of MVK and *p*-nitrobenzaldehyde performed under an atmosphere of elemental deuterium are consistent with this interpretation. The aldol adduct incorporates a single deuterium atom at the former enone β-position.[22e] This result excludes Morita-Baylis-Hillman pathways *en route* to aldol product, as deuterium incorporation at the α-carbon is not observed. Irreversible enone hydrometallation is suggested by the incorporation of a single deuterium atom. A catalytic cycle involving enone-aldehyde oxidative coupling (mechanism **C**, Scheme 1.7) cannot be excluded and may account for the fact that easily reduced enones participate in the coupling, whereas α,β-unsaturated esters do not (Scheme 1.12).

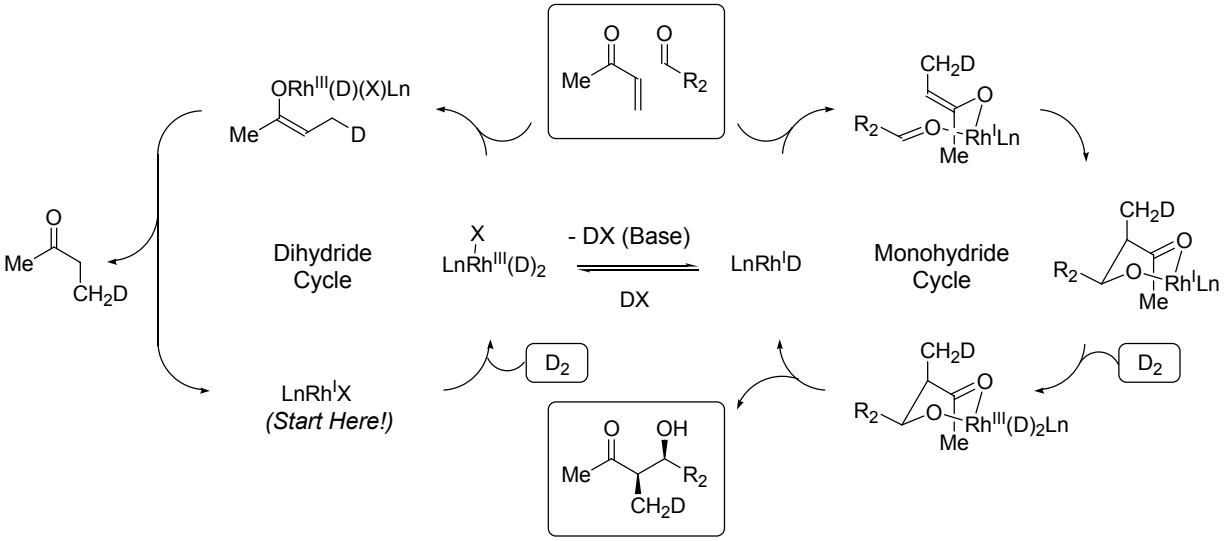

Scheme 1.12: Rhodium catalyzed hydrogenative aldol coupling under an atmosphere of deuterium: partitioning of carbonyl addition and 1,4-reduction manifolds.

The use of metallo-aldehyde enolates in aldol coupling typically suffers from polyaldolization, product dehydration and competitive Tishchenko-type processes.[8d,39] Indeed, catalytic cross aldolization of aldehyde donors only has been achieved through amine catalysis and the use of aldehyde-derived enol silanes.[40] The first use of metallo-aldehyde enolates in catalytic cross aldolization was achieved by hydrogenating enals in the presence of α-ketoaldehydes.[22d] The resulting *β*-hydroxy-*γ*-ketoaldehydes are highly unstable, but may be trapped through condensation with hydrazine to afford 3,5-disubsituted pyridazines (Scheme 1.13).

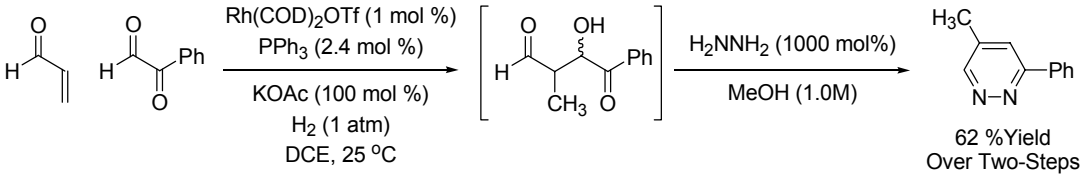

Scheme 1.13: Acrolein as a metallo-aldehyde enolate precursor in hydrogenative aldol additions to α-ketoaldehydes.

Under hydrogenation conditions, the cyclization of enone and enal donors tethered to aldehyde and ketone acceptors is readily achieved with high levels of *syn*-diastereoselectivity.[22a,b,c] The observance of *syn*-aldol adducts is consistent once again with the intermediacy of a Z-enolate and a closed Zimmerman-Traxler type transition structure. Reversible aldol addition is suggested by an inversion in diastereoselectivity observed in connection with aliphatic enone pronucleophiles and the results of isotopic labeling. In the latter case, hydrogenative aldol cyclization under an atmosphere of

deuterium results in deuterium incorporation exclusively at the former enone β-position, but as a distribution of deuterated products. This result supports reversible enone hydrometallation in the case of ketone acceptors, where reversible aldol addition is anticipated (Scheme 1.14).

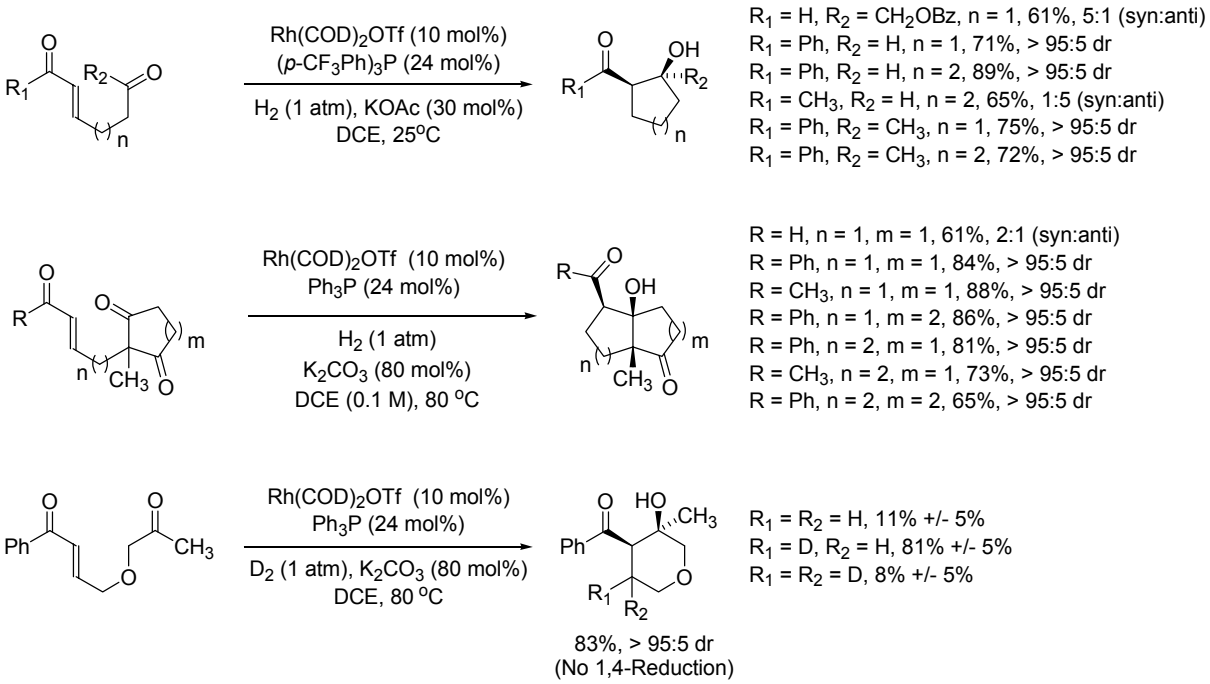

Scheme 1.14: Aldol cycloreduction *via* rhodium catalyzed hydrogenation.

1.2.3 COBALT

In 1989, a cobalt catalyzed reductive aldol coupling mediated by phenylsilane was reported by Mukaiyama.[23a] The reaction exhibits broad scope and is applicable to the coupling of α,β-unsaturated nitriles, amides and esters to a diverse assortment of aldehydes. While good yields of coupling product are obtained, roughly equimolar distributions of diastereomers are observed. Later in 2001, an intramolecular variant of

the cobalt catalyzed reductive aldol reaction was reported.[23b,c] Unlike the intermolecular coupling, the cyclization occurs with high levels of *syn*-diastereoselectivity for aryl- and heteroaryl-substituted enones. α,β-Unsaturated nitriles, amides and esters do not participate in the cyclization, instead providing products of conjugate reduction. This methodology is applicable to the formation of 5- and 6-membered ring aldol adducts (Scheme 1.15).

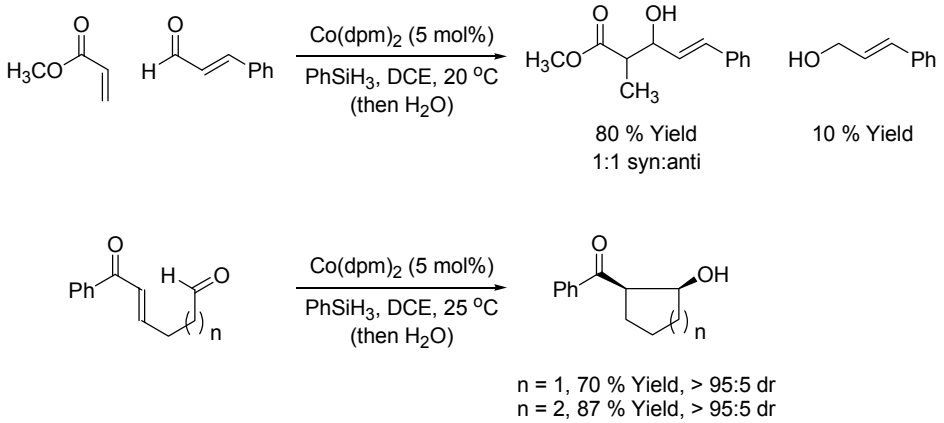

Scheme 1.15: Cobalt catalyzed intermolecular reductive aldol coupling.

The catalytic mechanism proposed for the cobalt catalyzed reductive aldol coupling takes into account the unique reactivity of $Co(dpm)_2$, a tetrahedral d^7-metal complex with three unpaired electrons. Tetrahedral d^7-metal complexes are known to engage in single electron oxidative addition through a free radical mechanism.[48] Additionally, Co(II) complexes are known to disproportionate.[42] Hence, two plausible mechanisms may account for generation of the (hydrido)cobalt intermediates required for entry into catalytic cycles involving enone hydrometallation: (A) single electron oxidative addition of silane to Co(II) or (B) disproportionation followed by two electron

oxidative addition of silane to Co(I). In either case, a Co(III) hydride is formed, suggesting a Co(I)-Co(III) cycle. Alkene geometry does not influence diastereoselection, which is consistent with a catalytic mechanism involving enone hydrometallation. Additionally, reductive cyclization mediated by $PhSiD_3$ results in the incorporation of a single deuterium atom at the former enone β-position as an equimolar mixture of epimers, as determined by single crystal neutron diffraction. The incorporation of a single deuterium atom suggests that β-hydride elimination of the metallo-enolate is slow with respect to subsequent steps in the catalytic cycle. The observance of an equimolar mixture of epimers suggests any combination of the following: (a) the enolate resides as the *O*-bound haptomer, (b) π-facial interconversion of the metallo-enolate is faster than aldehyde addition, or (c) aldol addition is reversible. The observed *syn*-diastereomers likely arise through addition of the (*Z*)-cobalt enolate to the tethered aldehyde through a chair-like transition structure (Scheme 1.16).

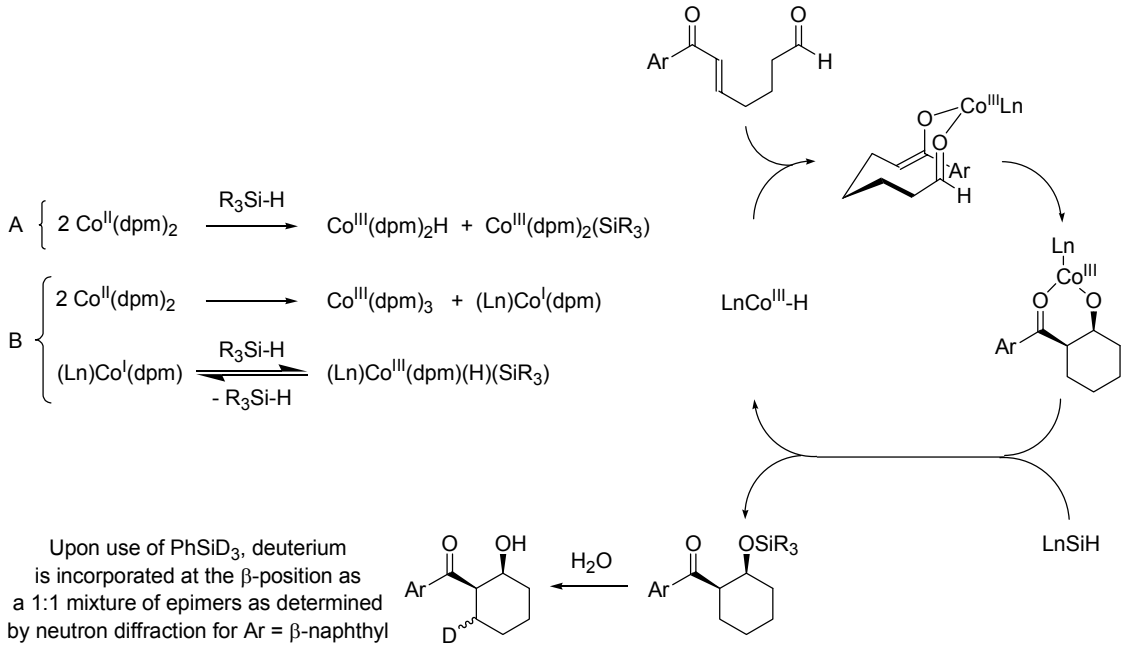

Scheme 1.16: Plausible mechanism for the cobalt catalyzed reductive aldol cyclization as supported by isotopic labeling studies.

Recently, a cobalt catalyzed reductive aldol cyclization reaction employing diethylzinc as the stoichiometric reductant was reported.[23d] Under optimal conditions, α,β-unsaturated amides are cyclized onto tethered ketones to provide a variety of 4-hydroxypiperdin-2-ones in excellent yield and with exceptional levels of diastereoselectivity (Scheme 1.17). A hydrometallative mechanism involving intermediacy of an amide enolate was proposed. Specifically, it was postulated that the cobalt precatalyst and diethylzinc engage in transmetallation-β-hydride elimination to furnish a cobalt-hydride. Hydrometallation of the α,β-unsaturated amide delivers a cobalt enolate that participates in a second transmetallation with diethylzinc to produce a zinc enolate and an ethylcobalt species. Addition of the zinc enolate to the tethered ketone

provides the zinc-aldolate of the cyclized product. β-Hydride elimination of the ethylcobalt species regenerates the cobalt hydride along with ethylene (Scheme 1.18).

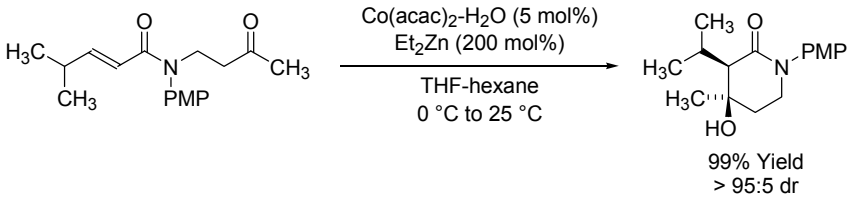

Scheme 1.17: Cobalt catalyzed reductive aldol cyclization mediated by diethylzinc.

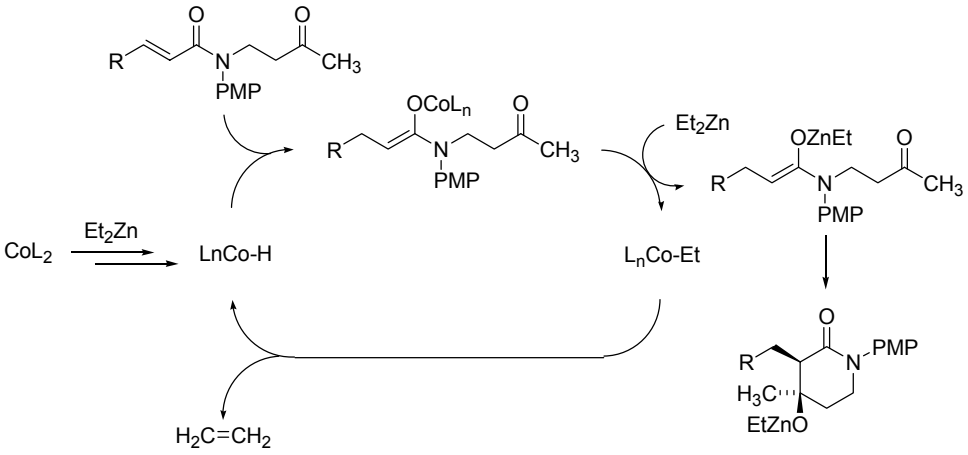

Scheme 1.18: Mechanism proposed for the cobalt catalyzed reductive aldol cyclization mediated by diethylzinc.

1.2.4 IRIDIUM

In 2001, an Ir(pybox) complex was reported to catalyze highly diastereo- and enantioselective reductive aldol couplings mediated by silane.[24] Simple aliphatic aldehydes are not sufficiently reactive to participate in the coupling. However, aldehydes bearing heteroatoms at the α- and β-positions, which benefit from σ-inductive effects, provide moderate yields of coupling product. For the indicated α-chiral aldehyde, highly

stereoselective reductive aldol addition is observed in the matched case. In the mismatched case, aldehyde reduction is observed. For the indicated β-chiral aldehyde, erosion in the level of *syn*-diastereoselectivity is observed. For both enantiomers of the β-chiral aldehyde, the ratio of the major and minor *syn*-aldol isomers is nearly identical, indicating good levels of catalyst directed asymmetric induction (Scheme 1.19).

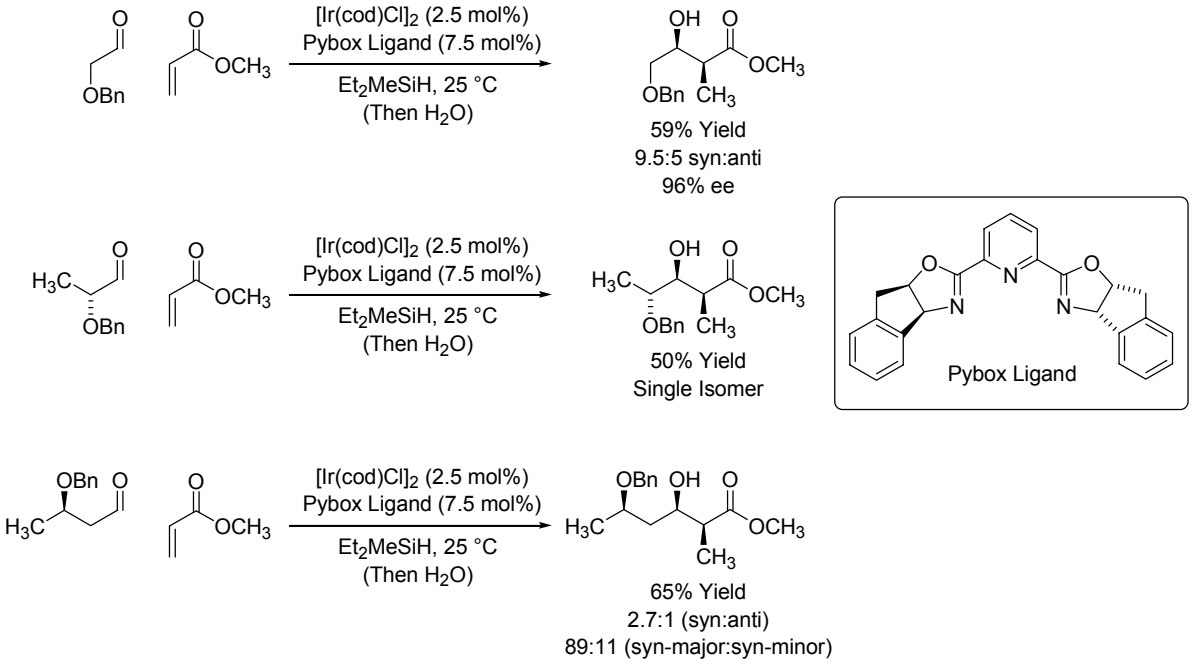

Scheme 1.19: Diastereo- and enantioselective reductive aldol coupling catalyzed by Ir(pybox).

1.2.5 RUTHENIUM

Recently, a $RuHCl(CO)(PPh_3)_3$ catalyzed reductive aldol dimerization of α,β-unsaturated aldehydes to provide α-hydroxymethyl ketones was reported that employs 2-

propanol as the terminal reductant.[25] The first step in the proposed catalytic mechanism involves enal hydrometallation to provide a ruthenium enolate. Addition of the enolate to a second molecule of aldehyde provides a ruthenium aldolate, which upon β-hydride elimination delivers an intermediate 1,3-dicarbonyl compound with regeneration of ruthenium hydride. Sequential hydrogen transfer from 2-propanol reduces the formyl moiety gives an unsaturated dimer, which upon further reduction provides the saturated dimer (Scheme 1.20).

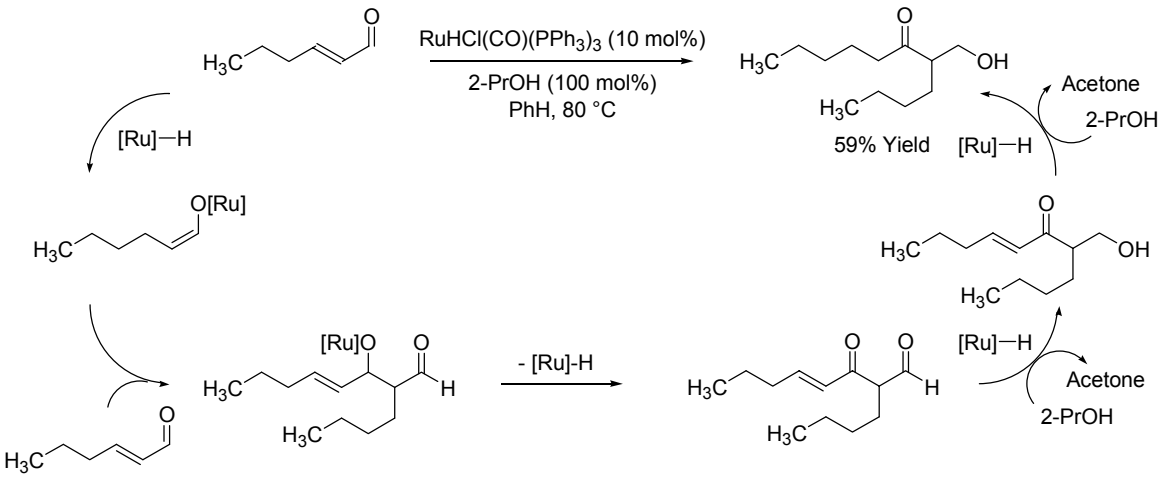

Scheme 1.20: Ruthenium catalyzed reductive dimerization of enals mediated by 2-propanol.

1.2.6 PALLADIUM

A singular example of palladium catalyzed reductive aldol coupling was disclosed in 1998.[26] This trichlorosilane-mediated coupling employs tetrakis(triphenylphosphine)palladium as the catalyst precursor. Under the reported

reaction conditions, the aldol product is obtained in good yield with modest levels of *anti*-diastereoselectivity. The first steps in the catalytic mechanism are postulated to involve oxidative addition of the trichlorosilane to palladium(0), followed by hydrometallation of the α,β-unsaturated compound. The remainder of the mechanism is unclear. It is not known whether the aldehydes addition occurs through the intermediacy of the palladium enolate or whether O-Si reductive elimination occurs to provide an enol silane that reacts with the aldehyde spontaneously (Scheme 1.21).

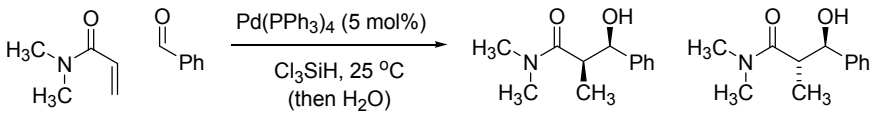

Scheme 1.21: Palladium catalyzed reductive aldol coupling mediated by silane.

1.2.7 COPPER

In 1998, the first use of Stryker's reagent, $[PPh_3CuH]_6$, in a reductive aldol cyclization was reported.[27] Scheme 1.22 demonstrates the conjugate reduction-intramolecular aldol *en route* to the synthesis of pseudolaric acid A. The initial report was not catalytic, but it paved the way for the development of catalytic variants.

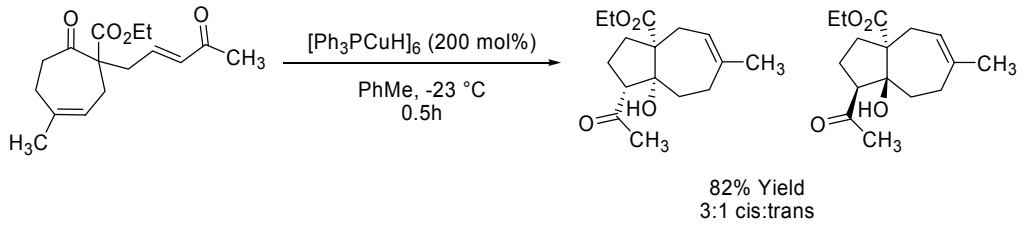

Scheme 1.22: Synthesis of pseudolaric acid A *via* conjugate reduction-intramolecular aldol.

The first catalytic variant of this transformation was reported in 2000 where a catalytic amount of Stryker's reagent was used with a silyl hydride to generate a silyl enol ether, that can be trapped by an aldehyde when a Lewis acid is present.[28a] For this reaction sequence to operate correctly the conjugate reduction had to proceed to completion before addition of the Lewis acid and aldehyde. The addition order was important to minimize the amount of reduced aldehyde. It is believed that Stryker's reagent delivers a hydride to the β-position of the enone and together with the silyl hydride reagent a silyl enol ether is generated. The silyl enol ether can be isolated. A variety of silyl hydrides were used such as: dimethylphenylsilane ($PhMe_2SiH$), tetramethyldisiloxane ($HMe_2SiOSiMe_2H$), and polymethylhydrosiloxane (PMHS). Once the enone is consumed by TLC analysis, then the Lewis acid and aldehyde are slowly added. For the Lewis acid portion of the reaction either $BF_3{\cdot}Et_2O$ or $TiCl_4$ was used. The reaction proceeded with a variety of enones and aldehydes in good yield. In all cases diastereomeric products were obtained (Scheme 1.23).

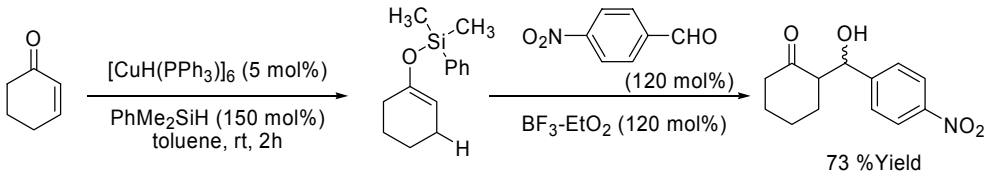

Scheme 1.23: Copper catalyzed reductive aldol reaction in the presence of Lewis acids.

One interesting use of a copper (I) catalyst in a reductive aldol reaction is as a radical initiator.[28b] It was discovered that copper (I) chloride can initiate the radical addition of Bu_3SnH to an enone in order to generate a tin enolate. Also, the copper (I) chloride catalyst can participate in the aldol reaction between the tin enolate and an aldehyde acting as a Lewis acid. This method is applicable to the coupling of vinyl ketones to aliphatic, aromatic and α,β-unsaturated aldehydes. The aldol products are obtained in good isolated yield with modest levels of *syn*-diastereoselection (Scheme 1.24).

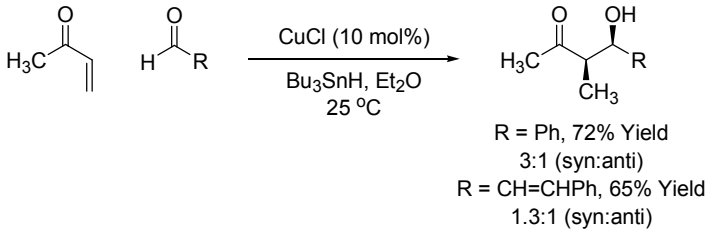

Scheme 1.24: Copper initiated radical addition of Bu_3SnH to enones resulting in reductive aldol coupling.

In 2005, a diastereo- and enantioselective copper(II) catalyzed reductive aldol cyclization mediated by 1,1,3,3-tetramethylhydroxysiloxane (TMDS) was developed by Lam and applied to the synthesis of β-hydroxylactones.[28c] The substrates for this

transformation are α,β-unsaturated esters of hydroxy ketones. The products form as single diastereomers, as determined by ^{1}H NMR analysis of the unpurified reaction mixtures. In an effort to develop an asymmetric variant of the cyclization, several chiral ligands were screened, revealing moderate levels of enantioselection. This methodology was extended to the synthesis of 4-hydroxypiperdin-2-ones, which are formed through the cycloreduction of corresponding α,β-unsaturated keto-amides. Again, exceptional levels of diastereoselection are observed (Scheme 1.25).[28d]

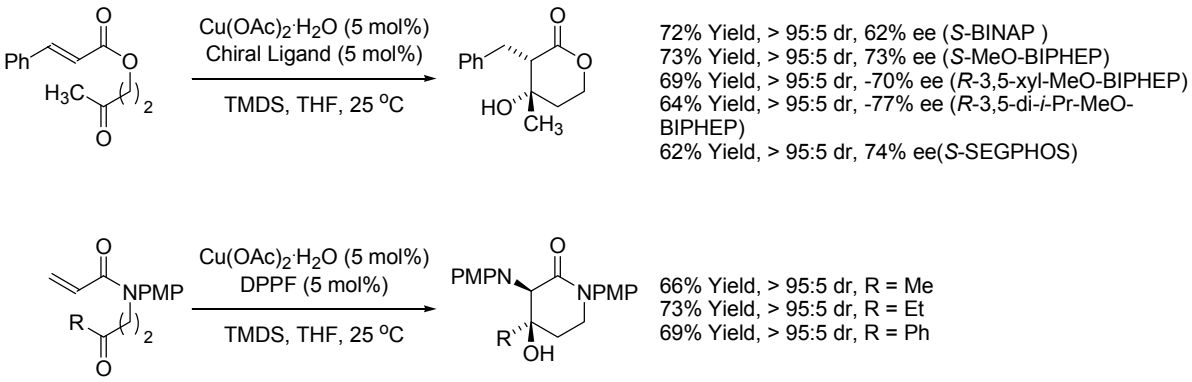

Scheme 1.25: Diastereo- and enantioselective copper(II) catalyzed reductive aldol cyclizations mediated by silane.

The authors propose a catalytic mechanism wherein silane-mediated reduction of $Cu(OAc)_2 \bullet H_2O$ provides a copper (I)-bisphosphine hydride complex, which initiates the catalytic cycle through hydrometallation of the α,β-unsaturated ester. The resulting copper enolate undergoes addition to the tethered ketone to give a copper aldolate, which upon σ-bond metathesis with siloxane delivers the product with concomitant regeneration of the copper (I)-bisphosphine hydride complex to close the cycle. The observed

stereoselectivity is postulated to arise through aldehyde addition of the (*Z*)-copper enolate in a closed transition structure (Scheme 1.26).

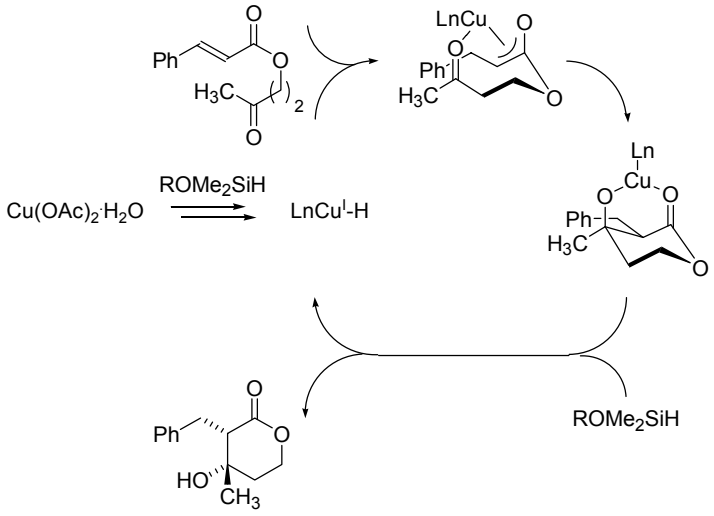

Scheme 1.26: Proposed catalytic cycle for the copper catalyzed reductive aldol cyclization mediated by silane.

The first highly diastereo- and enantioselective intermolecular reductive aldol coupling to simple ketones was reported by Riant using $[CuF(PPh_3)_3]$•2MeOH as a precatalyst and phenylsilane as the stoichiometric reductant.[28e] Entry into the catalytic cycle is achieved through the reaction of hydrosilane and $[CuF(PPh_3)_3]$•2MeOH to generate a copper(I) hydride, which initiates a hydrometallative mechanism akin to that previously described (Scheme 1.26). Under optimum conditions employing a "TANIAPHOS" ligand, methyl acrylate couples to methyl ketones such as acetophenone with remarkable levels of *anti*-diastereoselectivity and absolute stereocontrol. Aldehydes

couplings performed under these conditions exhibit modest levels of diastereoselection and highly variable levels of enantioselection.[28f] Very similar conditions for intermolecular reductive aldol coupling of acrylates, β-substituted acrylates and allenic esters to simple ketones using $[CuF(PPh_3)_3]$•2EtOH as precatalyst and triethoxysilane as the stoichiometric reductant were concurrently reported by Shibasaki and Kanai.[28g] In these reactions, which employ (*R*)-tol-BINAP as ligand, modest levels of relative and absolute stereocontrol were observed. Later it was found that using a "TANIAPHOS" ligand with pinacolborane as reductant, selectivities in reductive aldol couplings of allenic esters to acetophenone were improved.[28h] Furthermore, through the use of $P(c\text{-}Hex)_3$ as an additive, highly enantioselective alkylation is directed to the γ-position of the purported dienolate intermediate (Scheme 1.27).

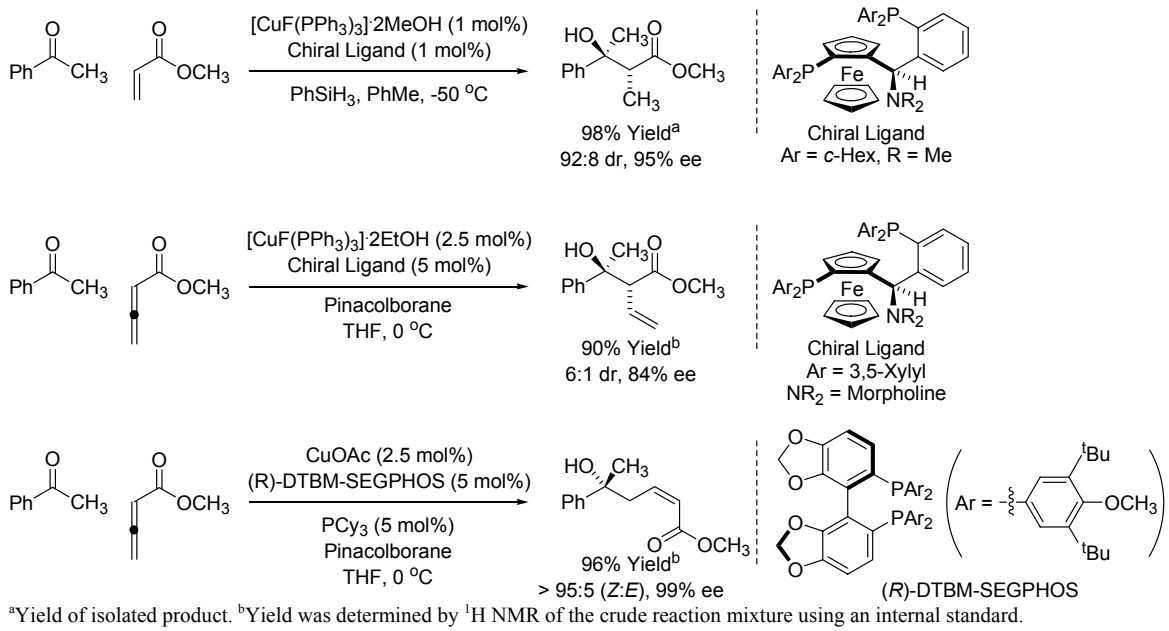

[a]Yield of isolated product. [b]Yield was determined by ^{1}H NMR of the crude reaction mixture using an internal standard.

Scheme 1.27: Diastereo- and enantioselective reductive aldol additions to ketones catalyzed by copper.

1.2.7 NICKEL

Recently, a nickel catalyzed reductive aldol addition of *tert*-butyl acrylate to aromatic and aliphatic aldehydes mediated by trialkylborane was reported.[29] Interestingly, an aryl iodide is required to initiate the catalytic process though it is not incorporated into the reaction product. In the absence of phenyl iodide no reaction occurrs and starting materials are recovered. It was found that the reaction requires sterically unencumbered aryl iodides, which led the authors to propose that phenyl iodide undergoes oxidative addition to the nickel(0) precatalyst. In agreement with this hypothesis, direct use of nickel(II) precatalysts results in an alternate reaction pathway involving ethyl transfer to the acrylate in advance of aldol addition. Based on the

collective data, the following catalytic mechanism was proposed. Oxidative addition of phenyl iodide to the nickel(0) precatalyst is followed by coordination of acrylate. The resulting complex is transforms to an ethyl(iodo)nickel species, along with an arylated boron enolate that spontaneously reacts with aldehyde to furnish trace quantities of tandem conjugate addition-aldol coupling product. The ethyl(iodo)nickel species, which represents the first point of entry into the actual catalytic cycle, eliminates ethylene and then coordinates another molecule of acrylate and triethylborane to generate the indicated nickel hydride complex. Acrylate hydrometallation provides a boron enolate and regenerates the ethyl(iodo)nickel species. The boron enolate is presumed to react spontaneously with the aldehyde to deliver the aldol product (Scheme 1.28).

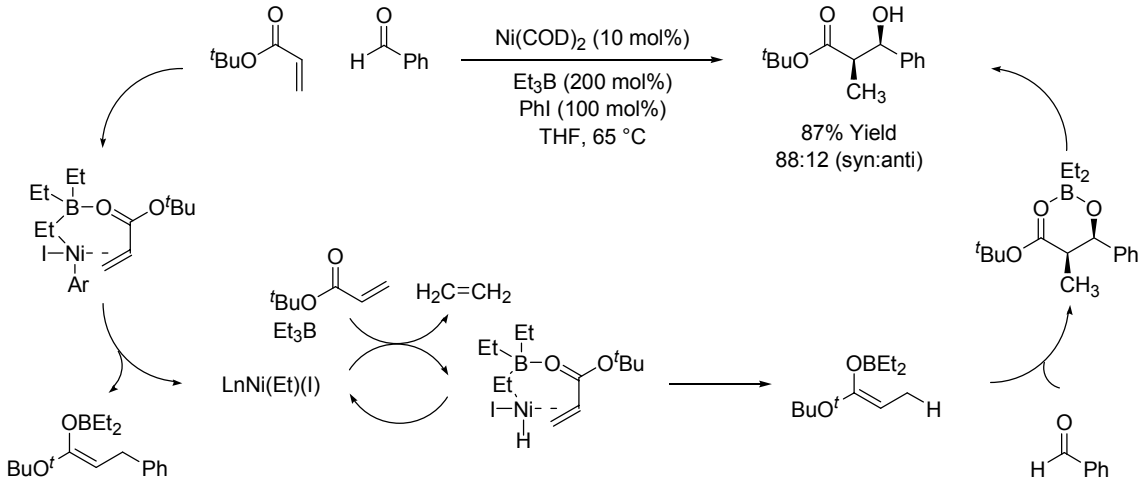

Scheme 1.28: Nickel catalyzed reductive aldol coupling initiated by aryl iodides and proposed catalytic mechanism.

1.2.8 INDIUM

In 2002, a reductive aldol coupling employing stoichiometric quantities of indium(III) bromide and tributylstannane was reported.[30] In 2004, it was found that use of triethylsilane as a terminal reductant enables corresponding catalytic processes.[31a] This protocol is applicable to the highly *syn*-diastereoselective coupling of enones to aldehydes. Entry into the catalytic mechanism is postulated to occur through transmetallation between $InBr_3$ and Et_3SiH to generate $HInBr_2$ and Et_3SiBr. The indium hydride is proposed to initiate a hydrometallative mechanism similar to that previously described (mechanism **D**, Scheme 1.7), but involving σ-bond metathesis between the intermediate indium aldolate and silane. It has been suggested that the hydrometallation event occurs through a 6-centered transition structure involving the *s-cis*-conformer of the enone, stereospecifically delivering the (*Z*)-indium enolate.[43] Aldehyde addition of the (*Z*)-indium enolate through a Zimmerman-Traxler type transition structure accounts for the observed *syn*-diastereoselectivity.[35] Concurrently, an indium catalyzed reductive aldol coupling employing indium(III) acetate as the catalyst and $PhSiH_3$ as reductant was reported.[31b] This catalyst system enables *syn*-diastereoselective intermolecular and intramolecular reductive coupling (Scheme 1.29).

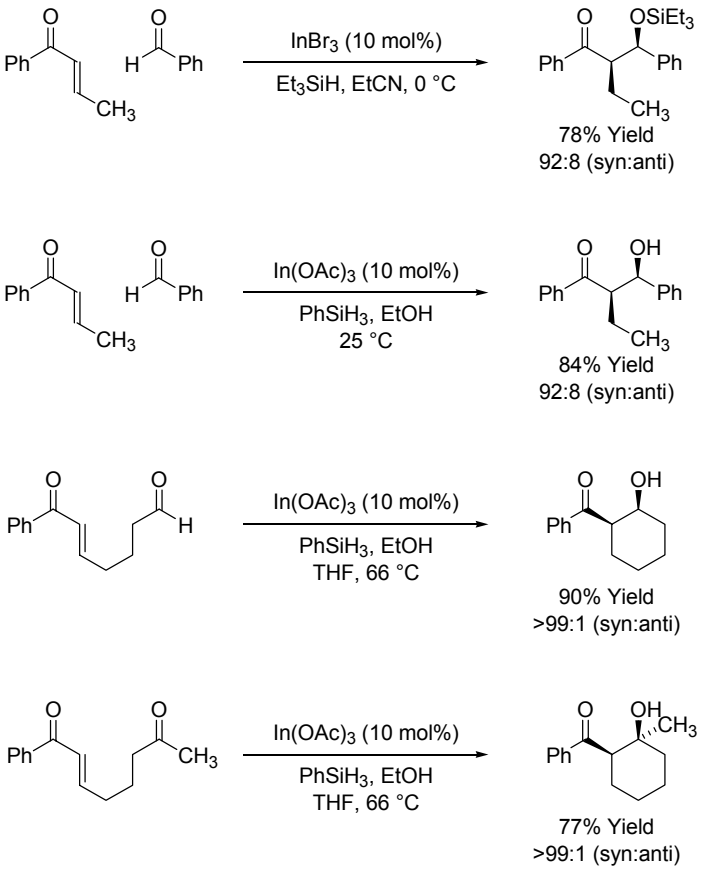

Scheme 1.29: Indium catalyzed reductive aldol coupling.

1.3.1 Reaction of Enones with Aldehydes (Morita-Baylis Hilman Reaction)

1.3.2 Rhodium

In the absence of hydrosilanes, Morita-Baylis-Hilman (MBH) type products can be obtained from the reductive coupling of enones and aldehydes by aldol addition followed by β-hydride elimination. It was discovered that enone and aldehydes couple to give Morita-Baylis-Hilman products in the presence of catalytic $RhH(PPh_3)_4$ or $RuH(PPh_3)_4$ and 20 mol% of 2-propanol (Scheme 1.30).[44] In the presence of ruthenium catalyst the alcohol additive was not needed to accelerate the reaction. This reaction is thought to proceed by hydrometallation of the enone by the rhodium or ruthenium

hydride to generate an enolate, which is trapped by the aldehyde (Scheme 1.30). Then an equilibrium is established between the aldolate and the enol. β-Hydride elimination provides the MBH product and regenerates the catalyst. Under these reaction conditions none of the reductive aldol product is isolated, but small amounts of the homocoupling product is obtained from the reaction of the enolate with another enone. Evidence supporting that this reaction is proceeding *via* reductive aldol addition/β-hydride elimination and not a classical MBH mechanism is that the addition of Bu_3P to the reaction does not alter the outcome of the reaction. Also, the addition of the alcohol additive enhances catalyst turnover.

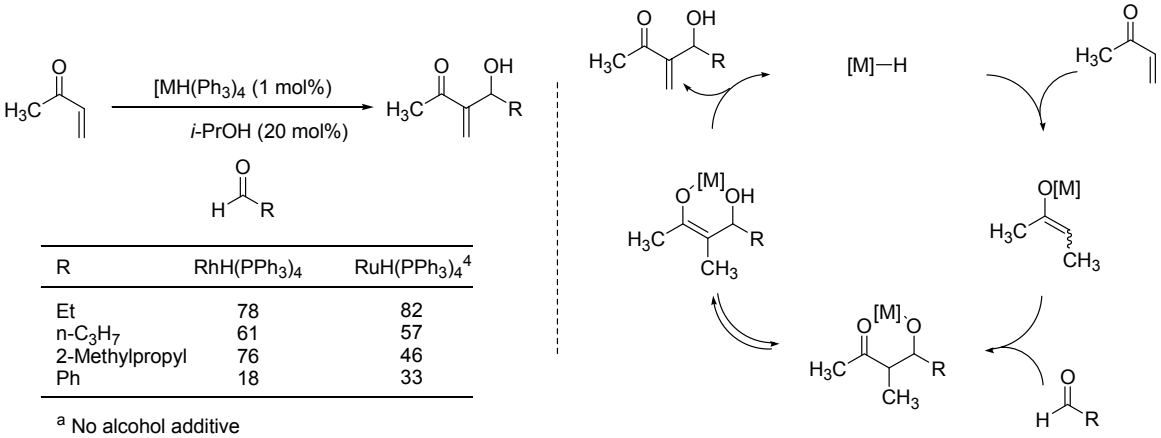

R	$RhH(PPh_3)_4$	$RuH(PPh_3)_4$[4]
Et	78	82
n-C_3H_7	61	57
2-Methylpropyl	76	46
Ph	18	33

[a] No alcohol additive

Scheme 1.30: Reductive coupling of enones and aldehydes to yield Morita-Baylis-Hilman products.

1.4.1 REACTION OF ENONES WITH IMINES (MANNICH REACTION)

In 1912, Carl Mannich realized the synthetic utility of the aminoalkylation of enolizable carbonyl compounds that would latter be named the Mannich reaction.[45] In the classical Mannich reaction an enolizable carbonyl compound is heated in the presence of an amine salt and an aldehyde. The amine salt and aldehyde react to form an iminium salt, which reacts further with the enol tautomer to provide the β-aminocarbonyl product, also called Mannich bases. Mannich bases are useful synthetic building blocks for many biologically significant compounds.

1.4.2 RHODIUM

In 2002, a rhodium catalyzed reductive coupling of enones to imines was reported. A cationic rhodium (I) catalyst, [Rh(COD){P(OPh_3)$_2$}]OTf, was used with Et_2MeSiH as the terminal reductant.[46] Reaction of the rhodium catalyst and the silane provide a rhodium hydride, which hydrometallates the enone to give a rhodium enolate. The rhodium enolate adds to the aldimine to generate the Mannich product. This reaction proceeded with good yield and modest selectivity (Scheme 1.31).

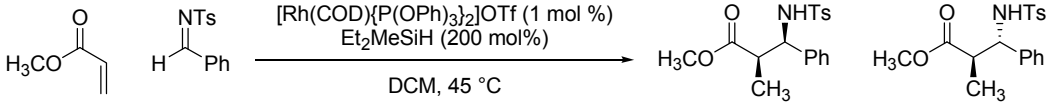

96% Yield
32:68 syn:anti

Scheme 1.31: Rhodium catalyzed Mannich reaction mediated by silanes.

The reductive Mannich coupling reactions of enones mediated by silane support the feasibility of developing a hydrogen-mediated variant. The use of hydrogen gas as the terminal reductant is completely atom economical and cost effective, because hydrogen gas is cheapest reductant known. Exposure of an enone and *N*-sulfonylimine to an atmosphere of hydrogen gas in the presence of a tri-2-furylphosphine ligated rhodium catalyst provides the desired Mannich addition product with good levels of *syn*-diastereoselectivity (Scheme 1.32).[47] Based on some mechanistic studies it is believed that this transformation proceeds by either Mechanism **C** or **D** as described in Scheme 1.7.

Scheme 1.32: Rhodium catalyzed Mannich reaction mediated by hydrogen gas.

1.4.3 IRIDIUM

Mannich bases are good synthetic building blocks for β-lactams as demonstrated in the 2002 report of an iridium catalyzed reductive coupling of aldimines and acrylates.[48] In this report Mannich addition followed by cyclization provides trans β-lactams with high levels of diastereoselectivity. It was found *via* an arrayed catalyst evaluation protocol that the optimal catalyst, ligand, and silane combination was $[(COD)IrCl]_2$,

$P(OPh)_3$, and Et_2MeSiH. Under these conditions a number of *trans*-β-lactams were produced in modest yield with good diastereoselectivity (Scheme 1.33).

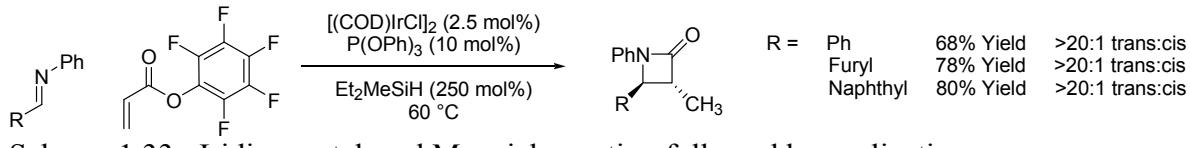

Scheme 1.33: Iridium catalyzed Mannich reaction followed by cyclization.

There are two plausible mechanisms for this transformation (Scheme 1.34). Cycle **E** depicts the same type of mechanism as described previously, *in situ* generation of an iridium hydride followed by hydrometallation of the acrylate. The iridium enolate is then trapped by the imine to furnish the Mannich addition product. The Mannich addition reaction proceeds *via* a boat-like transition state. The final product is obtained by the cyclization of the Mannich base. In Cycle **F** the iridium enolate is converted to a methyl ketene which engages the imine in a [2 + 2] cycloaddition reaction. Though both mechanisms are possible, it is believed that the reaction probably follows Cycle **E**. Due to the fact that a similar methyl ketene [2 + 2] cycloaddition reaction proceeds with only 3:1 *trans:cis* selectivity not the >20:1 *trans:cis* selectivity obtained by this transformation.

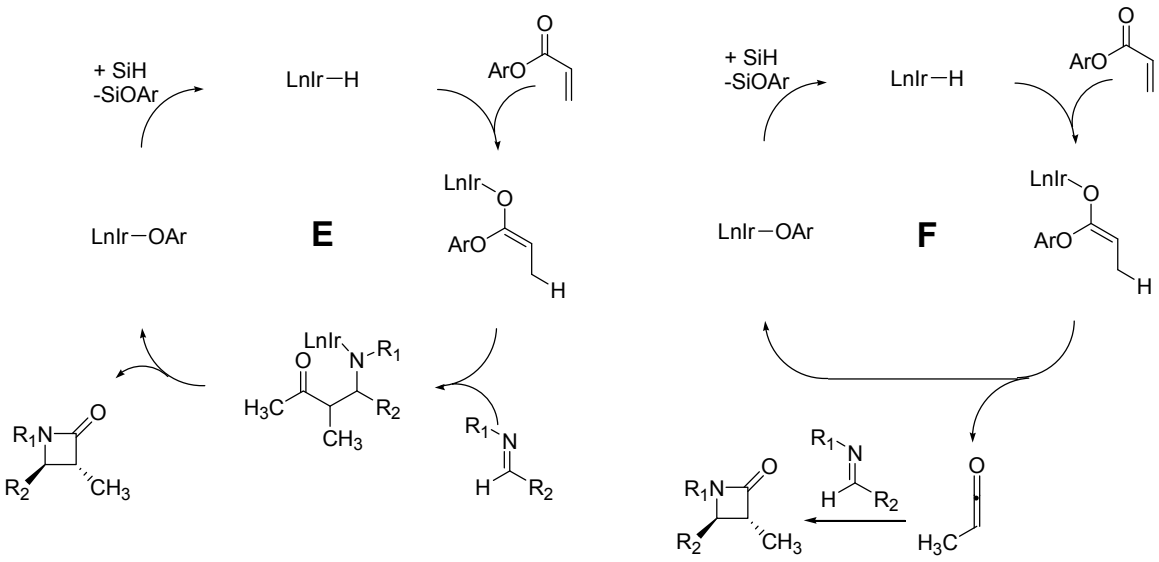

Scheme 1.34: Plausible mechanism for Iridium catalyzed Mannich reaction followed by cyclization.

1.5.1 Reaction of Enones with Michael Acceptors (Michael Reaction)

In 1894, Michael developed the reaction of enolates adding to the β position of an α,β-unsaturated carbonyl compound to make a new C-C bond.[49] Since this time much interest has been directed to this method of C-C bond formation. The number of Michael acceptors has been increased from just α,β-unsaturated carbonyl compounds to include other α,β-unsaturated carbonyl compound equivalents such as: α,β-unsaturated nitriles and nitro compounds. Recent work in this field has been focused on the reductive generation an enolate from an enone, and then the enolate is trapped by the Michael acceptor to provide a new C-C bond.

1.5.2 Cobalt

In 2002, a cobalt catalyzed reductive Michael process was reported that used a phenylsilane as the terminal reductant.[23] This work was an extension of the previously described cobalt catalyzed reductive aldol reaction (Scheme 1.16). This is the first catalytic system for reductive Michael condensation reactions, where α,β-coupling products were obtained. Both 5- and 6-membered rings are formed in good yields with complete diastereoselection. Aryl- and heteroaryl-substituted enones serve as the pronucleophilic partners. It is believed that the Michael cycloreduction reaction proceeds by the hydrometallation of the enone by a low-valent cobalt hydride, which is generated by the reaction of the cobalt (II) catalyst and phenylsilane. The hydrometallation generates an oxy-π-allyl, which is a mesomeric form of the enone anion radical. Another interesting piece about this methodology is that the choice a silane is critical. Exposure of the bis(enone) to $Co(dpm)_2$ (dpm = dipivaloymethane) in the presence of phenylsilane gives the reductive Michael cyclization product, whereas the use of phenylmethylsilane promotes formation of the [2 + 2] cycloadduct (Scheme 1.35). Mechanistic studies of the metal catalyzed [2 +2] cycloaddition reaction reveal that the reactive intermediate is an anion radical.[50]

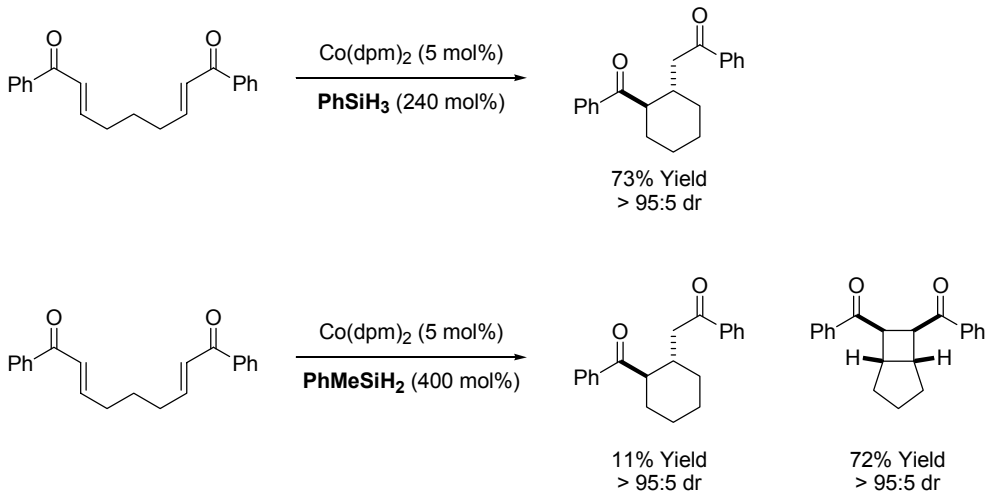

Scheme 1.35: Cobalt catalyzed reductive Michael reaction.

1.5.3 NICKEL

In contrast to the cobalt catalyzed reductive Michael reactions, Nickel catalyzed reductive coupling of bis(enones) provides the β,β-coupling product and a bicyclic product arising from aldol cyclization.[51] This methodology is also applied to the reductive cyclization of enones to dienes. At this time the mechanistic details are uncertain, but it is believed that a nickel-hydride plays a role. Due to the fact that organozincs possessing β-hydrogens are required in order to suppress competitive simple reduction (Scheme 1.36).

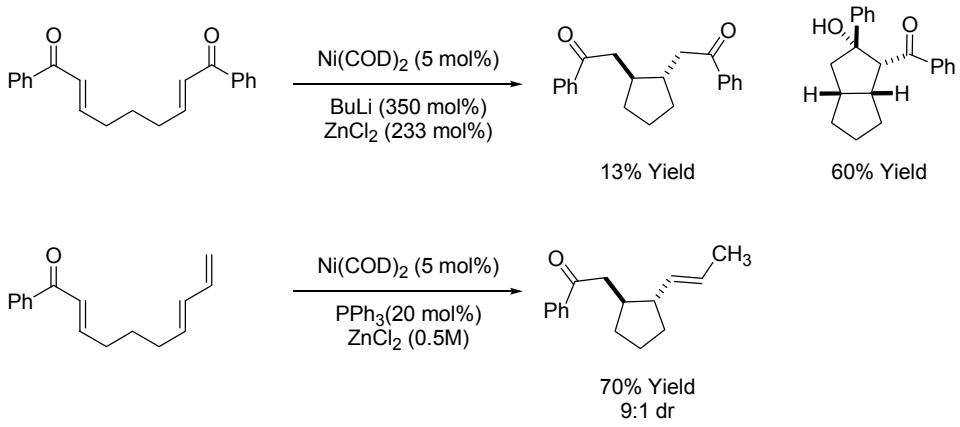

Scheme 1.36: Nickel catalyzed reductive cyclization of enones tethered to enones and dienes.

1.5.4 INDIUM

Another entry into the reductive Michael cyclization reaction is an indium (III) acetate catalyzed reductive coupling of bis(enones).[31b] This methodology discussed previously (Scheme 1.29) proceeds with good yield and excellent *trans* selectivity (Scheme 1.37).

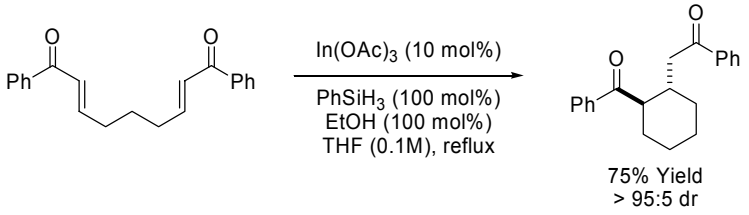

Scheme 1.37: Indium catalyzed Michael cyclization.

1.6.1 Reactions of Enones with Allylic Carbonates (Formal Hydroallylation)

1.6.2 Rhodium

Three component coupling reactions mediated by rhodium catalysts and silane reductants have found application in a number of reaction classes; another application is the coupling of enones and allylic carbonates to afford products of formal hydroallylation (Scheme 1.38).[52] The formal hydroallylation provides coupling exclusively at the α-carbon, but discrimination between allylic termini is case dependent. For linear allylic carbonates very little regioselectivity is observed.

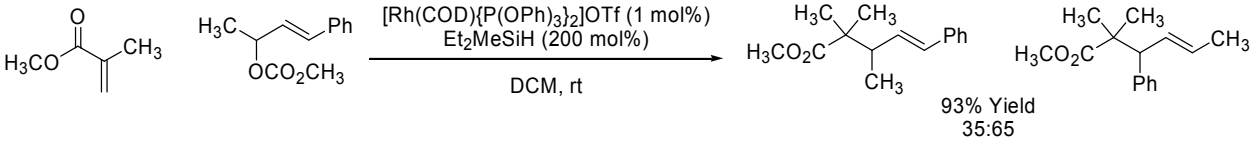

Scheme 1.38: Rhodium catalyzed hydroallylation of α,β-unsaturated carbonyl compounds.

One plausible mechanism for this transformation is shown in Scheme 1.39. It is well established that the first step is oxidative addition of the hydrosilane to the cationic rhodium (I) metal. Hydrometallation of the rhodium hydride to the enone provides the rhodium enolate. The reaction between the rhodium enolate and the allylic carbonate provides a η^3-allyl rhodium enolate and methyl trialkylsilyl carbonate as products. Reaction of the enolate and the π-allyl provides the mixture of products and a rhodium complex; which reacts with another molecule of hydrosilane to generate the active

catalyst. At the present time this transformation needs more fine tuning in order to make is synthetically useful, but it offers advantages over classical methods of allylation of enolates[53] and allylation of enoxysilanes.[54]

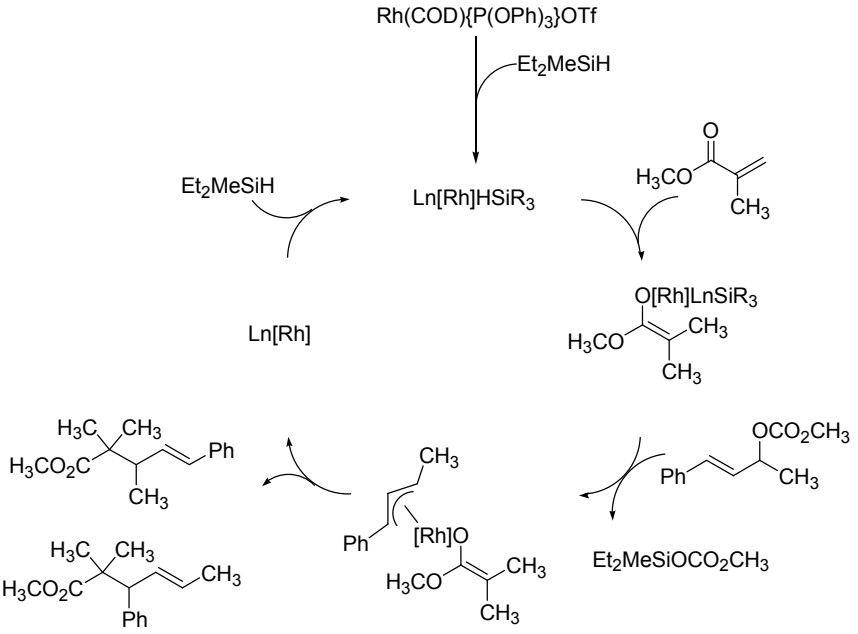

Scheme 1.39: Plausible catalytic cycle for rhodium catalyzed hydroallylation of α,β-unsaturated carbonyl compounds.

1.7.1 Reactions of Enones with Aryl Isocyanates (Formal Hydrocarbamoylation)

1.7.2 Rhodium

In 2001, it was discovered that aryl isocyanates are viable electrophiles to react with rhodium enolates providing products of formal hydrocarbamoylation.[55] This transformation is selective for the coupling of the central carbon of the isocyanate with the α-carbon of the enone. A variety of aryl isocyanates participated in this reaction, but

alkyl isocyanates are not reactive enough. The products of formal hydrocarbamoylation are obtained in good to excellent yield (Scheme 1.40).

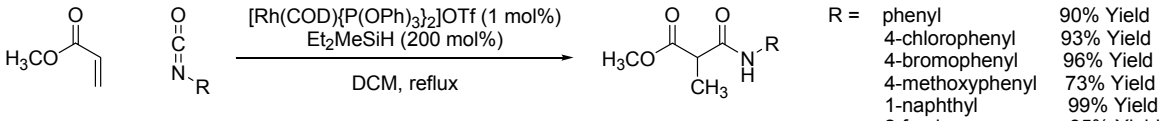

Scheme 1.40: Rhodium catalyzed formal hydrocarbamoylation of α,β-unsaturated esters.

A plausible mechanism for this transformation is shown in Scheme 1.41. Starting with a cationic rhodium (I) catalyst oxidative addition with the hydrosilane provides the rhodium hydride, which adds to the α,β-unsaturated carbonyl compounds to give an enolate. The next step addition of the enolate to the central carbon of the isocyanate. Reductive elimination provides the silyl imidate and the rhodium hydride catalyst is regenerated by oxidative addition of the hydrosilane. The final product is generated from the silyl imidate during workup.

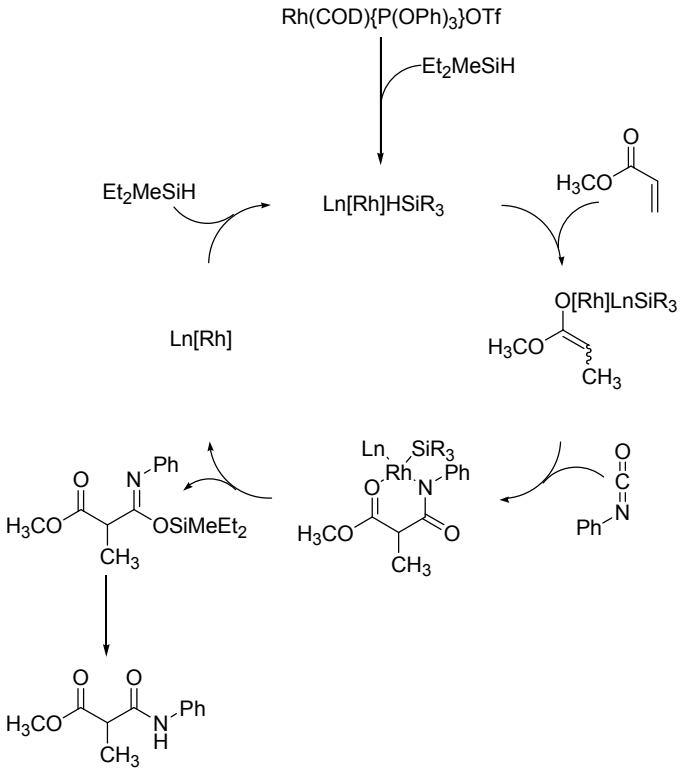

Scheme 1.41: Possible mechanism for the rhodium catalyzed formal hydrocarbamoylation of α,β-unsaturated esters.

1.8.1 Reactions of Enones with Allylic Esters (Claisen Rearrangement)

1.8.2 Rhodium

The claisen rearrangement is a useful synthetic tool for the construction of C-C bonds. One limitation is the necessity for the performation of the enolate with a stoichiometic amount of a strong base. The ability to catalytically generate an enolate under neutral conditions has enabled the development of a catalytic reductive claisen rearrangement.[56] This reaction proceeds by the use of a rhodium catalyst, $[(COD)RhCl]_2$, and Cl_2MeSiH as the terminal reductant. Previous work had established that reaction of

the rhodium catalyst, Cl_2MeSiH, and α,β-unsaturated ester would generate a *E*-silylketene acetals.[21d] Obtaining a single alkene isomer is critical for the control of the stereoselectivity for the reductive claisen. Another important factor is that the pendant alkene is not hydrosilated before the acrylate. Table 1.1 shows some examples from this body of work. The geometry of the appendant alkene dictates the stereochemistry of the product, notice entry 1 the *trans* alkene provides the *anti* diastereomer as the major product in 74% yield. The *cis* alkene (entry 2) gives the *syn* product as the major diastereomer in 49% yield. Trisubstituted alkenes are viable substrates (entry 3). Also all-carbon quaternary centers can be made *via* this methodology. Another interesting example is entry 4 under these conditions the reductive claisen product is obtained, indicating that formation of the *E*-silylketene acetal occurs faster than the formation of a rhodium-π-allyl.[52]

Table 1.1: Rhodium catalyzed reductive Claisen rearrangement.

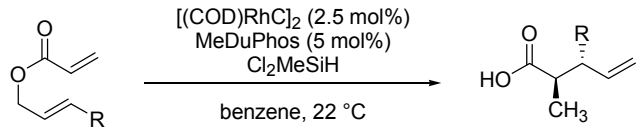

Entry	Substrate	Product	%Yield	dr
1	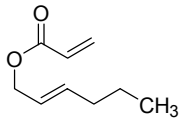	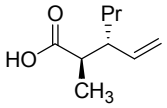	74%	11:1
2	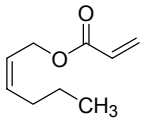	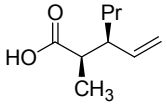	49%	23:1
3	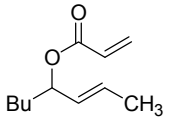	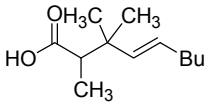	74%	na
4	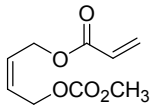	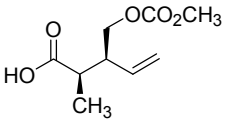	45%	>25:1

1.9.1 REACTIONS OF ENONES WITH ALKYNES

1.9.2 RHODIUM

Described previously, elemental hydrogen can replace other hydride sources in the reductive aldol and reductive mannich reactions, thus providing a completely atom economical process.[22, 47, 57] It was also discovered that the reductive cyclization of acetylenic enones could be mediated by elemental hydrogen and a cationic rhodium catalyst.[58] The reductive cyclization of 1,6-enynes proceeded readily at ambient temperature and pressure to afford cyclized products in good yield and excellent enantioselectivity. The product of this transformation contains an alkene (Scheme 1.42), and notice that over-hydrogenation is not observed. It is believed that the mechanism for

this transformation proceeds by the oxidative coupling of the alkyne and alkene, followed by hydrogenolytic cleavage *via* sigma bond metathesis (Scheme 1.7, Mechanism **C**).

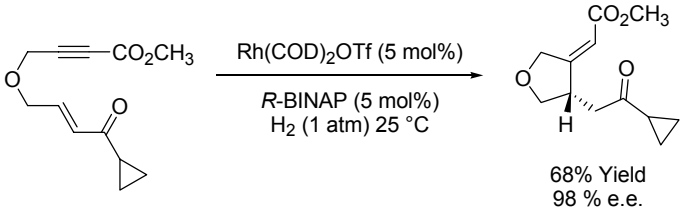

Scheme 1.42: Enantioselective rhodium catalyzed reductive cyclization of acetylenic enones.

1.8.3 NICKEL

Another reductive cyclization of acetylenic enones has been reported that is mediated by nickel catalyst (Scheme 1.43). This transformation uses organozincs possessing β-hydrogens, such as diethylzinc, as the terminal reductant. The reductive cylization product is formed in excellent yield. At this time a detailed reaction mechanism is uncertain. It is thought that the reaction proceeds *via* the intermediacy of a nickel (II) metallacycle.[59]

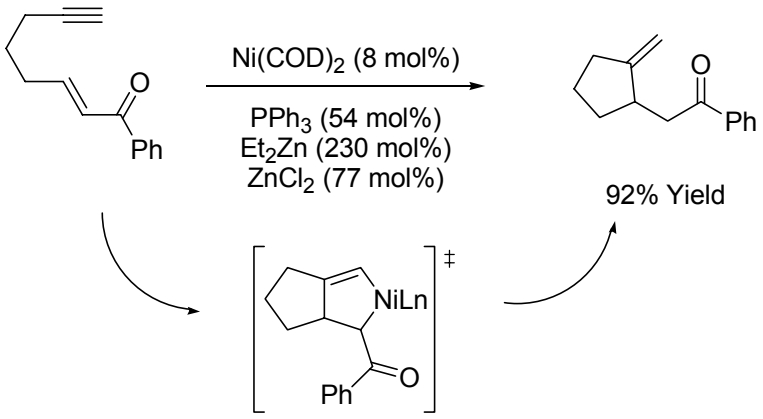

Scheme 1.43: Nickel catalyzed reductive cyclization of acetylenic enones.

1.10.1 CONCLUSIONS

Since the first catalytic reductive coupling to enones was reported in 1987 by Revis,[21a] this field of research has flourished. Many insightful methods for the reductive generation of enolates from α,β-unsaturated carbonyl compounds have been developed, along with a variety of enolate/electrophile combinations. But more work needs to be done in order to overcome current shortcomings such as: the need for stoichiometric silane in many of the transformations. One elegant method that has overcome the need for stoichiometric silane is the use of hydrogen gas as the terminal reductant.[22, 47, 57, 58] This provides a completely atom economical reaction, and hydrogen gas is the cheapest reductant available. Another area of growth will be the development of more enantioselective transformations with the evolution of new chiral phosphines. The synthetic potential of the metal catalyzed reductive coupling to α,β-unsaturated carbonyl compounds is great, but the full potential of this reaction type has yet to be realized.

References:

[1] Though largely attributed to Würtz, the aldol reaction was reported first by Borodin: (a) von Richter, V. *Ber. Deut. Chem. Ges.* **1869**, *2*, 552. (Borodin's earliest results are cited in this article); (b) Würtz, A. *Bull. Soc. Chim. Fr.* **1872**, *17*, 436. (c) Borodin, A. *Ber. Dtsch. Chem. Ges.* **1873**, *6*, 982. See also: Kane, R. *Ann. Phys. Chem., Ser. 2* **1838**, *44*, 475.

[2] (a) Hauser, C. R.; Puterbaugh, W. H. *J. Am. Chem. Soc.* **1951**, *73*, 2972. (b) Hauser, C. R.; Puterbaugh, W. H. *J. Am. Chem. Soc.* **1953**, *75*, 1068. (c) Hauser, C. R.; Lindsay, J. K. *J. Am. Chem. Soc.* **1955**, *77*, 1050. (d) Dunnavant, W. R.; Hauser, C. R. *J. Org. Chem.* **1960**, *25*, 503.

[3] For additional papers on the advancement of enolate generation, see: (a) Wittig, G.; Frommeld, H. D.; Suchanek, P. *Angew. Chem.* **1963**, *75*, 978. (b) Wittig, G.; Reiff, H. *Angew. Chem., Int. Ed. Engl.* **1968**, *7*, 7. (c) Wittig, G. *Rec. Chem. Prog.* **1967**, *28*, 45. (d) Rathke, M. W. *J. Am. Chem. Soc.* **1970**, *92*, 3222. (e) Rathke, M. W.; Lindert, A. *J. Am. Chem. Soc.* **1971**, *93*, 2318. (f) Posner, G. H.; Loomis, G. L. *J. Chem. Soc., Chem. Commun.* **1972**, 892. (g) Ireland, R. E.; Meuller, R. H.; Willard, A. K. *J. Am. Chem. Soc.* **1976**, *98*, 2868.

[4] (a) House H. O.; Czuba, L. J.; Gall, M.; Olmstead, H. D. *J Org. Chem*. **1969**, *34*, 2324. (b) Krafft, M. E.; Holton, R. A. *Tetrahedron Lett*. **1983**, *24*, 1345.

[5] (a) Stork, G.; Rosen, P.; Goldman, N. L. *J. Am. Chem. Soc*. **1961**, *83*, 2965. (b) Stork, G.; Rosen, P.; Goldman, N,; Coombs, R. V.; Tsuji, J. *J. Am Chem Soc*. **1965**, *87*, 275.

[6] For cobalt catalyzed conjugate reduction of α,β-unsaturated carbonyl compounds, see: (a) Leutenegger, U.; Madin, A.; Pfaltz, A. *Angew. Chem*. **1989**, *101*, 61; *Angew. Chem. Int. Ed. Engl*. **1989**, *28*, 60. (b) Misun, M.; Pfaltz, A. *Helv. Chim. Acta*. **1996**, *79*, 961. (c) von Matt, P.; Pfaltz, A. *Tetrahedron: Asymmetry* **1991**, *2*, 691. (d) Yamada, T.; Ohtsuka, Y.; Ikeno, T. *Chem Lett*. **1998**, 1129. (e) Ohtsuka, Y.; Ikeno, T.; Yamada, T. *Tetrahedron: Asymmetry* **2003**, *14*, 967. (f) Geiger, C.; Kreitmeier, P.; Reiser, O. *Adv. Synth. Catal.* **2005**, *347*, 249.

[7] For selected reviews encompassing metal catalyzed conjugate reduction mediated by silanes and borohydrides, see: (a) Keinan, E.; Greenspoon, N. In *Comprehensive Organic Synthesis*; Trost, B. M., Fleming, I., Eds.; Pergamon Press: Oxford, 1991; Vol. 8, Chapter 3.5, p 523. (b) Sibi, M. P.; Manyem, S. *Tetrahedron* **2000**, *56*, 8033. (c) Shibata, I. *Organomet. News* **2004**, *2*, 53. (e) Rendler, S.; Oestreich, M. *Angew. Chem. Int. Ed.* **2007**, *46*, 498.

[8] For selected reviews encompassing metal catalyzed conjugate reduction mediated by hydrogen, see: (a) Haskel, A.; Keinan, E. In *Handbook of Organopalladium Chemistry*

for Organic Synthesis; Negishi, E.-I., Ed.; John Wiley & Sons: New York, 2002; Vol. 2, p 2767. (b) Farina, V.; Reeves, J. T.; Senanayake, C. H.; Song, J. J. *Chem. Rev.* **2006**, *106*, 2734. (c) Jäkel, C.; Paciello, R. *Chem. Rev.* **2006**, *106*, 2912.

[9] For rhodium catalyzed conjugate reduction of α,β-unsaturated carbonyl compounds, see: (a) Ojima, I.; Kogure, T. *Organometallic.* **1982**, *1*, 1390. (b) Evans, D.; Fu, G. *J. Org. Chem*. **1990**, *55*, 5678. (c) Revis, A.; Hilty, T. *J. Org. Chem*. **1990**, *55*, 2972. (d) Tsuchiya, Y.; Kanazawa, Y.; Shiomi, T.; Kobayashi, K.; Nishiyama, H. *Synlett*. **2004**, *14*, 2493. (e) Kanazawa, Y.; Nishiyama, H. *Synlett*. **2006**, *19*, 3343. (f) Kanazawa, Y.; Tsuchiya, Y.; Kobayashi, K.; Shiomi, T.; Itoh, J.; Kikuchi, M.; Yamamoto, Y.; Nishiyama, H. *Chem. Eur. J.* **2006**, *12*, 63.

[10] For copper catalyzed conjugate reduction of α,β-unsaturated carbonyl compounds, see: (a) Mahoney, W. S.; Stryker, J. M. *J. Am .Chem. Soc*. **1989**, *111*, 8818. (b) Appella, D. H.; Moritani, Y.; Shintani, R.; Ferreira, E. M.; Buchwald, S. L. *J. Am. Chem. Soc*. **1999**, *121*, 9473. (c) Moritani, Y.; Appella, D. H.; Jurkauskas, V.; Buchwald, S. L. *J. Am. Chem. Soc*. **2000**, *122*, 6797. (d) Hughes, G.; Kimura, M.; Buchwald, S. L. *J. Am. Chem. Soc*. **2003**, *125*, 11258. (e) Lipshutz, B. H.; Keith, J.; Papa, P. P.; Vivian, R. *Tetrahedron Lett*. **1998**, *39*, 4627. (f) Lipshutz, B. H.; Servesdo, J. M. *Angew. Chem. Int. Ed*. **2003**, *42*, 4789. (g) Lipshutz, B. H.; Servesdo, J. M.; Petersen, T. B.; Papa, P. P.; Lover, A. A. *Org. Lett*. **2004**, *6*, 1273. (h) Lipshutz, B. H.; Servesdo, J. M.; Taft, B. R. *J. Am. Chem. Soc*. **2004**, *126*, 8352. (i) Lipshutz, B. H.; Frieman, B. A.; Tomaso, A. E. *Angew. Chem. Int. Ed*. **2006**, *45*, 1259.

[11] For palladium catalyzed conjugate reduction of α,β-unsaturated carbonyl compounds, see: (a) Keinan, E.; Greenspoon, N. *J. Am. Chem. Soc*. **1986**, *108*, 7314. (b) Tsuchiya, Y.; Hamashima, Y.; Sodeoda, M. *Org. Lett*. **2006**, *8,* 4851.

[12] For platinum catalyzed conjugate reduction of α,β-unsaturated carbonyl compounds, see: Johnson, C. R. and Raheja, R. K. *J. Org. Chem*. **1994**, *59*, 2287.

[13] For reviews encompassing general physical organic and stereochemical principles associated with the aldol reaction, see: (a) Evans, D.A.; Nelson, J. V.; Taber, T. R.; *Topics of Stereochemistry.* **1982**, *13*, 1. (b) Heathcock, C. H.; *ACS Symp Ser*. **1982**, *185*, 55. (c) Heathcock, C. H. *Asymmetic Synthesis* **1984**, *3*, 111. (d) Heathcock C. H. In: *Comprehensive Organic Synthesis*. Trost B. M., Fleming, I.; Heathcock C. H. (eds) New York. **1991**, Vol. *2*, p 181.

[14] For selected reviews encompassing recent developments in catalytic aldol coupling, see: (a) Machajewski, T. D.; Wong, C.-H. *Angew. Chem. Int. Ed.* **2000**, *39*, 1352. (b) Palomo, C.; Oiarbide, M.; García, J. M. *Chem. Eur. J.* **2002**, *8*, 36. (c) Palomo, C.; Oiarbide, M.; García, J. M. *Chem. Soc. Rev.* **2004**, *33*, 65. (d) Schetter, B.; Mahrwald, R. *Angew. Chem., Int. Ed.* **2006**, *45*, 7506.

[15] For a recent review on the use of metallic catalysts for direct enantioselective aldol additions, see: Shibasaki, M.; Matsunaga, S.; Kumagai, N. In *Modern Aldol Reactions*; Mahrwald, R., Ed.; Wiley-VCH: Weinheim, 2004; Vol. 2, Chapter 6.

[16] For a recent review on the use of organic catalysts for direct enantioselective aldol addition, see: List, B. In *Modern Aldol Reactions;* Mahrwald, R., Ed.; Wiley-VCH: Weinheim, 2004; Vol. 1, Chapter 4.

[17] Sakthivel, K.; Notz, W.; Bui, T.; Barbas, C. F., III *J. Am. Chem. Soc.* **2001**, *123*, 5260.

[18] Using amides of L-proline, direct catalyzed aldol coupling of 2-butanone to *p*-nitrobenzaldehyde affords mixtures of regioisomeric products: Tang, Z.; Yang, Z.-H.; Chen, X.-H.; Cun, L.-F.; Mi, A.-Q.; Jiang, Y.-Z.; Gong, L.-Z. *J. Am. Chem. Soc.* **2005**, *127*, 9285.

[19] Yoshikawa, N.; Yamada, Y. M. A.; Das, J.; Sasai, H.; Shibasaki, M. *J. Am. Chem. Soc.* **1999**, *121*,4168.

[20] For reviews encompassing the topic of reductive aldol coupling, see: (a) Motherwell, W. B. *Pure Appl. Chem.* **2002**, *74*, 135. (b) Huddleston, R. R.; Krische, M. J. *Synlett* **2003**, 12. (c) Jang, H.-Y.; Huddleston, R. R.; Krische, M. J. *Chemtracts* **2003**, *16*, 554. (d) Jang, H.-Y.; Krische, M. J. *Eur. J. Org. Chem.* **2004**, *19*, 3953. (e) Jang, H.-Y.; Krische, M. J. *Acc. Chem. Res.* **2004**, *37*, 653. (f) Chiu, P. *Synthesis*, **2004**, 2210. (g) Nishiyama, H.; Shiomi, T. *Topp. Curr. Chem.* In Press.

[21] For rhodium catalyzed reductive aldol reaction mediated by silane or other reductants see: (a) Revis, A.; Hilty, T. K. *Tetrahedron Lett*. **1987**, *28*, 4809. (b) Matsuda, I.; Takahashi, K.; Sato, S. *Tetrahedron Lett*. **1990***, 31*, 5331. (c) Taylor, S. J.; Morken, J. P. *J. Am. Chem. Soc.* **1999,** *121,* 12202. (d) Zhao, C.-X.; Bass, J.; Morken, J. P. *Org Lett*. **2001**, *3*, 2839. (e) Taylor, S. J.; Duffey, M. O.; Morken, J. P. *J. Am. Chem. Soc.* **2000**, *122,* 4528. (f) Fuller, N. O.; Morken, J.P. *Synlett*. **2005**, 1459. (g) Emiabata-Smith, D.; McKillop, A.; Mills, C.; Motherwell, W. B.; Whitehead, A. J. *Synlett*. **2001**, 1302. (h) Freiría, M.; Whitehead, A. J.; Tocher, D. A.; Motherwell, W. B. *Tetrahedron*. **2004**, *60*, 2673. (i) Nishiyama, H.; Shiomi, T.; Tsuchiya, Y.; Matsuda, I. *J. Am. Chem. Soc*. **2005**, *127*, 6972. (j) Ito, J. I.; Shiomi, T.; Nishiyama, H. *Adv. Synth. Catal*. **2006**, *348*, 1235. (k) Shiomi, T.; Ito, J.-I.; Yamamoto, Y.; Nishiyama, H. *Eur, J. Org. Chem.* **2006**, 5594. (l) Willis, M. C.; Woodward, R. L. *J. Am. Chem. Soc*. **2005**, *127*, 18012.

[22] For rhodium catalyzed reductive aldol reaction mediated by hydrogen, see: (a) Jang, H.Y.; Huddleston, R. R.; Krische, M. J. *J. Am. Chem. Soc*. **2002** *124*, 15156. (b) Huddleston, R. R.; Krische, M. J.; *Org. Lett*. **2003,** *5,* 1143. (c) Koech, P. K.; Krische, M. J. *Org. Lett*. **2004**, *6,* 691. (d) Marriner, G. A.; Garner, S. A.; Jang, H. Y.; Krische, M. J. *J. Org. Chem.* **2004,** *69*, 1380. (e) Jung, C. K.; Garner, S. A.; Krische, M. J. *Org. Lett*.

2006, *8*, 519. (f) Han, S. B.; Krische M. J. *Org. Lett*. **2006,** *8*, 5657. (g) Jung, C. K.; Krische, M, J. *J. Am. Chem. Soc.* **2006**, *128*, 17051.

[23] For cobalt catalyzed reductive aldol reaction, see: (a) Isayama. S.; Mukaiyama, T. Chem. *Lett.* **1989**, 2005. (b) Baik, T. G.; Luis, A. L.; Wang, L. C.; Krische, M. J. *J. Am. Chem. Soc.* **2001**, *123*, 5112. (c) Wang, L. C.; Jang, H.-Y.; Roh, Y.; Lynch, V.; Schultz, A. J.; Wang, X.; Krische, M. J. *J. Am. Chem. Soc.* **2002,** *124*, 9448. (d) Lam, H. W.; Joensuu, P. M.; Murray, G. J.; Fordyce, E. A. F.; Prieto, O.; Luebbers, T. *Org. Lett*. **2006**, *8*, 3729.

[24] For iridium catalyzed reductive aldol reaction, see: (a) Zhao. C. X.; Duffey, M. O.; Taylor, S. J.; Morken, J. P. *Org. Lett*. **2001**, *3*, 1829.

[25] For ruthenium catalyzed reductive aldol reaction, see: Doi, T.; Fukuyama, T.; Minamino, S.; Ryu, I. *Synlett* **2006**, *18*, 3013.

[26] For palladium catalyzed reductive aldol reaction, see: (b) Kiyooka, S. I.; Shimizu, A.; Torii, S. *Tetrahedron Lett* **1998**, *39*, 5237.

[27] For copper promoted reductive aldol reaction, see: (a) Chiu, P.; Chen, B.; Cheng, K. F. *Tetrahedron Lett*. **1998**, *39*, 9229. (b) Chiu, P. *Synthesis* **2004**, *13*, 2210. (c) For copper promoted reductive intramolecular Henry reaction, see: Chung, W. K.; Chiu, P. *Synlett* **2005**, *1*, 55. (d) For copper promoted and catalyzed reductive cyclizations of ąb-acetylenic ketones tethered to ketones, see: Chiu, P.; Leung, S. K. *Chem. Commun*. **2004**, 2308.

[28] For copper catalyzed reductive aldol reaction, see: (a) Lipshutz, B. H.; Chrisman, W.; Noson, K.; Papa, P.; Sclafani, J. A.; Vivian, R. W.; Keith, J. M. *Tetrahedron* **2000**, *56*, 2779. (b) Ooi. T.; Doda, K.; Sakai, D.; Maruoka, K.; *Tetrahedron Lett*. **1999**, *40*, 2133. (c) Lam, H. W.; Joensuu, P. M. A. *Org. Lett*. **2005**, *7*, 4225. (d) Lam, H. W.; Murray, G. J.; Firth, J. D. *Org Lett* **2005**, *7*, 5743. (e) Deschamp, J.; Chuzel, O.; Hannedouche, J.; Riant, O. *Angew. Chem. Int. Ed*. **2006**, *45*, 1292. (f) Chuzel, O.; Deschamp, J.; Chauster, C.; Riant, O. *Org. Lett.* **2006**, 8, 5943. (g) Zhao, D.; Oisaki, K.; Kanai, M.; Shibasaki, M. *Tetrahedron Lett.* **2006**, *47*, 1403. (h) Zhao, D.; Oisaki, K.; Kanai, M.; Shibasaki, M. *J. Am. Chem. Soc*. **2006**, *128,* 14440. (i) Welle, A; Diez-Gonzalez, S.; Tinant, B.; Nolan, S. P.; Riant, O. *Org. Lett.* **2006**, 8, 6059.

[29] For nickel catalyzed reductive aldol reaction, see: Chrovian, C. C.; Montgomery, J. *Org Lett.* **2007**, *9*, 537.

[30] For a reductive aldol coupling employing stoichiometric quantities of indium reagent, see: Inoue, K.; Ishida, T.; Shibata, I.; Baba, A. *Adv. Synth. Catal.* **2002**, 344, 283.

[31] For indium catalyzed reductive aldol reaction, see: (a) Shibata, I.; Kato, H.; Ishida, T.; Yasuda, M.; Baba, A. *Angew. Chem. Int. Ed*. **2004**, *43*, 711. (b) Miura, K.; Yamada, Y.; Tomita, M.; Hosomi, A. *Synlett* **2004**, 1985.

[32] Slough, G. A.; Bergman, R. C.; Heathcock, C. H. *J. Am. Chem. Soc.* **1989**, *111*, 938.

[33] Wright, M. E.; Cochran, B. B. *J. Am. Chem. Soc.* **1993**, *115*, 2059.

[34] For tri-2-furylphosphine and triphenylarsine effects in metal catalyzed reactions, see: (a) Farina, V.; Krishnan, B. *J. Am. Chem. Soc.* **1991**, *113*, 9585. (b) Farina, V. *Pure Appl. Chem.* **1996**, *68*, 73. (c) Anderson, N. G.; Keay, B. A. *Chem. Rev.* **2001**, *101*, 997.

[35] Zimmerman, H. E.; Traxler, M. D. *J. Am. Chem. Soc*. **1957**, *79*, 1920.

[36] For mechanistic studies on alkene hydrogenation catalyzed by neutral Rh(I) complexes, see: (a) Tolman, C. A.; Meakin, P. Z.; Lindner, D. L.; Jesson, J. P. *J. Am. Chem. Soc.* **1974**, *96*, 2762. (b) Halpern, J.; Wong, C. S. *Chem. Commun.* **1973**, 629. (c) Halpern, J.; Okamoto, T.; Zakhariev, A. *J. Mol. Catal.* **1976**, *2*, 65.

[37] Monohydride catalytic cycles initiated *via* deprotonation of cationic rhodium dihydrides have been postulated and their veracity further established through the stoichiometric conversion of cationic rhodium(I) complexes to the corresponiding rhodium(I) monohydrides via expsoure to hydrogen in the presence of a tertiary amine base: (a) Schrock, R. R.; Osborn, J. A. *J. Am. Chem. Soc.* **1976**, *98*, 2134. (b) Schrock, R. R.; Osborn, J. A. *J. Am. Chem. Soc.* **1976**, *98*, 2143. (c) Schrock, R. R.; Osborn, J. A. *J. Am. Chem. Soc.* **1976**, *98*, 4450.

[38] For a review of the acidity of metal hydrides, see: "Acidity of Hydrido Transition Metal Complexes in Solution," J. R. Norton, In *Transition Metal Hydrides*; Dedieu, A. Ed., New York, 1992, Chapter 9.

[39] Alcaide, B.; Almendros, P. *Angew. Chem. Int. Ed*. **2003**, *42*, 858.

[40] (a) Denmark, S.; Ghosh, S. K. *Angew. Chem. Int. Ed.* **2001**, *40*, 4759. (b) Northrup, A. B.; MacMillan, D. W. C. *J. Am. Chem. Soc.* **2002**, *124*, 6798. (c) Pidathala, C.; Hoang, L.; Vignola, N.; List, B. *Angew. Chem. Int. Ed.* **2003**, *42*, 2785.

[41] For a review ecompassing single electron oxidative addition, see: Halpern, J. *Acc. Chem. Res.* **1970**, *3*, 386.

[42] Socol, S. M.; Verkade, J. G. *Inorg. Chem.* **1986**, *25*, 2658 and references therein.

[43] (a) Boldrini, G. P.; Mancini, F.; Tagliavini, E.; Trombini, C.; Umani-Ronchi, A. *J. Chem. Soc. Chem. Commun.* **1990**, 1680. (b) Boldrini, G. P.; Bortolotti, M.; Mancini, F.; Tagliavini, E.; Trombini, C.; Umani-Ronchi, A. *J. Org. Chem.* **1991**, *56*, 5820.

[44] (a) Sato, S.; Matsuda, I.; Izumi, Y. *Chem. Lett*. **1985**, 1875. (b) Matsuda, I.; Shibata, M.; Sato, S. *J. Organomet.Chem*. **1988**, *340*, C5. (c) Sato, S.; Matsuda, I.; Shibata, M.; *J. Organomet.Chem*. **1989**, *377*, 347.

[45] Mannich, C.; Krosche, W. Arch. Pharm. **1912**, 250, 647.

[46] Moraoka, T.; Kamiya, S.; Matsuda, I.; Itoh, K. *Chem. Comm*. **2002**, 1284.

[47] Garner, S. A.; Krische, M. J. Manuscript in Preparation.

[48] Townes, J.; Evans, M. Queffelec, J. Taylor, S. J. Morken, J. P. *Org. Lett.* **2002**, *4*, 2537.

[49] Michael, A. *J. Prakt. Chem.* **1887**, *36*, 349-356; ibid., **1894**, *49*, 20. Kohler. *J. Am. Chem. Soc.* **1907**, *37*, 385; ibid., **1935**, *57*, 1316.

[50] For mechanistic studies establishing anion radical chain cyclobutanation of bis(enones), see: (a) Roh, Y.; Jang, H. –Y.; Bauld, N. L.; Krische, M. J. *Org. Lett*. **2002**, *4*, 611. (b) Yang, J.; Felton, G. A. N.; Bauld, N. L.; Krische, M. J. *J. Am. Chem. Soc*. **2004**, *126*, 1634. (c) Yang, J.; Cauble, D. C.; Berro, A. J.; Bauld, N. L.; Krische, M. J. *J. Org. Chem*. **2004**, *69*, 7979.

[51] (a) Savchenko, A.; Montgomery, J. *J. Org. Chem*. **1996**, *61*, 1562. (b) Montgomery, J.; Oblinger, E.; Savchenko, A. *J. Am. Chem. Soc*. **1997**, *119*, 4911. (c) Montgomery, J.; Chevliakov, M. V.; Brielmann, H. L. *Tetrahedron*, **1997**, *53*, 16449. (d) Seo, J.; Fain, H.; Blanc, J. –B.; Montgomery, J. *J. Org. Chem*. **1999**, *64*, 6060.

[52] Muraoka, T.; Matsuda, I.; Itoh, K. *J. Am. Chem. Soc*. **2000**, *122*, 9552.

[53] (a) Kazmaier, U.; Zumpe, F. L. Angew. Chem. Int. Ed. Engl. 2000, 39, 802. (b) Tsuji, J. Palladium Reagents and Catalysts; John Wiley & Sons: New York, 1995, and references therein.

[54] (a) Malkov, A. V.; Baxendale, I. R.; Dvorák, D.; Mansfield, D. J.; Kocovsky, P. J. Org Chem. 1999, 64, 2737. (b) Tsuji, J.; Takahashi, K.; Minami, I.; Shimizu, I. Tetrahedron Lett. 1984, 25, 1325. (c) Reetz, M. T. Angew. Chem. Int. Ed. Engl. 1982, 21, 96 and references therein.

[55] Muraoka, T.; Matsuda, I.; Itoh, K. *Organometallics* **2001**, *20*, 4676.

[56] Miller, S. P.; Morken, J. P. *Org. Lett*. **2002**, *4*, 2743.

[57] For reviews on hydrogen-mediated C-C bond formation see: (a) Jang, H. –Y.; Huddleston, R. R.; Krische, M. J. *Chemtracts* **2003**, *16*, 554. (b) Jang, H. –Y.; Krische, M. J. *Eur. J. Org. Chem.* **2004**, 3953. (c) Jang, H. –Y.; Krische, M. J. *Acc. Chem. Res*. **2004**, *37*, 653.

[58] (a) Jang, H. –Y.; Krische, M. J. *J. Am. Chem. Soc*. **2004**, *126*, 7875. (b) Jang, H. –Y.; Hughes, F. W.; Gong, H.; Zhang, J.; Brodbelt, J. S.; Krische, M. J. *J. Am. Chem. Soc*. **2005**, *127*, 6174.

[59] Amarsinghe, K. K. D.; Chowdhury, S. K.; Heeg, M J.; Montogomery, J. *Organometallics*. **2001**, *20*, 370.

CHAPTER 2. HYDROGEN-MEDIATED CARBON-CARBON BOND FORMATION

2.1 INTRODUCTION

Catalytic hydrogenation of alkenes is one of the oldest and most utilized organic reactions. The addition of the molecular hydrogen to an alkene can be accomplished *via* the use of transition metal catalysis such as: iridium, nickel, palladium, platinum, rhodium and ruthenium.[1] Paul Sabatier reported the first catalytic hydrogenation. He used fine nickel particles as heterogeneous catalysts to accomplish the reduction of benzene to cyclohexane.[2] Another historic breakthrough came about in the 1960s when Wilkinson developed chlorotris(triphenylphosphine) rhodium, $[RhCl(PPh_3)_3]$.[3] For the first time, a homogeneous hydrogenation catalyst was able to achieve the same reactivity as other heterogeneous catalysts. Soon after, Knowles had the idea to combine Wilkinson's catalyst with the use of chiral phosphanes in order to create a chiral environment around the metal center. The result was the first asymmetric homogeneous hydrogenation that he used in his synthesis of L-DOPA.[4]

At the present time catalytic asymmetric hydrogenation is the leading catalytic asymmetric process used in industry. In fact, over half of the chiral compounds produced industrially that are not made by resolution are made *via* asymmetric hydrogenation.[5] This is due to two reasons: (1) Knowles' catalytic asymmetric hydrogenation was the first highly enantioselective process available to the chemical community and (2) The efficiency of catalytic hydrogenation makes it an attractive process for industry. In catalytic hydrogenation there are no stoichiometric byproducts and hydrogen gas is

cheap, ($0.02 / mole). Even though catalytic hydrogenation has been practiced for over a century, the full synthetic potential of this transformation has not been realized.

The first carbon-carbon bond forming hydrogenation involved the migratory insertion of carbon monoxide into alkenes, known as alkene hydroformylation[6] (Fischer-Tropsch Reaction).[7] Currently the Fischer-Tropsch process is the largest volume application of homogeneous metal catalysis, and this process is used to produce over 7 million metric tons of aldehydes annually (Scheme 2.1). The Fischer-Tropsch reaction is a very powerful process, but it does have one limitation, it is to restricted couplings with carbon monoxide.

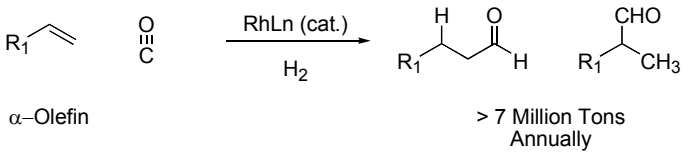

Scheme 2.1: Fischer-Tropsch reaction.

The ability to generalize this process to the coupling of basic chemical feedstocks would have profound impact on the synthetic community (Scheme 2.2). Most reductive methods for catalytic carbon-carbon bond formation need stoichiometric silane, borane, and stannane to complete the catalytic cycle, and therefore generate stoichiometric byproducts. The ability to conduct these transformations in the presence of hydrogen gas would provide a completely atom economical and cost efficient process.

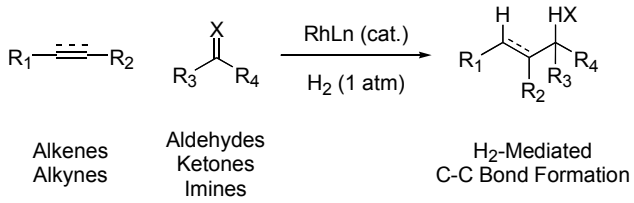

Scheme 2.2: H_2-mediated C-C bond formation of basic chemical feedstocks.

As a starting point for this reaction development one must understand how hydrogen gas interacts with transition metals. There are three mechanisms in which a molecule of hydrogen can be activated by a transition metal complex: (1) oxidative addition, (2) homolytic cleavage of hydrogen or (3) heterolytic cleavage of hydrogen.[8] Homolytic activation molecular hydrogen requires 100 kcal/mol of energy obtain two atoms, each with one of the former bonding electrons ($H_2 \rightarrow 2H^{\cdot}$). Heterolytic activation requires 37 kcal/mol of energy and one hydride ion is generated along with a proton ($H_2 \rightarrow H^- + H^+$).

The addition of H_2 to a metal center can occur by three general types of mechanisms: (1) concerted oxidative addition giving rise to a dihydride metal complex; (2) a radical chain mechanism providing a monohydride metal complex; or (3) a S_N2-like (polar) process that also provides a monohydride metal complex (Scheme 2.3).[8] The dihydride formation requires a low oxidation state for the transition metal. Electron rich ligands help to stabilize the resulting high oxidation state of the dihydride complex. Homolytic Cleavage of molecular hydrogen can occur with both monomeric and dimeric metal complexes and increases the oxidation state of the metal complex by one unit.

Heterolytic activation of hydrogen can be promoted by exogenous base or by a basic ligand. Scheme 2.3 demonstrates how the base assists in the heterolytic activation of hydrogen by stabilizing the proton as it is being formed. This mechanism can be thought of as a concerted ionic splitting of hydrogen.

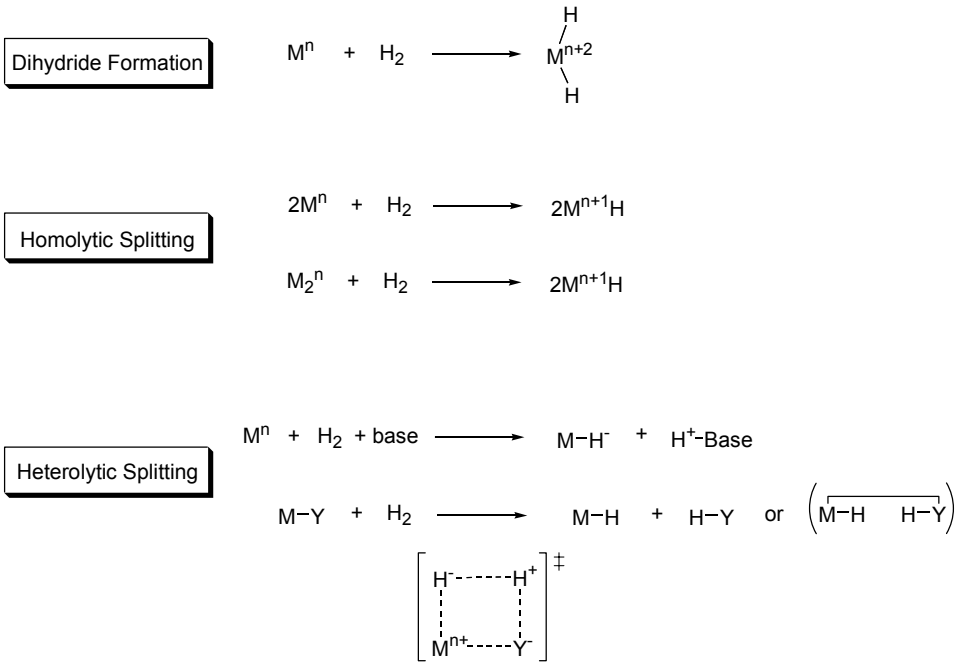

Scheme 2.3: Mechanisms for the activation of hydrogen.

Another method for achieving the same stoichiometry as heterolytic activation is by formation of a dihydride complex followed by deprotonation. It may be impossible to distinguish between this mechanism and actual heterolytic splitting if the relative rates are fast. This addition-elimination sequence shown in Scheme 2.4 should not be considered heterolytic activation of molecular hydrogen, but often it is impossible to detect.[8]

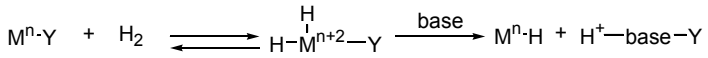

Scheme 2.4: Monohydride formation *via* addition-elimination mechanism.

It is a common formalism in the chemical literature to refer to the hydrogen of a M—H bond as an anionic hydride ligand, even if the hydride ligand is acidic. This formalism gives an increase in the oxidation state of the metal by one unit per hydride ligand. But with heterolytic activation of hydrogen both of the bonding electrons are being supplied by the hydride ligand and there is no formal oxidation of the metal center. Throughout this thesis, it will be shown that the ability to generate a monohydride metal complex is key in achieving a carbon-carbon bond forming hydrogenation.

Considerable mechanistic studies have been conducted on alkene hydrogenation catalyzed by Wilkinson's catalyst, $Rh(PPh_3)_3Cl$, a neutral rhodium source. It is known that this metal complex forms a dihydride rhodium complex under hydrogenation conditions (Scheme 2.5).[9, 10]

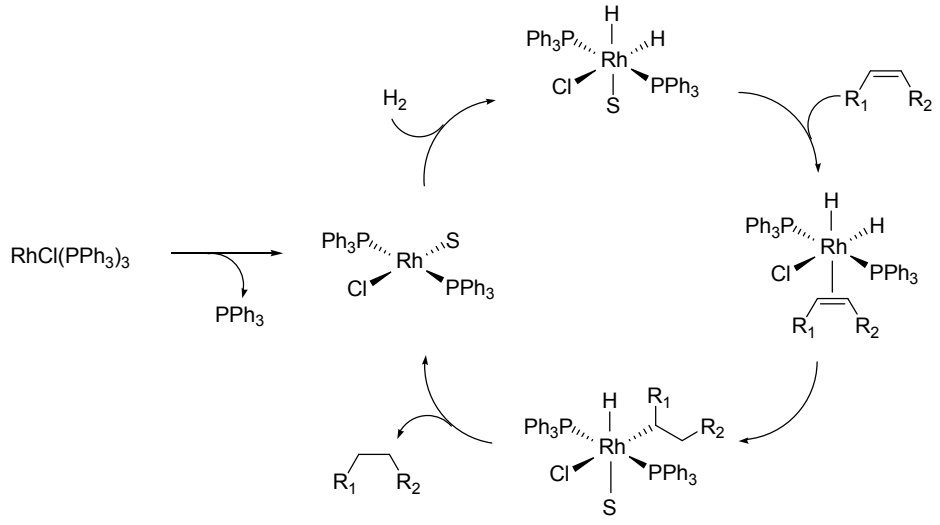

Scheme 2.5: Alkene hydrogenation catalyzed by Wilkinson's catalyst.

Seminal studies conducted by Schrock and Osborn revealed that for cationic rhodium complexes two different rhodium complexes, dihydride (RhH_2Ln) and monohydride (RhHLn), exist in equilibrium (Scheme 2.6).[11,12,13] Also, these studies revealed that the formation of the monohydride complex could be promoted by addition of exogenous base. Therefore the activation of molecular hydrogen by cationic rhodium(I) salts in the presence of base follows the mechanism of oxidative addition followed by deprotonation (formal heterolytic activation) (Scheme 2.4). Additional support for this mechanism comes from the fact that rhodium(III)-hydride complexes have low pKa values (Scheme 2.7).[14]

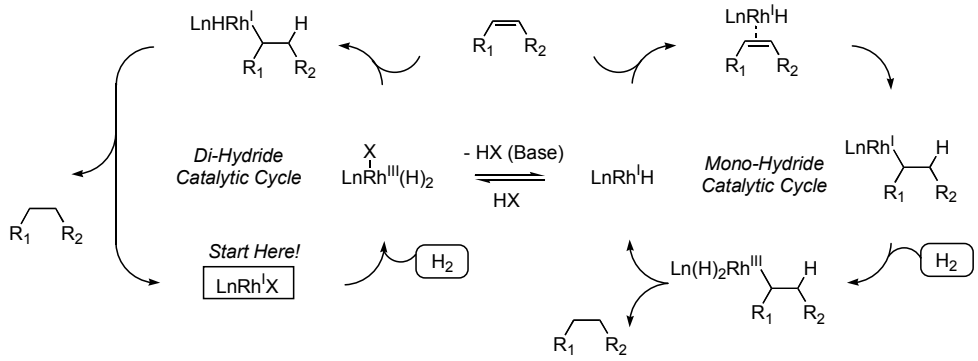

Scheme 2.6: Catalytic cycle for olefin hydrogenation *via* a cationic rhodium source.

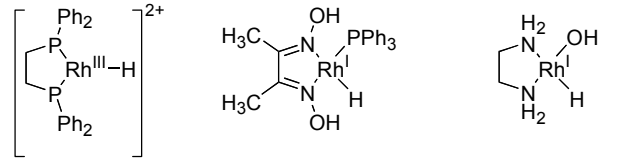

Scheme 2.7: pKa Values for some rhodium hydrides.

With the knowledge gained from these mechanistic studies one can hypothesize that hydrogenation intermediates that occur transiently during the course of the reaction can be intercepted with an electrophile in order to form a carbon-carbon bond. Historically, catalytic hydrogenation has been viewed only as a method of reduction (Scheme 2.8, eq 1). In catalytic hydrogenation, homolytic activation of molecular hydrogen gives a (dihydrido)metal intermediate, which hydrometallates the alkene to afford an (alkyl)(hyrdrido)metal complex, which upon C-H reductive elimination provides the product of conventional hydrogenation. But the ability to heterolytically activate hydrogen allows the transformation of this reaction from simple reduction to carbon-carbon bond formation. Heterolytic activation provides a monohydrio metal

complex, which hydrometallates the alkene. The product of this reaction lacks the appendent hydride ligand. This extends the lifetime of the monohydride species allowing it to be trapped with an electrophile to make a new carbon-carbon bond (Scheme 2.8, eq 2). Another possible mechanism involves oxidative coupling of the reactants prior to hydrogen activation. Because cationic rhodium complexes are slow to activate hydrogen, this mechanism is also plausible (Scheme 2.8, eq 3).[15] In this case σ-bond metathesis of hydrogen to the rhodium center affords the product and regenerates the catalyst

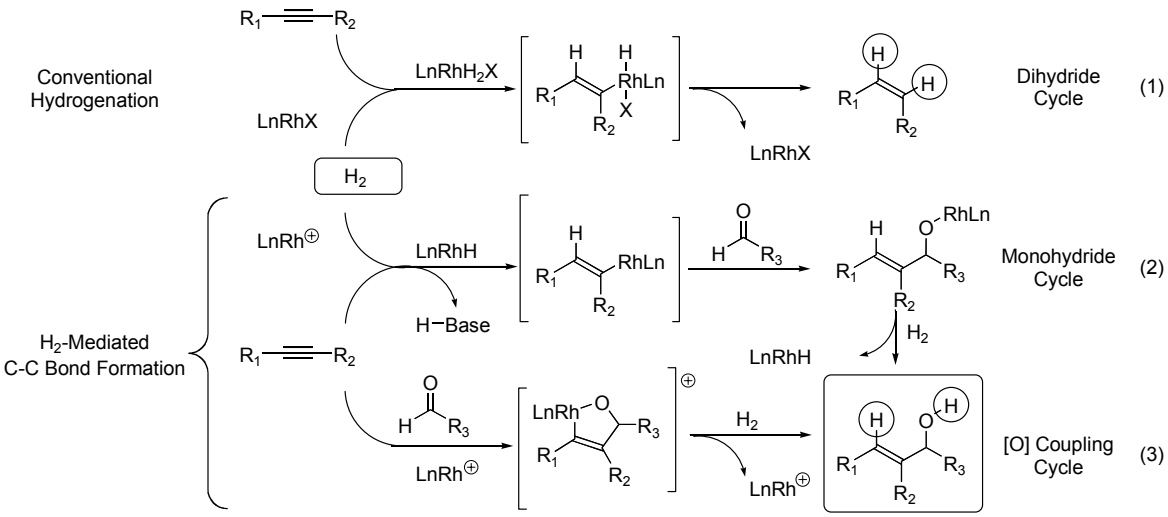

Scheme 2.8: Potential pathway for hydrogen mediated C-C bond formation.

In this thesis, hydrogen mediated carbon-carbon bond formation utilizing a cationic rhodium source and hydrogen gas is described as applied to the reductive aldol and Mannich reactions (Scheme 2.9). This methodology offers great improvements over traditional methods. In that it is catalytic in transition metal and uses hydrogen gas as the terminal reductant, the cheapest reductant known to man.

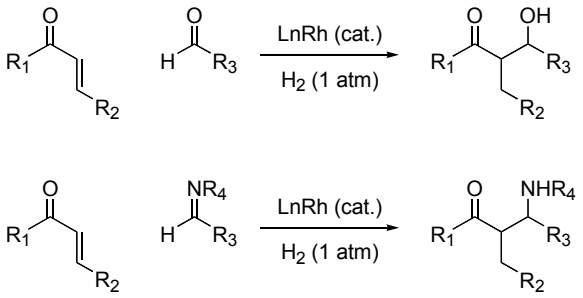

Scheme 2.9: Hydrogen-mediated C-C bond formation.

[1] Reviews for hydrogenation see: (a) Schmit, O. *Chem. Rev*. **1933**, *12*, 363. (b) Hoelscher, H. E.; Poynter, W. G.; Weger, E . *Chem. Rev*. **1954**, *54*, 575. (c) Kieboom, A. P. G.; Van Rantwijk, F. Hydrogenation and Hydrogenolysis in Synthetic Organic Chemistry; Delft University Press, **1977**. (d) Muetterties, E. L.; Bleeke, J. R. *Acc. Chem. Res*. **1979**, *12*, 324. (e) Knowles, W. S. *Acc. Chem. Res*. **1983**, *16*, 106. (f) Jessop, P. G.; Ikariya, T.; Noyori, R. *Chem. Rev*. **1995**, *95*, 259. (g) Genet, J. –P. *Acc. Chem. Res*. **2003**, *36*, 908.

[2] (a) Sabatier, P.; Senderens, J. B. *Comptes Rendus Hebdomadaries des Seances de l' Academic des Sciences,* **1897**, 1358. (b) Sabatier, P.; Senderens, J. B. *Comptes Rendus Hebdomadaries des Seances de l' Academic des Sciences,* **1899**, 1173.

[3] Young, J. F.; Osborn, J. A.; Jardine, F. H.; Wilkinson, G. *J. Chem. Soc. Chem. Commun.* **1965**, 131.

[4] (a) Knowles, W. S.; Sabacky, M. L. *J. Chem. Soc. Chem. Commun.* **1968**, 1445. (b) Knowles, W. S.; Sabacky, M. J.; Vineyard, B. D. *J. Chem. Soc. Chem. Commun.* **1972**, 10. (c) Vineyard, B. D.; Knowles, W. S.; Sabacky, M. J. *J. Am. Chem. Soc.* **1997**, *99*, 5946. (d) Knowles, W. S. *Acc. Chem. Res*. **1972**, *16*, 106. (e) Knowles, W. S.; *Angew. Chem. Int. Ed.* **2002**, *41*, 1998.

[5] *Chemical and Engineering News* **2005**, *83*, 40.

[6] Reviews for hydroformylation, see: (a) Breit, B.; Seiche, W. *Synthesis* **2001**, 1. (b) Breit, B. *Acc. Chem. Res*. **2003**, *36*, 264. (c) Tang, W.; Zhang, X. *Chem. Rev*. **2003**, *103*, 3029.

[7] Reviews for Fischer-Tropsch process, see: (a) Herrmann, W. A. *Angew. Chem. Int. Ed*. **1982**, *21*, 117. (b) Rofer-Depoorter, C. K. *Chem Rev.* **1981**, *81*, 447.

[8] Brothers, P. J. *Progress in Inorganic Chemistry*; John Wiley & Sons: New York, **1981**; Vol. *28*, 1.

[9] Hapern, et. Al. *Inorg. Chim. Acta.* **1981**, *50*, 11.

[10] Collman, J. P.; Hegedus, L. S.; Norton, J. R.; Finke, R. G. *Principles and Applications of Organotransition Metal Chemistry*, University Science Books, Mill Valley, **1987**, 523.

[11] Schrock, R. R.; Osborn, J. A. *Chem. Commun.* **1970**, 567.

[12] Schrock, R. R.; Osborn, J. A. *J. Am. Chem. Soc.* **1976**, *98*, 2134.

[13] Schrock, R. R.; Osborn, J. A. *J. Am. Chem. Soc.* **1976**, *98*, 2143. (b) Schrock, R. R.; Osborn, J. A. *J. Am. Chem. Soc.* **1976**, *98*, 4450.

[14] Norton, J. R. *Transition metal hydrides*; Wiley-VCH: New York, **1992**, 309.

[15] Cao, P.; Wang, B.; Zhang, X. *J. Am. Chem. Soc*. **2000**, *122*, 6490.

CHAPTER 3. HYDROGEN-MEDIATED REDUCTIVE ALDOL REACTIONS

3.1 INTRODUCTION

The aldol reaction is one of the oldest and most utilized organic transformations. Much attention has been devoted to improving this reaction and making it more synthetically useful. In Chapter 1 of this thesis, the reductive aldol reaction is discussed in detail. One reason for the wealth of interest in the aldol reaction is that nature uses enolates as nucleophiles in polypropionate and polyacetate biosynthesis. For instance, one can see that Erythromycin-A is obtained from Erythromycin seco-acid, which can be further simplified to seven propionate subunits (Scheme 3.1). A hydrogen mediated reductive aldol reaction would provide access to polypropionates in a completely atom economical process from basic chemical feedstocks under neutral conditions.

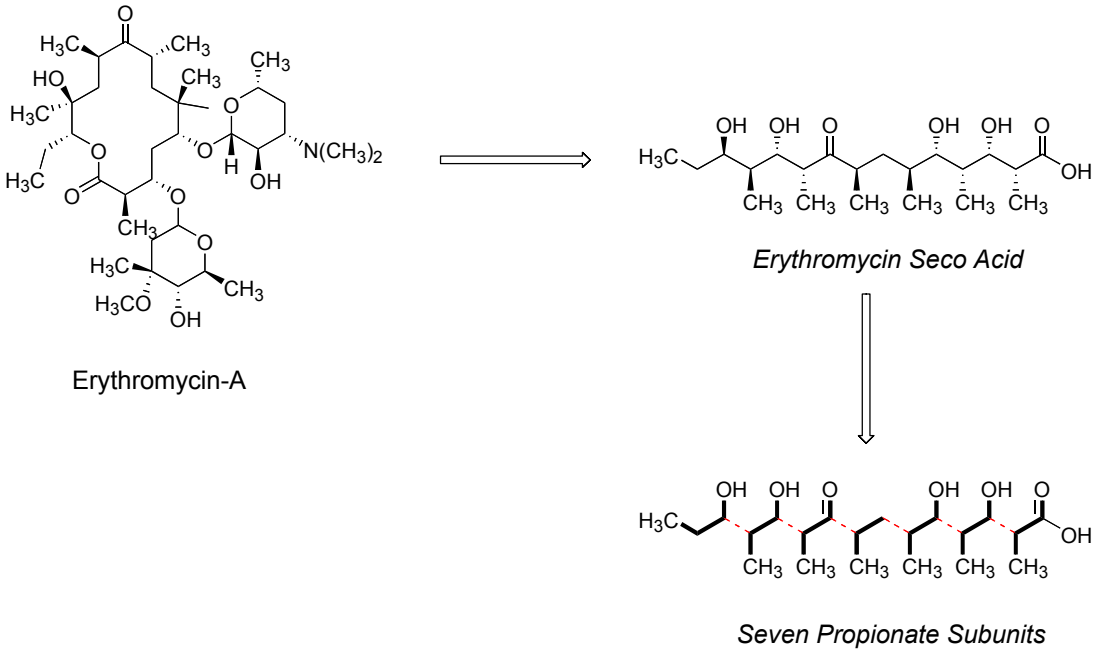

Scheme 3.1: The seven propionate subunits of Erythromycin A.

3.2.1 BACKGROUND

In order to assess the feasibility of a hydrogen mediated reductive aldol reaction, a phenyl substituted mono-enone mono-aldehyde substrate was exposed to a neutral rhodium (I) source, Wilkinson's catalyst, at ambient temperature and pressure.[1] The result was the product of convention hydrogenation (Table 3.1). By changing the catalyst to a cationic rhodium (I) source, $Rh(COD)_2OTf$, now a 21% yield of the reductive aldol product can be obtained along with 25% yield of the convention hydrogenation product. The addition of a substoichiometric amount of a mild basic additive, 30 mol% of potassium acetate, increases the yield of the reductive aldol product to 59%. The optimized reaction conditions were obtained by using the cationic rhodium (I) source, $Rh(COD)_2OTf$, a more electron deficient ligand, $(p\text{-}CF_3Ph)_3P$, and a substoichiometric amount of potassium acetate. These conditions allowed for the complete partitioning between the conventional hydrogenation and carbon-carbon bond forming hydrogenation manifold.

Table 3.1: Partitioning between conventional hydrogenation and C-C bond forming hydrogenation.

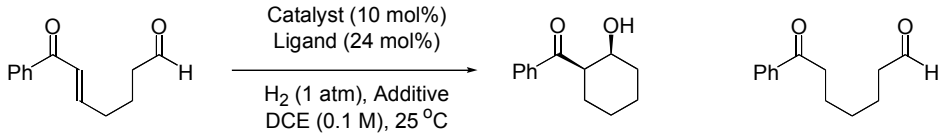

Catalyst	Ligand	Additive (mol%)	Aldol (syn-anti)	1,4-Reduction
$Rh(PPh_3)_3Cl$	**---**	---	1% (99:1)	57%
$Rh(COD)_2OTf$	PPh_3	---	21% (99:1)	25%
$Rh(COD)_2OTf$	PPh_3	KOAc (30%)	59% (58:1)	21%
$Rh(COD)_2OTf$	$(p\text{-}CF_3Ph)_3P$	---	57% (14:1)	22%
$Rh(COD)_2OTf$	**$(p\text{-}CF_3Ph)_3P$**	**KOAc (30%)**	**89% (10:1)**	**0.1%**

[a]As product ratios were found to vary with surface area to volume ratio of the reaction mixture, all transformations were conducted on 1.48 mmol scale in 50 mL round bottomed flasks.

Mechanistic studies where conducted in order to confirm that the reaction was in fact proceeding via the interception of hydrogenation intermediates. First, the mono-enone mono-aldehyde substrate was subjected to the reaction conditions in the absence of hydrogen gas (Scheme 3.2). The result was no reaction with full recovery of the mono-enone mono-aldehyde substrate; the reaction does require hydrogen gas. Also, the fact that Mortia-Baylis-Hillman adducts were not isolated reveals that the reaction is not preceding *via* tandem phosphine catalyzed cyclization-conjugate reduction. Reexposure of the conventional hydrogenation product to the reaction conditions does not produce the aldol product. Additionally, exposure of the convention hydrogenation product to one equivalent of potassium acetate does not produce the aldol product, only starting material was recovered.

Mono-enone Mono-aldehdyde without H_2

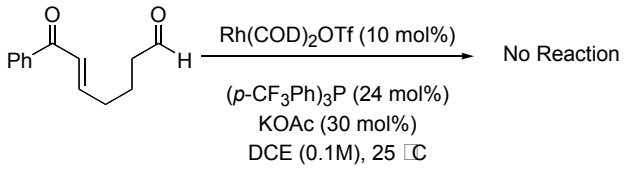

1,4-Reduction Product Resubmitted to Reaction Conditions

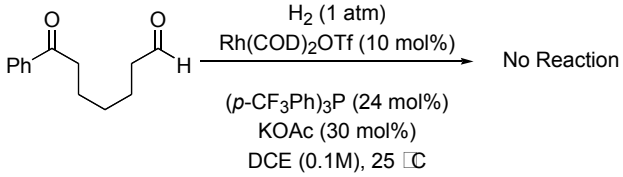

1,4-Reduction Product with KOAc Only

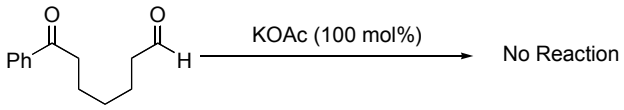

Scheme 3.2: Control experiments.

Next, the reaction was conducted in the presence of deuterium gas.[2] This experiment revealed exclusive deuterium incorporation at the former β-position of the enone (Scheme 3.3). The distribution of deuterated products supports reversible enone hydrometallation, which is not surprising for ketone acceptors. Deuterium incorporation at the α-position of the former enone is not observed.

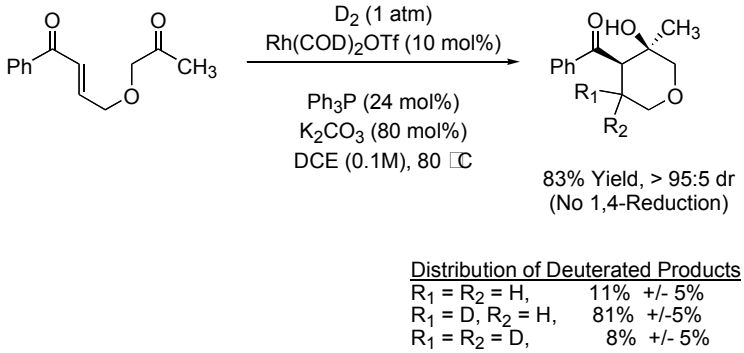

Scheme 3.3: Deuterium labeling experiments.

At this time it is not clear if this reaction is proceeding via the monohydride catalytic cycle or the enone-aldehyde oxidative coupling mechanism (Scheme 2.8). The profound effect of basic additives on partitioning between the reductive aldol and the conventional hydrogenation pathway supports the monohydride catalytic cycle. Based on this effect, a catalytic cycle can be proposed (Scheme 3.4). Beginning with a cationic rhodium (I) source in the presence of hydrogen gas, oxidative addition occurs to give a rhodium (III) dihydride complex. This rhodium (III) dihydride complex can enter either the dihydride catalytic cycle or the monohydride catalytic cycle. If the rhodium (III) dihydride enters the dihydride catalytic cycle, hydrometallation of the enone provides a rhodium (III) enolate. Notice, that this enolate processes an appendant hydride ligand. Rapid C-H reductive elimination occurs producing the undesired product of conventional hydrogenation and regenerates the catalyst.

One important point to remember is that the cationic rhodium hydrides are quite acidic as discussed in Scheme 2.7. Therefore, by the addition of a mild basic additive the acidic rhodium (III) hydride can be deprotonated to afford a neutral rhodium (I)

monohydride. This in effect shifts the catalytic cycle toward the monohydride catalytic cycle. Hydrometallation of the enone by the neutral rhodium (I) catalyst provides a rhodium (I) enolate, which lacks a hydride ligand. This extends its lifetime and allows the enolate to be trapped by an electrophile. Upon carbonyl addition a rhodium (I) aldolate is generated. Oxidative addition of another molecule of hydrogen to the rhodium produces a rhodium (III) complex. Lastly, O-H reductive elimination delivers the reductive aldol product and regenerates the rhodium (I) monohydride catalyst. Notice, that this reaction produces no stoichiometric byproducts. The key feature is the deprotonation of the rhodium (III) dihydride to obtain the rhodium (I) monohydride, which allows for the reaction mechanism to be shifted to the monohydride catalytic cycle favoring carbon-carbon bond formation.

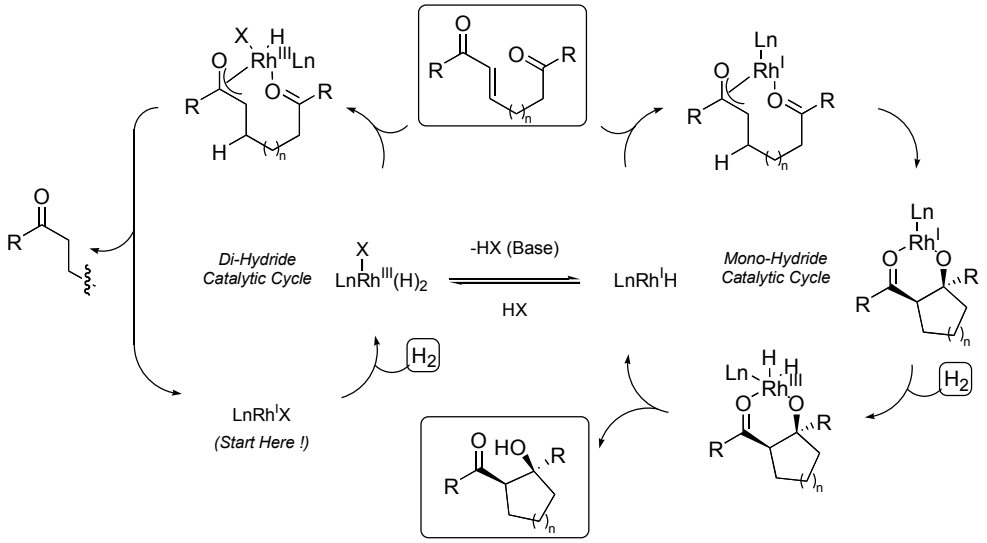

Scheme 3.4: Proposed catalytic cycle for hydrogen-mediated reductive aldol reactions.

3.2.2 SUBSTRATE SCOPE

This reaction manifold has a wide substrate scope that encompasses aromatic, heteroaromatic, and aliphatic enones to form 5- and 6- membered ring products. The reductive aldol products are obtained in good yields and diastereoselectivity (Scheme 3.5).[1]

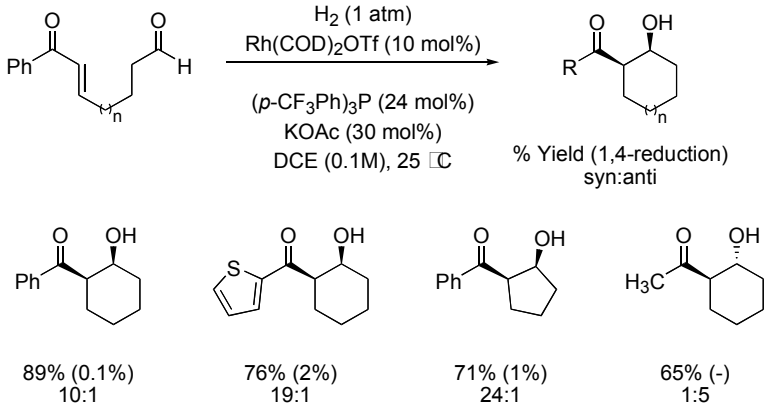

Scheme 3.5: Hydrogen-mediated intramolecular reductive aldol cyclizations with aldehyde acceptors.

We have been able to expand substrate scope of this reductive aldol process to more challenging electrophiles such as ketones.[2] Since ketones are less electrophilic than aldehydes, competitive conventional hydrogenation is more of a problem. Nevertheless, sufficient yields of the reductive aldol products were obtained. The reductive aldol cyclization of keto-enones proceeded with good yields for 5- and 6- membered rings with a variety of aromatic and heteroaromatic enones (Scheme 3.6). The reductive aldol products were obtained with excellent syn diastereoselectivity, which suggests the reaction proceeds through a *Z*-enolate and a Zimmerman-Traxler-type transition state.[3]

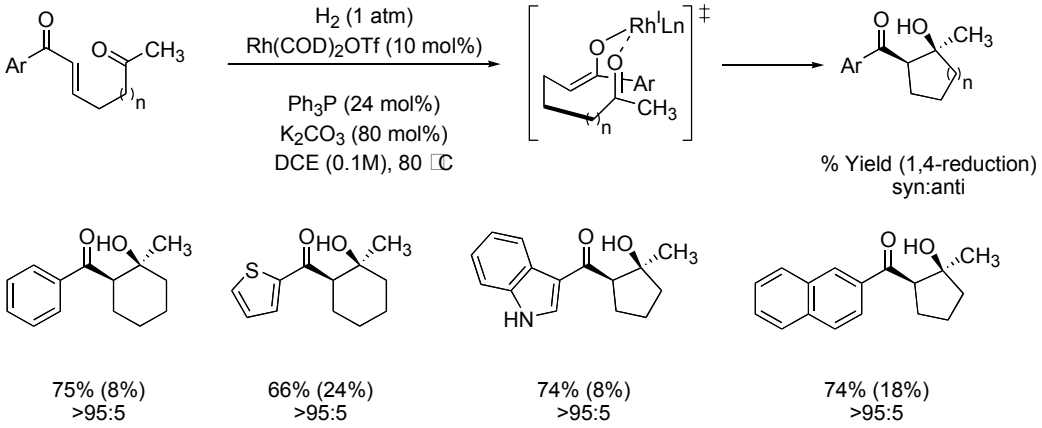

Scheme 3.6: Hydrogen-mediated intramolecular reductive aldol cyclizations with ketone acceptors

Another class of potential substrates were enone-diones.[2] These substrates have increased electrophilicity due to the inductive effects of an adjacent electron withdrawing group and carbonyl addition relieves unfavorable dipole-dipole interactions. These reductive aldol cyclizations proceeded with good yield and excellent *syn*-diastereoselectivity. Conventional hydrogenation is not observed for most cases (Scheme 3.7).

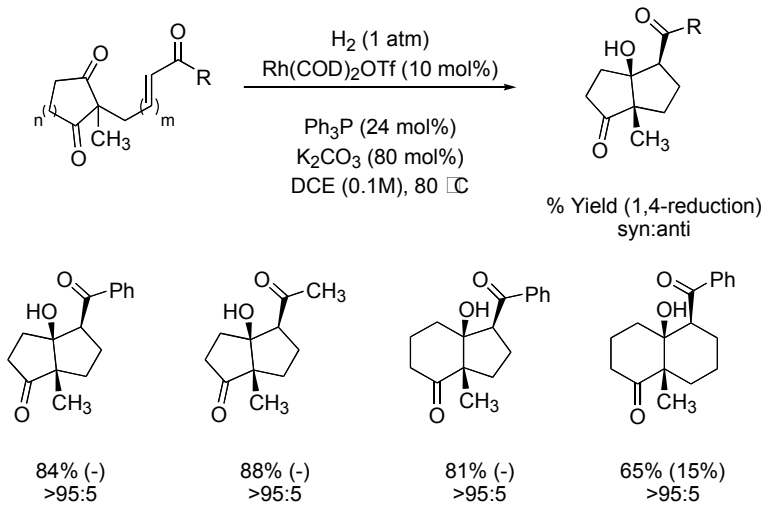

Scheme 3.7: Hydrogen-mediated intramolecular reductive aldol cyclizations with dione acceptors.

One of the most difficult variants of the aldol reaction is the addition of metallo-aldehyde enolates to ketones. This reaction is challenging for several reasons. First, aldehyde enolates are less nucleophilic than traditional enolates, and second, the addition to ketones is difficult due to reduced electrophilicity. In the chemical literature there is only one stoichiometric variant of this transformation.[4] Under optimized carbon-carbon forming hydrogenation conditions, this transformation was achieved by the intramolecular addition of metallo-aldehyde enolates to activated ketones (Scheme 3.8).[5]

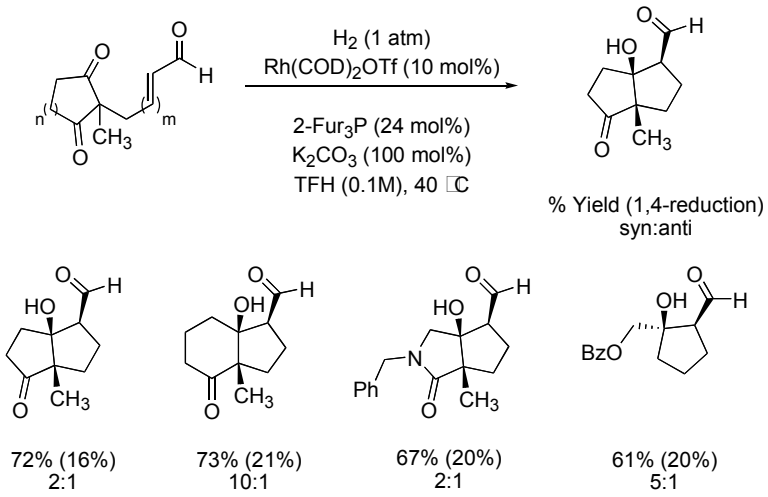

Scheme 3.8: Hydrogen-mediated intramolecular reductive aldol cyclizations of metallo-aldehyde enolates with ketone acceptors.

3.3.1 INTERMOLECULAR REDUCTIVE ALDOL ADDITIONS

Next, we focused our attention to the development of an intermolecular variant of the reductive aldol reaction. An intermolecular reductive aldol reaction is an attractive target for several reasons. First, the products obtained from this transformation are polypropionate synthons that map onto many natural products; recall the structure of Erythromycin A (Scheme 3.1). Also, the starting materials for this transformation are inexpensive and commercially available. An intermolecular reductive aldol reaction presents a greater challenge for competitive conventional hydrogenation; therefore a slight excess of enone is required. Under optimized hydrogenation conditions the reaction was conducted with methyl vinyl ketone (MVK) and *p*-nitrobenzaldehyde as coupling partners. The reaction proceeded with poor chemical yield and poor diastereoselectivity (Scheme 3.9). In order to make this reaction synthetically useful,

the yield and diastereoselectivity must be improved. The structure of compound **3.1a** was confirmed by the resonances at δ 5.28-5.29 (m, 1H) and 2.86 (dq, 1H) in the ^{1}H NMR spectrum corresponding to the methine proton adjacent to the hydroxyl group and the methine proton at the α-position to the carbonyl group. Also, HRMS data calculated [M + 1] for $C_{11}H_{13}NO_4$: 224.0923 and found 224.0925.

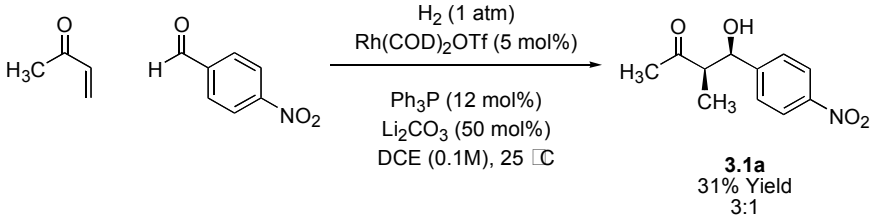

Scheme 3.9: Hydrogen-mediated intermolecular reductive aldol addition to aldehyde acceptors.

3.3.2 METHODS OF INCREASING DIASTEREOSELECTIVITY

In 1980 Heathcock and *et. al.* found that increasing the size of the acyl substituent resulted in increased diastereoselectivity.[6] The larger the acyl substituent the greater the preference for the *Z*-enolate due to minimization of $A^{1,2}$ strain. This in turn increases the preference for the syn product since the aldol reaction is a stereospecific transformation (Scheme 3.10). Notice, that when the acyl substituent is an ethyl group the syn to anti selectivity is only 64:36, but compared to an acyl *tert*-butyl group the syn:anti ratio increases to >98:2. Even though the size of the acyl substituent provides enhanced diastereoselection, this was not an attractive choice for us.

A more useful method would allow for diastereoselection irrelevant of the size of the acyl substituent. One contributing factor to the poor diastereoselection for the intermolecular hydrogen-mediated reductive aldol reaction is that the rhodium-oxygen bond length is approximately 4 Å. We envisioned that a diastereoselective variant could be achieved by using a weakly coordinating, π-acidic ligand. A π-acidic ligand should make the rhodium center more Lewis acidic, and therefore provide a shorter and stronger rhodium-oxygen bond. The overall effect would result in a tighter chair-like transition state rendering the aldol addition step more stereoselective.

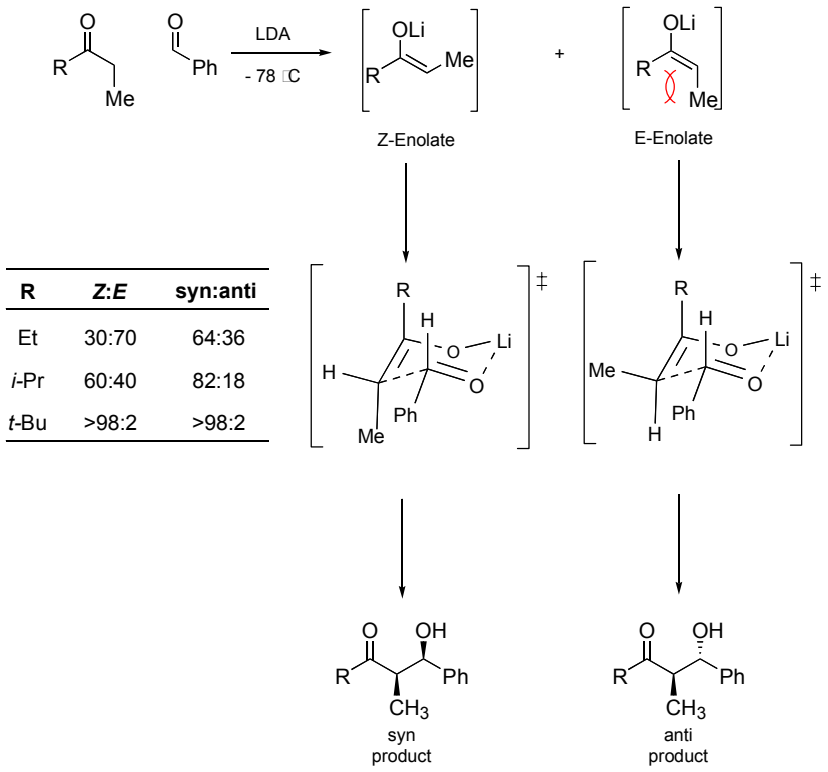

R	*Z*:*E*	syn:anti
Et	30:70	64:36
i-Pr	60:40	82:18
t-Bu	>98:2	>98:2

Scheme 3.10: Increasing acyl substitiuent size in order to increase diastereoselectivity.

The use of π-acidic ligands in order to confer increased electrophility at the metal center was a technique used by Farina in his modification of the Stille coupling reaction.[7] Farina observed nearly a 17 fold rate enhancement when the π-acidic ligand, tri-2-furylphosphine was used instead of triphenylphosphine. Triphenylphosphine and tri-2-furylphosphine are similar in size, but tri-2-furylphosphine is π-acidic due to the electron withdrawing furyl rings. Farina reports that the use of a less coordinating, poorer electron donating phosphine renders the Pd(II)allyl intermediate more electrophilic, therefore more reactive in the rate determining transmetallation step in his synthesis of Cephalasporin derivatives (Scheme 3.11).[7] Notice, that the reaction with tri-2-furyl phosphine as ligand proceeds at room temperature. In the case when triphenylphosphine was used the reaction required elevated temperature which resulted in substrate decomposition.

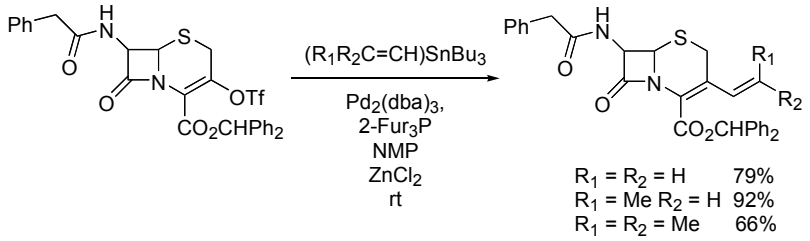

Scheme 3.11: Farina's use of tri-2-furylphosphine as a π-acidic ligand.

3.3.3 REACTION OPTIMIZATION

The steric and electronic properties of ligands dramatically influence the reactivity of the metal center, therefore in order to improve the yield and

diastereoselectivity of the intermolecular reductive aldol reaction a ligand screen was conducted. The ligand triphenylphosphine provided a 31% yield with a 3:1 syn:anti ratio (Table 3.2, entry 1). In order to test our hypothesis, the π-acidic ligand tri-2-furylphosphine was chosen as a ligand (Table 3.2, entry 4). The change from the electron rich triphenylphosphine to the π-acidic ligand, tri-2-furylphosphine had a dramatic effect. With the π-acidic ligand the reductive aldol product was obtained in 74% yield with a 19:1 syn:anti ratio. Interestingly, it was found that a sequential replacement of the phenyl residues on the ligand for 2-furyl residues (Ph_3P, 2-$FurPh_2P$, 2-Fur_2PhP, 2-Fur_3P) resulted in increased the yields and diastereoselectivity (Table 3.2, entries 1-4).[8] Two additional weakly coordinating π-acidic ligands, Ph_3As and $(PhO)_3P$, were screened in this reaction (Table 3.2, entries 5-6), and they also promote enhanced diastereoselectivity. The electron deficient ligand, $(p\text{-}CF_3Ph)_3P$, was screened in this reaction, and it provided poor yield and moderate selectivity (Table 3.2, entry 7). π-Acidic ligands such as tri-2-furylphosphine are weakly coordinating, and it is interesting that this reaction still proceeds in the absence of ligand to give a 9% yield with 2:1 syn:anti selectivity (Table 3.2, entry 8). Several other ligands were screened (Table 3.2, entries 9-12), though none provided the high levels of reactivity and selectivity that tri-2-furylphosphine afforded. When chiral ligands were used (Table 3.2, entries 11 & 12) poor enantioselectivity was observed. From the ligand screen it is obvious that tri-2-furylphosphine is the ideal ligand for the intermolecular hydrogen-mediated reductive aldol reaction.

Table 3.2: Ligand effect on the intermolecular hydrogen-mediated reductive aldol reaction.

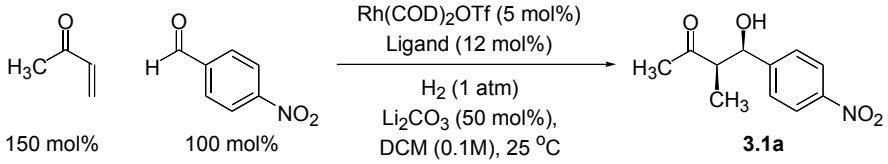

Entry	Ligand	Yield%	dr
1	PPh_3	31	3:1
2	$FurPh_2P$	24	6:1
3	Fur_2PhP	52	15:1
4	**Fur_3P**	**74**	**19:1**
5	Ph_3As	17	7:1
6	$(PhO)_3P$	28	6:1
7	$(p\text{-}CF_3Ph)_3P$	30	4:1
8	No Ligand	9	2:1
9	S-Phos	21	1.3:1
10	2-Diphenylphosphino-6-Methylpyridine	27	2:1
11	(R)-Cl-MeO-BIPHEP[b]	18	4:1
12	(R)BINAP[c]	8	7:1

[a]As product ratios were found to vary with surface to volume ratio of the reaction mixture, all transformations were conducted on 0.66 mmol scale in 13x100 mm test tubes. [b]14 %ee [c] 28 %ee

Next, the additive effect was screened for the intermolecular hydrogen-mediated reductive aldol reaction. Interestingly, the additive effect had profound impact on the reaction outcome. Lithium carbonate was discovered to be the best basic additive for the intermolecular reductive aldol reaction affording a 74% yield and 19:1 dr (Table 3.3, entry 1). Sodium and potassium carbonate both gave poor yield and selectivity (Table 3.3, entry 2 &3). When lithium acetate was used as the additive the reductive aldol product **3.1a** was obtained in 31% yield with a 3:1 syn:anti selectivity (Table 3.3, entry 4). This demonstrates the importance of the appropriate metal ion and counter ion.

Potassium acetate provided only a 6% yield and 1.7:1 diastereoselectivity (Table 3.3, entry 5). The major product obtained when potassium acetate was utilized was the simple reduction of the *p*-nitrobenzaldehyde. No reaction occurred when lithium hexafluorophosphate was used (Table 3.3, entry 6). The reaction proceeded when the amine base, *N,N*-diisopropylethylamine (DIPEA), was used, but with poor yield and selectivity (Table 3.3, entry 7). In the absence of any additive the hydrogen-mediated reductive aldol reaction occurred with modest yield, and the high level of syn diastereoselectivity is retained (Table 3.3, entry 8). This is a very interesting result because it shows that the high *syn* diastereoselectivity it not the result of a transmetallation between rhodium and lithium.

Table 3.3: Additive effect on the intermolecular hydrogen-mediated reductive aldol reaction.

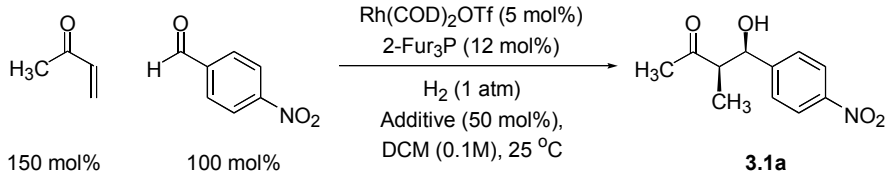

entry	Additive	Yield%	dr
1	**Li_2CO_3**	**74**	**19:1**
2	Na_2CO_3	16	4:1
3	K_2CO_3	39	1:2
4	LiOAc	31	3:1
5	KOAc	6	1.7:1
6	$LiPF_6$	NR	--
7	DIPEA	26	3:1
8	No Additive	61	16:1

[a]As product ratios were found to vary with surface to volume ratio of the reaction mixture, all transformations were conducted on 0.66 mmol scale in 13x100 mm test tubes.

Solvent can play an important role in transition metal catalyzed reactions. Often solvent molecules will occupy open coordination sites on the metal and must dissociate before substrate coordination. For this intermolecular hydrogen-mediated reductive aldol reaction the optimal solvent is dichloromethane providing a 74% yield with 19:1 diastereoselectivity (Table 3.4, entry 1). A polar coordinating solvent such as tetrahydrofuran provides **3.1a** in good yield but diminished selectivity (Table 3.4, entry 4).

Table 3.4: Solvent effect on the intermolecular hydrogen-mediated reductive aldol reaction

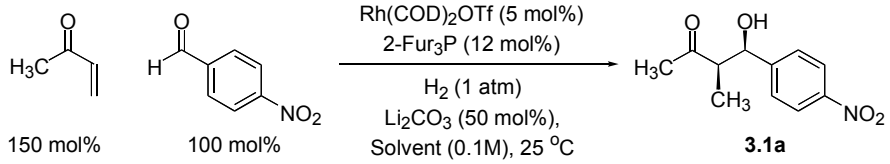

Entry	Solvent	Yield%	dr
1	**DCM**	**74**	**19:1**
2	DCE	64	12:1
3	Toluene	34	2.6:1
4	THF	70	2:1

[a]As product ratios were found to vary with surface to volume ratio of the reaction mixture, all transformations were conducted on 0.66 mmol scale in 13x100 mm test tubes.

Lastly, considering that the best two results were obtained when 50 mol% of Li_2CO_3 was used or no additive at all, (Table 3.3, entry 1 & 8 respectively) we examined the stoichiometry of the basic additive. Varying the amount of Li_2CO_3 had little effect on the reaction outcome (Table 3.5). The loading of Li_2CO_3 could go as low as 10 mol% without compromising the reaction outcome.

Table 3.5: Stoichiometry of Li_2CO_3 on the intermolecular hydrogen-mediated reductive aldol reaction.

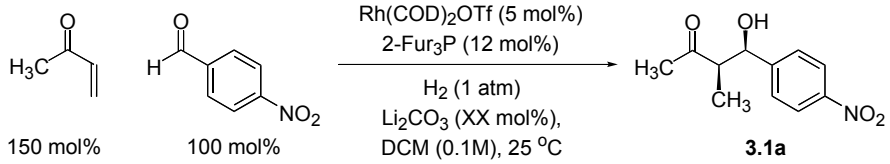

150 mol% 100 mol% **3.1a**

Entry	Li_2CO_3 (mol %)	Yield%	dr
1	Li_2CO_3 (50 mol%)	74	19:1
2	Li_2CO_3 (25 mol%)	80	16:1
3	Li_2CO_3 (10 mol%)	73	16:1
4	Li_2CO_3 (5 mol%)	78	9:1
5	No Additive	61	16:1

[a]As product ratios were found to vary with surface to volume ratio of the reaction mixture, all transformations were conducted on 0.66 mmol scale in 13x100 mm test tubes.

The final optimized reaction conditions are shown in Scheme 3.12. Tri-2-furylphosphine is the optimal ligand choice for the cationic $Rh(COD)_2OTf$ catalyst. Lithium carbonate is the basic additive at 10 mol% loading. Conducting the reaction in dichloromethane at 0.3M concentration provides the reductive aldol product **3.1a** in 91% yield with 16:1 *syn:anti* diastereoselectivity.

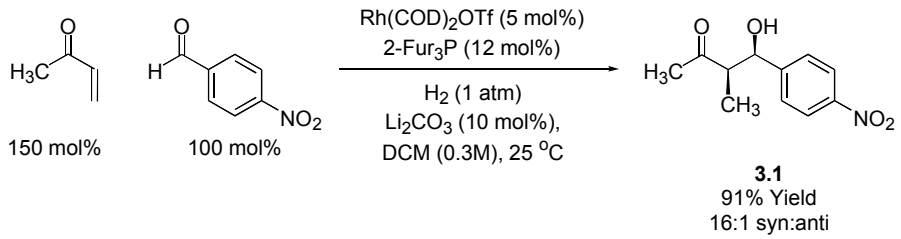

Scheme 3.12: Optimized reaction conditions for the intermolecular hydrogen-mediated reductive aldol.

The diastereoselectivities that are obtained in this hydrogen-mediated reductive aldol reaction are greater than the diastereoselectivities observed in traditional aldol reactions with lithium enolates (Scheme 3.13).[9] Notice that the hydrogen-mediated reductive aldol reaction proceeds at ambient temperature and pressure. The traditional aldol reaction is conducted at -78 °C with a preformed lithium enolate.

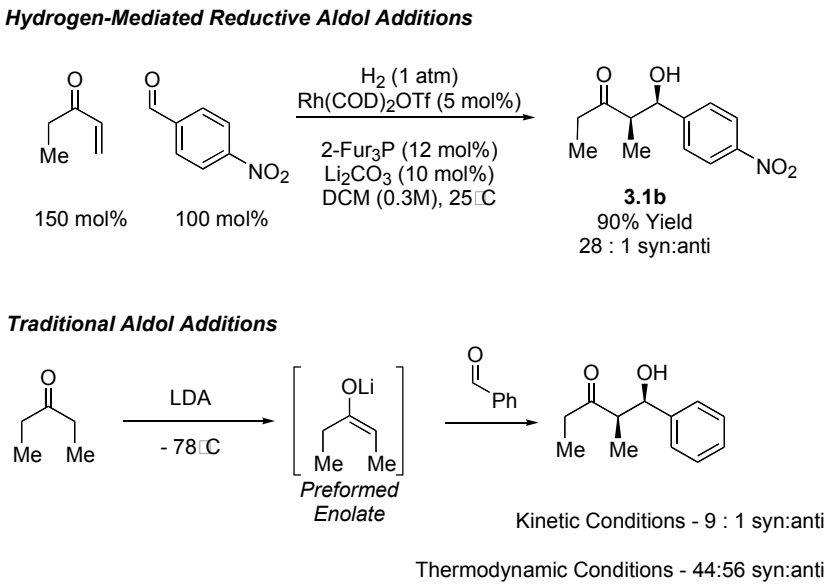

Scheme 3.13: Hydrogen-mediated reductive aldol additions verses traditional aldol additions.

In order to confer such high levels of syn diastereoselection the reaction must proceed with kinetic control during both the enolization step and the aldol addition step. For the intermolecular aldol reaction the anti product is the thermodynamically preferred, therefore high levels of syn selectivity indicate kinetic control of the reaction. The syn selective aldol product is the result of the reaction proceeding through a *Z*(O)-enolate. The enolization step is stereospecific via rhodium hydride addition to the *s*-cis conformer of the enone (Scheme 3.14).[10] The *Z*(O)-enolate adds to the aldehyde through a Zimmermna-Traxler type transition structure to stereospecitifically deliver the *syn*-aldol product.[3] The π-acidic tri-2-furylphosphine ligand contributes to the enhanced syn-selectivity by making the Rh—O bond stronger and shorter, which has the overall effect of tightening the transition state. The aldol reaction is reversible, but the strong Rh—O

bond will provide a strong chelate. Chelation of aldolate products is a major driving force for the aldol reaction.[11]

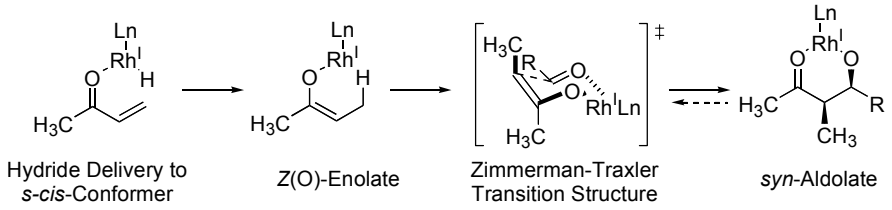

Scheme 3.14: Kinetically controlled enolization and carbonyl addition.

Another piece of evidence that suggests the reaction proceeds *via* a *Z*(O)-enolate and Zimmerman-Traxler type transition structure is that the aldol addition to an α-chiral aldehyde proceeds with *anti*-Felkin-Anh selectivity. It is known that additions of *Z*(O)-enolates to α-chiral aldehydes proceed through a Zimmerman-Traxler type transition structure to provide products with *anti*-Felkin-Anh selectivity in order to avoid the syn-pentane interactions that occur with Felkin-Anh selectivity.[12] Scheme 3.15 demonstrates the hydrogen-mediated reductive aldol addition reaction with an α-chiral aldehyde to give the reductive aldol product **3.10** with *anti*-Felkin-Anh selectivity and high levels of *syn*-diastereoselectivity (8:1 syn:all other isomers). The stereochemical assignment of **3.10** is based on a single crystal X-ray diffraction analysis of the corresponding 3,5-dinitrobenzoate **3.11** (Figure 3.1). At this time chelation controlled addition can not be ruled out, but this result does support that the reaction is proceeding *via* the intermediacy of a *Z*(O)-enolate and a Zimmerman-Traxler transition structure.

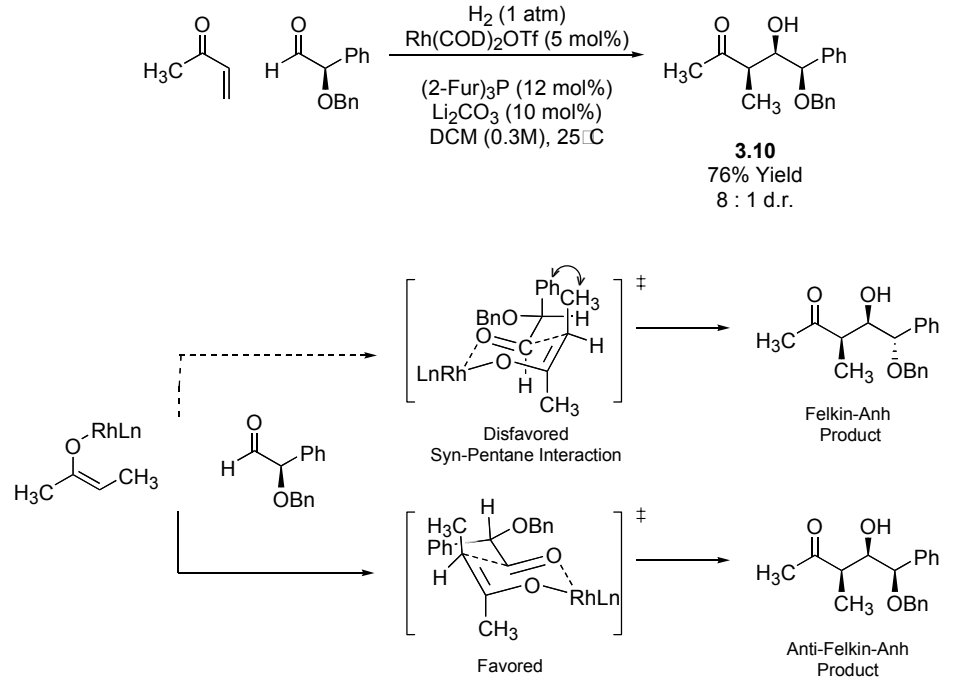

Scheme 3.15: *Anti*-Felkin-Anh addition of *Z*(O)-enolates to α-chiral aldehydes.

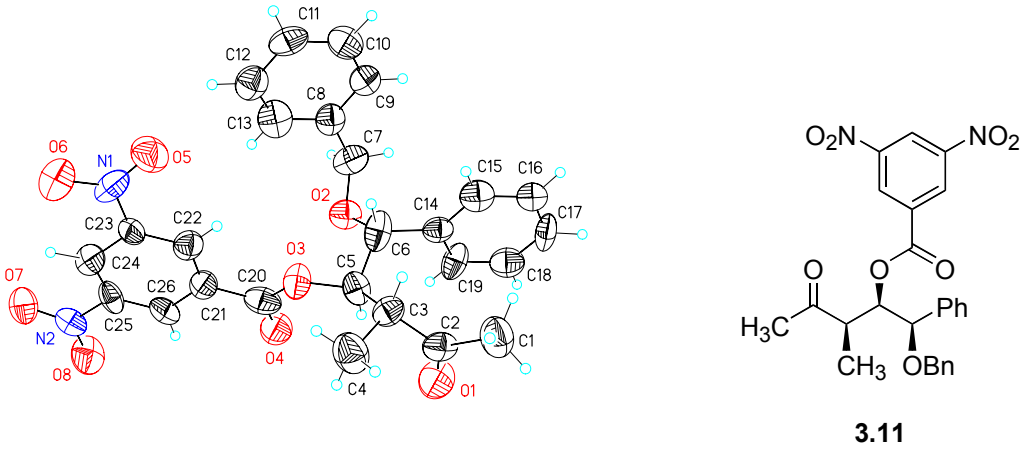

Figure 3.1: Single crystal x-ray diffraction analysis of **3.11.**

A deuterium labeling study was conducted to gain further insight to the reaction mechanism (Scheme 3.16). The result provided *deuterio*-**3.1** with incorporation of a single deuterium atom at the former enone β-position exclusively. This is consistent with irreversible enolization via enone hydrometallation. Also, the fact that deuterium incorporation at the α-carbon is not observed rules out Morita-Baylis-Hillman pathways en route to the product. This is consistent with the proposed catalytic cycle shown in Scheme 3.4.

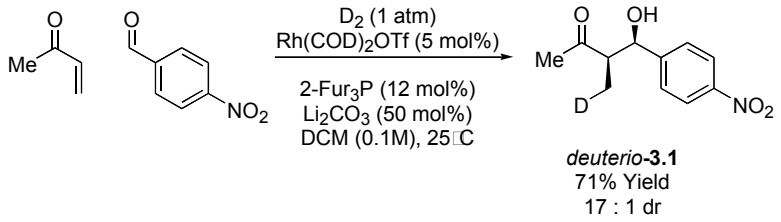

Scheme 3.16: Reductive coupling under an atmosphere of deuterium gas.

Two control experiments were conducted in order to further support the proposed catalytic cycle (Scheme 3.17). First, the reaction was carried out under optimal conditions, but under an atmosphere of argon gas instead of hydrogen. The result was no reaction; only unreacted starting material was recovered, therefore hydrogen gas is required in order for the reaction to proceed. In another control experiment MVK was replaced with 2-butanone. Again the result was no reaction with only unreacted starting material recovered. All of the experimental evidence collected thus far is consistent with the proposed catalytic cycle.

Intermolecular Reductive Aldol without H_2

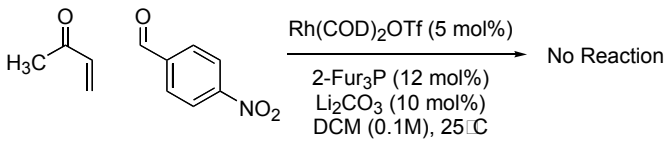

Intermolecular Reductive Aldol without Enone

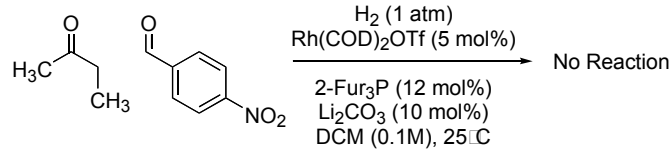

Scheme 3.17: Control experiments for the hydrogen-mediated intermolecular reductive aldol reaction.

3.3.4 SUBSTRATE SCOPE

Under optimum conditions the tri-2-furylphosphine ligated rhodium catalyst and commercially available methyl and ethyl vinyl ketone (MVK and EVK) participate in the hydrogen-mediated intermolecular reductive aldol additions to a diverse set of aldehydes with high *syn*-diastereoselectivity (Table 3.6 & Table 3.7). This reaction proceeds with high chemoselectivity, functional groups that are considered to by "hydrogen-labile" such as alkyenes, alkenes, benzylic ethers, and nitroarenes remain unreduced. In all cases the reductive aldol product was obtained in good yield with high levels of *syn*-diastereoselectivity.[8] The level of diastereoselectivity was increased when EVK was used as the nucleophilic partner, presumably due to enhanced $A^{1,2}$ strain giving a greater preference for the *Z*(O)-enolate. The products obtained from the reductive aldol coupling with EVK incorporate two propionate subunits. When *p*-nitrobenzaldehyde is used as the aldehyde acceptor only 150 mol% of the MVK or EVK is needed in order to achieve

good yields (entries **3.1a,b**), but when less electrophilic aldehydes are used then 300 mol% of enone is required. For entries **3.2a,b-3.33a,b** and **3.5a,b-3.9a,b** the reaction was conducted at 1.0M concentration using 300 mol% of enone. The acetylenic aldehyde used in entries **3.4a** and **3.4b** is very reactive, and therefore the catalysts loading had to be decreased to 2 mol% $Rh(COD)_2OTf$ and 500 mol% of enone was used in order to achieve a optimal result. The aliphatic aldehyde, heptanal, required increasing the catalyst loading to 10 mol% $Rh(COD)_2OTf$ due to low reactivity (entries **3.8a,b**).

Table 3.6: Hydrogen-mediated intermolecular reductive aldol additions with MVK employing cationic rhodium catalysts ligated by tri-2-furylphosphine.

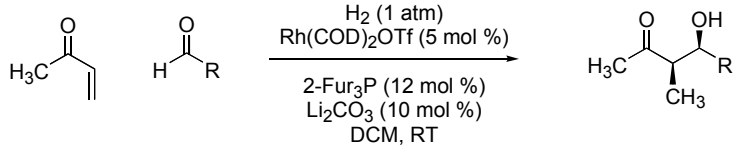

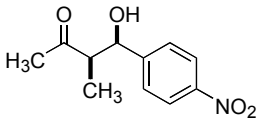	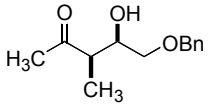	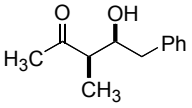
3.1a 91%Yield 16:1 dr	**3.2a** 90%Yield 17:1 dr	**3.3a** 84%Yield 16:1 dr
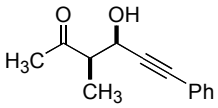	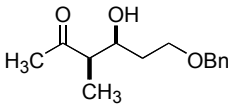	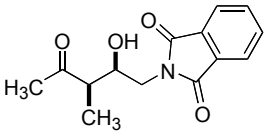
3.4a 65%Yield 8:1 dr	**3.5a** 71%Yield 15:1 dr	**3.6a** 95%Yield 50:1 dr
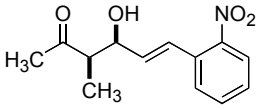	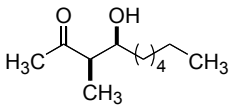	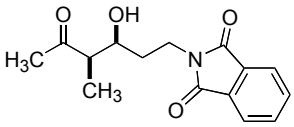
3.7a 92%Yield 8:1 dr	**3.8a** 62%Yield 10:1 dr	**3.9a** 87%Yield 28:1 dr

[a]As product ratios were found to vary with surface to volume ratio of the reaction mixture, all transformations were conducted on 0.66 mmol scale in 13x100 mm test tubes. [b] The cited yields are of isolated material and represent the average of two runs. [c] Diastereomeric ratios were established by ^{1}H NMR or HPLC analysis.

Table 3.7: Hydrogen-mediated intermolecular reductive aldol additions with EVK employing cationic rhodium catalysts ligated by tri-2-furylphosphine.

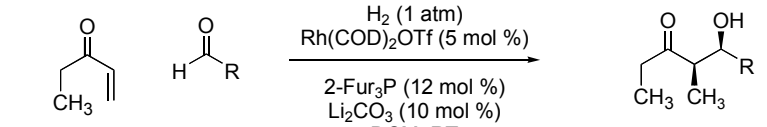

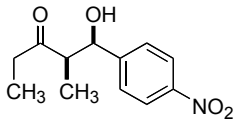 **3.1b** 90 %Yield 28:1 dr	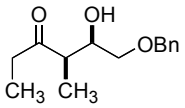 **3.2b** 88 %Yield 18:1 dr	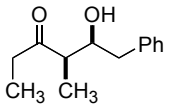 **3.3b** 89 %Yield 30:1 dr
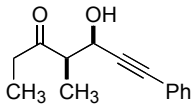 **3.4b** 70 %Yield 10:1 dr	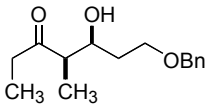 **3.5b** 73 %Yield 20:1 dr	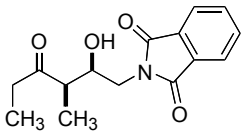 **3.6b** 97 %Yield >99:1 dr
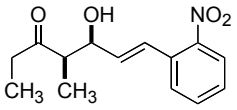 **3.7b** 99 %Yield 10:1 dr	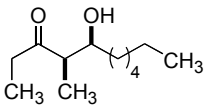 **3.8b** 60 %Yield 19:1 dr	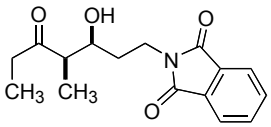 **3.9b** 94 %Yield 65:1 dr

[a]As product ratios were found to vary with surface to volume ratio of the reaction mixture, all transformations were conducted on 0.66 mmol scale in 13x100 mm test tubes. [b] The cited yields are of isolated material and represent the average of two runs. [c] Diastereomeric ratios were established by ^{1}H NMR or HPLC analysis.

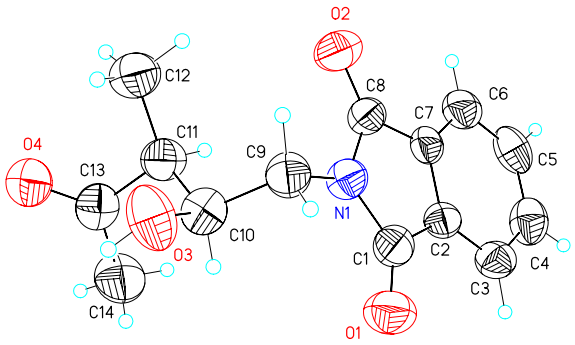

Figure 3.2: Single crystal x-ray diffraction analysis of **3.6a.**

3.3.5 Future Work For The Intermolecular Reductive Aldol Reaction

This reaction methodology is a very attractive synthetic tool that allows for the formation of aldol products at ambient temperature and pressure without the formation of any stoichiometric byproducts. This intermolecular reductive aldol reaction is the first diastereoselective reductive aldol reaction of vinyl ketones. The reductive aldol products are obtained in higher regio- and stereoselectivities than with traditional aldol additions conducted at low-temperature. One remaining challenge is the development of an enantioselective variant of this transformation. Initial screening of commercially available chiral ligands provided poor results (Table 3.2, entries 11 & 12). Currently, chirally modified monophosphines bearing 2-furyl residues are being synthesized and screened in hope of achieving an enantioselective variant of the intermolecular reductive aldol reaction.

3.4.1 Intermolecular Hydrogen-Mediated Reductive Coupling to Activated Ketones

Upon completion of the intermolecular reductive aldol coupling with aldehydes we turned our attention to a more challenging variant of the aldol reaction, intermolecular reductive couplings to activated ketones. Ketone aldol additions are challenging for a number of reasons. The biggest challenge is the reduced electrophilicity of ketones compared to aldehydes making addition more difficult. Also, aldol addition reactions are reversible. The major driving force for aldol additions under protic conditions is the formation of strong O-H bond,[13] and under aprotic conditions chelation is the major driving force.[11] For the ketone aldol, steric compression in the aldol product increases reversibility (Scheme 3.18). Another challenge for this transformation will be controlling diastereoselectivity. To date there are no direct catalytic asymmetric ketone aldol additions known.

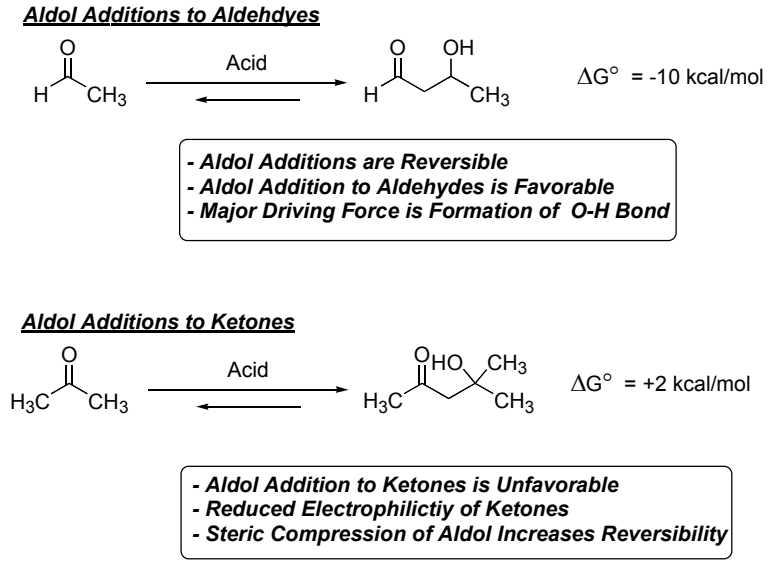

Scheme 3.18: Thermodynamic of aldol additions under protic conditions.

3.4.2 BACKGROUND

Kobayashi reported the first stereoselective aldol addition to activated ketones in 1992.[14] In this transformation one equivalent of tin(II) triflate is required along with a chiral promoter, (S)-1-pentyl-2-[(piperidin-1-yl)methyl]pyrrolidine (Scheme 3.19). Under the reaction conditions the aldol product is obtained in good yield and selectivity.

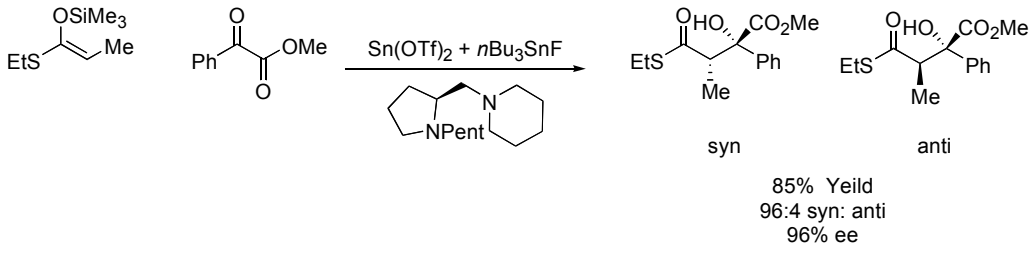

Scheme 3.19: First stereoselective intermolecular aldol addition to ketones.

Evans reported the first catalytic enantioselective aldol addition to activated ketones in 1997.[15] The study used chiral Cu(II)-based Lewis acids as catalysts. Aldol additions between enolsilanes and pyruvate esters were accomplished in excellent yield and selectivity. In both of the previous reports the reaction required the use of preformed enolates. To date there are no reports of direct catalytic aldol additions to ketones.

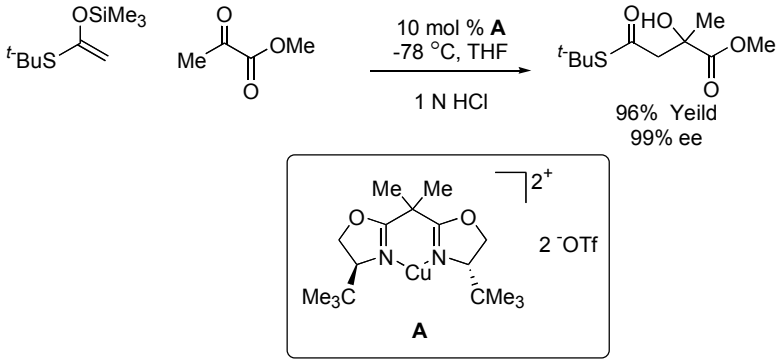

Scheme 3.20: First catalytic enantioselective intermolecular aldol addition to ketones.

3.4.3 Reaction Optimization for Hydrogen-Mediated Intermolecular Reductive Coupling to Activated Ketones

The initial screen for the hydrogen-mediated intermolecular reductive aldol addition to ketones began with attempting to couple MVK and ethyl pyruvate under standard hydrogenation conditions (Scheme 3.21). The reductive aldol product was obtained in trace yield with poor diastereoselectivity.

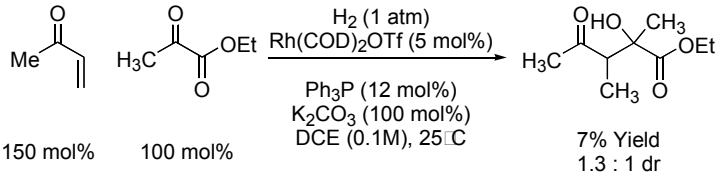

Scheme 3.21: Hydrogen-mediated reductive aldol reaction of MVK and ethyl pyruvate.

Next, a more reactive α-ketoester, 1-(3-bromophenyl)propane-1,2-dione, was employed. This α-ketoester participated in the reaction to a greater extent. The first reaction with the bromo-α-ketoester resulted in a 13% yield of **3.12** and 38% recovered starting material (Table 3.8, entry 1). By increasing the reaction temperature from room temperature to 40 °C the yield of the yield of the reductive aldol product increased to 45% (Table 3.8, entry 2). A ligand screen of tri-2-furylphosphine and triphenylarsine did not provide increased yield or diastereoselectivity (Table 3.8, entries 4 & 5). Also, electron rich phosphines such as $(p\text{-MeOPh})_3P$ did not improve the reaction outcome (Table 3.8, entry 6). By increasing the catalyst loading from 2 mol% to 5 mol% provided an increase in yield and diastereoselectivity (Table 3.8, entry 7). The final optimal conditions were obtained by conducting the reaction at 35 °C in dichloromethane at 0.3M concentration (Table 3.8, entry 8). These conditions furnished the reductive aldol product **3.12** in 90% yield with a 2:1 diastereoselectivity. At this time it is not known if this transformation is proceeding *via* a closed Zimmerman-Traxler type transition state or *via* an open transition state. Both scenarios are possible. The structure of compound **3.12** was confirmed by the resonances at δ 3.48-3.56 (q, 1H) and 0.98 (d, 3H) for the syn isomer and 3.60-3.67 (q, 1H) and 1.27 (d, 3H) for the anti isomer in the ^{1}H NMR

spectrum corresponding to the methine proton placed at the α-position to the carbonyl group and the methyl group at the former enone β-position. Also, HRMS data calculated [M + 1] for $C_{13}H_{16}O_4Br$: 315.0232 and found 315.0219 for the syn isomer and for the anti isomer $C_{13}H_{16}O_4Br$: 315.0232 and found 315.0219. For both syn and anti isomers the mass spectra had the characteristic M + 2 peak diagnostic for bromide.

Table 3.8: Reaction optimization of intermolecular cross aldol additions with activated ketones.

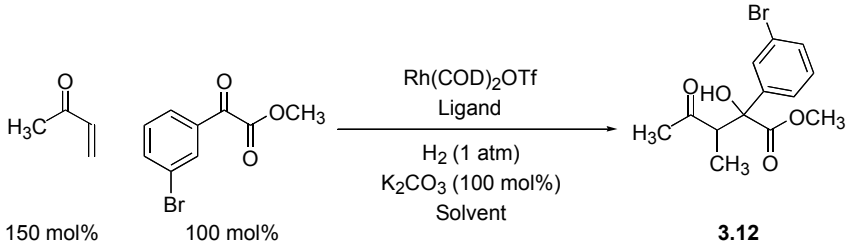

entry	$Rh(COD)_2OTf$	Ligand	Solvent	Temperature	% Yield (SM)	dr
1	2 mol%	Ph_3P (5 mol%)	DCE (0.1M)	RT	13% (38%)	1.3:1
2	2 mol%	Ph_3P (5 mol%)	DCE (0.1M)	40 °C	45% (46%)	2:1
3	2 mol%	2-Fur_3P (5 mol%)	DCE (0.1M)	40 °C	23% (21%)	1.5:1
4	2 mol%	Ph_3As (5 mol%)	DCE (0.1M)	40 °C	16% (66%)	1:1
5	2 mol%	(*p*-MeOPh)$_3$P (5 mol%)	DCE (0.1M)	40 °C	20% (25%)	1.3:1
6	5 mol%	Ph_3P (12 mol%)	DCE (0.1M)	40 °C	72% (7%)	2:1
7	**5 mol%**	**Ph_3P (12 mol%)**	**DCM (0.3M)**	**35 °C**	**90% (0%)**	**2:1**

[a]As product ratios were found to vary with surface to volume ratio of the reaction mixture, all transformations were conducted on 1.0 mmol scale in 50 mL round bottom flasks with a reflux condensor.

3.4.4 SUBSTRATE SCOPE

Employing optimal conditions the substrate scope was screened. Due to the fact that only highly activated α-ketoesters are viable electrophiles for this transformation, we

turned our attention to screening a variety of enones in hope of increasing the diastereoselectivity by increasing the size of the acyl substitiuent.[6] Unfortunately, the substrate scope for this transformation is limited. The diastereoselectivity remains unchanged when the acyl substitiuent is changed to ethyl (Table 3.9, entry 2). The diastereoselectivity is increased to 3:1 when the acyl substitiuent is a phenyl group (Table 3.9, entry 3). An x-ray crystal structure was obtained for the syn isomer of **3.14** (Figure 3.3). When the acyl substitiuent is equal to an isopropyl group the product **3.15** is obtained in trace yield with 63% recovered α-ketoester (Table 3.9, entry 4). When tert-butyl vinyl ketone is used as the enone no reaction occurs (Table 3.9, entry 5). In the isopropyl vinyl ketone and tert-butyl vinyl ketone reactions, the size of the acyl substitiuent may be too large thus hindering hydrometallation of the enone.

Table 3.9: Substrate scope for hydrogen-mediated intermolecular cross-aldol reactions with activated ketones.

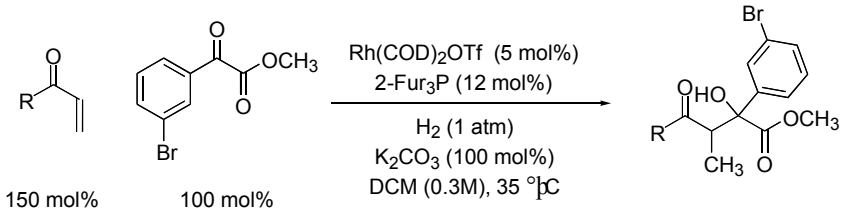

150 mol% 100 mol%

entry	R	Product	% Yield (SM)	dr syn:anti
1	Me	**3.12**	90% (0%)	2:1
2	Et	**3.13**	96% (0%)	2:1
3	Ph	**3.14**	90% (0%)	3:1
4	*i*Pr	**3.15**	9% (63%)	--
5	*t*Bu	**3.16**	No Rxn	--

[a]As product ratios were found to vary with surface to volume ratio of the reaction mixture, all transformations were conducted on 1.0 mmol scale in 50 mL round bottom flasks with a reflux condensor.

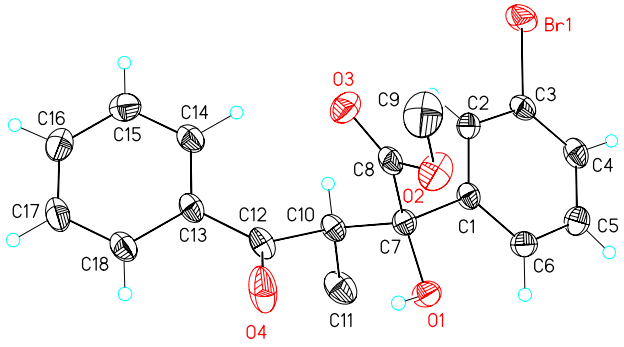

Figure 3.3: Single crystal x-ray diffraction analysis of *syn*-**3.14.**

3.4.5 Future Work For The Hydrogen-Mediated Intermolecular Cross-Aldol Reactions with Activated Ketones

This methodology proves that direct catalytic intermolecular ketone-aldol additions can be achieved, but considerable work needs to be done in order to make this reaction synthetically useful. At the present time this reaction suffers from a limited substrate scope and poor diastereocontrol. Interestingly, the reaction has high chemoselectivity in that the aryl bromide is not reduced under the reaction conditions.

3.5.1 Synthesis of 3,5-Disubstituted Pyridazines *via* Intermolecular Cross Aldol Additions of Enals and Glyoxals

After the development of the highly syn-selective hydrogen-mediated aldol coupling reaction, a new hypothesis was raised: Can we use an enal (α, β-unsaturated aldehyde) as our nucleophilic partner? Previously, we had utilized enones as pronucleophiles in an intra and intermolecular fashion. An enal is a more challenging pronucleophilic partner. Hydrometallation of the enal would result in a metallo-aldehyde enolate that could possibly be trapped by an electrophile such as an aldehyde. The product of this reaction would be a β-hydroxyaldehyde (Scheme 3.22). β-Hydroxyaldehydes are important synthons; evidence for this is found in nature. Nature uses enolates as nucleophiles in the aldol reaction in polypropionate and polyacetate biosynthesis (Scheme 3.1). The ability to utilize aldehyde enolates in the aldol reaction would be a major advance to field of aldol research.

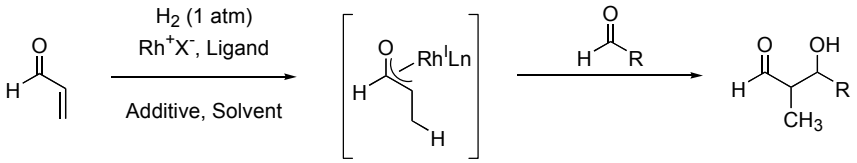

Scheme 3.22: Can enals serve as pronucleophilic partners for Rh-catalyzed hydrogenation?

3.5.2 BACKGROUND

Even though the field of aldol chemistry is quite advanced, the use of aldehyde enolates has remains a challenge. Aldehyde enolates are problematic due to the number of competing reactions such as dehydration, polyaldolization, oligomerization, Tishchenko reactions, and homo-aldolizations (problem for cross-aldol reactions) (Scheme 3.23).[13] Scheme 3.23 illustrates that the product of this transformation, a β-hydroxyaldehyde, contains a reactive aldehyde functional group. With such a reactive product, polyaldolization is a major competing reaction through secondary additions to the β-hydroxyaldehyde adduct. Another competing reaction is the Tishchenko reaction where the desired product is transformed to a β-hydroxyester. Other competing reactions, such as oligomerization, dehydration, and homo-aldolization, are common problems with all aldol reactions not those involving aldehyde enolates.

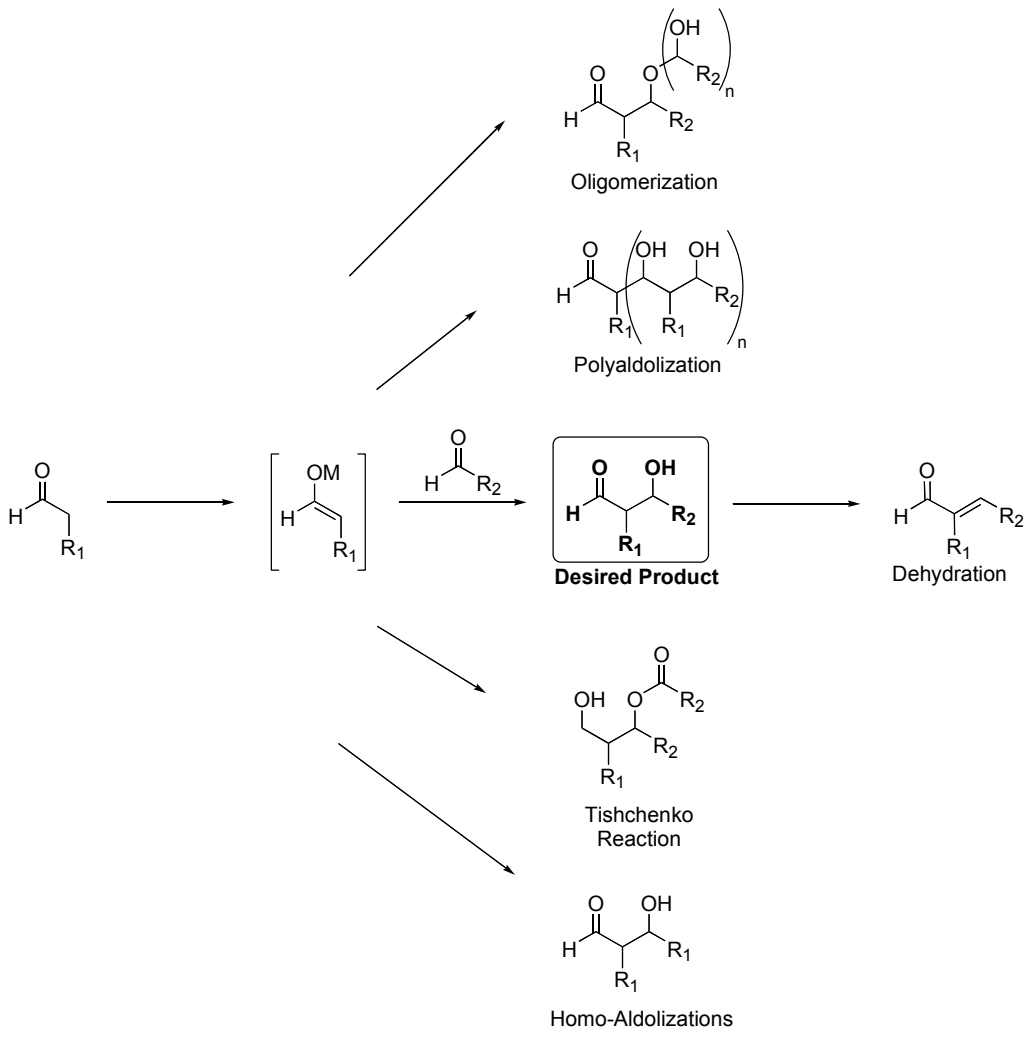

Scheme 3.23: Potential problems with aldehyde enolates.

Another major concern when using aldehyde enolates in the aldol reaction is the stability of the resulting β-hydroxyaldehyde product. Rychnovsky and co-workers report that simple β-hydroxyaldehydes are unstable at room temperature and preferentially exist as dimers (Scheme 3.24).[16] The product contains a very reactive aldehyde functional

group and the electrophilicity of the aldehyde is enhanced *via* the induction of the β-hydroxy group.

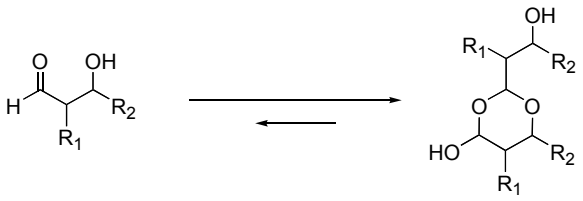

Scheme 3.24: Simple β-hydroxy-aldehydes exist preferentially as dimers.

Recently, there have been some reports of catalytic cross-aldol reactions *via* the use of aldehyde enolates. The first report comes from Denmark's research group, where the cross aldolization was achieved indirectly *via* employment of a preformed trichlorosilyl enol ether (Scheme 3.25).[17] The trichlorosilyl enol ether used in this reaction is highly reactive and can only be isolated by distillation. This reaction is catalyzed by a chiral phosphoramide. The chiral phosphoramide serves two purposes: (1) it activates the trichlorosilyl enol ether through the formation of an 'ate' complex and (2) it provides a chiral environment for asymmetric induction. This methodology works very well to produce the cross aldol products in high yield and high diastereoselectivity, but the enantioselectivity is variable. Denmark reports that the product stability was problematic therefore the cross aldol product was not isolated directly. Instead the β-hydroxyaldehyde product was derivatized *in situ* as the dimethyl acetal.

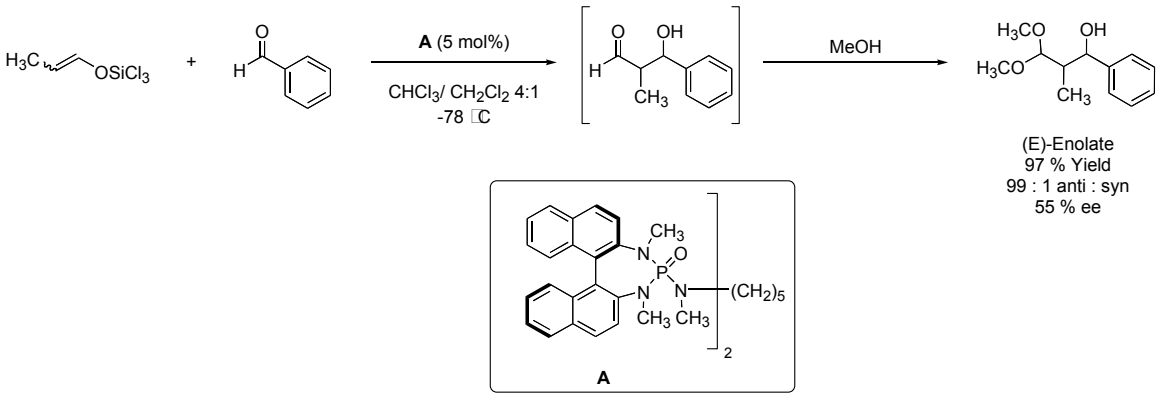

Scheme 3.25: Catalytic intermolecular cross-aldol reaction.

In 2002, MacMillan and co-workers reported the first direct and enantioselective cross-aldol reaction of aldehydes (Scheme 3.26).[18] This methodology uses L-proline as a catalyst. The aldehyde donor is added to the reaction *via* syringe pump addition inorder to suppress homo-aldolization. Again, product stability was an issue and the β-hydroxyaldehyde product was not isolated directly, but reduced to the 1,3-diol by sodium borohydride reduction. This methodology provides the desired product in high yield and high enantioselectivity but with only moderate diastereoselectivity.

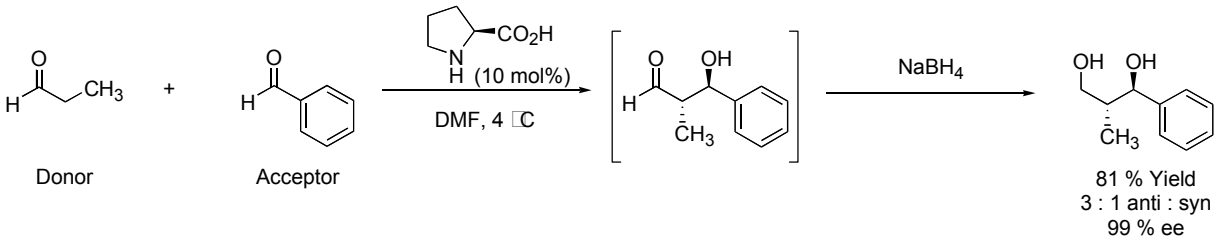

Scheme 3.26: First direct catalytic intermolecular cross-aldol reaction.

In 2003 List and co-workers reported an intramolecular cross-aldolization methodology similar to MacMillan's report (Scheme 3.27).[19] In this methodology L-proline was used as the catalyst. Again the β-hydroxyaldehyde product could not be isolated directly due to instability, and was derivatized *in situ* to the 1,3 diol. The isolated diols were obtained in high yield, diastereoselectivity, and enantioselectivity.

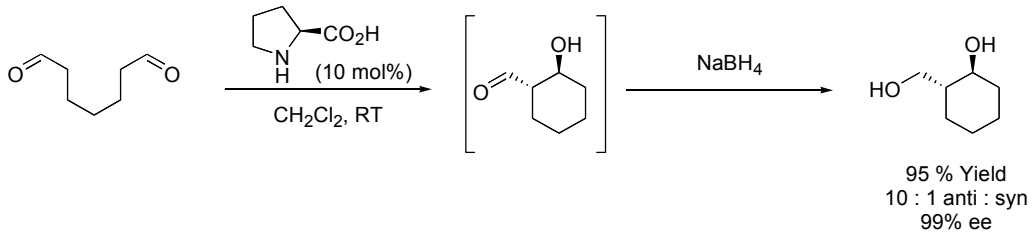

Scheme 3.27: Direct catalytic intramolecular cross-aldol reaction.

3.5.3 RESULTS AND DISCUSSION

To investigate the use of enals as pronucleophilic partners the reaction of acrolein with various electron deficient aldehydes was performed (Scheme 3.28). The conditions for these reactions are similar to those previously described in the intermolecular reductive aldol reaction (Scheme 3.12). For this transformation we were able to decrease the catalyst loading to 1 mol% $Rh(COD)_2OTf$. Triphenylphosphine was used as ligand in 2.4 mol% and one equivalent of potassium acetate was used. An excess of the enal was used due to competitive conjugate reduction. These reactions were carried out at room temperature with 1,2-dichloroethane (0.1M) as solvent.

The starting point of this investigation was the reaction between acrolein and *p*-nitrobenzaldehyde. We had previously discovered that methyl vinyl ketone and *p*-nitrobenzaldehyde coupled in 91% yield (Scheme 3.12). But when acrolein and *p*-nitrobenzaldehyde were subjected to the reaction conditions no coupling, occurred. Aldehyde enolates are less nucleophilic than those derived from ketones so a more electrophilic partner is required in order to trap the aldehyde enolate. The next electrophilic partner that was tried was chlorodifluoroacetaldhyde monohydrate, but the aldolization did not occur between these two partners. Finally, aldol addition did occur between acrolein and the very electrophilic phenyl glyoxal monohydrate to give the β-hydroxy-γ-ketoaldehyde as the product in 52% yield as a 1:1 mixture of diastereomers (Scheme 3.28).

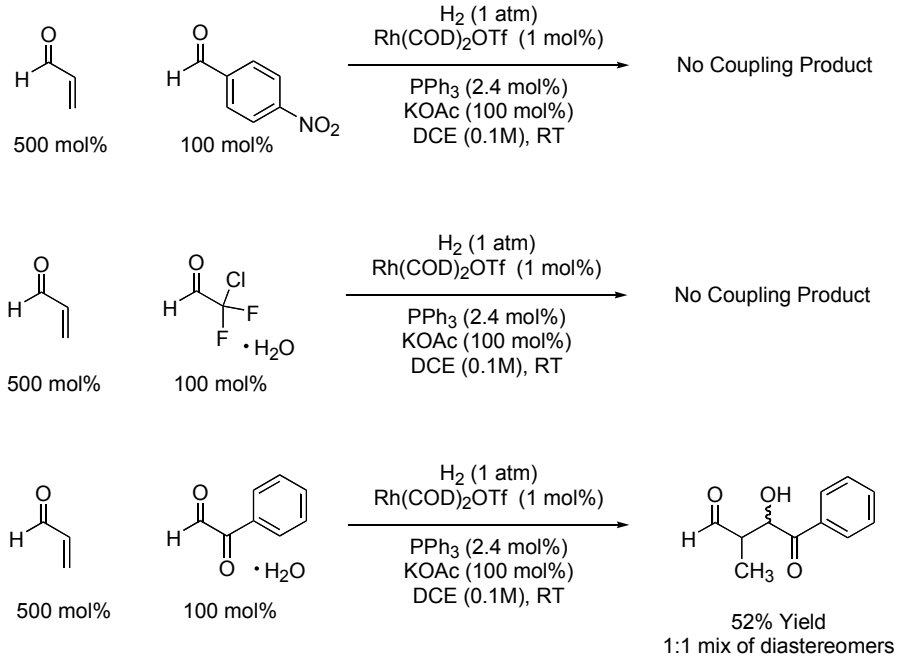

Scheme 3.28: Enal and aldehyde reductive coupling.

It was difficult to obtain reproducible results for the aldolization of acrolein and phenyl glyoxal monohydrate due to the instablility of the β-hydroxyaldehyde. A method to derivatize the β-hydroxyaldehyde was sought in order to overcome product instability. The reaction was quenched with acidic methanol in hope of isolating the dimethyl acetal protected aldehyde, as Denmark and coworkers had done (Scheme 3.29). This reaction did not give complete conversion, but instead an inseparable mixture of protected and unprotected aldehyde.

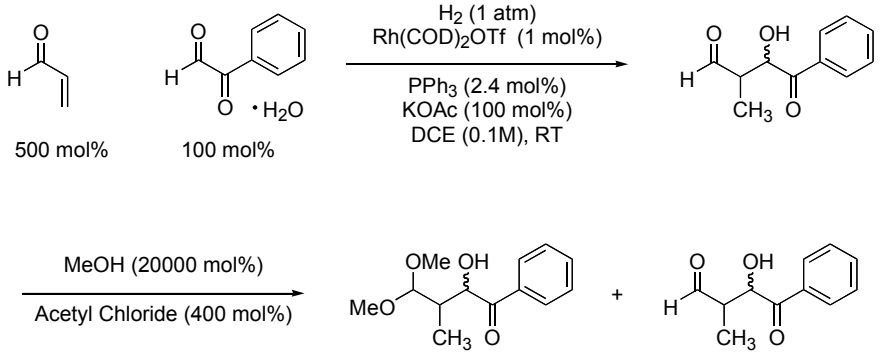

Scheme 3.29: Attempted dimethyl acetal derivatization.

Upon reevaluation of our product we hypothesized that quenching the reaction with hydrazine could generate a 3,5-disubstituted pyridazine with the elimination of three equivalents of water. Our product, a β-hydroxy-γ-ketoaldehyde appeared to be a good substrate for pyridazine formation (Scheme 3.30).

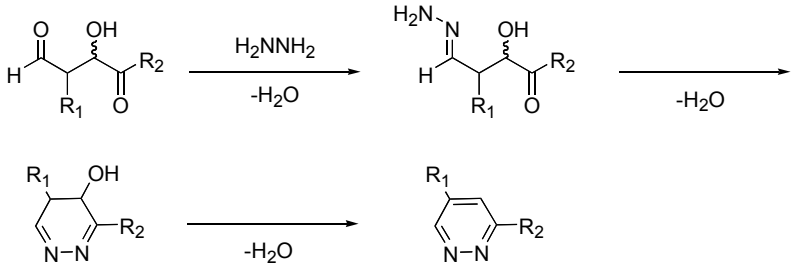

Scheme 3.30: Proposed 3,5-disubstituted pyridazine formation.

Recently there has been increased interest in the synthesis of pyridazines, with the commercialization of the antihypertensive hydralazine and the antibacterial sulfamethoxypyridazine (Scheme 3.31).[19]

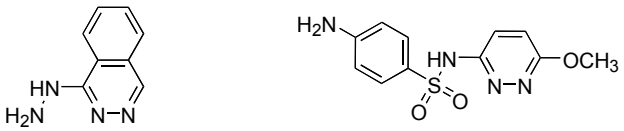

Hydralazine Sulfamethoxypyridazine

Scheme 3.31: Pyridazine pharmaceuticals.

Also, it was discovered that pyridazines of the 3,5-disubstitution pattern are known to possess unique biological activity. These pyridazines have a "bleaching" herbicidal activity, which inhibits the plant's growth. The known methods for the synthesis of this class of compounds require many steps, and are low yielding. Scheme 3.32 demonstrates one method developed by Sauer in which a [4+2] cycloaddition between 3-aryl-1,2,4,5-tetrazines and ethynyltributyltin is used to form the pyridazine ring.[20] This is followed by

a Stille coupling of the 3-phenyl-5-tributylstannyl-pyridazine with an aryl halide to afford the 3,5-disubstituted pyridazine.

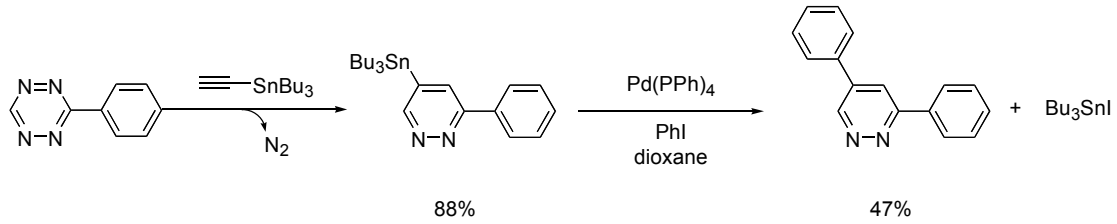

Scheme 3.32: Sauer's synthesis of 3,5-disubstituted pyridazines.

Another method shown in Scheme 3.33 developed by South utilizes haloazodienes in inverse electron demand [4+2] hetero Diels-Alder reaction.[21] The haloazodiene is prepared in two steps from 2-bromoacetophenone. Next, the haloazodiene is treated with Hünig's base followed by the addition of an enamine to provide the pyridazine in modest yield. There are no known one-pot syntheses of pyridazines.

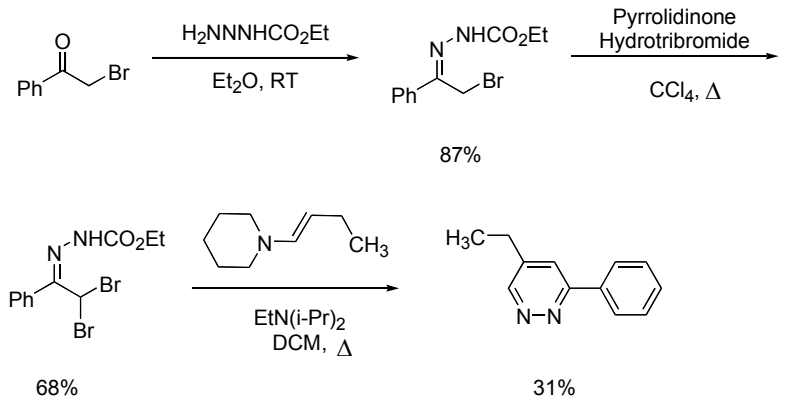

Scheme 3.33: South's synthesis of 3,5-disubstituted pyridazines.

In order to test our hypothesis of pyridazine formation, we conducted the reaction of acrolein and phenyl glyoxal under our optimized conditions which are hydrogen gas at one atmosphere of pressure, with a cationic rhodium (I) source, $Rh(COD)_2OTf$, at a loading of 1 mole percent. The ligand used is triphenylphosphine at 2.4 mole percent loading; with one equivalent of a basic additive, potassium acetate. The solvent was 1,2-dichloroethane and the reaction was conducted at room temperature. The reaction was monitored by thin layer chromography for the consumption of phenyl glyoxal. Then a solution of hydrazine in methanol was added to quench the reaction. Gratifyingly, the *in situ* trapping of the aldolization product with hydrazine gave the 3,5-disubstituted pyridazines **3.17** in 62% isolated yield, an increase of the overall yield compared to previous methods (Scheme 3.34). The structure of compound **3.17** was confirmed by a previous report by South where he synthesized and fully characterized the same compound.[21]

This results shows that the yield of the aldolization reaction is higher than the isolated yield due to product instability. Notice that without derivatization the yield of the aldol product is 52% and now we are adding an additional step to our reaction, our isolated yield is increasing 10%. It was found that this reaction worked best with the glyoxal partner in its' crystalline monohydrate state.

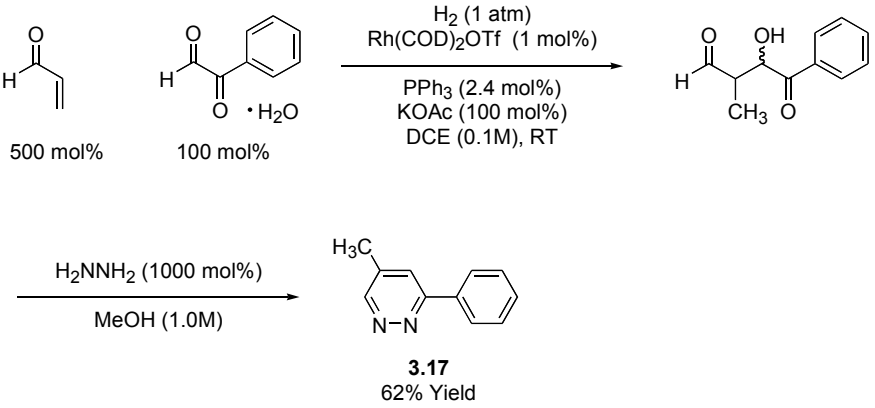

Scheme 3.34: Derivatization with hydrazine to yield 3,5-disubstituted pyridazines.

3.5.4 SUBSTRATE SCOPE

This methodology worked well for aromatic glyoxals such as phenyl and napthyl. We are also able to extend the scope to use heteroaromatic glyoxal as electrophiles in this reaction (Table 3.10). Aliphatic glyoxals, such as tert-butyl glyoxal, were not viable electrophilic partners for this transformation.

Table 3.10: Synthesis of 3,5-disubstituted pyridazines *via* enal aldehyde reductive coupling.

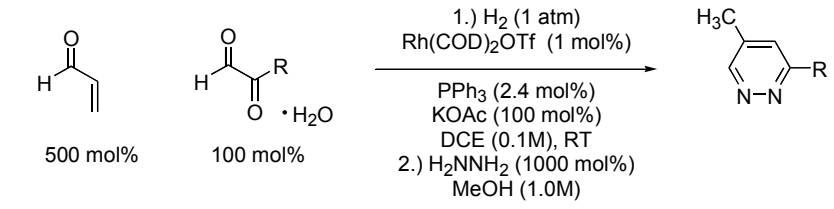

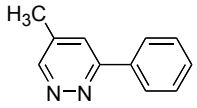

3.17
62 %

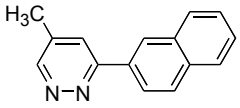

3.18
59 %

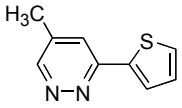

3.19
31 %

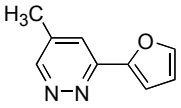

3.20
29 %

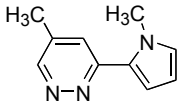

3.21[b]
30 %

[a]As product ratios were found to vary with surface to volume ratio of the reaction mixture, all transformations were conducted on 1.0 mmol scale in 50 mL round bottom flasks. [b]3 mol% $Rh(COD)_2OTf$ was used.

This methodology was also extended to the use of β-substituted enals. β-Substituted enals were viable pronucleophilic partners, but more forcing conditions were required in order to get the reaction to proceed. The catalyst loading was increased from 1 mol% to 5 mol%, and triphenylphosine loading was increased to 12 mol%. The solvent was changed from 1,2-dichloroethane to the more polar tetrahydrofuran. The reaction was carried out at an elevated temperature, 40 °C (Table 3.11). These conditions were needed due to the steric hindrance from the β-substituent, which retards the

hydrometallation step. Under more forcing conditions, the β-substituted enals were efficiently trapped by aromatic glyoxals in modest yield (Table 3.11).

Table 3.11: Synthesis of 3,5-disubstituted pyridazines *via* β-substituted enal aldehyde reductive coupling.

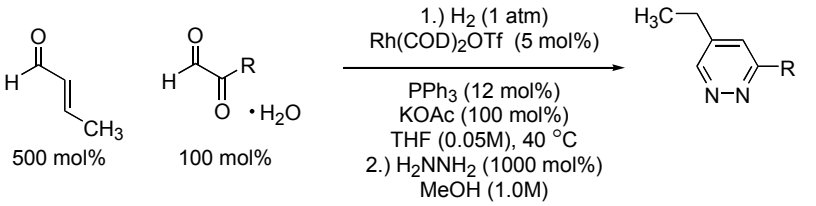

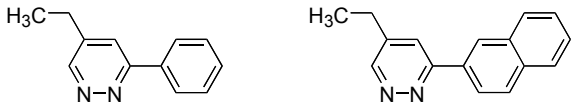

3.22
47 %

3.23
50 %

[a]As product ratios were found to vary with surface to volume ratio of the reaction mixture, all transformations were conducted on 1.0 mmol scale in 50 mL round bottom flasks.

In order to corroborate this reaction mechanism with the mechanism previously discussed for the reductive coupling of enones and aldehydes, (Scheme 3.35) a deuterium labeling study was conducted. The reaction was carried out as described above, except in the presence of one atmosphere of deuterium gas instead of hydrogen gas (Scheme 3.35). The result was the incorporation of a single deuterium at the β-position of the enal, which is consistent with the proposed mechanism.

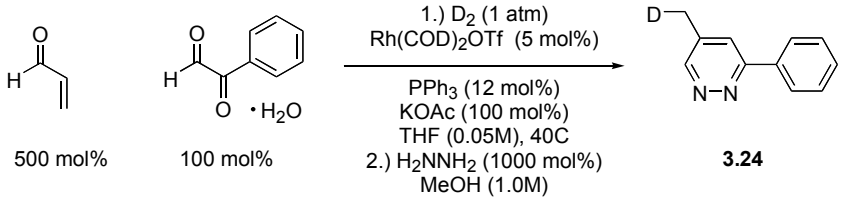

Scheme 3.35: Deuterium labeling study.

Scheme 3.36 shows the proposed catalytic cycle for the rhodium catalyzed hydrogenation-aldolization reaction. Starting with the cationic Rh (I), $Rh(COD)_2OTf$, the catalytic cycle begins with the heterolytic activation of hydrogen ($H_2 + Rh^+X^- \rightarrow Rh—H + HX$). In the presence of hydrogen gas at one atmosphere, the cationic Rh (I) undergoes oxidative addition to yield the Rh (III) dihydride species. At this point, there are two different reactive pathways that the Rh (III) dihydride complex can follow. One pathway is the dihydride catalytic cycle, where the next step is hydrometallation by the Rh (III) dihydride complex to the enal to give a Rh (III) enolate. Notice that this Rh^{III} enolate has a hydride ligand, which allows for rapid C—H reductive elimination to give the undesired product of conjugate reduction. By the addition of the basic additive, the reaction can be shifted to the monohydride catalytic cycle. The Rh (III) dihydride complex can be deprotonated by exogenous base to yield the Rh (I) monohydride species. The deprotonation of the Rh (III) dihydride complex disables the dihydride catalytic cycle, therefore shifting the reaction into the monohydride catalytic cycle. Upon generation of the Rh (I) monohydride complex, the enal is hydrometallated to yield the Rh (I) enolate. Notice that the Rh (I) enolate does not have any hydride ligands. Which therefore extends the lifetime of this intermediate by eliminating the possibility for

conjugate reduction. The Rh (I) enolate is then trapped by the electrophile to provide the Rh (I) aldolate. Oxidative addition of elemental hydrogen to the Rh (I) aldolate gives the Rh (III) dihydride, which upon oxygen-hydrogen reductive elimination provide the aldol product and regenerates the active Rh (I) monohydride complex. The aldol product was then trapped *in situ* with excess hydrazine in order to obtain the 3,5-disubtituted pyridazine.

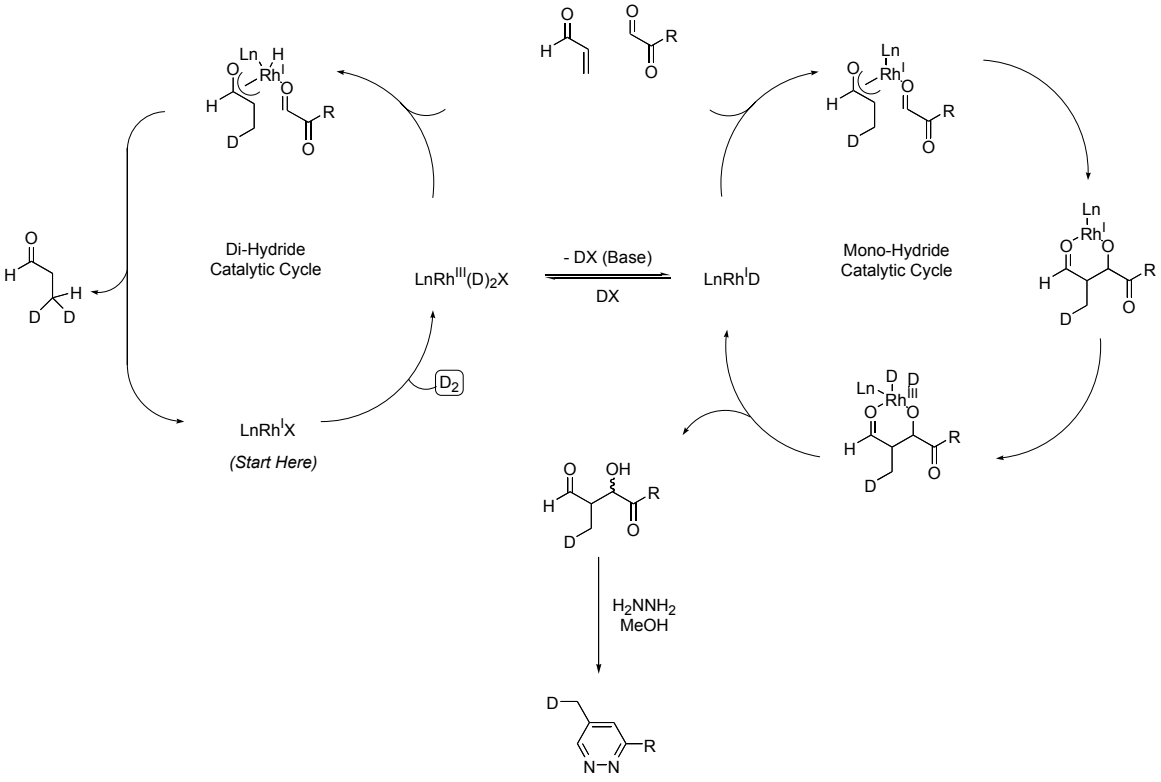

Scheme 3.36: Proposed catalytic cycle for the reductive aldol condensation of enals with glyoxal partners.

3.5.5 CONCLUSION

In conclusion, this methodology shows the first example of a catalytically generated metallo-aldehyde enolate, which is generated in the presence of the electrophilic partner. The generation of the metallo-aldehyde enolate is carried out under mild and atom economical conditions by the use of hydrogen as the terminal reductant. This methodology can produce a variety of 3,5-disubtituted pyridazines in good yields *via* a one-pot process.[23]

3.6.1 INTERMOLECULAR REDUCTIVE ALDOL ADDITIONS WITH ACRYLATES AND RELATED ACYL DERIVATIVES AS THE NUCLEOPHILIC PARTNER

Thus far, enones and enals have been used in the hydrogen-mediated reductive aldol addition methodology. One way to greatly expand the synthetic utility of this transformation would be the ability to use acrylates and other acyl derivatives as the nucleophilic partner. Subjecting a variety of acrylates and other acyl derivatives to our standard hydrogenation conditions resulted in conventional hydrogenation and none of the aldol addition product was obtained. Table 3.12 shows the reductive coupling of phenyl vinyl ketone and *p*-nitrobenzaldehyde under optimal conditions producing the aldol product in 92% yield with a 1.8:1 syn:anti ratio.[1] All of the acrylates and acyl derivatives shown in Table 3.12 are commercially available or prepared according to known procedures. Unfortunately, none of the acrylates or other acyl derivatives participated in this reaction, only simple reduction of the acyl derivative occurred.

Table 3.12: Acrylates and related acyl derivatives as the nucleophilic partners for hydrogen-mediated reductive aldol additions.

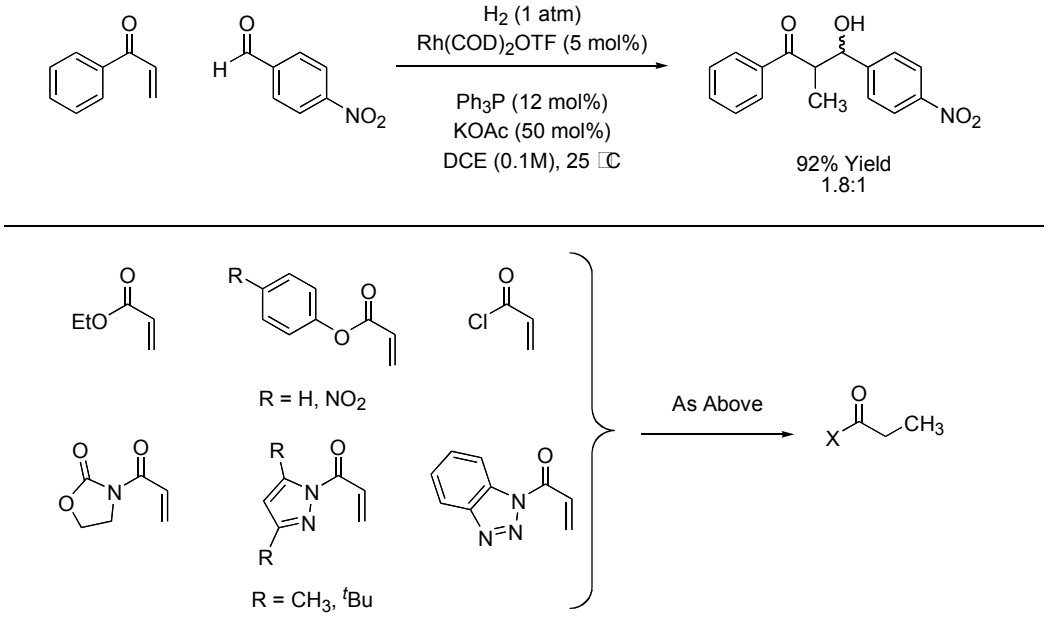

[a]As product ratios were found to vary with surface to volume ratio of the reaction mixture, all transformations were conducted on 1.0 mmol scale in 50 mL round bottom flasks.

At this time it is unclear why the reductive coupling does not occur. One possible reason for the failure of acrylates or other acyl derivatives to participate in this transformation is that the heteroatom at the acyl position shifts the equilibrium of enolate haptomers from an *O*-bound rhodium enolate to a *C*-bound rhodium enolate (Scheme 3.37). As previously discussed it is believed that the hydrogen-mediated aldol additions occur *via* a closed Zimmerman-Traxler type transition state. The formation of a *C*-bound rhodium enolate can hinder aldol addition, leading to formation of the simple reduction product. Molecular calculations using Spartan were performed on the acrylates and other

acyl derivatives, but the results were inconclusive. More work is needed in this area in order to develop a synthetically useful reaction.

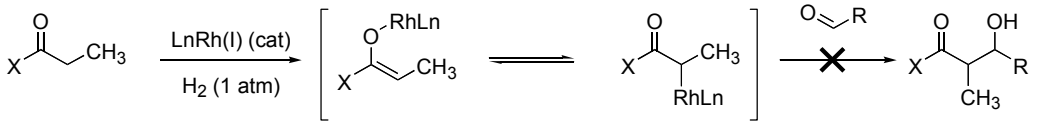

Scheme 3.37: *O*-bound verses *C*-bound rhodium enolates.

3.7 CONCLUSION

The hydrogen-mediated reductive aldol reaction is an elegant alterative to the traditional aldol reaction. The ability to reductively couple an enone and a carbonyl compound in the presence of hydrogen gas and a rhodium salt at ambient temperature and pressure is a true advance to the field of synthetic organic chemistry. This reaction methodology allows for the synthesis of complex molecules in a one-pot reaction without the need to preform the enolate and no stoichiometric byproducts are generated. One of the greatest challenges in the future of this chemistry is the development of an enantioselectivity variant. Much progress has been made in the field of hydrogen-mediated reductive aldol additions, but the full potential of the reaction has yet to be realized.

3.8.1 EXPERIMENTAL SECTION

GENERAL

All reactions were run under an atmosphere of argon, unless otherwise indicated. Anhydrous solvents were transferred by an oven-dried syringe. Flasks were flame-dried and cooled under a stream of nitrogen. Dichloromethane (DCM) and 1,2-Dichloroethane (DCE) were distilled from calcium hydride. Tetrahydrofuran (THF) was purified by distillation from sodium-benzophenone/ketyl radical. Methanol was distilled from Mg/I_2. Chemical reagents were purchased from Aldrich and Strem Chemicals. Commercially available aldehydes and enones were purified prior to usage. Deuterated solvents were used as received from Cambridge Isotope Laboratories. Analytical thin-layer chromatography (TLC) was carried out using 0.2-mm commercial silica gel plates (DC-Fertigplatten Kieselgel 60 F_{254}). Flash chromatography was performed on silica gel 60 (200-400 mesh) according to the method of Still.[23] Proton nuclear magnetic resonance (^{1}H NMR) spectra were recorded on a Varian Mercury 400, or Unity+ 300 spectrometer. ^{1}H NMR spectra were obtained at 400 MHz or 300 MHz, as indicated. Chemical Shifts are reported in delta (δ) units, parts per million (ppm) downfield from trimethylsilane. Coupling constants are reported in Hertz (Hz). Carbon-13 nuclear magnetic resonance (^{13}C-NMR) spectra were recorded on a Varian Mercury 400, or Unity+ 300 spectrometer. ^{13}C-NMR spectra were obtained at either 100MHz or 75 MHz, as indicated. Chemical Shifts are reported in delta (δ) units, parts per million (ppm) relative to the center triplet at 77.0 ppm for deuteriochloroform. ^{13}C-NMR spectra were routinely run with broadband decoupling. High-resolution mass spectra (HRMS) were obtained on a Micromass ZAB-

E spectrometer and are reported as m/z (relative intensity). Accurate masses are reported for the molecular ion (M+1) or a suitable fragment ion. FT-IR spectra were obtained using a Nicolet Impact 410 spectrometer. Melting points were obtained on a Thomas-Hoover Unimelt apparatus in open capillaries and are uncorrected.

3.8.2 General Procedure for the Intermolecular Hydrogen-Mediated Reductive Coupling of Enones and Aldehydes

To a 13 mm x 100 mm test-tube charged with Li_2CO_3 (0.662 mmol, 10 mol%), Fur_3P (0.0790 mmol, 12 mol%), $Rh(COD)_2OTf$ (0.0331 mmol, 5 mol%), and aldehyde (0.662 mmol, 100 mol%) was added dichloromethane (1.0 M). Then the test-tube was sealed and the reaction system was purged with argon and then with hydrogen for 20 seconds each. The reaction was placed under one atmosphere of hydrogen using a balloon. Enone (1.99 mmol, 300 mol%) was added to the reaction mixture and it was stirred until consumption of aldehyde, which was monitored by TLC. The products were separated by column chromatography. For entry **3.1a** and **3.1b** the reaction was conducted in dichloromethane (0.3 M) using enone (150 mol%). For entry **3.4a** and **3.4b**, the reaction was conducted using $Rh(COD)_2OTf$ (2 mol%), 2-Fur_3P (4.8 mol%), Li_2CO_3 (4 mol%), and enone (500 mol%). For entry **3.8a** and **3.8b**, the reaction was conducted using $Rh(COD)_2OTf$ (10 mol%), 2-Fur_3P (24 mol%), Li_2CO_3 (20 mol%), and enone (300 mol%).

3.8.3 PREPARATION OF THE 3,5 DINITROBENZOATE OF 3.11

A solution of alcohol **3.10** (0.23 mmol, 100 mol%) in THF (1.0 mL, 0.23 M) was cooled to 0 °C under an atmosphere of argon. To the reaction mixture was added pyridine (0.25 mmol, 110 mol%) and 3,5-dinitrbenzoyl chloride (0.25 mmol, 110 mol%). The reaction mixture was allowed to stir for 18 hours, at which point the reaction mixture was diluted with ether and the ethereal layer was washed with water. The organic phase was collected, dried ($MgSO_4$), filtered and evaporated. Chromatographic purification of the residue provides the title compound as a viscous oil in 68% yield. Crystallization from an ether-hexane mixture provides **3.11** as clear needles (MP = 105-106 °C).

3.8.4 GENERAL PROCEDURE FOR THE INTERMOLECULAR HYDROGEN-MEDIATED REDUCTIVE COUPLING OF ENONES AND ACTIVATED KETONES

To a 50 mL round-bottomed flask charged with K_2CO_3 (1.00 mmol, 100 mol%), Ph_3P (0.12 mmol, 12 mol%), $Rh(COD)_2OTf$ (0.05 mmol, 5 mol%), and α-ketoester, 1-(3-bromophenyl)propane-1,2-dione, (1.00 mmol, 100 mol%) was added dichloromethane (0.3 M). Next, the 50 mL round-bottom flask was equipped with a reflux condenser. The reaction system was purged with argon and then with hydrogen for 20 seconds each. The reaction was placed under one atmosphere of hydrogen using a balloon, and enone (1.50 mmol, 150 mol%) was added to the reaction mixture. The reaction mixture was stirred at 35 °C until consumption of α-ketoester, which was monitored by TLC. The products were separated by column chromatography.

3.8.5 General Procedure for the Synthesis of 3,5-Disubstituted Pyridazines *via* Intermolecular Cross Aldol Additions of Enals and Glyoxals

To a 50 mL round-bottomed flask under an atmosphere or argon (g) charged with KOAc (1.0 mmol, 100 mol%), Ph_3P (0.024 mmol, 2.4 mol%), $Rh(COD)_2OTf$ (0.01 mmol, 1 mol%), was added 1,2-dichloroethane (10 mL, 0.1 M). The resulting solution stirred for 5 min at which point the glyoxal monohydrate[24] (1.0 mmol, 100 mol%) was added. The system was flushed with hydrogen (g) and stirred under 1 atmosphere of hydrogen (g) at ambient temperature until complete consumption of the glyoxal was observed by TLC, at which point hydrazine (10 mmol, 1000 mol%), was added as a methanolic solution (10 mL, 1.0 M). The reaction mixture was allowed to stir for 45 minutes. Evaporation of the reaction mixture onto silica gel and purification by silica gel chromatography provides the 3,5-disubstituted pyridazines.

The reactions preformed with crotonaldehyde were conducted in tetrahydrofuran (0.05M) at 40 °C with a 5 mol% loading of $Rh(COD)_2OTf$ and a 12 mol% loading of Ph_3P. Compounds **3.17** and **3.22** are known and fully characterized.[21]

3.9 SPECTROSCOPIC CHARACTERIZATION DATA

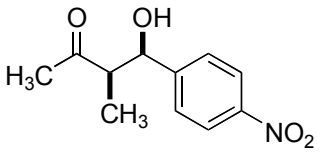

3.1a

4-Hydroxy-3-methyl-4-(4-nitro-phenyl)-butan-2-one (3.1a). ^{1}H NMR (400 MHz, $CDCl_3$): δ 1.06 (d, *J* = 7.2 Hz, 3H), 2.24 (s, 3H), 2.86 (dq, *J* = 3.0, 7.3 Hz, 1H), 3.57 (d, *J* = 2.4 Hz, 1H), 5.28-5.29 (m, 1H), 7.51-7.55 (m, 2H), 8.18-8.22 (m, 2H). ^{13}C NMR (75 MHz, $CDCl_3$): δ 9.4, 29.1, 52.3, 71.6, 123.5, 126.7, 147.1, 149.1, 213.4. HRMS: Calcd [M+1] for $C_{11}H_{13}NO_4$: 224.0923; Found: 224.0925. FTIR (film): 3447, 3057, 2985, 1701, 1604, 1522, 1348, 1264, 1176, 1109, 853, 737 cm^{-1}.

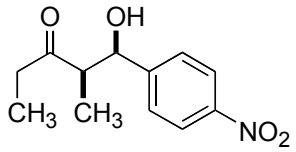

3.1b

1-Hydroxy-2-methyl-1-(4-nitro-phenyl)-pentan-3-one (3.1b). ^{1}H NMR (300 MHz, $CDCl_3$): δ 1.04 (d, *J* = 7.2 Hz, 3H), 1.07 (t, *J* = 7.3 Hz, 3H), 2.46 (dq, *J* = 18.2, 7.2 Hz, 1H), 2.62 (dq, *J* = 18.2, 7.3 Hz, 1H), 2.85 (dq, *J* = 3.2, 7.3 Hz, 1H), 3.63 (d, *J* = 2.3 Hz, 1H), 5.22-5.24 (m, 1H), 7.50-7.54 (m, 2H), 8.18-8.22 (m, 2H). ^{13}C NMR (75 MHz, $CDCl_3$): δ 7.5, 9.9, 35.1, 51.4, 72.0, 123.4, 126.7, 147.1, 149.1, 216.1. HRMS: Calcd [M+1] for $C_{12}H_{15}NO_4$: 238.1079; Found: 238.1080. FTIR (film): 3945, 3686, 3500,

3054, 2984, 2877, 2686, 2306, 1699, 1606, 1522, 1422, 1349, 1265, 1111, 979, 896, 852, 738 cm^{-1}.

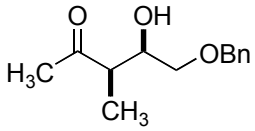

3.2a

5-Benzyloxy-4-hydroxy-3-methyl-pentan-2-one (3.2a). ^{1}H NMR (400 MHz, $CDCl_3$): 1.14 (d, *J* = 7.2 Hz, 3H), 2.16 (s, 3H), 2.61-2.77 (dq, *J* = 5.1, 7.2 Hz, 1H), 2.90 (d, *J* = 2.7 Hz, 1H), 3.41-3.53 (m, 2H), 4.09-4.10 (m, 1H), 4.51 (s, 2H), 7.26-7.36 (m, 5H). ^{13}C NMR (100 MHz, $CDCl_3$): 11.0, 29.2, 48.6, 70.2, 71.6, 73.3, 127.6, 127.7, 128.3, 137.7, 212.2. HRMS Calcd [M+1] for $C_{13}H_{18}O_3$: 223.1334; Found: 223.1330. FTIR (film): 3439, 3031, 2920, 2867, 1704, 1455, 1360, 1252, 1207, 1181, 1094, 1028, 957, 916, 739, 699 cm^{-1}.

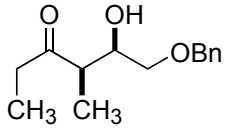

3.2b

6-Benzyloxy-5-hydroxy-4-methyl-hexan-3-one (3.2b). ^{1}H NMR (400 MHz, $CDCl_3$): 1.00 (t, *J* = 7.4, 3H), 1.12 (d, *J* = 7.2 Hz, 3H), 2.40-2.57 (m, 2H), 2.73-2.80 (dq, *J* = 5.1, 7.2 Hz, 1H), 2.93 (s, 1H), 3.40-3.47 (m, 2H), 4.05 (q, *J* = 5.4, 1H), 4.50 (s, 2H), 7.26-7.36 (m, 5H). ^{13}C NMR (100 MHz, $CDCl_3$): 7.4, 11.5, 35.2, 47.6, 70.5, 71.6, 73.3, 127.7, 128.3, 137.7, 214.9. HRMS Calcd [M+1] for $C_{14}H_{20}O_3$: 237.1491; Found:

237.1488. FTIR (film): 3502, 3064, 3031, 2977, 2938, 1705, 1497, 1455, 1410, 1376, 1250, 1208, 1099, 1028, 976, 915, 738, 699 cm^{-1}.

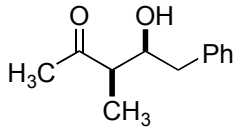

3.3a

4-Hydroxy-3-methyl-5-phenyl-pentan-2-one (3.3a.) ^{1}H NMR (400 MHz, $CDCl_3$): δ 1.23 (d, *J* = 7.2 Hz, 3H), 2.16 (s, 3H), 2.56 (dq, *J* = 3.4, 7.2 Hz, 1H), 2.67-2.68 (br, 1H), 2.69 (dd, *J* = 13.7, 5.8 Hz, 1H), 2.79 (dd, *J* = 13.7, 7.9 Hz, 1H), 4.18-4.22 (m, 1H), 7.20-7.26 (m, 3H), 7.28-7.33 (m, 2H). ^{13}C NMR (100 MHz, $CDCl_3$): δ 9.9, 29.1, 40.3, 49.9, 72.0, 126.5, 128.5, 129.2, 138.1, 213.4. HRMS: Calcd [M+1] for $C_{12}H_{16}O_2$: 193.1229; Found: 193.1227. FTIR (film): 3501, 3054, 2985, 2685, 2306, 1701, 1603, 1496, 1455, 1358, 1266, 1171, 1031, 909, 896,734 cm^{-1}.

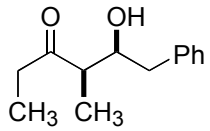

3.3b

5-Hydroxy-4-methyl-6-phenyl-hexan-3-one (3.3b). ^{1}H NMR (400 MHz, $CDCl_3$): δ 1.03 (t, *J* = 7.4 Hz, 3H), 1.22 (d, *J* = 7.2 Hz, 3H), 2.43 (dq, *J* = 18.1, 7.3 Hz, 1H), 2.52 (dq, *J* = 18.1, 7.3 Hz, 1H), 2.59 (dq, *J* = 3.4, 7.2 Hz, 1H), 2.68 (dd, *J* = 13.5, 6.0 Hz, 1H), 2.72-2.72 (m, 1H), 2.79 (dd, *J* = 13.7, 8.2 Hz, 1H), 4.14-4.19 (m, 1H), 7.20-7.33 (m, 5H). ^{13}C NMR (100 MHz, $CDCl_3$): δ 7.5, 10.3, 35.0, 40.3, 48.8, 72.2, 126.4,

128.4, 129.1, 138.2, 216.1. HRMS: Calcd [M+1] for $C_{13}H_{18}O_2$: 207.1385; Found: 207.1385. FTIR (film): 3943, 3512, 3054, 2984, 2941, 2685, 2305, 1698, 1604, 1496, 1455, 1421, 1379, 1265, 1110, 1030, 976, 896, 737 cm^{-1}.

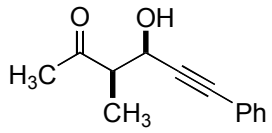

3.4a

4-Hydroxy-3-methyl-6-phenyl-hex-5-yn-2-one (3.4a). ^1H NMR (400 MHz, $CDCl_3$): 1.37 (d, *J* = 7.2 Hz, 3H), 2.25 (s, 3H), 2.83-2.89 (dq, *J* = 4.4, 7.2 Hz, 1H), 3.21 (s, 1H), 4.90 (d, *J* = 4.4 Hz, 1H), 7.27-7.32 (m, 3H), 7.41-7.43 (m, 2H). ^{13}C NMR (100 MHz, $CDCl_3$): 11.6, 29.0, 52.0, 63.5, 85.6, 87.6, 122.2, 128.2, 128.5, 131.6, 211.6. HRMS Calcd [M+1] for $C_{13}H_{14}O_2$: 203.1072; Found: 203.1075. FTIR (film): 3436, 3057, 2984, 2937, 1705, 1599, 1491, 1457, 1443, 1420, 1359, 1266, 1028, 967, 759, 737 cm^{-1}.

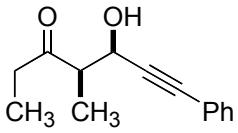

3.4b

5-Hydroxy-4-methyl-7-phenyl-hept-6-yn-3-one (3.4b). ^1H NMR (400 MHz, $CDCl_3$): 1.07 (t, *J* = 7.2 Hz, 3H), 1.36 (d, *J* = 7.2 Hz, 3 H), 2.52-2.64 (m, 2H), 2.85-2.91 (dq, *J* = 4.6, 7.2 Hz,, 1H), 3.26 (s, 1H), 4.87 (d, *J* = 4.4 Hz, 1H), 7.26-7.33 (m, 3H), 7.39-

7.43 (m, 2H). ^{13}C NMR (100 MHz, $CDCl_3$): 7.4, 11.9, 35.0, 51.2, 63.6, 85.5, 87.8, 122.3, 128.2, 128.4, 131.6, 214.3. HRMS: Calcd [M+1] for $C_{14}H_{16}O_2$: 217.1229; Found: 217.1230. FTIR (film): 3426, 2978, 2938, 1707, 1643, 1599, 1490, 1459, 1443, 1407, 1378, 1266, 1029, 978, 758, 737 cm^{-1}.

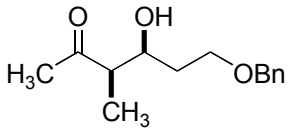

3.5a

6-Benzyloxy-4-hydroxy-3-methyl-hexan-2-one (3.5a). ^{1}H NMR (400 MHz, $CDCl_3$): 1.14 (d, *J* = 7.2 Hz, 3H), 1.61-1.68 (m, 1H), 1.73-1.82 (m, 1H), 2.18 (s, 3H), 2.57-2.66 (m, 1H), 3.28 (d, *J* = 2.1, 1 H), 3.60-3.71 (m, 2H), 4.10-4.13 (m, 1H), 4.51 (s, 2H), 7.26-7.36 (m, 5H). ^{13}C NMR (100 MHz, $CDCl_3$): 10.6, 29.3, 33.6, 51.5, 68.5, 70.5, 73.2, 127.5, 127.6, 128.3, 137.8, 212.8. HRMS Calcd [M+1] for $C_{14}H_{20}O_3$: 237.1491; Found: 237.1496. FTIR (film): 3433, 3031, 2924, 2868, 1701, 1455, 1362, 1207, 1181, 1098, 1028, 737, 699 cm^{-1}.

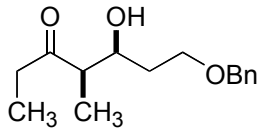

3.5b

7-Benzyloxy-5-hydroxy-4-methyl-heptan-3-one (3.5b). ^{1}H NMR (400 MHz, $CDCl_3$): 1.03 (t, *J* = 7.4 Hz, 3H), 1.13 (d, *J* = 7.2 Hz, 3H), 1.60-1.67 (m, 1H), 1.80-1.71

(m, 1H), 2.45-2.56 (dq, *J* = 2.7, 7.2 Hz, 2H), 2.58-2.65 (dq, *J* = 4.4, 8.2 Hz, 1H), 3.35 (s, 1H), 3.60-3.70 (m, 2H), 4.06-4.09 (m, 1H), 4.5 (s, 2H), 7.25-7.36 (m, 5H). ^{13}C NMR (100 MHz, $CDCl_3$): 7.5, 11.0, 33.6, 35.3, 50.4, 68.5, 70.6, 73.2, 127.5, 127.6, 128.3, 137.8, 215.5. HRMS Calcd [M+1] for $C_{15}H_{22}O_3$: 251.1647; Found: 251.1648. FTIR (film): 3501, 2975, 2938, 2876, 1707, 1455, 1411, 1364, 1099, 1028, 975, 739, 699 cm^{-1}.

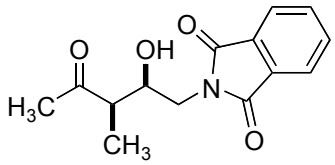

3.6a

2-(2-Hydroxy-3-methyl-4-oxo-pentyl)-isoindole-1,3-dione (3.6a). ^{1}H NMR (400 MHz, $CDCl_3$): δ 1.29 (d, *J* = 7.5 Hz, 3H), 2.23 (s, 3H), 2.68 (dq, *J* = 4.2, 7.2 Hz, 1H), 2.93-2.95 (m, 1H), 3.75 (dd, *J* = 14.4, 4.4 Hz, 1H), 3.85 (dd, *J* = 14.2, 7.4 Hz, 1H), 4.25-4.30 (m, 1H), 7.72-7.74 (m, 2H), 7.84-7.88 (m, 2H). ^{13}C NMR (100 MHz, $CDCl_3$): δ 10.9, 29.2, 41.7, 49.4, 69.9, 123.7, 132.1, 134.4, 169.0, 212.4. HRMS: Calcd [M] for $C_{14}H_{15}NO_4$: 261.1001; Found: 261.1004. FTIR (film): 3435, 3053, 2978, 2935, 2872, 2306, 1640, 1446, 1383, 1351, 1266, 1114, 1076, 896, 743 cm^{-1}. MP = 140-141 °C.

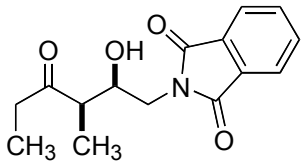

3.6b

2-(2-Hydroxy-3-methyl-4-oxo-hexyl)-isoindole-1,3-dione (3.6b). ^{1}H NMR (400 MHz, $CDCl_3$): δ 1.05 (t, *J* = 7.2 Hz, 3H), 1.27 (d, *J* = 7.2 Hz, 3H), 2.51 (dq, *J* = 18.1, 7.2 Hz, 1H), 2.60 (dq, *J* = 18.1, 7.2 Hz, 1H), 2.69 (dq, *J* = 4.3, 7.2 Hz, 1H), 3.10 (d, *J* = 3.8 Hz, 1H), 3.73 (dd, *J* = 14.2, 4.6 Hz, 1H), 3.85 (dd, *J* = 14.0, 7.5 Hz, 1H), 4.23-4.28 (m, 1H), 7.71-7.76 (m, 2H), 7.83-7.88 (m, 2H). ^{13}C NMR (100 MHz, $CDCl_3$): δ 7.4, 10.9, 34.7, 41.3, 48.2, 69.6, 123.3, 131.8, 134.0, 168.6, 214.8. HRMS Calcd [M] for $C_{15}H_{17}NO_4$: 275.1158; Found: 275.1158. FTIR (film): 3454, 3054, 2986, 2305, 2254, 1773, 1714, 1642, 1422, 1397, 1265, 909, 748 cm^{-1}.

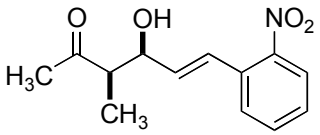

3.7a

4-Hydroxy-3-methyl-6-(2-nitro-phenyl)-hex-5-en-2-one (3.7a). ^{1}H NMR (400 MHz, $CDCl_3$): 1.22 (d, *J* = 7.5 Hz, 3H), 2.26 (s, 3H), 2.80-2.86 (dq, *J* = 3.8, 7.3 Hz, 1H), 3.29 (s, 1H), 4.70 (t, *J* = 4.8 Hz, 1H), 6.14-6.20 (dd, *J* = 15.7, 5.8 Hz, 1H), 7.04-7.10 (dd, *J* = 15.7, 1.4 Hz, 1 H), 7.36-7.43 (m, 1H), 7.53-7.58 (m, 2H), 7.91 (d, *J* = 8.2, 1H). ^{13}C NMR (100 MHz, $CDCl_3$): 10.7, 29.3, 51.3, 71.9, 124.3, 126.4, 128.1, 128.7, 132.4, 133.0, 134.6, 147.6, 212.8. HRMS Calcd [M+1] for $C_{13}H_{15}NO_4$: 249.1001; Found: 249.1003.

FTIR (film): 3426, 2981, 2937, 2878, 1704, 1607, 1571, 1522, 1477, 1443, 1422, 1346, 1267, 1180, 1144, 1127, 1064, 1022, 968, 861, 786, 738, 702 cm^{-1}.

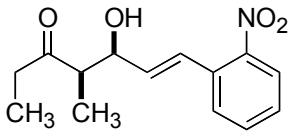

3.7b

5-Hydroxy-4-methyl-7-(2-nitro-phenyl)-hept-6-en-3-one (3.7b). ^{1}H NMR (400 MHz, $CDCl_3$): 1.06 (t, *J* = 7.4 Hz, 3H), 1.21 (d, *J* = 7.2 Hz, 3H), 2.51-2.67 (m, 2H), 2.81-2.88 (dq, *J* = 3.9, 7.4 Hz, 1H), 3.31 (d, *J* = 2.7 Hz, 1H), 4.66 (bs, 1H), 6.14-6.20 (dd, *J* = 15.7, 5.8 Hz, 1H), 7.05-7.09 (dd, *J* = 15.9, 1.2 Hz, 1H), 7.37-7.42 (m, 1H), 7.53-7.58 (m, 2H), 7.9 (d, *J* = 8.2 Hz, 1H). ^{13}C NMR (100 MHz, $CDCl_3$): 7.4, 11.0, 35.3, 50.2, 72.1, 124.3, 126.3, 128.0, 128.7, 132.4, 133.0, 134.6, 147.6, 215.5. HRMS Calcd [M+1] for $C_{14}H_{17}NO_4$: 264.1236; Found: 264.1230. FTIR (film): 3425, 2980, 2939, 2880, 1704, 1648, 1607, 1572, 1525, 1460, 1408, 1347, 1305, 1266, 1112, 1020, 969, 861, 785, 739, 703 cm^{-1}.

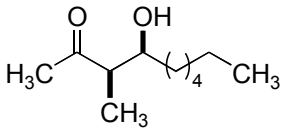

3.8a

4-Hydroxy-3-methyl-decan-2-one (3.8a.) ^{1}H NMR (400 MHz, $CDCl_3$): δ 0.88 (t, *J* = 6.8 Hz, 3H), 1.15 (d, *J* = 7.5 Hz, 3H), 1.26-1.36 (m, 2H), 1.43-1.52 (m, 8H), 2.21

(s, 3H), 2.57 (dq, *J* = 3.0, 7.3 Hz, 1H), 3.92-3.96 (m, 1H). ^{13}C NMR (100 MHz, $CDCl_3$): δ 9.6, 14.0, 22.5, 26.0, 29.1, 29.2, 31.7, 34.0, 50.8, 71.0, 214.0. HRMS: Calcd [M+1] for $C_{11}H_{22}O_2$: 187.1698; Found: 187.1699. FTIR (film): 3942, 3512, 3054, 2931, 2858, 2685, 2306, 1701, 1422, 1359, 1265, 1175, 896, 738 cm^{-1}.

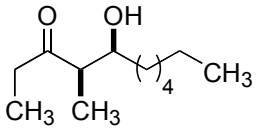

3.8b

5-Hydroxy-4-methyl-undecan-3-one (3.8b). ^{1}H NMR (400 MHz, $CDCl_3$): δ 0.88 (t, *J* = 6.8 Hz, 3H), 1.06 (t, *J* = 7.2 Hz, 3H), 1.13 (d, *J* = 7.2 Hz, 3H), 1.25-1.35 (m, 8H), 1.43-1.52 (m, 2H), 2.48 (dq, *J* = 17.9, 7.3 Hz, 1H), 2.57 (dq, *J* = 18.0, 7.3 Hz, 1H), 2.58 (dq, *J* = 3.0, 7.2 Hz, 1H), 2.73 (br, 1H), 3.87-3.93 (m, 1H). ^{13}C NMR (100 MHz, $CDCl_3$): δ 7.6, 9.9, 14.0, 22.6, 26.0, 29.2, 31.8, 34.0, 35.1, 50.0, 71.1, 216.8. HRMS: Calcd [M] for $C_{12}H_{24}O_2$: 200.1776; Found: 200.1778. FTIR (film): 3447, 3053, 2985, 2932, 2858, 2305, 2253, 1698, 1461, 1422, 1379, 1265, 912, 743 cm^{-1}.

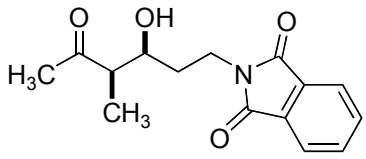

3.9a

2-(3-Hydroxy-4-methyl-5-oxo-hexyl)-isoindole-1,3-dione (3.9a). ^{1}H NMR (400 MHz, $CDCl_3$): δ 1.17 (d, *J* = 7.2 Hz, 3H), 1.67-1.85 (m, 2H), 2.19 (s, 3H),

2.61 (dq, J = 3.8, 7.2 Hz, 1H), 3.20 (d, J = 3.8 Hz, 1H), 3.77-3.93 (m, 3H), 7.71-7.75 (m, 2H), 7.83-7.87 (m, 2H). ^{13}C NMR (100 MHz, $CDCl_3$): δ 10.5, 29.3, 33.0, 34.8, 51.1, 68.4, 123.2, 131.9, 134.0, 168.6, 212.8. HRMS: Calcd [M] for $C_{15}H_{17}NO_4$: 275.1158; Found: 275.1156. FTIR (film): 3469, 3054, 2986, 2305, 2254, 1771, 1710, 1468, 1397, 1372, 1265, 1177, 951, 910, 741 cm^{-1}.

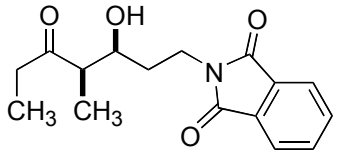

3.9b

2-(3-Hydroxy-4-methyl-5-oxo-heptyl)-isoindole-1,3-dione (3.9b). ^{1}H NMR (400 MHz, $CDCl_3$): δ 1.03 (t, J = 7.2 Hz, 3H), 1.15 (d, J = 7.2 Hz, 3H), 1.67-1.84 (m, 2H), 2.49 (dq, J = 18.1, 7.2 Hz, 1H), 2.57 (dq, J = 18.1, 7.3 Hz, 1H), 2.64 (dq, J = 4.4, 7.2 Hz, 1H), 3.34 (d, J = 4.1 Hz, 1H), 3.77-3.91 (m, 3H), 7.71-7.75 (m, 2H), 7.81-7.87 (m, 2H). ^{13}C NMR (100 MHz, $CDCl_3$): δ 7.4, 11.0, 33.0, 34.8, 35.3, 50.1, 68.6, 123.2, 131.9, 133.9, 168.6, 215.5. HRMS: Calcd [M] for $C_{16}H_{19}NO_4$: 289.1314; Found: 289.1316. FTIR (film): 3466, 3054, 2985, 2305, 2254, 1771, 1710, 1468, 1397, 1265, 952, 911, 741 cm^{-1}.

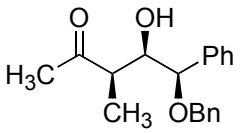

3.10

5-Benzyloxy-4-hydroxy-3-methyl-5-phenyl-pentan-2-one (3.10a). ^{1}H NMR (400 MHz, $CDCl_3$): δ 1.14 (d, *J* = 7.2 Hz, 3H), 2.03 (s, 3H), 2.31 (dq, *J* = 4.3, 7.1 Hz, 1H), 2.81-2.82 (m, 1H), 4.17-4.23 (m, 1H), 4.26 (d, *J* = 11.3 Hz, 1H), 4.32 (d, *J* = 7.2 Hz, 1H), 4.46 (d, *J* = 11.3 Hz, 1H), 7.27-7.43 (m, 10H). ^{13}C NMR (100 MHz, $CDCl_3$): δ 10.1, 28.3, 48.2, 70.7, 75.0, 82.6, 127.6, 127.8, 128.0, 128.4, 128.5, 128.8, 137.6, 137.9, 210.5. HRMS: Calcd [M+1] for $C_{19}H_{22}O_3$: 299.1647; Found: 299.1647. FTIR (film): 3943, 3568, 3055, 2986, 2878, 2306, 1710, 1604, 1494, 1454, 1357, 1265, 1178, 1066, 1028, 988, 910, 738 cm^{-1}.

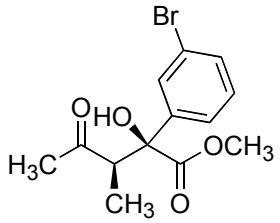

***syn*-3.12**

***syn*-2-(3-Bromo-phenyl)-2-hydroxy-3-methyl-4-oxo-pentanoic acid methyl ester (*syn*-3.12**.) ^{1}H NMR (400 MHz, $CDCl_3$): δ 0.98 (d, *J* = 7.47 Hz, 3H), 2.29 (s, 3H), 3.48-3.56 (q, *J* = 7.5 Hz, 1H), 3.71 (s, 3H), 4.56 (s, 1H), 7.20-7.26 (t, *J* = 7.93 Hz, 1H), 7.31-7.50 (m, 2H), 7.75 (s, 1H). ^{13}C NMR (100 MHz, DMSO): δ 10.5, 28.5, 52.4, 53.7, 78.0, 121.7, 124.6, 128.3, 130.4, 130.5, 143.5, 174.1, 210.1. HRMS: Calcd [M+1] for

$C_{13}H_{16}O_4Br$: 315.02320; Found: 315.0219. FTIR (film): 3498, 2984, 1735, 1592, 1566, 1458, 1361, 1253, 1192, 730 cm^{-1}.

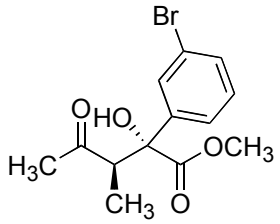

***anti*-3.12**

***anti*-2-(3-Bromo-phenyl)-2-hydroxy-3-methyl-4-oxo-pentanoic acid methyl ester (*anti*-3.12)**. ^{1}H NMR (400 MHz, $CDCl_3$): δ 1.27 (d, *J* = 7.02 Hz, 3H), 2.02 (s, 3H), 3.60-3.67 (q, *J* = 7.10 Hz, 1H), 3.80 (s, 3H), 4.49 (s, 1H), 7.20-7.24 (t, *J* = 7.93 Hz, 1H), 7.41-7.44 (m, 1H), 7.52-7.55 (m, 1H), 7.80 (t, *J* = 1.91 Hz 1H). ^{13}C NMR (100 MHz, DMSO): δ 12.3, 29.5, 52.7, 54.5, 78.9, 121.5, 125.2, 125.8, 128.6, 130.2, 130.6, 143.6, 172.7, 208.3, 208.3. HRMS: Calcd [M+1] for $C_{13}H_{16}O_4Br$: 315.02320; Found: 315.02253. FTIR (film): 3498, 2984, 1735, 1592, 1566, 1458, 1361, 1253, 1192, 730 cm^{-1}.

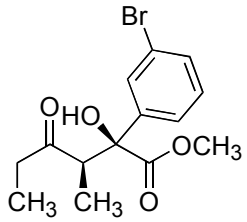

***syn*-3.13**

***syn*-2-(3-Bromo-phenyl)-2-hydroxy-3-methyl-4-oxo-hexanoic acid methyl ester (*syn*-3.13)**. ^{1}H NMR (400 MHz, $CDCl_3$): δ 0.97 (d, *J* = 7.5 Hz, 3H), 1.15 (t, *J* = 7.2

Hz 3H), 2.59-2.74 (m, 2H), 3.50 (q, J = 7.4 Hz, 1H), 3.72 (s, 3H), 4.74 (s, 1H), 7.19-7.28 (t, J = 7.9 Hz, 1H), 7.40-7.54 (m, 2H), 7.76 (s, 1H). ^{13}C NMR (100 MHz, $CDCl_3$): δ 7.4, 10.8, 34.7, 52.2, 53.0, 79.3, 122.7, 123.6, 129.9, 131.0, 141.0, 174.5, 217.5. HRMS: Calcd [M+1] for $C_{14}H_{18}O_4Br$: 329.03886; Found: 329.03973. FTIR (film) 3496, 2980, 2941, 1729, 1699, 1593, 1567, 1434, 1255, 1170, 1112, 789 cm^{-1}.

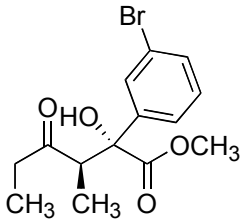

***anti*-3.13**

***anti*-2-(3-Bromo-phenyl)-2-hydroxy-3-methyl-4-oxo-hexanoic acid methyl ester (*anti*-3.13)**. ^{1}H NMR (400 MHz, $CDCl_3$): δ 0.84 (t, J = 7.2 Hz, 3H), 1.27 (d, J = 7.2 Hz 3H), 2.13-2.24 (m, 1H), 2.42-2.56 (m, 1H), 3.65 (q, J = 7.2 Hz, 1H), 3.80 (s, 3H), 4.68 (s, 1H), 7.19-7.24 (t, J = 7.9 Hz, 1H), 7.40 (d, J = 7.9 Hz, 1H), 7.54 (d, J = 7.3 Hz, 1H), 7.79 (s, 1H). ^{13}C NMR (100 MHz, $CDCl_3$): δ 7.1, 13.0, 36.4, 52.3, 53.2, 79.4, 122.7, 124.2, 128.7, 129.9, 131.2, 142.9, 172.2, 215.1. HRMS: Calcd [M+1] for $C_{14}H_{18}O_4Br$: 329.03886; Found: 329.03973. FTIR (film) 3496, 2980, 2941, 1729, 1699, 1593, 1567, 1434, 1255, 1170, 1112, 789 cm^{-1}.

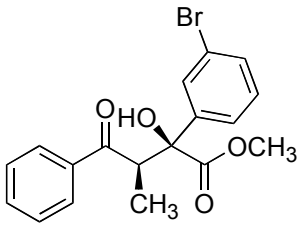

***syn*-3.14**

***syn*-2-(3-Bromo-phenyl)-2-hydroxy-3-methyl-4-oxo-4-phenyl-butyric acid methyl ester (*syn*-3.14)**. ^{1}H NMR (400 MHz, $CDCl_3$): δ 1.0 (d, *J* = Hz, 3H), 3.64 (s 3H), 4.28-4.41 (q, *J* = Hz, 1H), 5.14 (s, 1H), 7.20-7.33 (t, *J* = Hz, 1H), 7.41-7.57 (q, *J* = Hz, 3H), 7.60 (d, *J* = Hz, 2H), 7.83 (s, 1H) 8.03 (d, *J* = Hz 2H). ^{13}C NMR (100 MHz, $CDCl_3$): δ 12.1, 48.0, 52.9, 79.7, 122.8, 123.7, 128.3, 128.5, 128.7, 129.9, 131.1, 133.9, 135.0, 141.1, 174.5, 206.6. HRMS: Calcd [M+1] for $C_{18}H_{18}O_4Br$: 377.0388; Found: 377.0390. FTIR (film) 3495, 3065, 2983, 1728, 1664, 1596, 1567, 1449, 1425, 1348, 1257, 1221, 1160, 1094, 790, 729, 689 cm^{-1}. MP = 87-89 °C

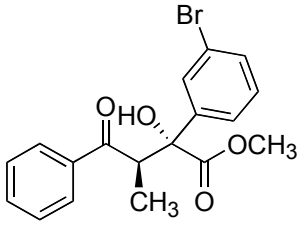

***anti*-3.14**

***anti*-2-(3-Bromo-phenyl)-2-hydroxy-3-methyl-4-oxo-4-phenyl-butyric acid methyl ester (*anti*-3.14)**. ^{1}H NMR (400 MHz, $CDCl_3$): δ 1.39-1.45 (d, *J* = 7.2 Hz, 3H), 3.82 (s 3H), 4.55-4.68 (q, *J* = 7.2 Hz, 1H), 5.06 (s, 1H), 7.06-7.14 (t, *J* = 7.9 Hz, 1H), 7.24-7.35 (m, 1H), 7.38-7.62 (m, 4H), 7.81-7.91 (t, *J* = 7.8 Hz, 3H). ^{13}C NMR (100

MHz, $CDCl_3$): δ 14.3, 46.7, 53.2, 80.1, 122.7, 124.0, 128.3, 128.8, 129.8, 131.1, 134.0, 135.5, 143.4, 172.1, 204.4. HRMS: Calcd [M+1] for $C_{18}H_{18}O_4Br$: 377.0388; Found: 377.0390. FTIR (film) 3495, 3065, 2983, 1728, 1664, 1596, 1567, 1449, 1425, 1348, 1257, 1221, 1160, 1094, 790, 729, 689 cm^{-1}.

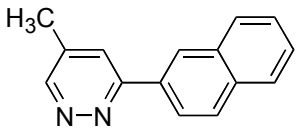

3.18

5-Methyl-3-naphthalen-2-yl-pyridazine (3.18). ^1H NMR (400 MHz, $CDCl_3$): δ 8.96 (d, *J* = 1.7 Hz, 1H); 8.50 (d, *J* = 1.0 Hz, 1H); 8.19 (dd, *J* = 8.7, 1.9 Hz, 1H); 7.94 (d, *J* = 8.5 Hz, 1H); 7.92 (m, 1H); 7.86 (m, 1H); 7.72 (m, 1H); 7.51 (m, 2H); 2.38 (s, 3H). ^{13}C NMR (100 MHz, $CDCl_3$): δ 158.5, 151.5, 137.8, 133.9, 133.6, 133.2, 128.6, 128.6, 127.6, 126.9, 126.9, 126.4, 124.2, 124.2, 18.4. . HRMS Calcd for $C_{15}H_{13}N_2$ [M+1]: 221.1079; Found: 221.1083. FTIR (film): 1636.31 cm^{-1}. MP = 137-140 °C.

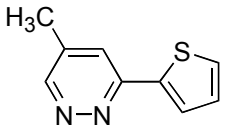

3.19

5-Methyl-3-thiophen-2-yl-pyrizadine (3.19). ^1H NMR (400 MHz, $CDCl_3$): δ 8.87 (d, 1H, *J* = 1.4 Hz); 7.65 (dd, 1H, *J* = 3.8, 1.0 Hz); 7.57 (d, 1H, *J* = 1.0 Hz); 7.47 (dd, 1H, *J* = 5.0, 0.9 Hz); 7.14 (dd, 1H, *J* = 5.1, 3.8 Hz); 2.38 (s, 3H). ^{13}C NMR (100 MHz, $CDCl_3$): δ 154.4, 151.4, 140.6, 137.8, 129.0, 128.0, 126.0, 122.4, 18.4. HRMS

Calcd for $C_9H_9N_2S$ [M+1]: 177.0486; Found: 177.0489. IR (film): 1647, 1598, 1445 cm^{-1}. MP = 118-120 °C.

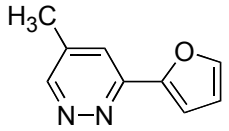

3.20

3-Furan-2-yl-5-methyl pyridazine (3.20). ^{1}H NMR (400 MHz, $CDCl_3$): δ 8.89 (d, 1H, *J* = 1.7 Hz); 7.65 (dd, 1H, *J* = 2.0, 1.0 Hz); 7.53 (dd, 1H, *J* = 1.7, 0.7 Hz); 7.32 (d,1H, *J* = 3.4 Hz); 6.58 (dd, 1H, J = 3.4, 1.7 Hz); 3.39 (s, 3H). ^{13}C NMR (100 MHz, $CDCl_3$): δ 151.6, 151.2, 150.8, 144.3, 137.8, 121.9, 112.4, 110.3, 18.5. HRMS Calcd for $C_9H_9N_2O$ [M+1]: 161.0715; Found 161.0723. IR (film): 1636, 1598, 1489 cm^{-1}. MP = 77-78 °C.

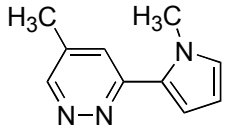

3.21

5-Methyl-3-(1-methyl-1H-pyrrol-2-yl)-pyridazine (3.21). ^{1}H NMR ($CDCl_3$, 400 MHz): δ 8.81-8.80 (d, *J* = 2.1 Hz, 1H); 7.48-7.47(q, *J* = 0.91 Hz, 1H); 6.80-6.79 (m, 1H); 6.65-6.63 (m, 1H); 6.22-6.21 (dd, *J* = 2.4, 1.4 Hz, 1H); 4.09 (s, 3H); 2.35 (s, 3H). ^{13}C NMR ($CDCl_3$, 100 MHz): δ 154.1, 150.0, 137.2, 128.9, 127.8, 124.4, 112.0, 108.0, 37.8, 18.3. HRMS Calcd for $C_{10}H_{12}N_3$ [M+1]: 174.1031; Found: 174.1032. FTIR (film) 2956.94,1601.28 cm^{-1}.

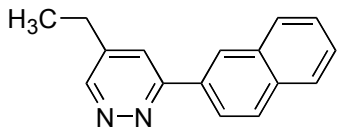

3.23

5-Ethyl-3-naphthalen-2-yl-pyridazine (3.23). ^{1}H NMR ($CDCl_3$, 400 MHz) δ 9.03 (s, 1H); 8.53(s, 1H); 8.23-8.21 (dd, *J* = 8.5, 1.4 Hz, 1H); 7.98-7.94 (m, 2H); 7.88-7.87 (d, *J* = 5.1 Hz, 1H); 7.78 (s, 1H); 7.54-7.52 (m, 2H); 2.77-2.71 (q, *J* = 7.6 Hz, 2H), 1.37-1.33 (t, *J* = 7.7 Hz, 3H). ^{13}C NMR ($CDCl_3$, 100 MHz) δ 158.8, 150.8, 143.4, 133.9, 133.7, 133.2, 128.7, 128.6, 127.6, 126.9, 126.8,126.4, 124.2, 122.9, 25.8, 13.7. HRMS Calcd for $C_{16}H_{15}N_2$ (M+1): 235.1235; Found: 235.1227. FTIR (film) 2969.52, 1641.61 cm^{-1}. MP = 102-104 ºC.

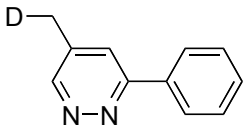

3.24

5-d_1-Methyl-3-phenyl pyridazine (3.24). ^{1}H NMR (400 MHz, $CDCl_3$): δ 8.97 (d, 1H, *J* = 2.0 Hz); 8.04 (dd, 2H, *J* = 8.0, 1.5 Hz); 7.63 (m, 1H); 7.48 (m, 3H); 2.38 (m, 2H). ^{13}C NMR (100 MHz, $CDCl_3$): δ 151.6, 136.4, 129.8, 128.9, 127.1 124.2, 18.3. HRMS Calcd for $C_{11}H_{10}DN_2$ [M+1]: 172.0985; Found 172.0980. FTIR (film) 3039, 1595. MP = 87-88 °C.

3.10 SPECTRA

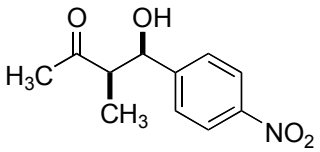

3.1a

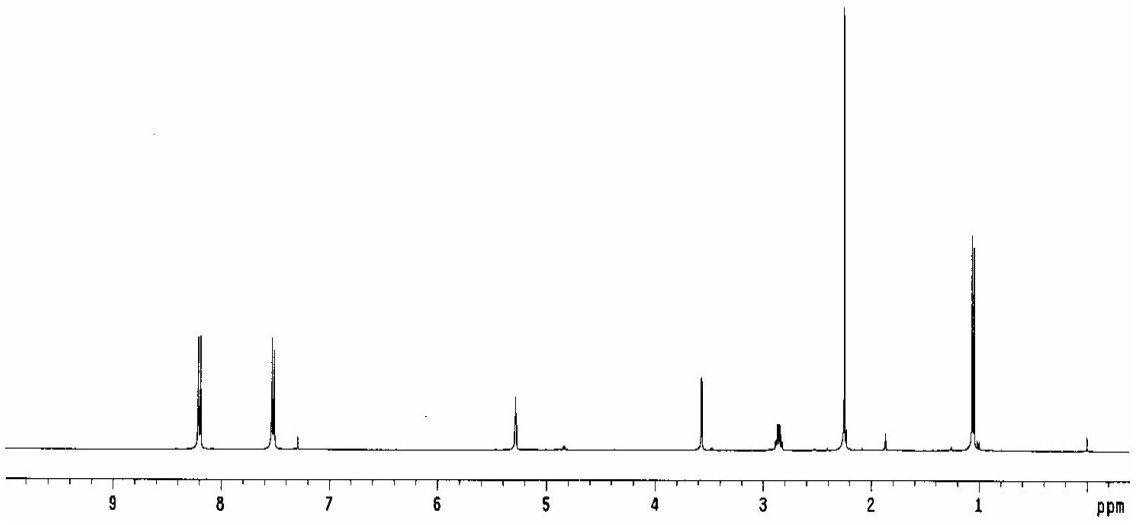

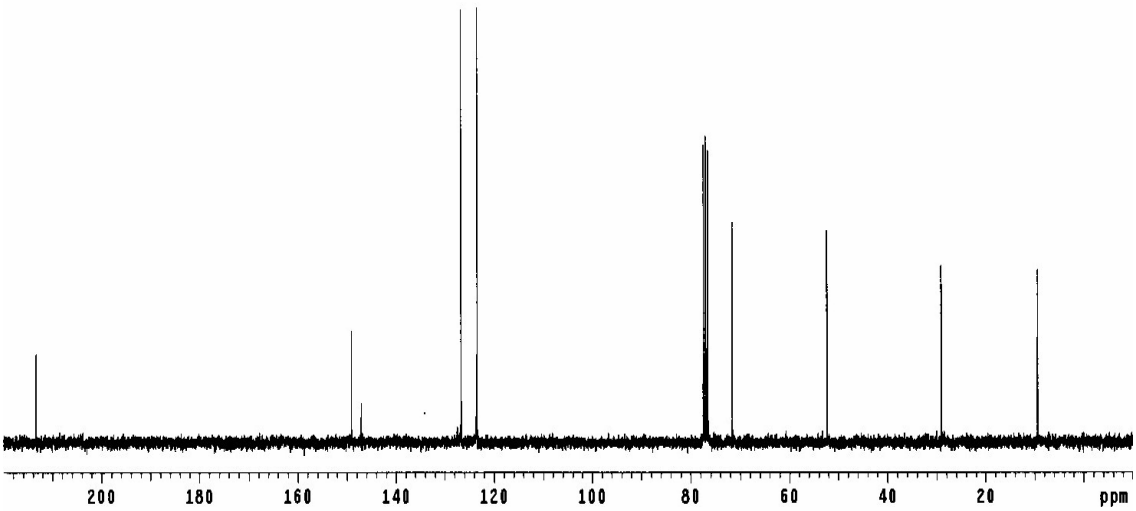

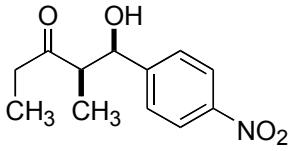
O
OH
CH3
CH3
NO2

3.1b

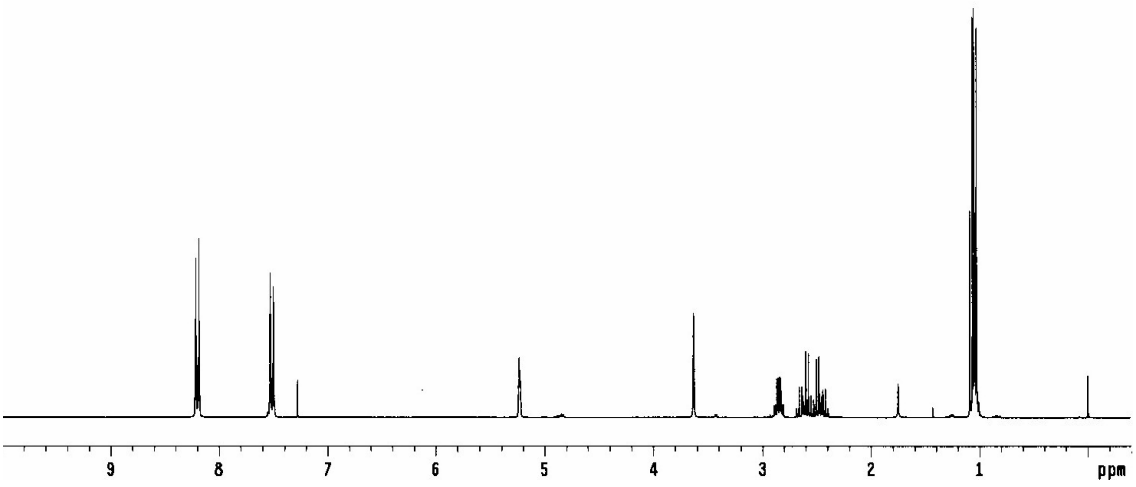
9
8
7
6
5
4
3
2
1
ppm

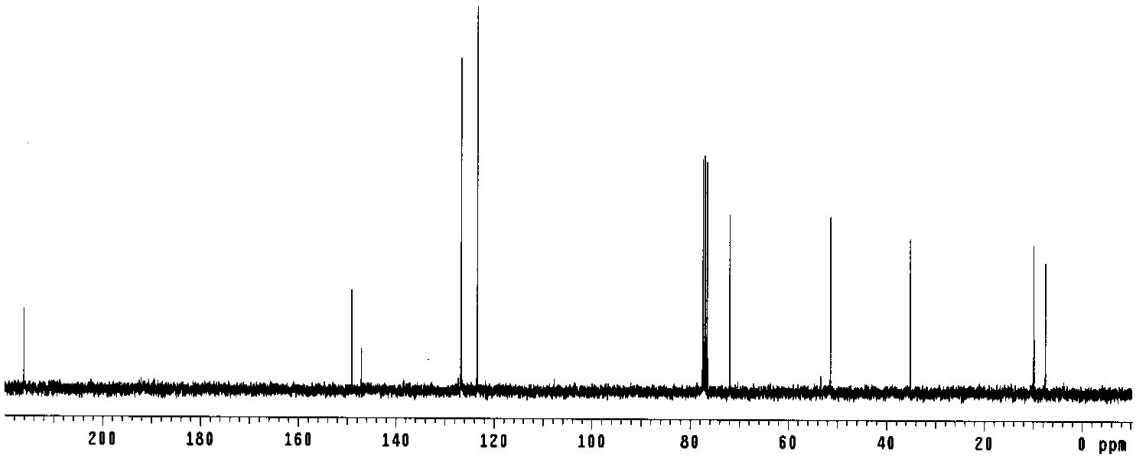
200
180
160
140
120
100
80
60
40
20
0 ppm

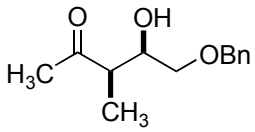
O
OH
OBn
H3C
CH3

3.2a

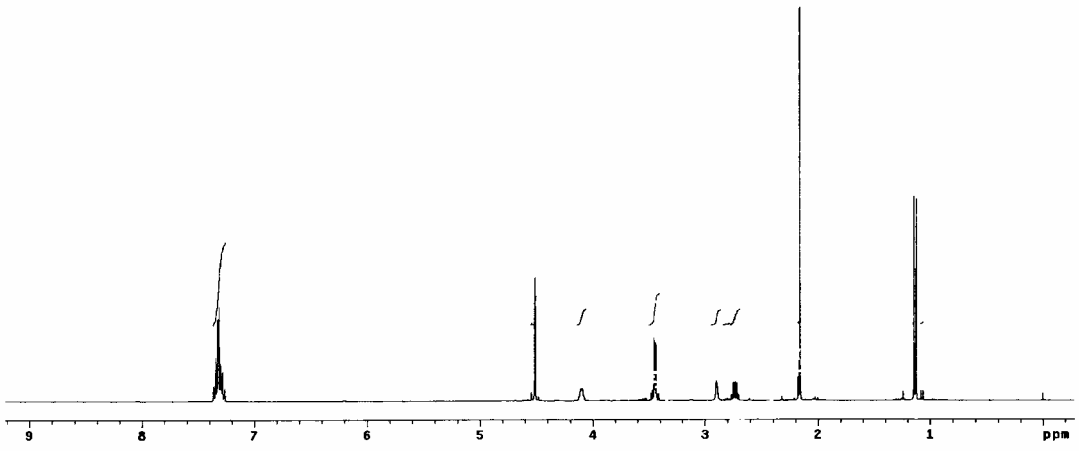
9
8
7
6
5
4
3
2
1
ppm

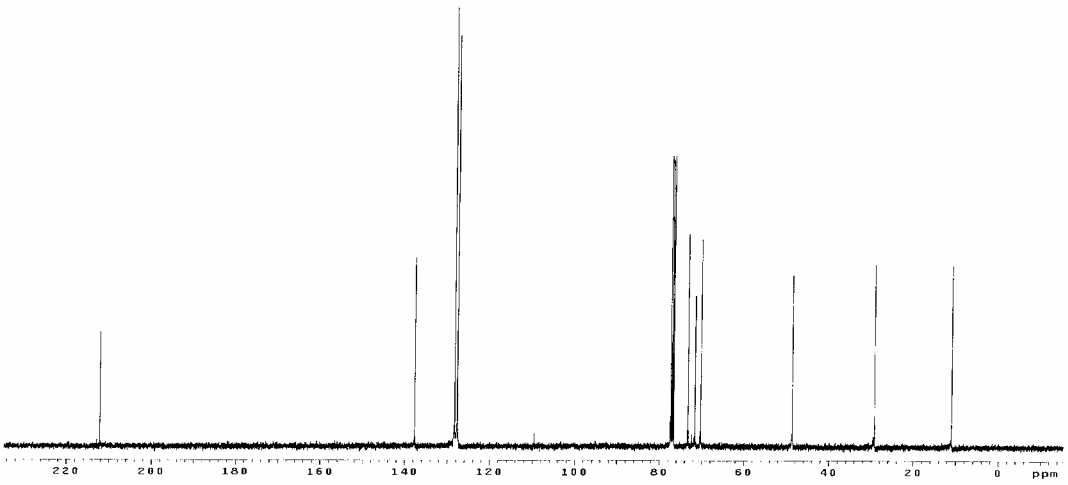
220
200
180
160
140
120
100
80
60
40
20
0
ppm

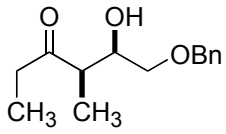
O
OH
OBn
CH3
CH3

3.2b

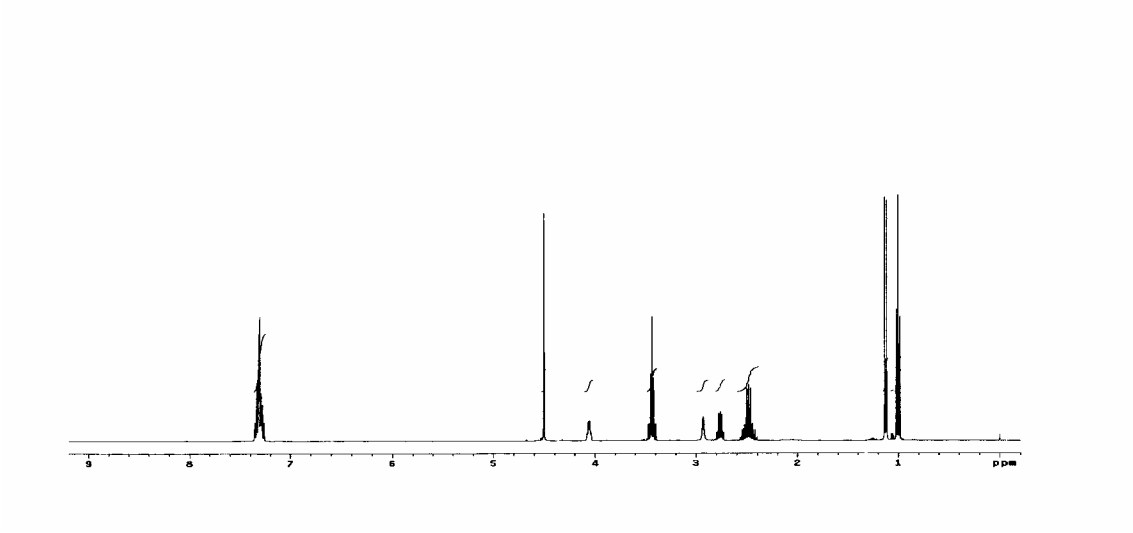
9
8
7
6
5
4
3
2
1
ppm

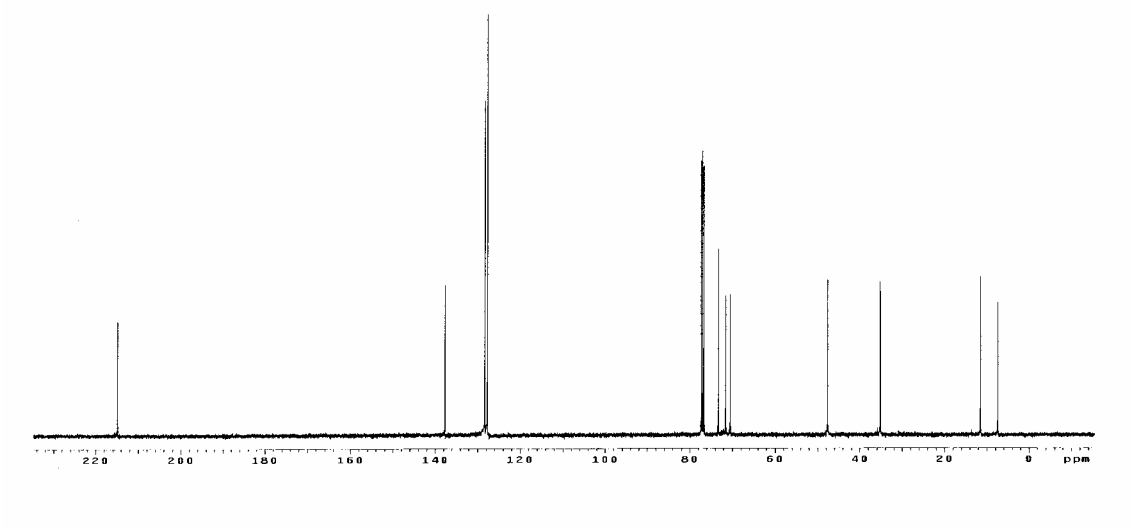
220
200
180
160
140
120
100
80
60
40
20
0
ppm

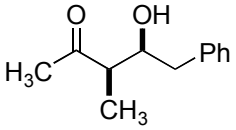
O
OH
Ph
H3C
CH3

3.3a

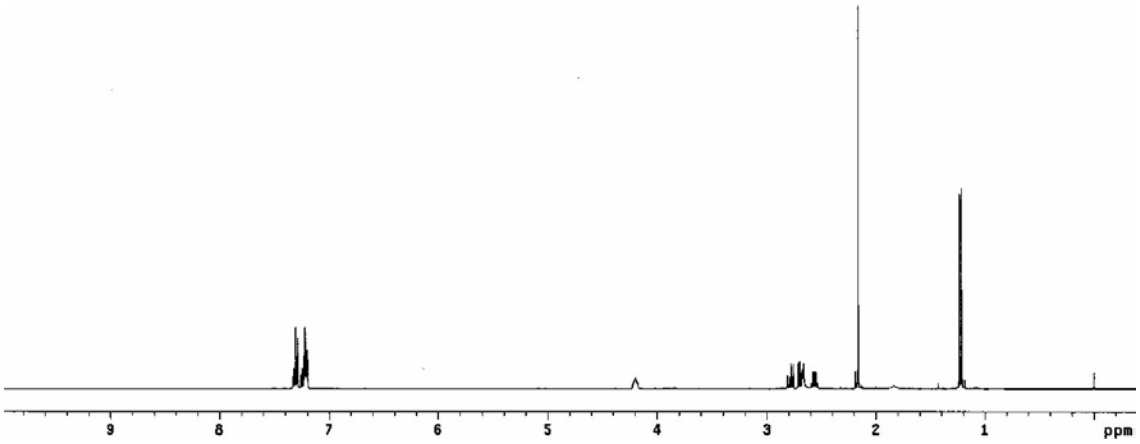
9
8
7
6
5
4
3
2
1
ppm

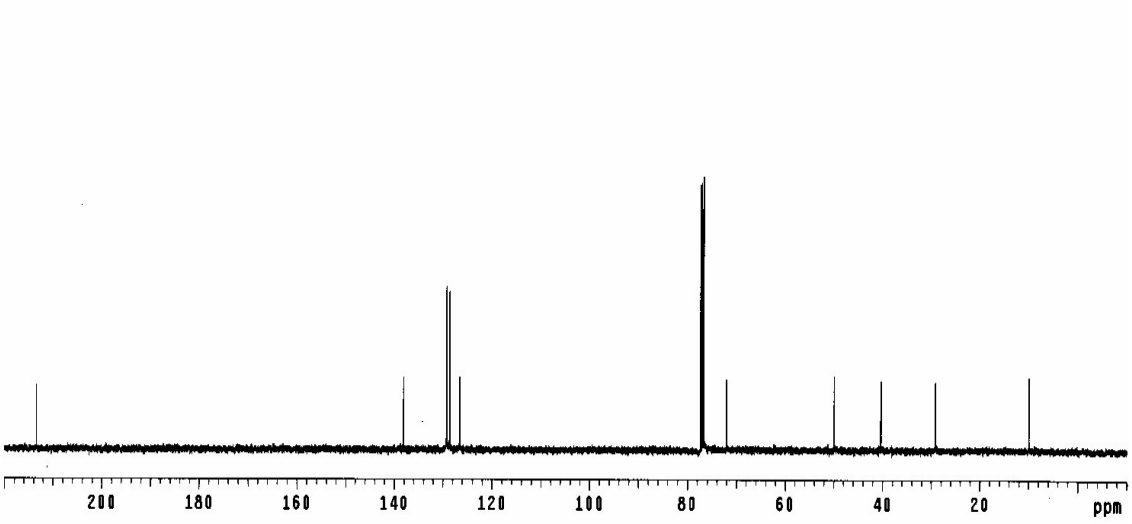
200
180
160
140
120
100
80
60
40
20
ppm

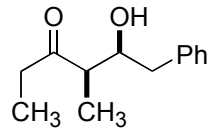
O
OH
Ph
CH3
CH3

3.3b

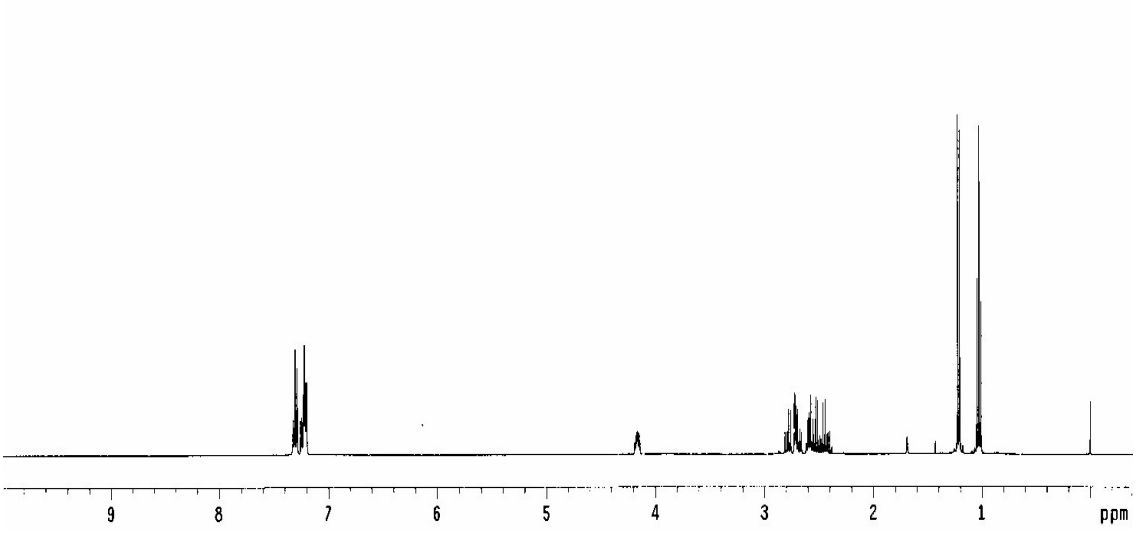
9
8
7
6
5
4
3
2
1
ppm

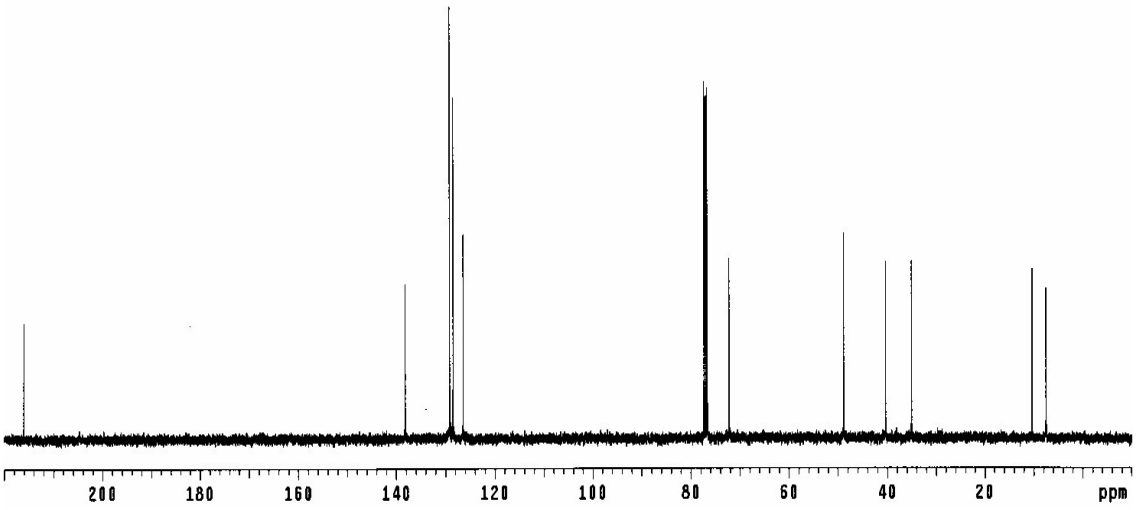
200
180
160
140
120
100
80
60
40
20
ppm

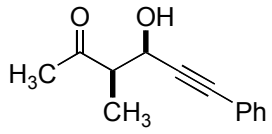
O
OH
H3C
CH3
Ph

3.4a

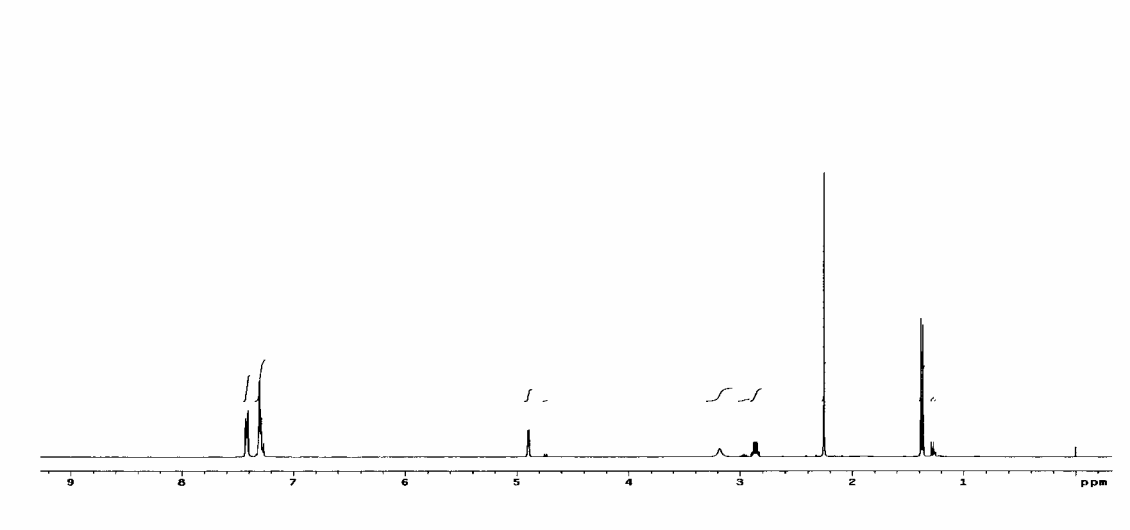
9
8
7
6
5
4
3
2
1
ppm

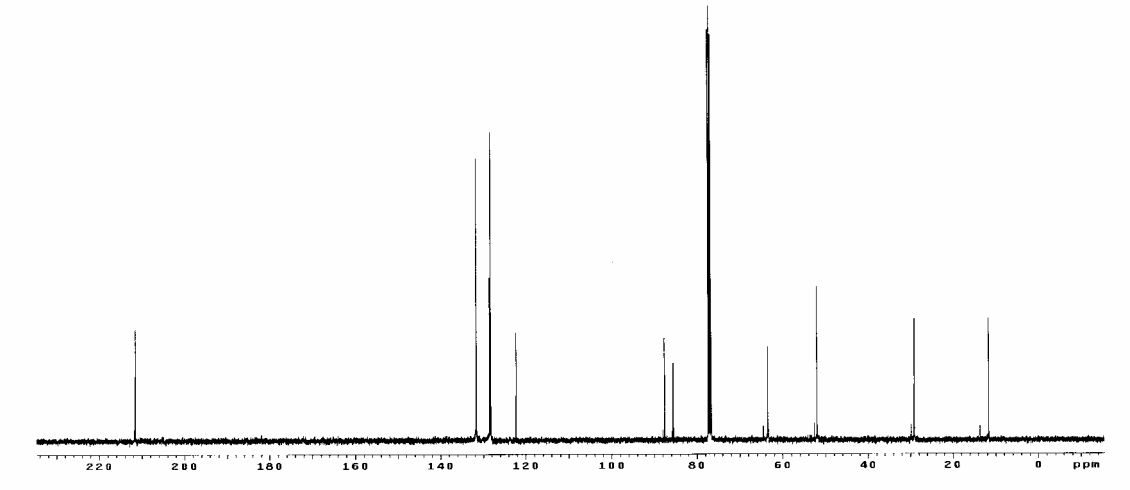
220
200
180
160
140
120
100
80
60
40
20
0
ppm

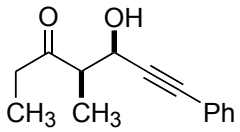
O
OH
CH3
CH3
Ph

3.4b

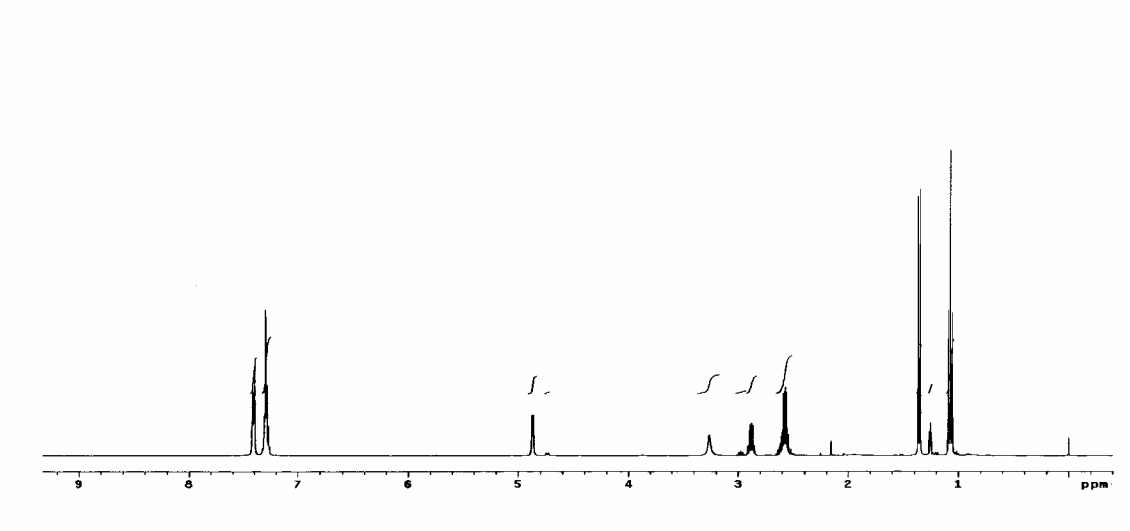
9
8
7
6
5
4
3
2
1
ppm

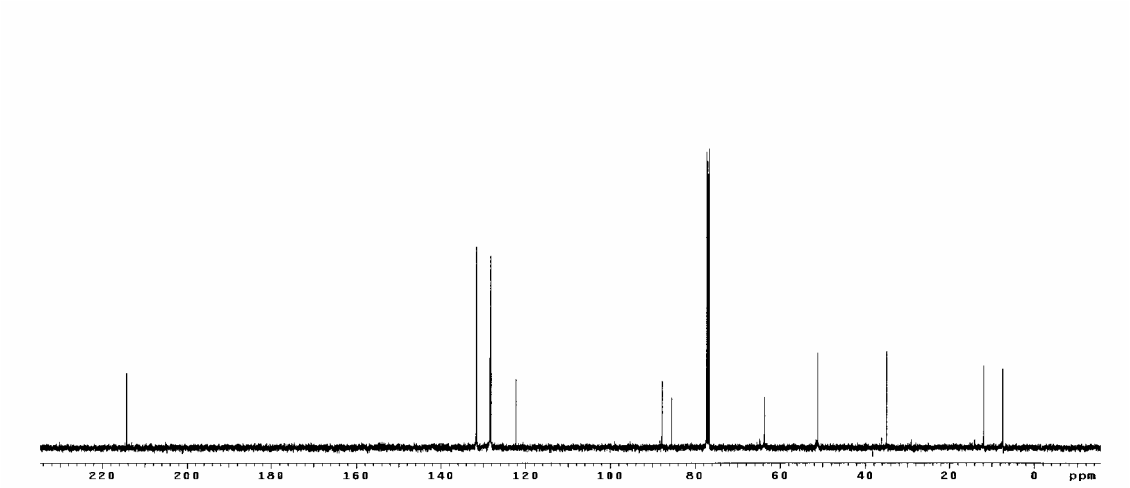
220
200
180
160
140
120
100
80
60
40
20
0
ppm

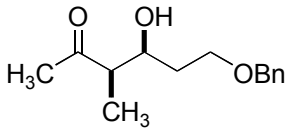
O
OH
H3C
OBn
CH3

3.5a

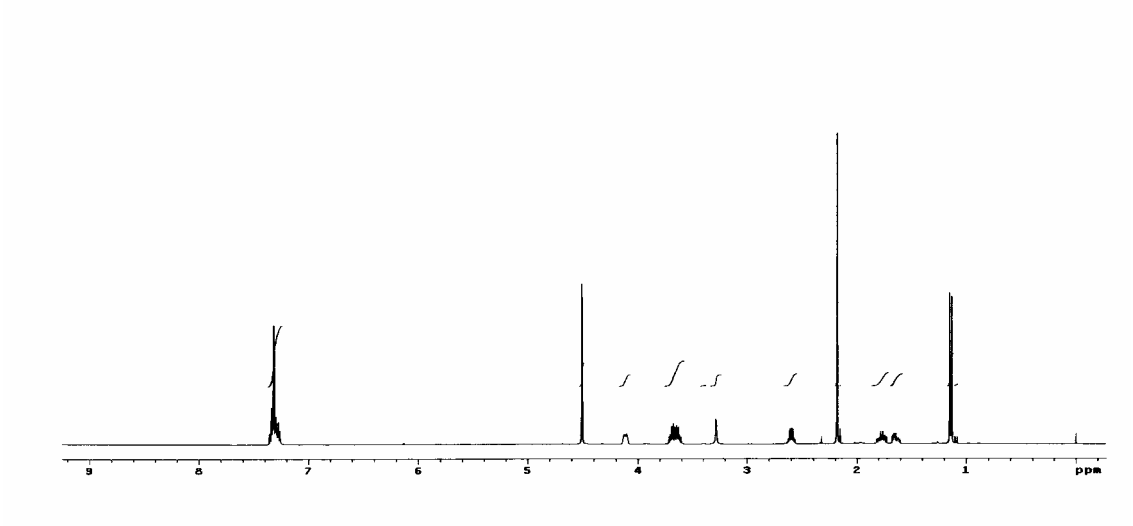
9
8
7
6
5
4
3
2
1
ppm

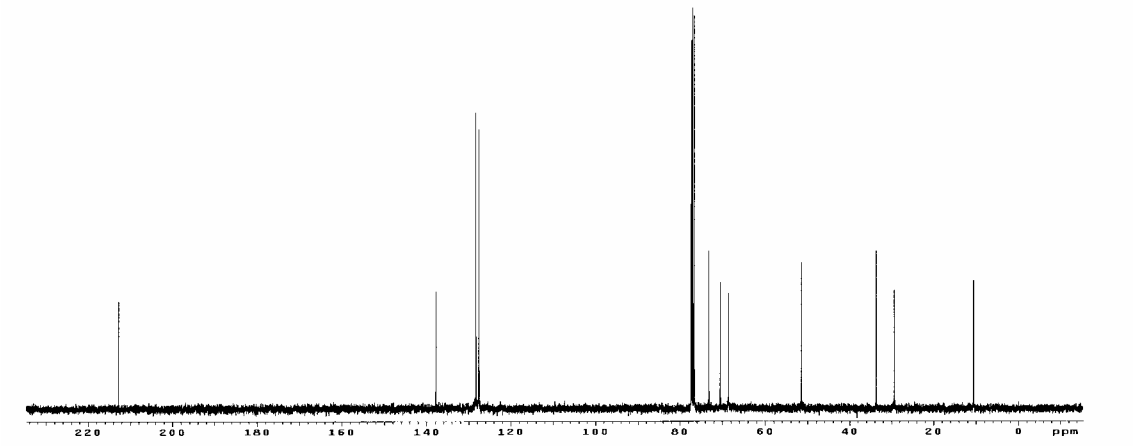
220
200
180
160
140
120
100
80
60
40
20
0
ppm

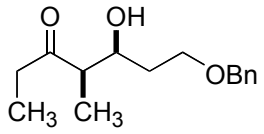
O
OH
OBn
CH3
CH3

3.5b

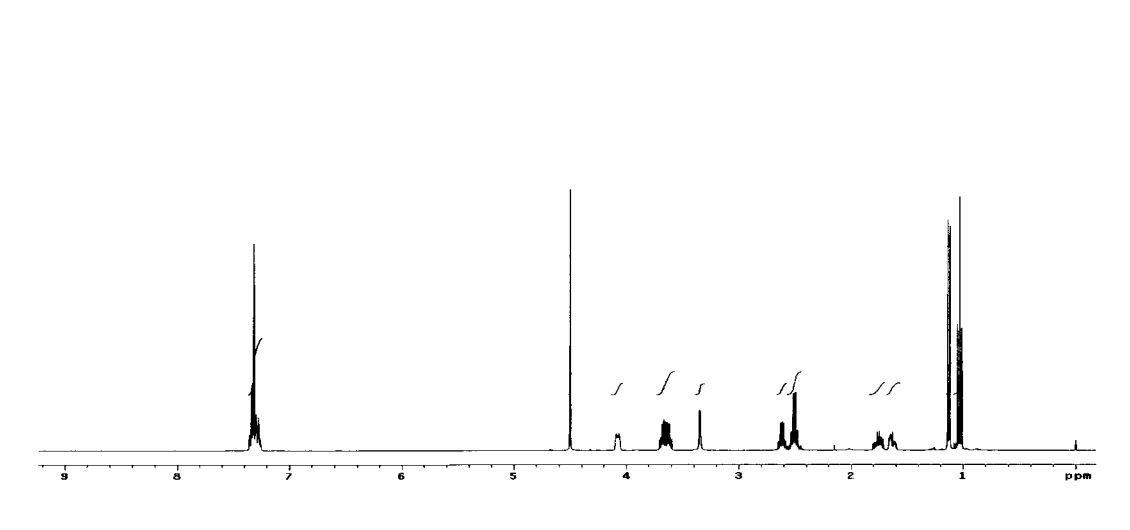
9
8
7
6
5
4
3
2
1
ppm

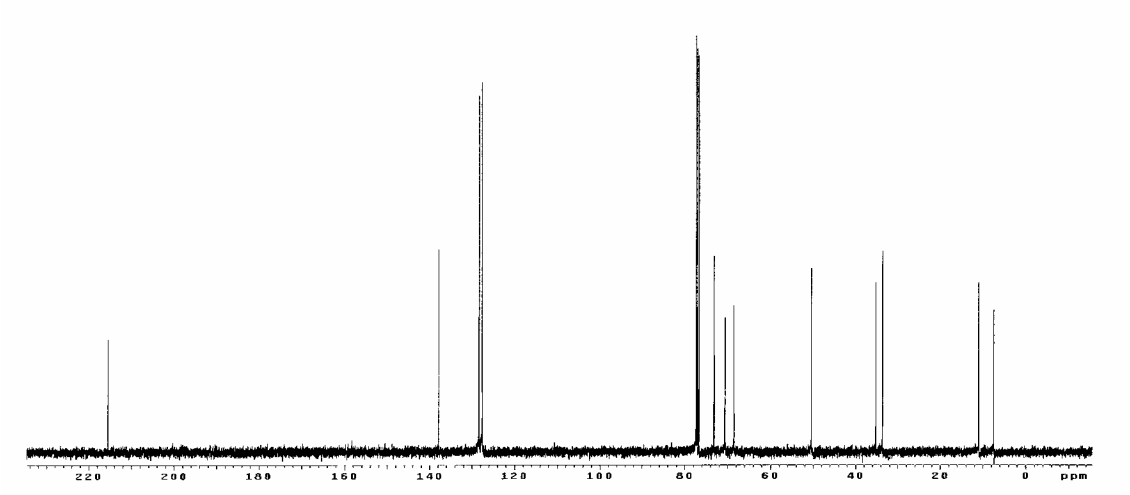
220
200
180
160
140
120
100
80
60
40
20
0
ppm

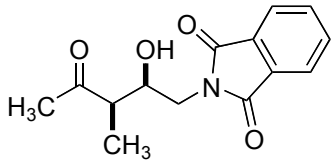
O
OH
O
H3C
N
CH3
O

3.6a

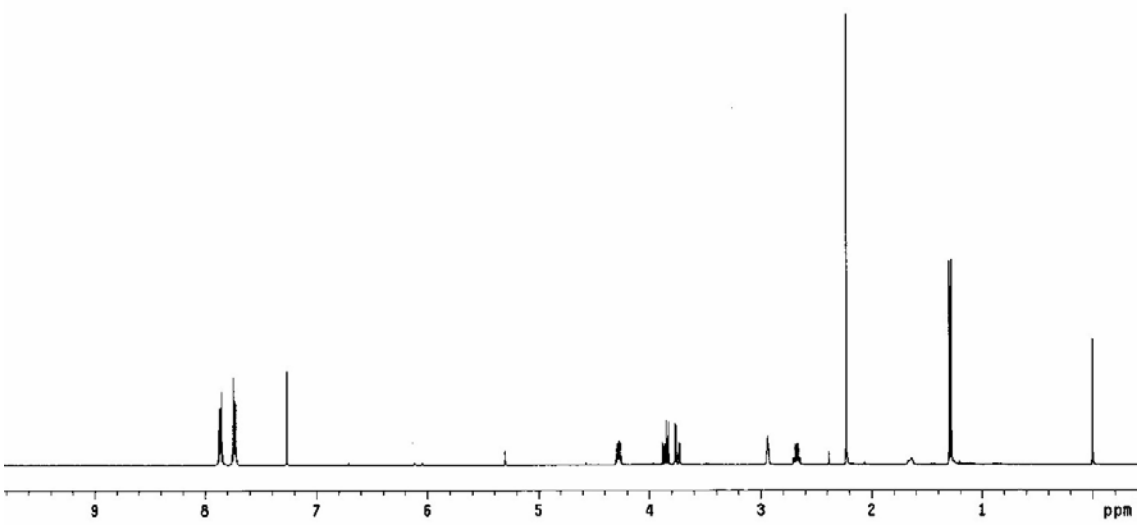
9
8
7
6
5
4
3
2
1
ppm

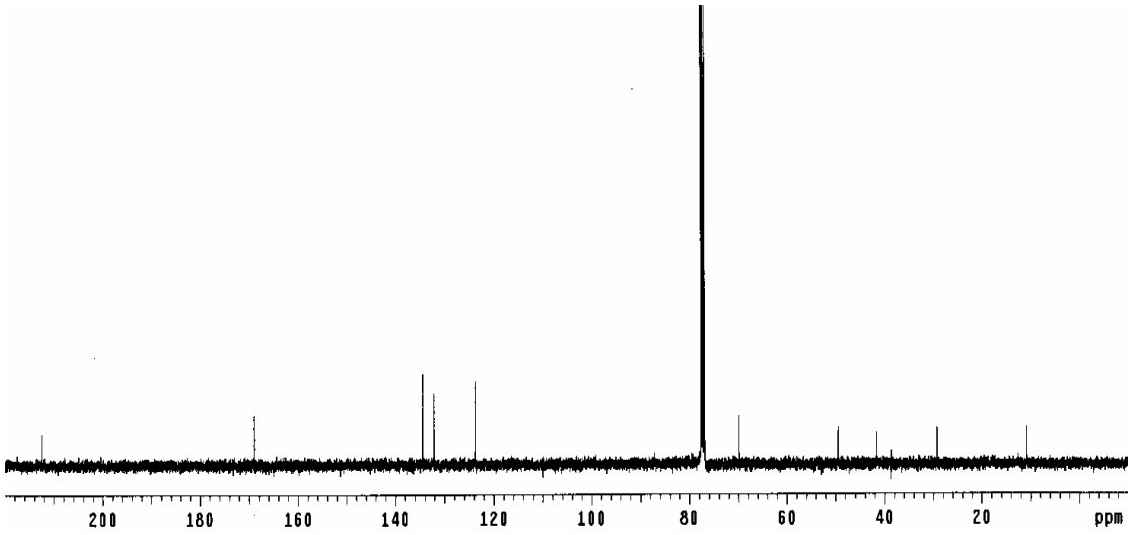
200
180
160
140
120
100
80
60
40
20
ppm

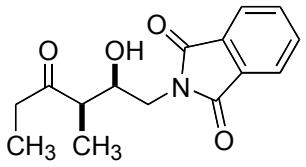
O
OH
O
N
O
CH3
CH3

3.6b

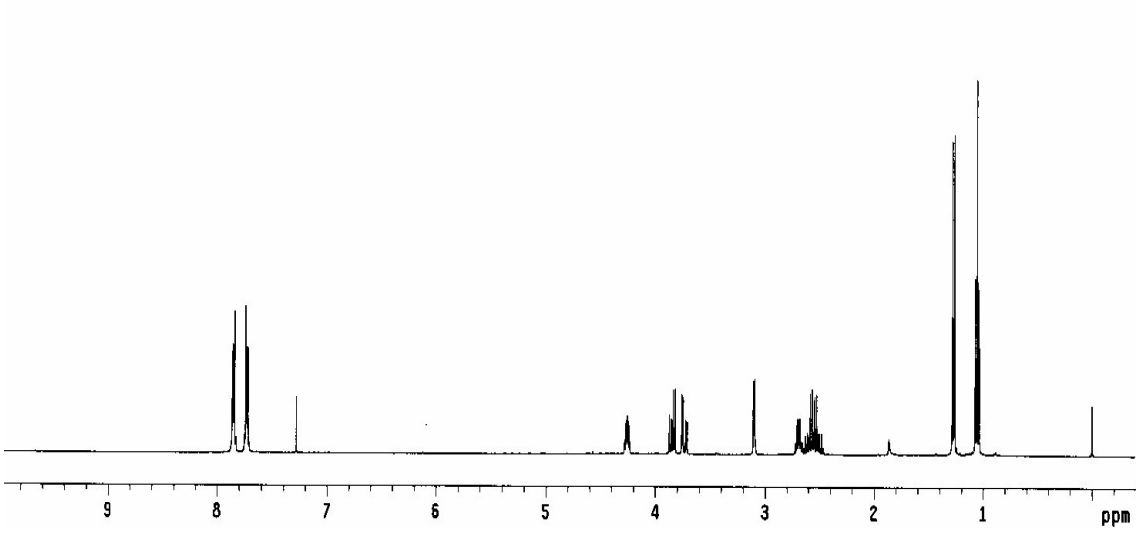
9
8
7
6
5
4
3
2
1
ppm

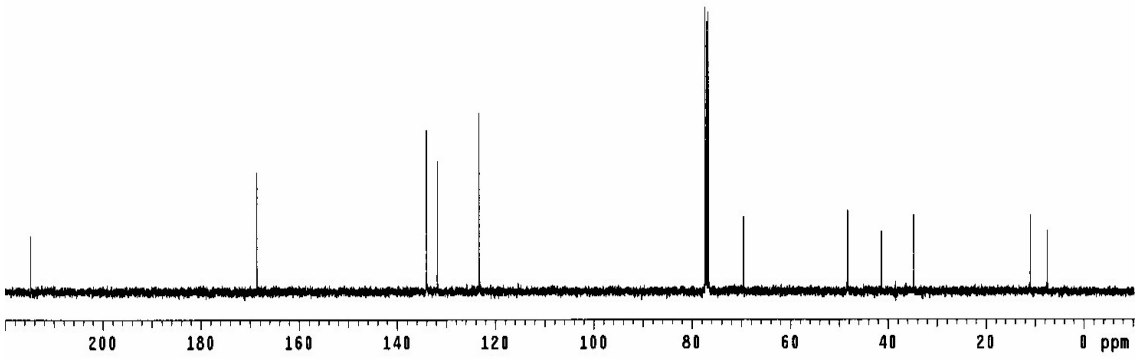
200
180
160
140
120
100
80
60
40
20
0 ppm

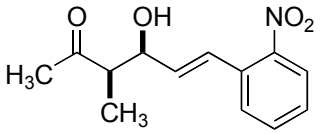
O
OH
NO2
H3C
CH3

3.7a

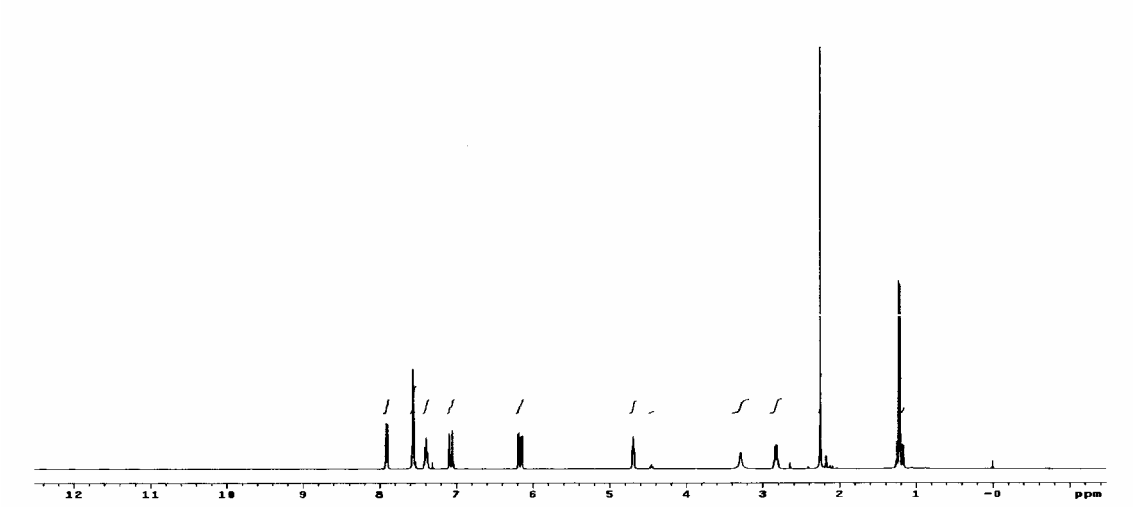
12
11
10
9
8
7
6
5
4
3
2
1
-0
ppm

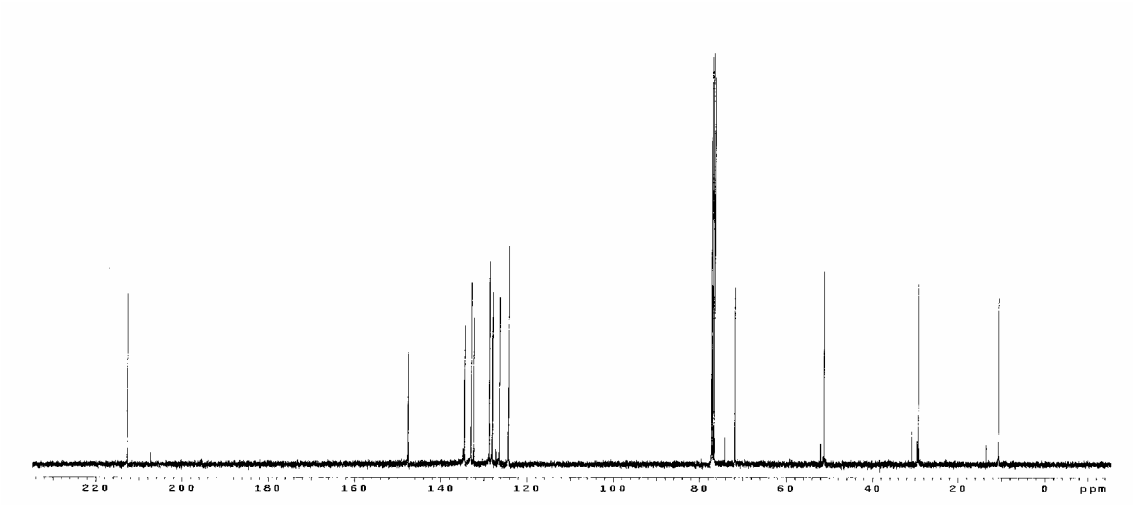
220
200
180
160
140
120
100
80
60
40
20
0
ppm

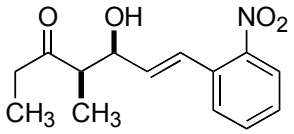
O
OH
NO2
CH3
CH3

3.7b

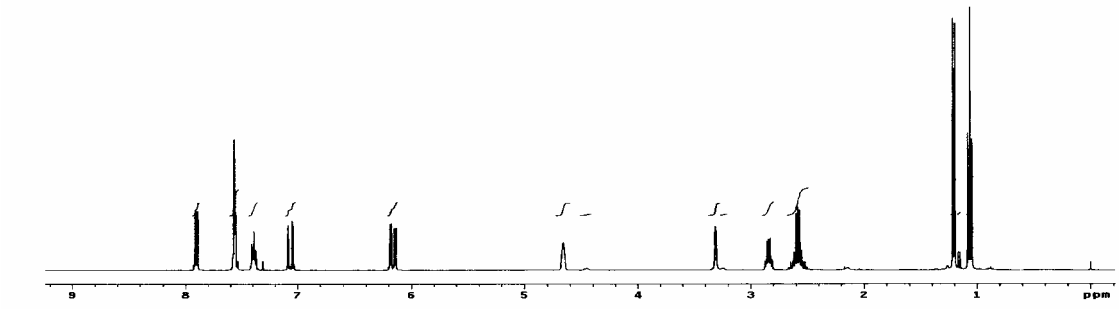
9
8
7
6
5
4
3
2
1
ppm

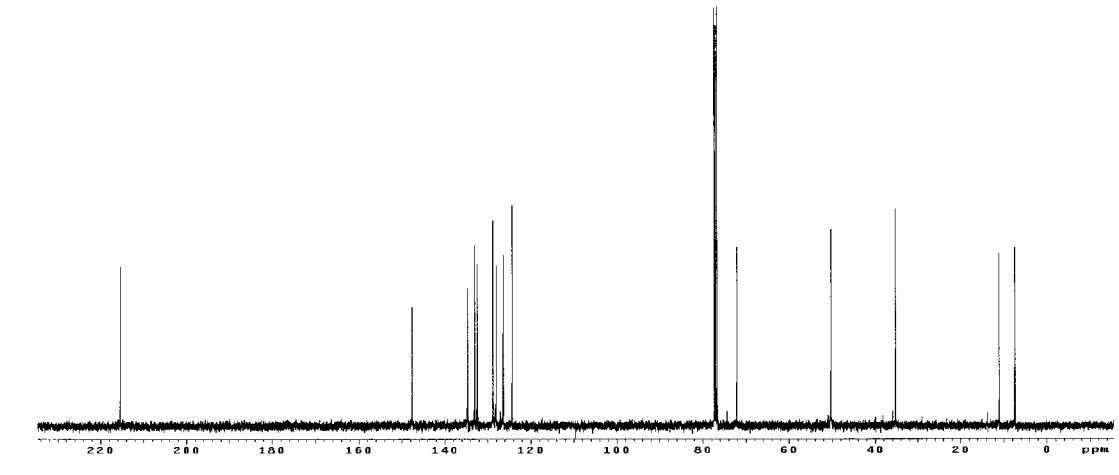
220
200
180
160
140
120
100
80
60
40
20
0
ppm

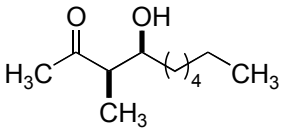
O
OH
H3C
4
CH3
CH3

3.8a

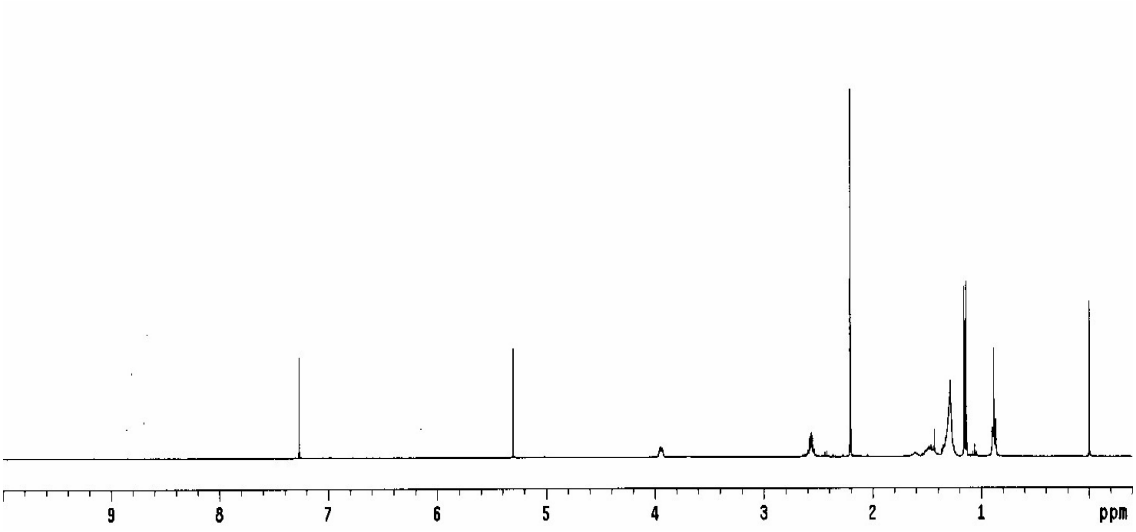
9
8
7
6
5
4
3
2
1
ppm

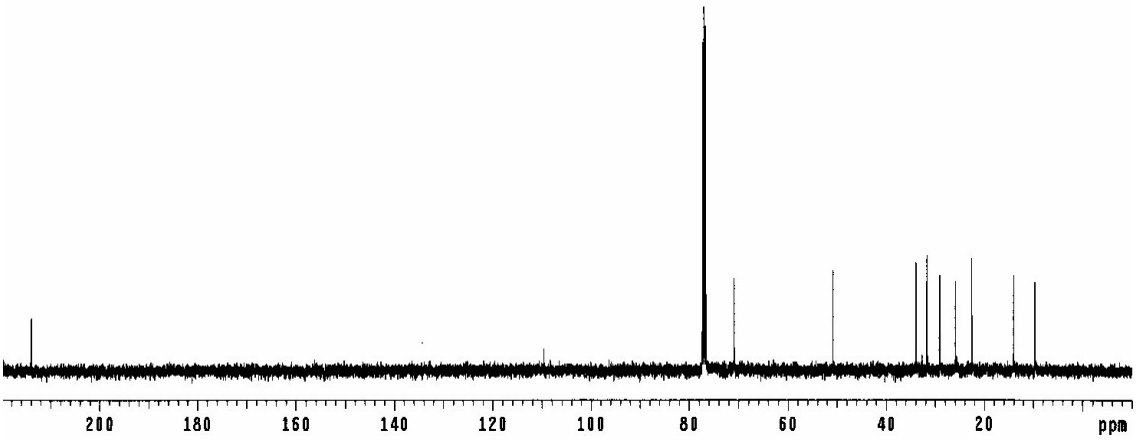
200
180
160
140
120
100
80
60
40
20
ppm

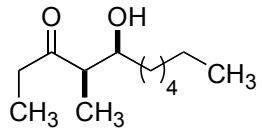
O
OH
CH3
4
CH3
CH3

3.8b

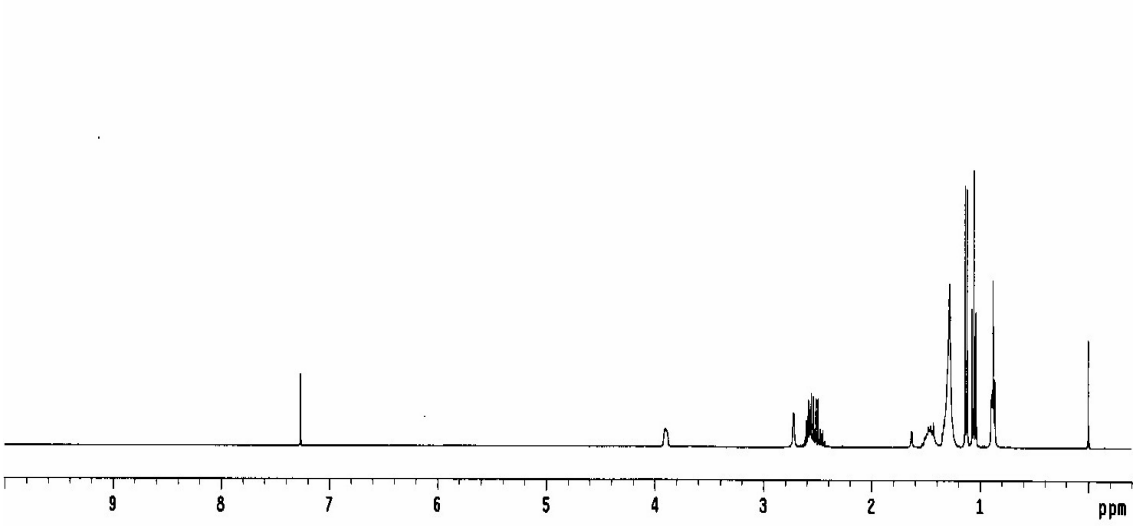
9
8
7
6
5
4
3
2
1
ppm

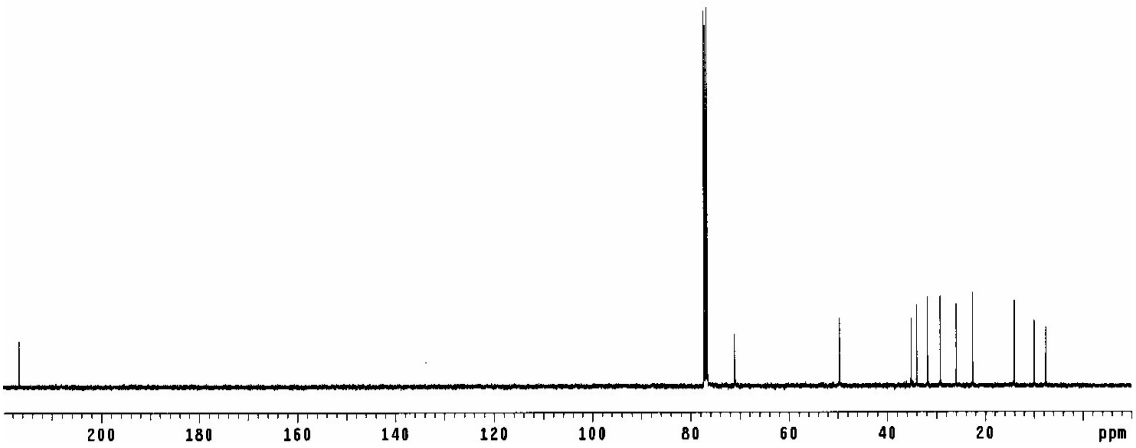
200
180
160
140
120
100
80
60
40
20
ppm

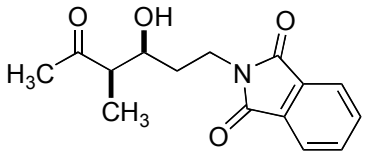
O
OH
O
H3C
N
CH3
O

3.9a

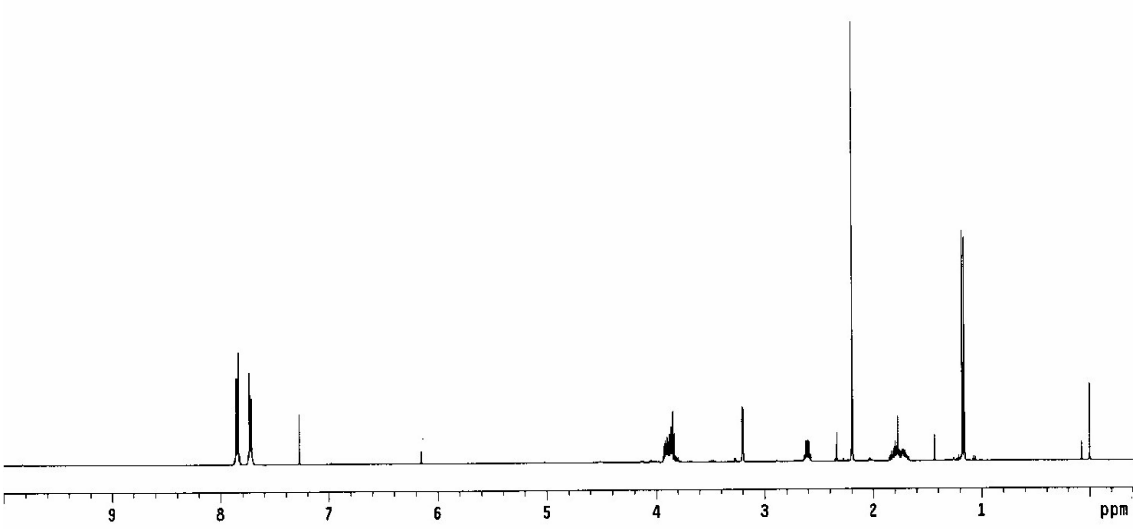
9
8
7
6
5
4
3
2
1
ppm

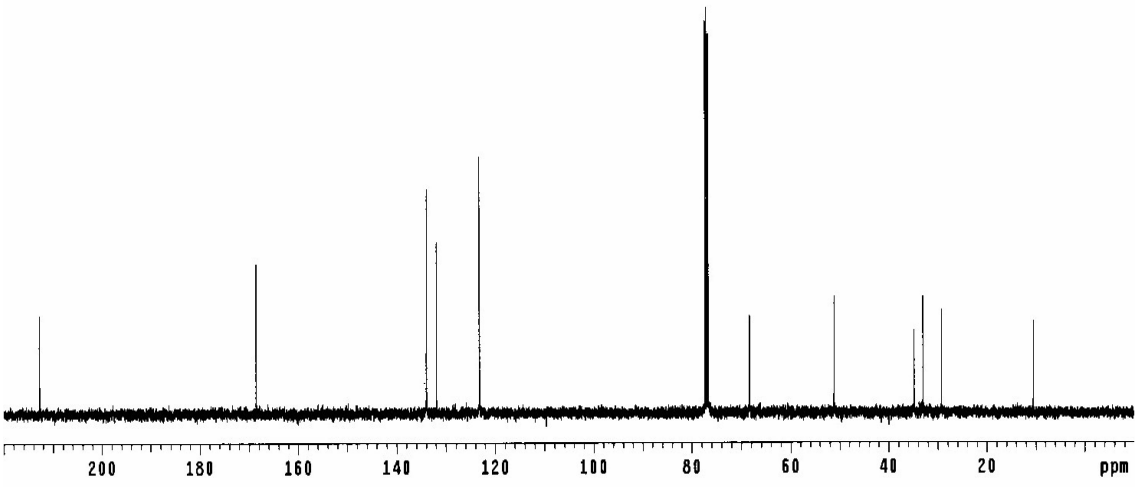
200
180
160
140
120
100
80
60
40
20
ppm

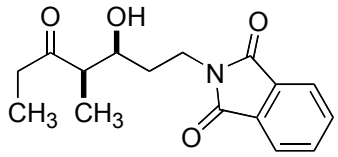
O
OH
O
N
O
CH3
CH3

3.9b

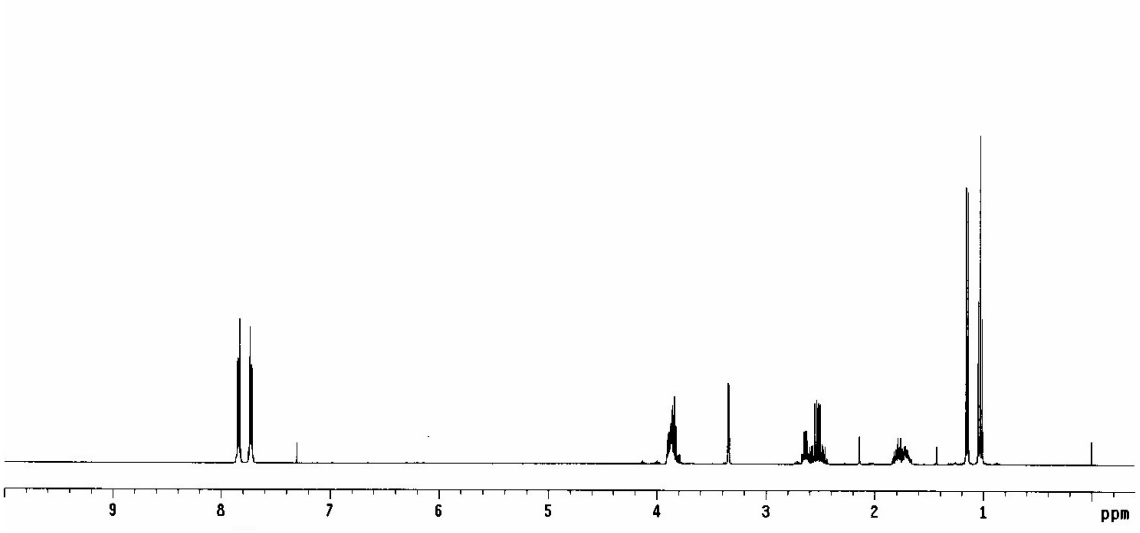
9
8
7
6
5
4
3
2
1
ppm

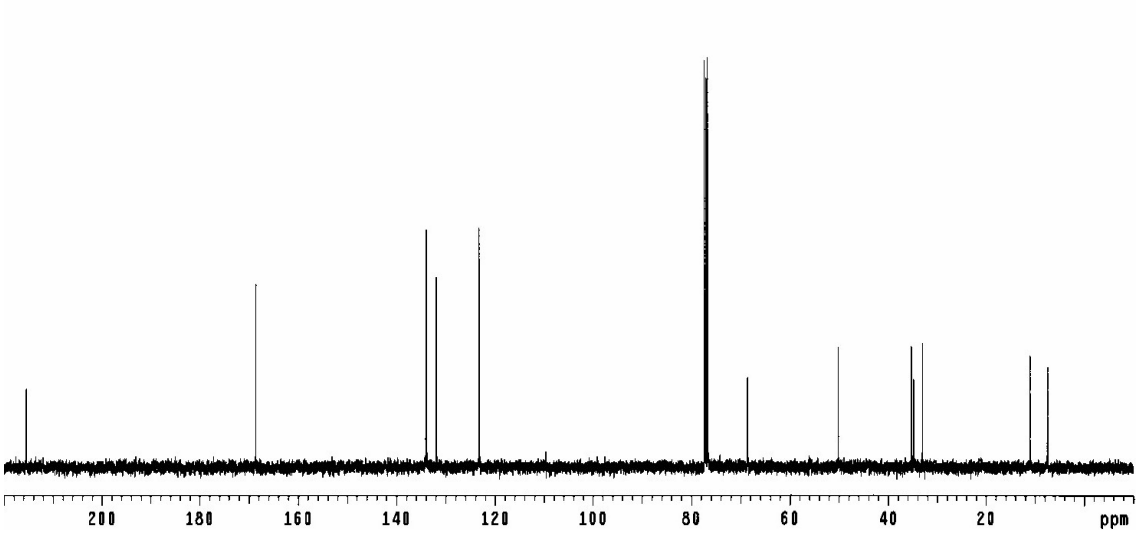
200
180
160
140
120
100
80
60
40
20
ppm

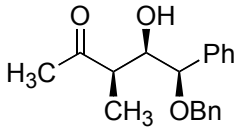
O
OH
Ph
H3C
CH3
OBn

3.10

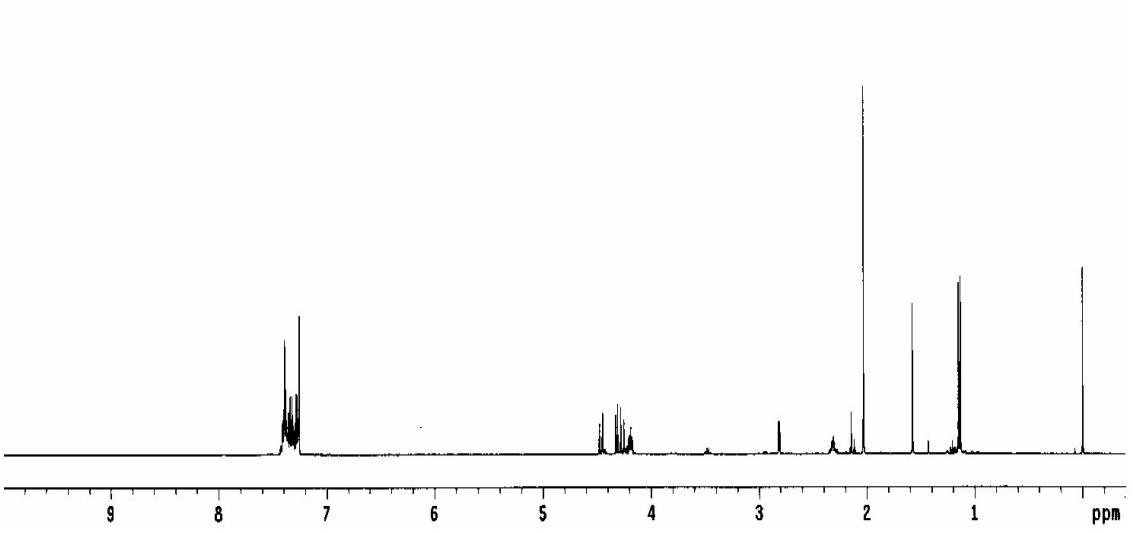
9
8
7
6
5
4
3
2
1
ppm

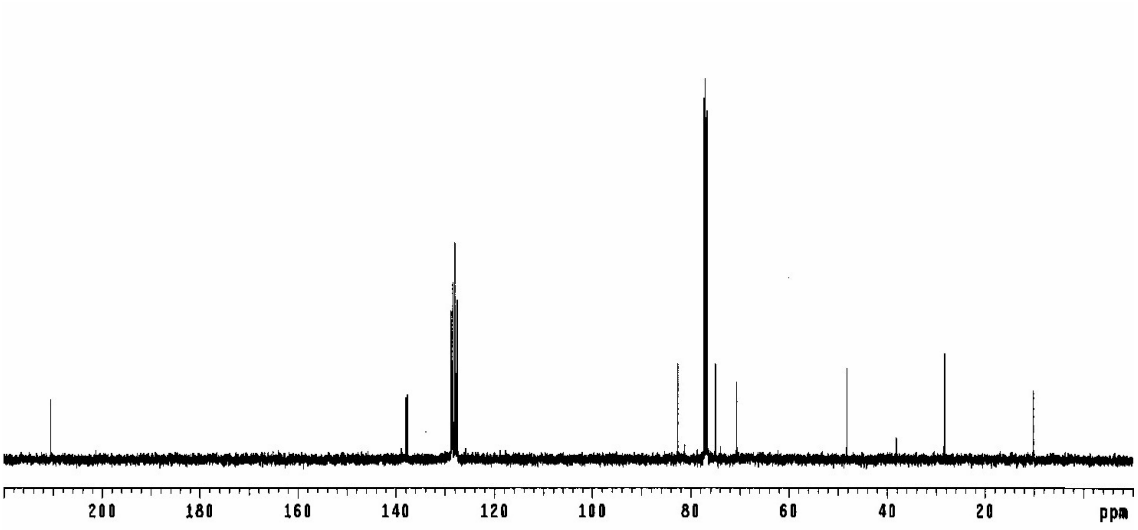
200
180
160
140
120
100
80
60
40
20
ppm

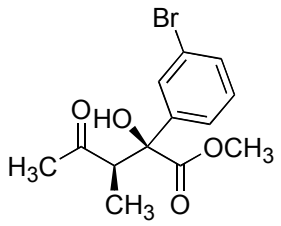
Br
O
HO
OCH3
H3C
CH3
O

***syn*-3.12**

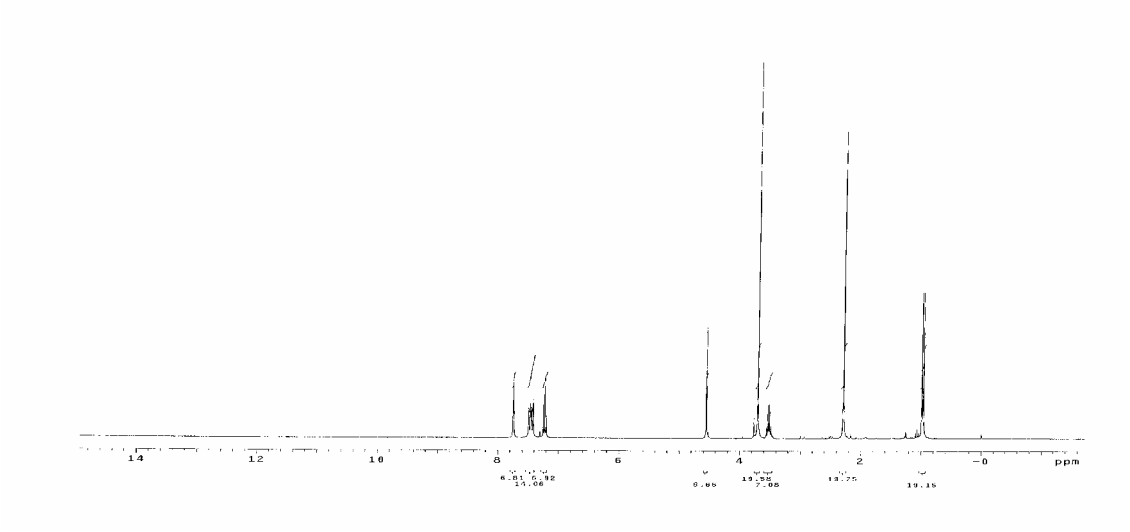
14
12
10
8
6
4
2
0
ppm

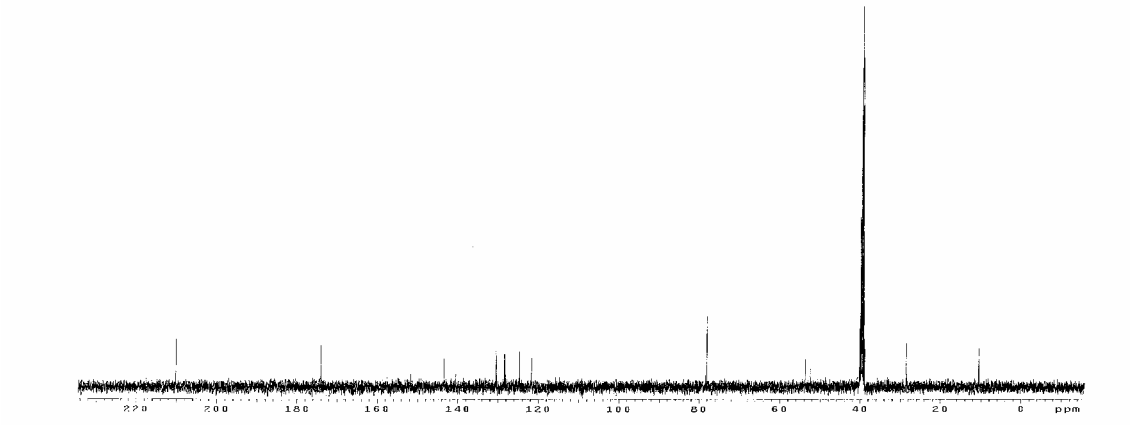
220
200
180
160
140
120
100
80
60
40
20
0
ppm

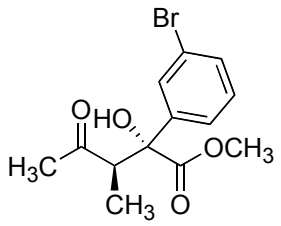
Br
O
HO
H3C
OCH3
CH3
O

***anti*-3.12**

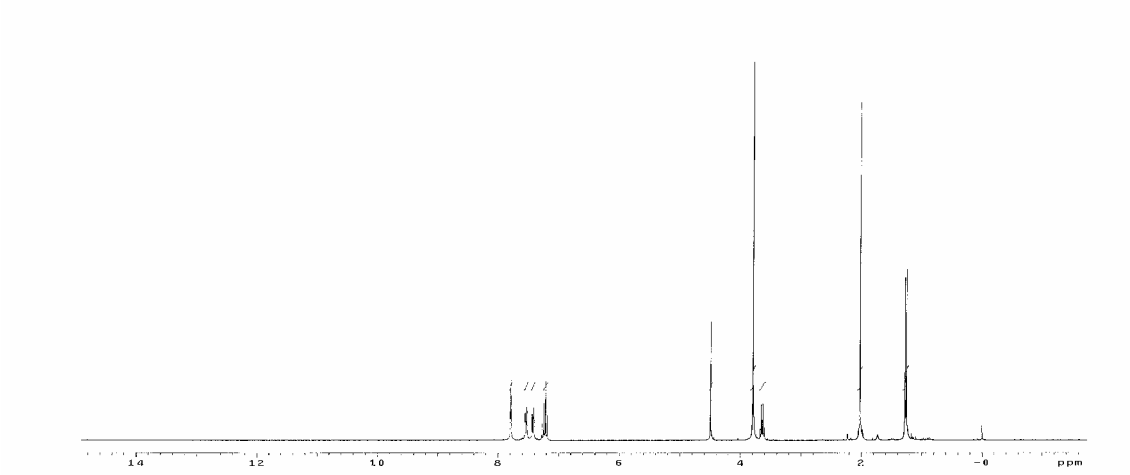
14
12
10
8
6
4
2
0
ppm

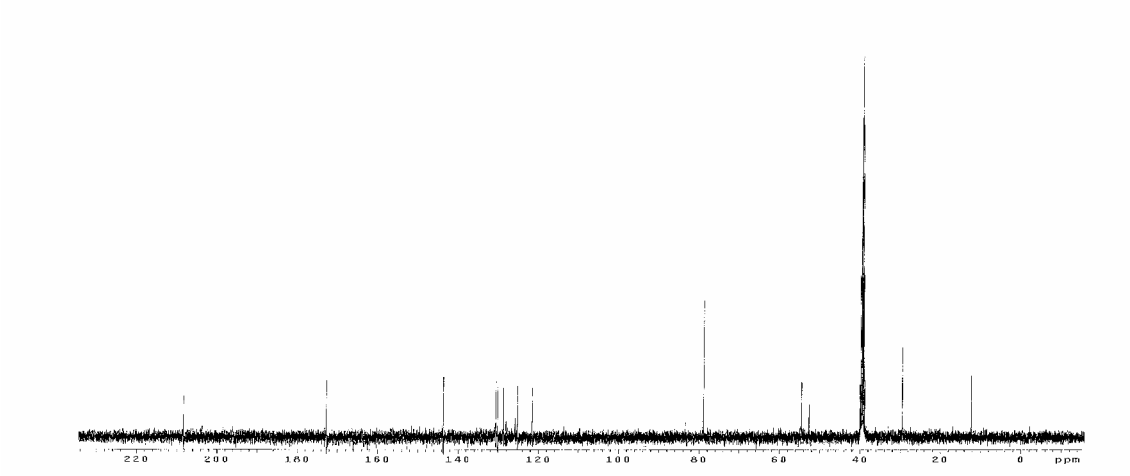
220
200
180
160
140
120
100
80
60
40
20
0
ppm

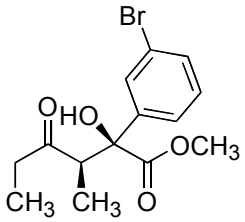
Br
O
HO
OCH3
CH3
CH3
O

***syn*-3.13**

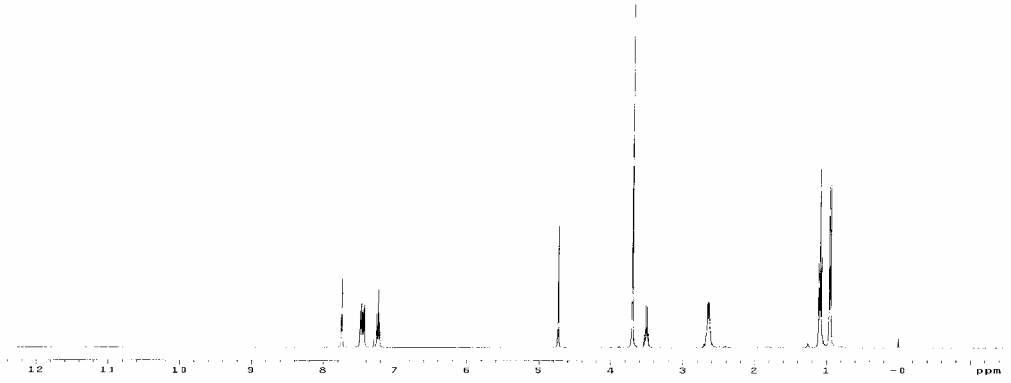
12
11
10
9
8
7
6
5
4
3
2
1
0
ppm

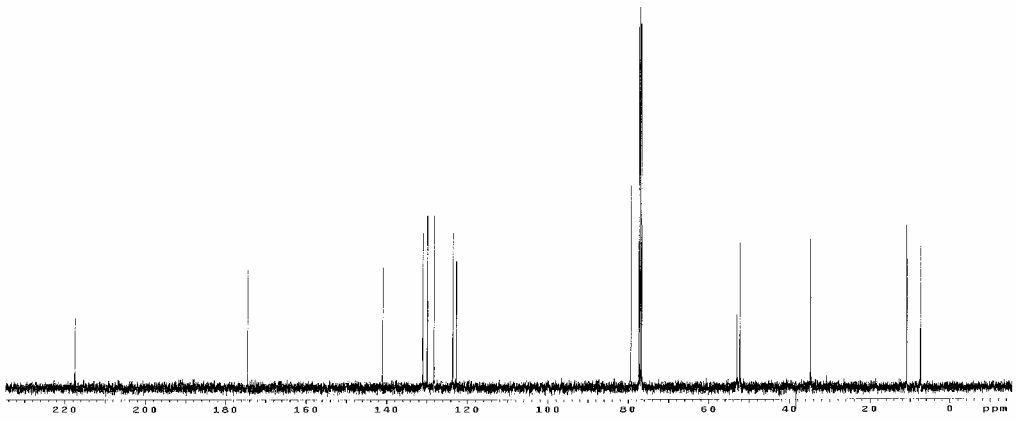
220
200
180
160
140
120
100
80
60
40
20
0
ppm

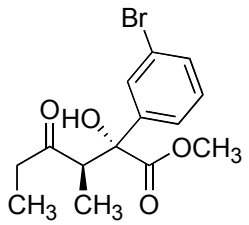
Br
O
HO
OCH3
CH3
CH3
O

***anti*-3.13**

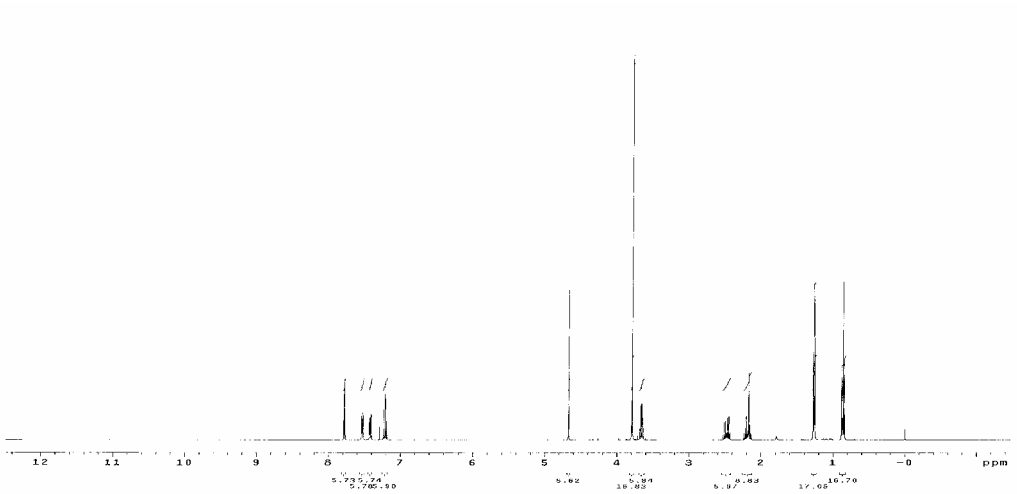
12
11
10
9
8
7
6
5
4
3
2
1
0
ppm

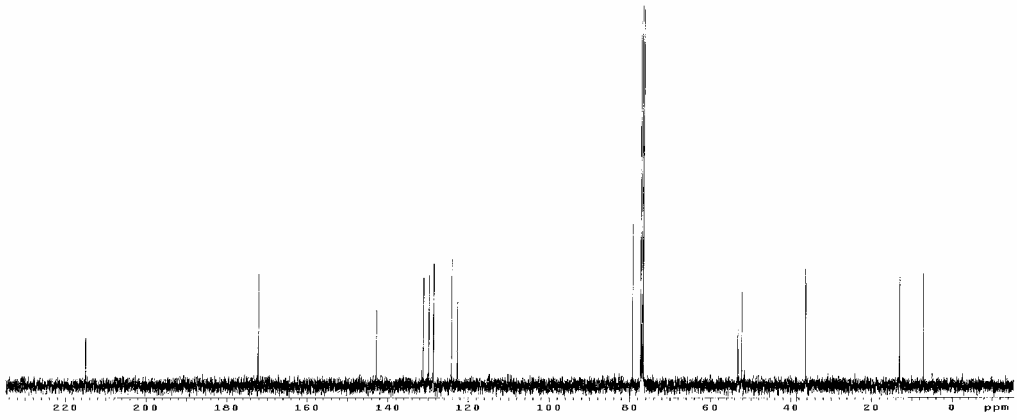
220
200
180
160
140
120
100
80
60
40
20
0
ppm

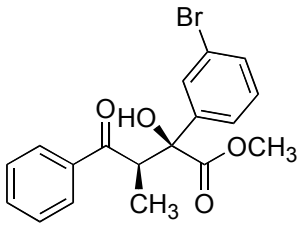
Br
O
HO
OCH3
CH3
O

***syn*-3.14**

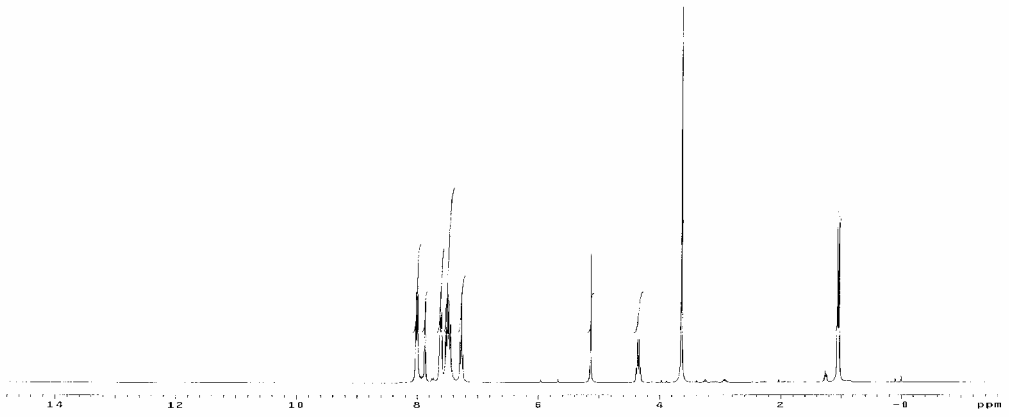
14
12
10
8
6
4
2
0
ppm

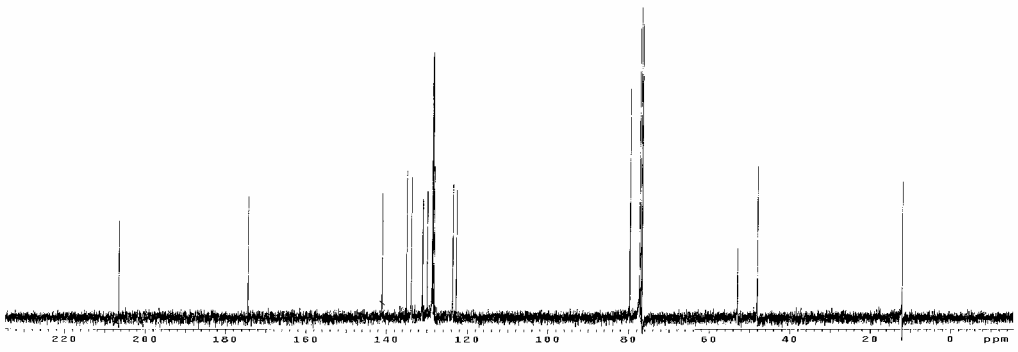
220
200
180
160
140
120
100
80
60
40
20
0
ppm

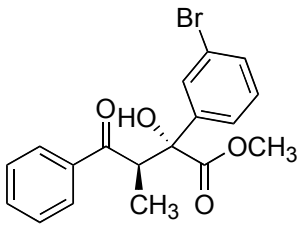
Br
O
HO
OCH3
CH3
O

***anti*-3.14**

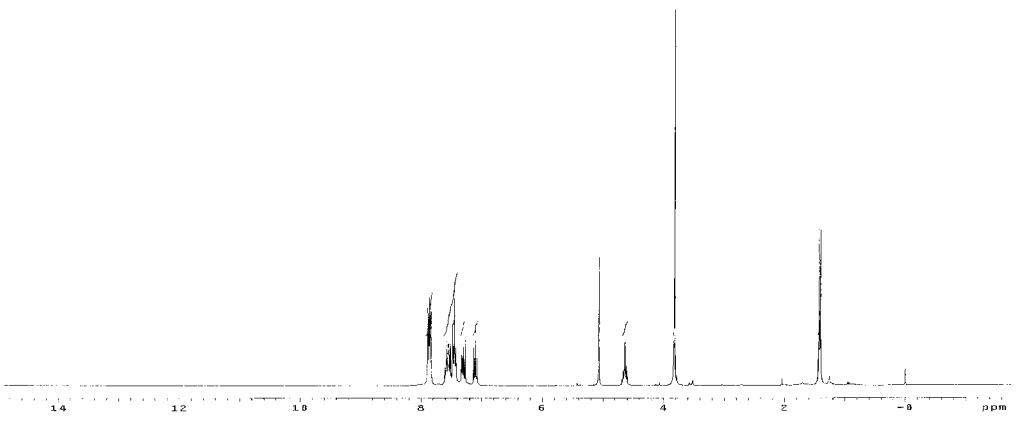
14
12
10
8
6
4
2
0
ppm

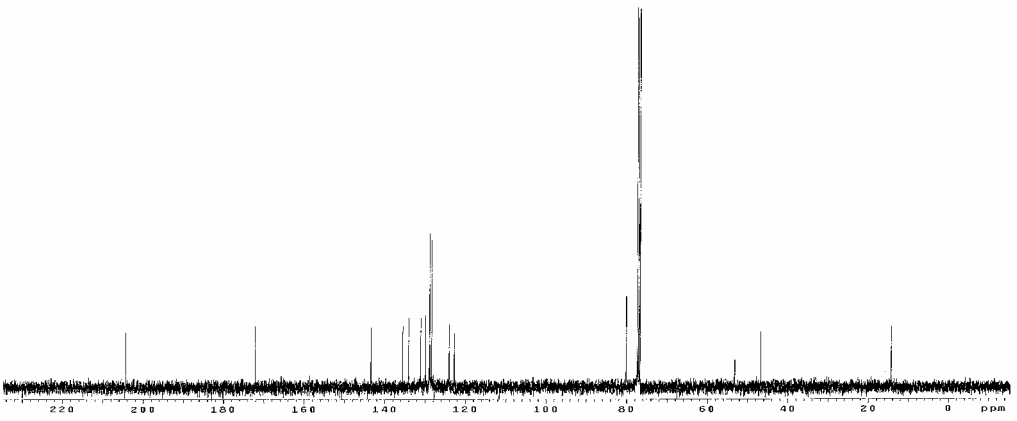
220
200
180
160
140
120
100
80
60
40
20
0
ppm

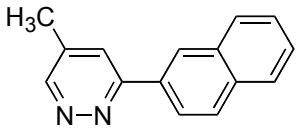
H3C
N–N

3.18

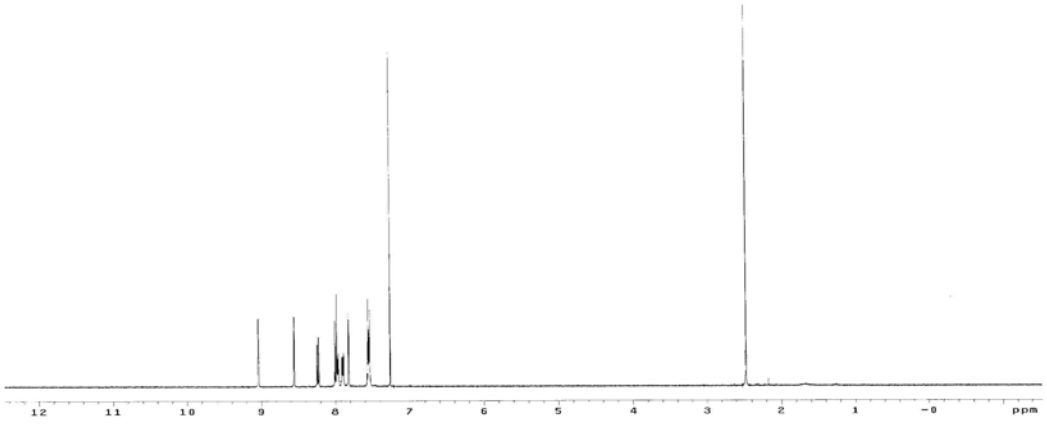
12
11
10
9
8
7
6
5
4
3
2
1
-0
ppm

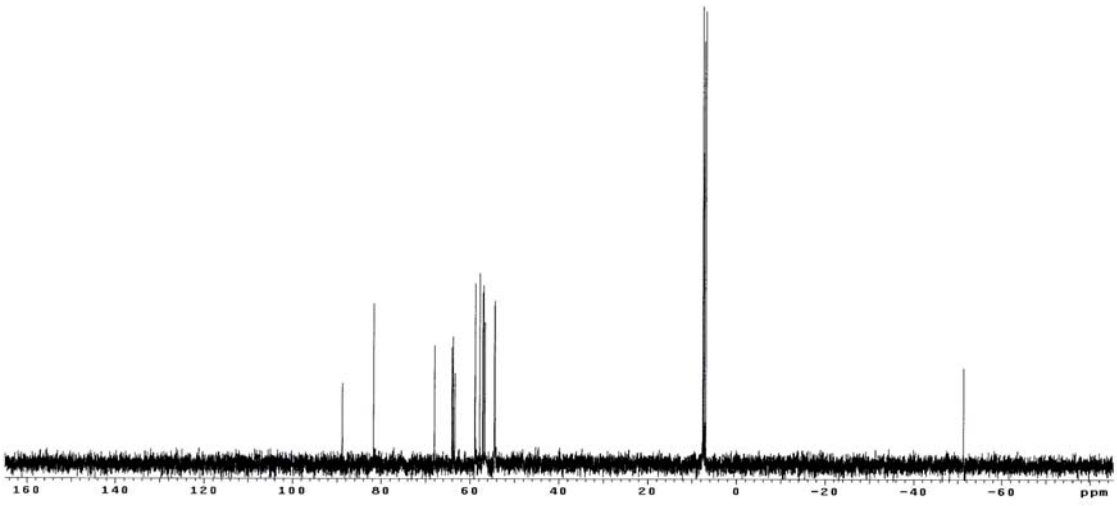
160
140
120
100
80
60
40
20
0
-20
-40
-60
ppm

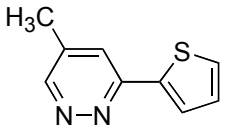
H3C
S
N–N

3.19

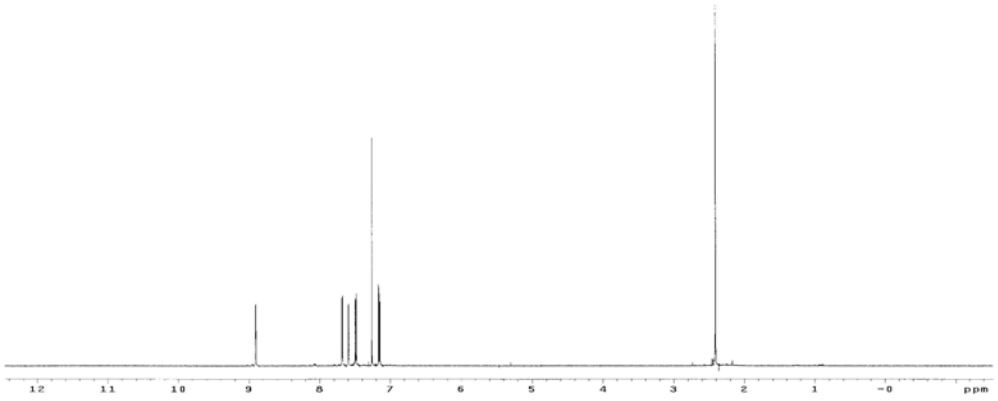
12
11
10
9
8
7
6
5
4
3
2
1
0
ppm

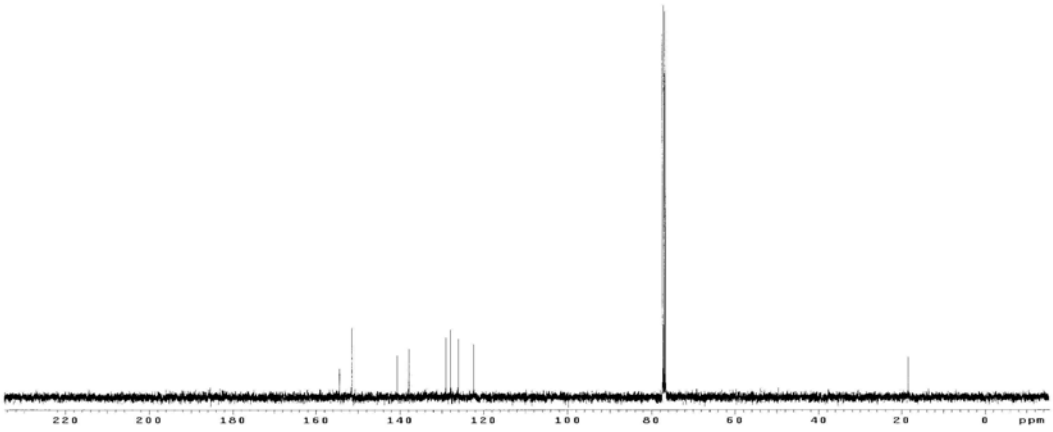
220
200
180
160
140
120
100
80
60
40
20
0
ppm

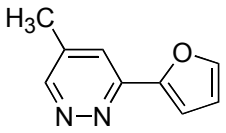
H3C
O
N–N

3.20

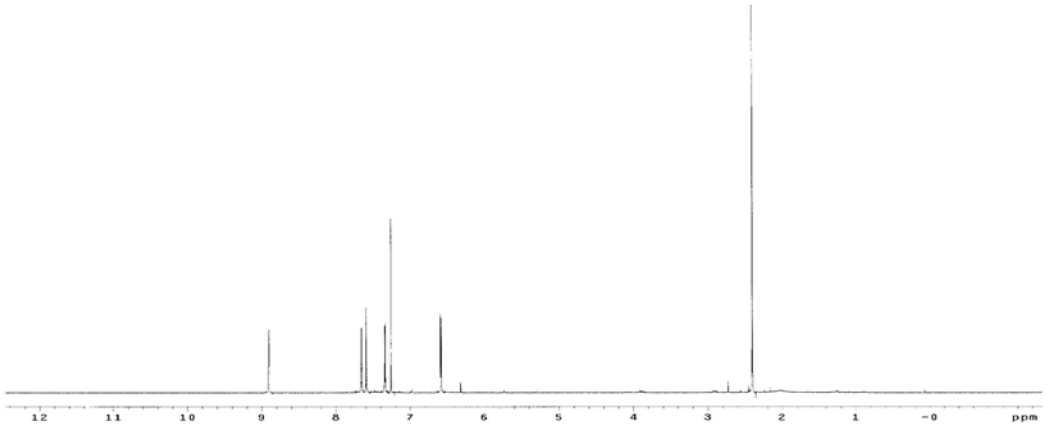
12
11
10
9
8
7
6
5
4
3
2
1
0
ppm

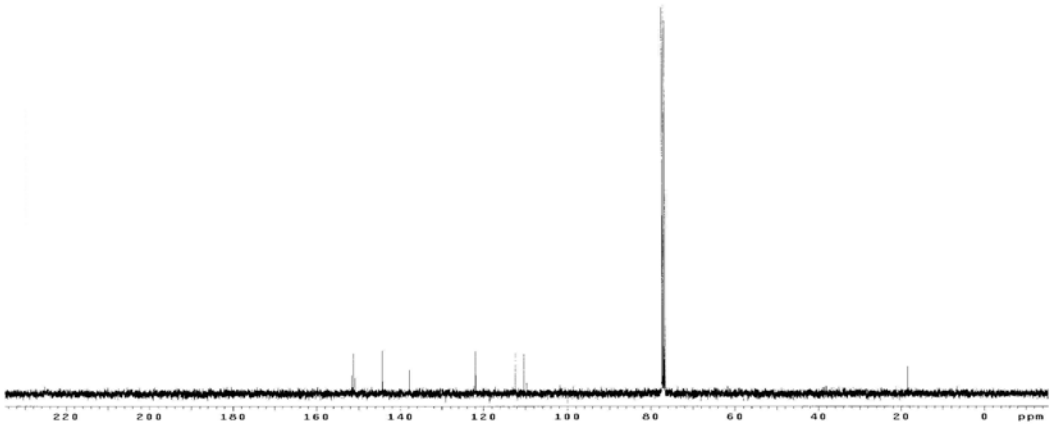
220
200
180
160
140
120
100
80
60
40
20
0
ppm

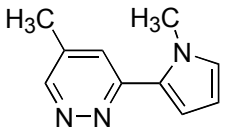
H3C
H3C
N
N–N

3.21

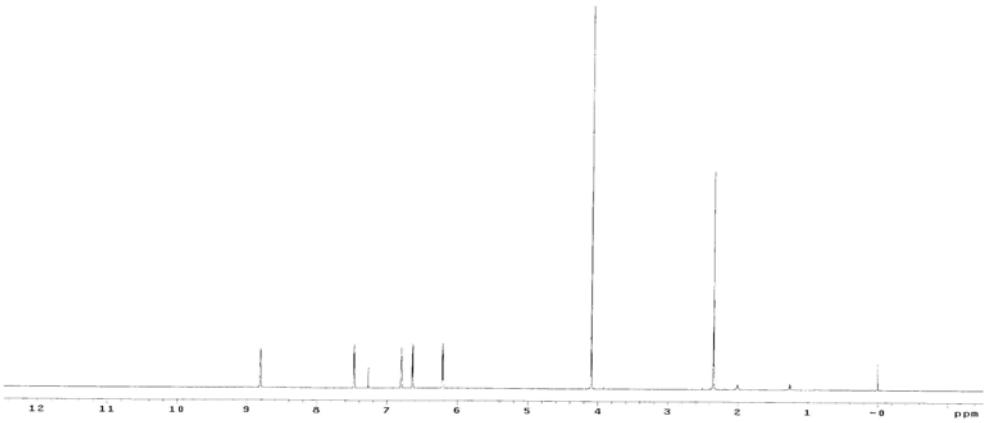
12
11
10
9
8
7
6
5
4
3
2
1
-0
ppm

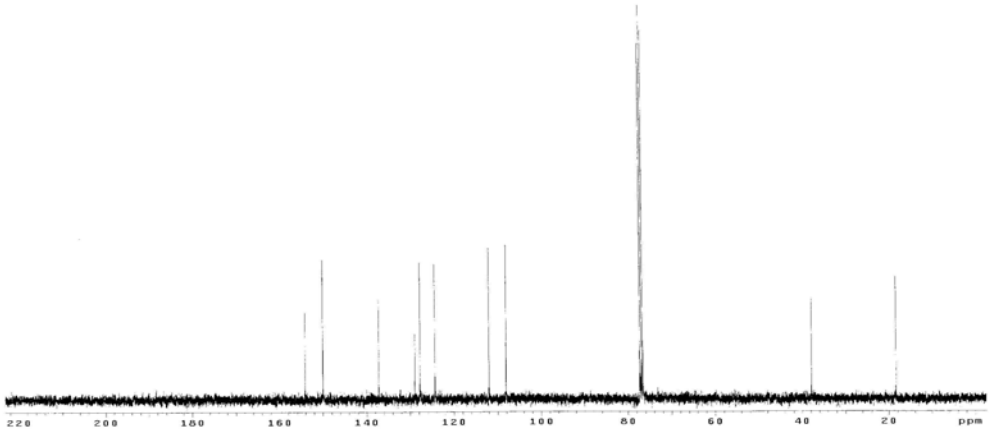
220
200
180
160
140
120
100
80
60
40
20
ppm

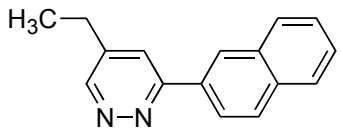
H3C
N–N

3.23

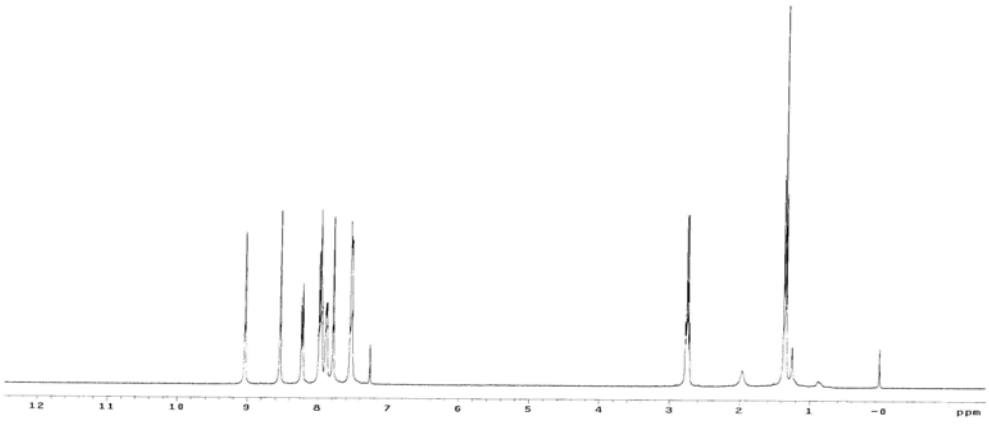
12
11
10
9
8
7
6
5
4
3
2
1
0
ppm

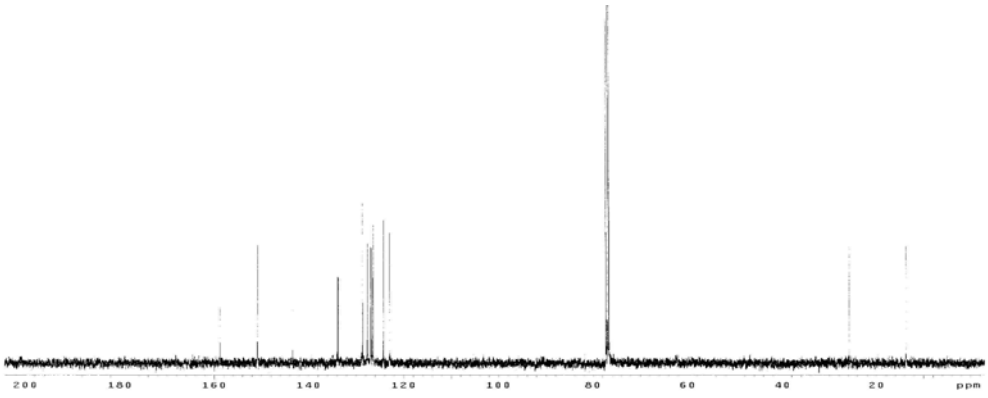
200
180
160
140
120
100
80
60
40
20
ppm

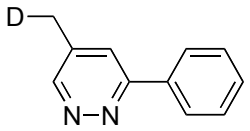

3.24

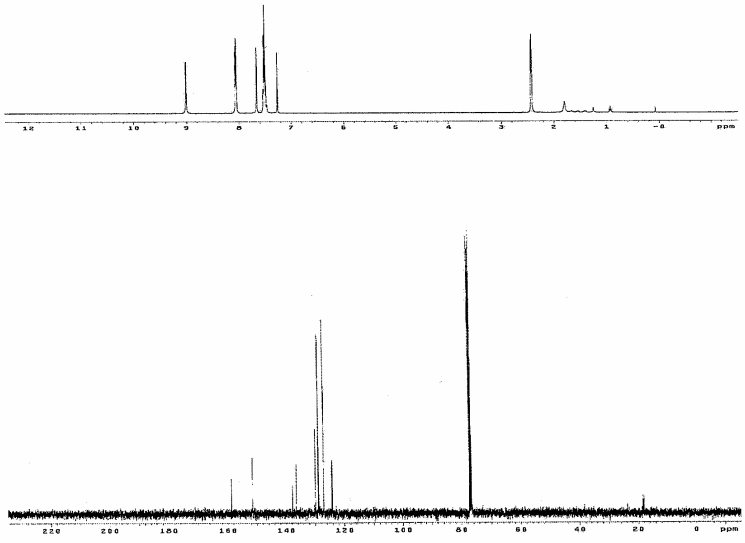

[1] Jang, H. –Y.; Huddleston, R. R.; Krische, M. J. *J. Am. Chem. Soc*. **2002**, *124*, 15156.

[2] Huddleston, R. R.; Krische, M. J. *Org. Lett*. **2003**, *5*, 1143.

[3] Zimmerman, H. E.; Traxler, M. D. *J. Am. Chem. Soc*. **1957**, *79*, 1920.

[4] Yachi, K.; Shinokubo, H.; Oshima, K. *J. Am. Chem. Soc*. **1999**, *121*, 9465.

[5] Koech, P. K.; Krische, M. J. *Org. Lett*. **2004**, *6*, 691.

[6] Heathcock, C. H.; Buse, C. T.; Kleschick, W. A.; Pirrung, M. C.; Sohn, J. E.; Lampe, J. *J. Org. Chem.* **1980**, *45*, 1066.

[7] (a) Farina, V.; Krishman, B. *J. Am. Chem. Soc*. **1991**, *113*, 9585. (b) Farina, V. *Pure Appl. Chem.* **1996**, *68*, 73. (c) Anderson, N. G.; Keay, B. A. *Chem. Rev*. **2001**, *101*, 997.

[8] Jung, C. –Y.; Garner, S. A.; Krische, M. J. *Org. Lett.* **2006**, *8*, 519.

[9] For selected reviews on stereoselective aldol additions, see: (a) Heathcock, C. H. *Science*, **1981**, *241*, 395. (b) Heathcock, C. H. *ACS Symp. Ser.* **1982**, *185*, 55. (c) Evans, D. A.; Nelson, J. V.; Taber, T. R. *Top. Stereochem*. **1982**, *185*, 55.

[10] Enones that are constrained to the *s*-trans confirguration, such as, cyclohexenone, do not participate in hydrogen-mediated reductive aldol coupling.

[11] Non-coordinating tris(dialkylamino)sulfonium enolates do not participate in aldol addition reactions: (a) Noyori, R.; Sakata, J.; Nishizawa, M. *J . Am. Chem. Soc*. **1980**, *102*, 1223. (b) Noyori, R.; Nishida, I.; Sakata, J. *J . Am. Chem. Soc*. **1981**, *103*, 2106. (c) Noyori, R.; Nishida, I.; Sakata, J. *J . Am. Chem. Soc*. **1983**, *105*, 1598.

[12] Roush, W. R. *J. Org. Chem*. **1991**, *56*, 4151.

[13] Heathcock, C. H. in *Comprehensive Organic Synthesis*. Vol. 2. Trost, B. M.; Fleming, I.; Heathcock, C. H.; Ed. Pergamon Press: New York, **1996**, 133.

[14] Kobayashi, S. Hachiya, I. *J. Org. Chem.* **1992**, *57*, 1324.

[15] Evans, D. A.; Kozlowski, M. C.; Burgey, C. S.; MacMillan, W. C. *J. Am. Chem. Soc*. **1997**, *119*, 7893.

[16] Rychnovsky, S.D.; Skalitzky, G. J. *J. Org.Chem*. **1992**, *57*,4336.

[17] Denmark, S. E.; Ghosh, S. K. *Angew. Chem. Int. Ed*. **2001**, *40*, 4759.

[18] Northup, A. B.; MacMillan, D. W. *J. Am. Chem. Soc*. **2002**, *124*, 6798.

[19] Pidathala, C.; Hoan, L.; Vignola, N.; List, B. *Angew. Chem. Int. Ed.* **2003**, *42*, 2785.

[19] Boulton, A. J. in *Comprehensive Heterocyclic Chemistry*. Eds. Katritzky, F. R.; Rees, C. W.; Scriven, E. F. **1996**, 3.

[20] Sauer, J.; Heldmann, D. K. *Tetrahedron*, **1998**, *54*, 4297.

[21] South, M. S.; Jakuboski, T. L.; Westmeyer, M. D.; Dukesherer, D. R. *J. Org. Chem*. **1996**, *61*, 8921.

[22] Marriner, G. A.; Garner, S. A.; Jang, H. –Y.; Krische, M. J. *J. Org. Chem*. **2004**, *69*, 1380.

[23] Still, W. C.; Kahn, M.; Mitra, M. *J. Org. Chem*. **1978**, *43*, 2923.

[24] Noncommercial glyoxals were made from the selenium dioxide oxidation of the corresponding methyl ketone. The glyoxal was then crystallized from boiling water, and then recrystallized from chloroform. (a) Beck, B.; Magin-Lachaux, M.; Herdtweck, E.; Dömling, A. *Org. Lett*. **2001**, *3*, 28. (b) Block, M. H.; Harrison, A.; Hargreaves, R. B. *Eur. Pat. Appl*. **1993**, EP 544445. (c) Reed, L. A. *Eur. Pat. Appl*. **1986**, EP 201221.

CHAPTER 4. HYDROGEN-MEDIATED REDUCTIVE MANNICH REACTIONS

4.1 INTRODUCTION

The success of the hydrogen-mediated reductive aldol reaction led us to explore other electrophiles such as imines, the nitrogen analogs of carbonyl compounds. The reductive coupling of imines and enones would provide Mannich-type products. In Chapter 1 of this thesis, the reductive Mannich reaction is discussed in detail, but there has not been a great deal of work conducted in this area. A hydrogen-mediated reductive Mannich reaction would provide a catalytic transformation under neutral conditions. The use of an enone as a latent enolate would remove the necessity for enolate preformation. Utilization of hydrogen gas as the terminal reductant is clean and environmentally friendly providing a reaction that will not generate any stoichiometric byproducts.

The products of Mannich reactions, Mannich bases, are useful synthetic building blocks.[1] Mannich bases can be easily modified to a variety of derivatives. Scheme 4.1 illustrates that elimination of the amine provides a Michael acceptor product. Also, Mannich bases can be converted to a 1,3-aminoalcohols *via* the addition of organometallic reagents to the carbonyl. Another useful manipulation of Mannich bases is displacement of the amine by nucleophiles. Mannich bases and their derivatives have been used in paint and polymers,[2] but the largest application is in pharmaceuticals.[2,3] Scheme 4.2 demonstrates the Mannich bases that are currently being used as pharmaceutical agents.

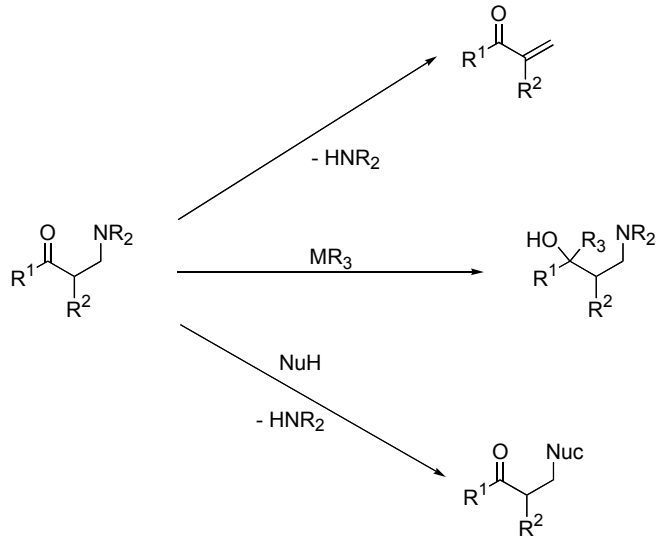

Scheme 4.1: Mannich bases are useful synthetic building blocks.[1]

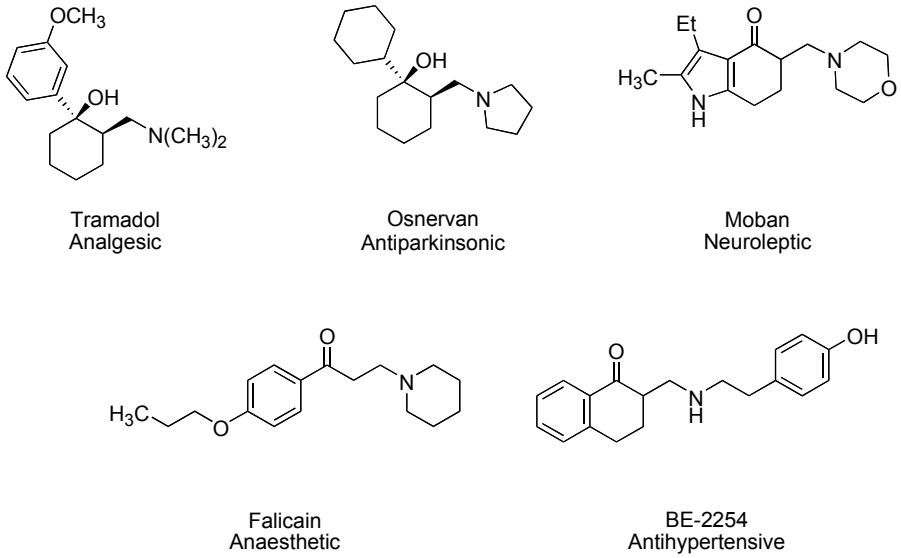

Scheme 4.2: Mannich bases as pharmaceutical agents.[1]

4.2.1 BACKGROUND

In 1912, Carl Mannich systematically developed the aminoalkylation of enolizable carbonyl compounds into the Mannich reaction.[4] In the classical Mannich reaction, an enolizable carbonyl compound is heated in the presence of an amine salt and an aldehyde. Scheme 4.3 shows a simplified reaction mechanism for the classical Mannich reaction.[1] Condensation of the amine salt and the aldehyde forms the reactive iminium salt in a low concentration *via* a series of equilibrium reactions. The iminium salt reacts with the enol tautomer of the enolizable carbonyl compound, which is also formed in low concentration to provide the product.

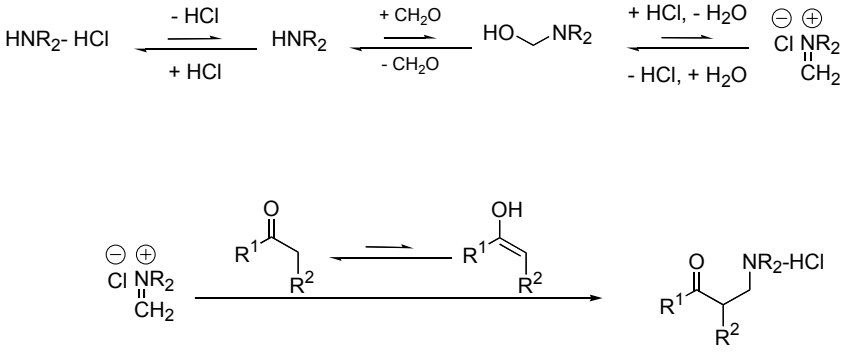

Scheme 4.3: Simplified mechanism of the classical Mannich reaction.[1]

The classical Mannich reaction has been used in numerous syntheses. One well-known example is Robinson's tropinone synthesis in 1917 (Scheme 4.4).[5] Tropinone is a derivative of the alkaloid tropine. There was a great demand for these alkaloids during World War I. The starting materials for this Mannich reaction were succindialdehdye, methyl amine, and acetone dicarboxylate. Robinsons's synthesis is an excellent example

of a biogenetic-type synthesis, because nature uses the identical starting materials to make this compound. The tandem one-pot reaction proceeds by two Mannich reactions, one intermolecular and one intramolecular, followed by decarboxylation to provide the product.

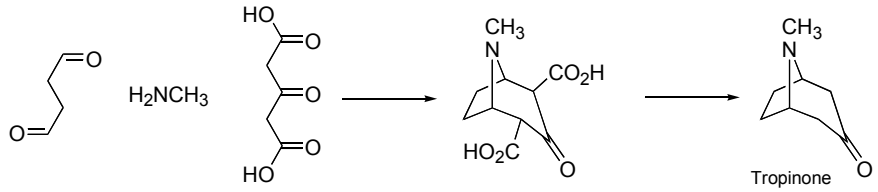

Scheme 4.4: Robinson's tropinone synthesis.

The classical Mannich reaction creates a number of problems for synthetic organic chemist to address. The classic Mannich reaction requires long reaction times and often side reactions occur such as bis-ketone formation, by deamination of the Mannich base to provide a Michael acceptor. Then Michael addition of the enol to the Michael acceptor provides the bis-ketone (Scheme 4.5).[1] Another limitation is if ammonia or a primary amine is used as the amine in the Mannich reaction, then repeated Mannich reactions will occur until all acidic hydrogens are removed. Also, the use of unsymmetrical ketones or ketones with two reactive α-positions can be problematic and leads to the formation of bis-Mannich bases.

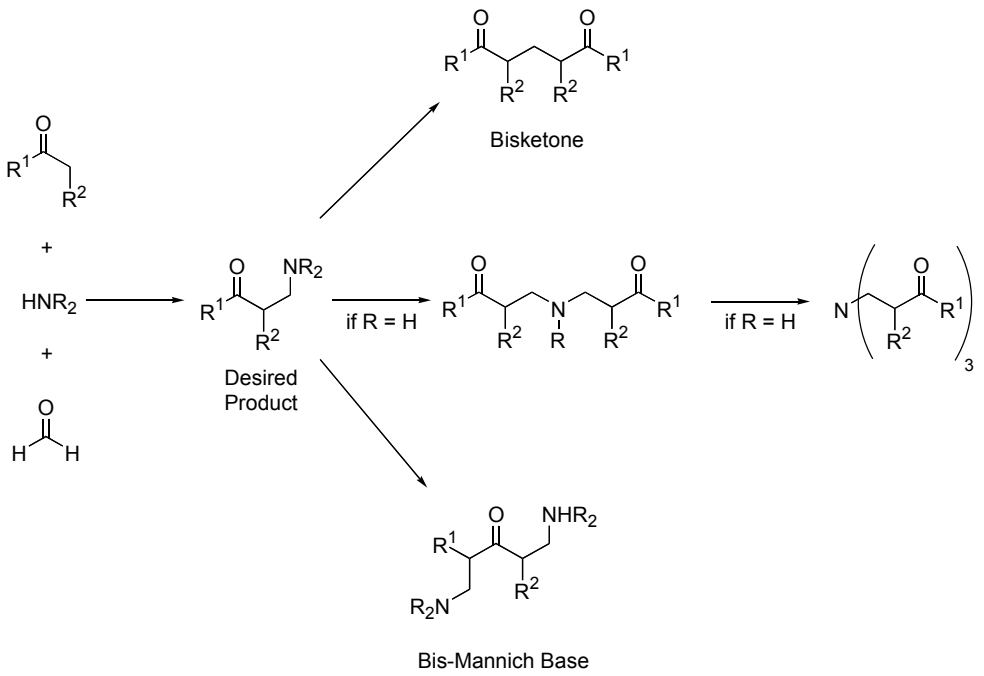

Scheme 4.5: Problems with the classic Mannich reactions.[1]

Even though the classic Mannich reaction possesses serious limitations, there has been considerable work conducted in order to overcome these problems. The solution is found in using preformed Mannich reagents. The use of preformed electrophiles, such as iminium salts or imines, provides a higher concentration of electrophile in the reaction mixture, which in turn allows the reactions to be conducted at a lower temperature with shorter reaction times.[1,6] The use of preformed nucleophiles, such as enolates, enol ethers, and enamines, also assists in preventing undesirable side reactions.[1]

4.2.2 Recent Developments in Mannich-Type Reactions

In 1997, Kobayashi reported the first catalytic enantioselective Mannich-type reaction using aldimines with silyl enolates in the presence of a novel zirconium catalyst.[7]

The zirconium catalyst is prepared *in situ* by the addition of $Zr(O^tBu)_4$, 6,6'-dibromo-1,1'-bi-2-naphthol, and N-methylimidazole (NMI) in dichloromethane. After an hour at room temperature the reaction is cooled to -45 °C and the aldimine and the ketene silyl acetal are added. The reaction proceeds with quantitative yield and 92% enantiomeric excess (Scheme 4.6).

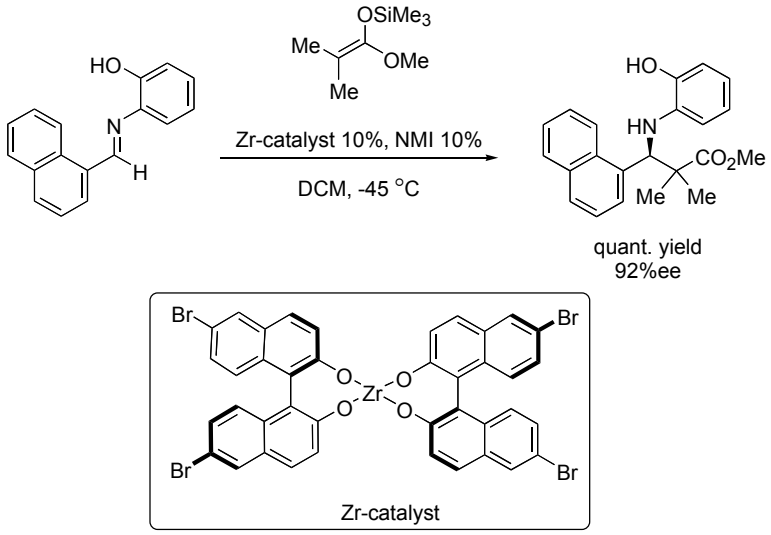

Scheme 4.6: First catalytic enantioselective Mannich-type reaction.

One of the most elegant Mannich methodologies is an organocatalytic one-pot three-component Mannich-type reaction developed by Barbas.[8] In this reaction the three reacting components (ketone, aniline, and aldehyde) are mixed together in the presence of L-proline at room temperature, and the desired Mannich product is obtained in good yield and selectivity (Scheme 4.7). One limitation of this methodology is regioselectivity. When unsymmetrical ketones possessing two reactive α-positions, as shown in Scheme

4.7, are used, regioisomers are generated. In the case of 2-butanone, two regioisomers are isolated as an inseparable mixture.

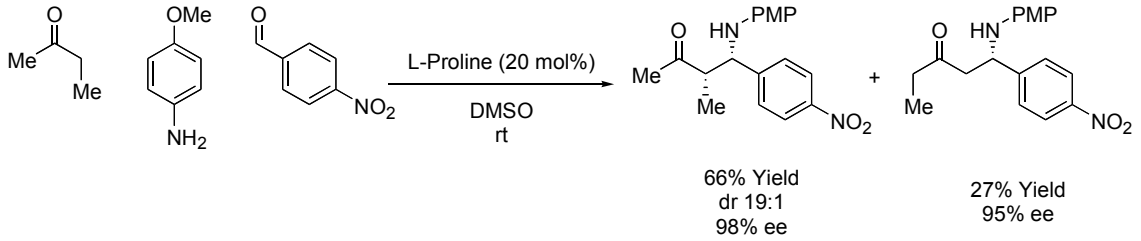

Scheme 4.7: Organocatalytic one-pot three-component Mannich-type reaction.

4.3.1 Development of a Hydrogen-Mediated Intermolecular Reductive Mannich Reaction

The development of a hydrogen-mediated reductive Mannich reaction by coupling of an enone and an imine would provide advantages over known Mannich-type reactions. This reaction would provide a catalytic reaction under neutral conditions with complete atom economy. Using an enone as a latent enolate would do away with the necessity for enolate preformation and the generation of regioisomers would not be an issue. Another advantage is that hydrogen gas is the cheapest and cleanest terminal reductant known to man (Scheme 4.8).

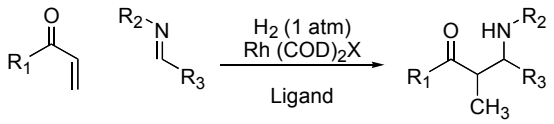

Scheme 4.8: Hydrogen-mediated intermolecular reductive Mannich reaction.

4.3.2 C-N DOUBLE BOND ISOMERIZATION

Performing selective reactions on imines can be very challenging due the *cis-trans* isomerization of imines.[9] Imines in solution at ambient temperature are in equilibrium with their *cis-trans* isomers.[10] Nucleophilic addition to an imine can occur *via* front-side or back-side attack. These two factors make selective addition to imines difficult (Scheme 4.9).

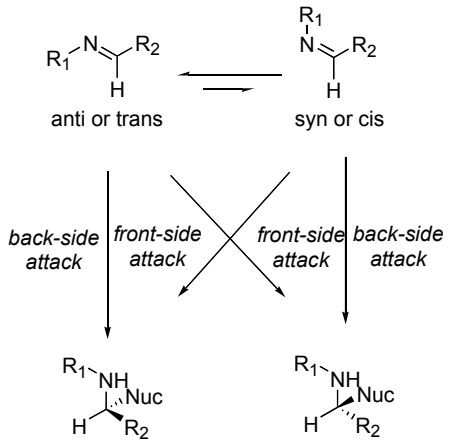

Scheme 4.9: C-N Double bond isomerization gives rise to poor selectivity.[9]

The *cis-trans* isomerization of imines can occur *via* one of three mechanisms: homolytic cleavage of the π-bond, heterolytic cleavage of the π-bond, or *via* a lateral shift mechanism.[11] Isomerization *via* homolytic cleavage of the π-bond would proceed through a transition state as shown in Scheme 4.10 and would require approximately 36 to 60 kcal/mol of energy. Homolytic cleavage of the π-bond is the accepted mechanism for the isomerization of many olefins, but for this case this reaction would have to be

photochemically induced in order to overcome such high-energy barriers. Therefore, isomerization *via* homolytic cleavage of the π-bond is possible, but not likely.

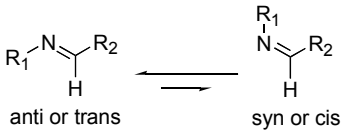

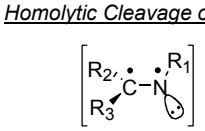

Scheme 4.10: *Cis-Trans* isomerization of imines by homolytic cleavage of the π-bond.

Cis-trans isomerization of imines by heterolytic cleavage of the π-bond could occur by destabilization of the C-N double bond by polarization. Heterolytic cleavage would create the structure shown in Scheme 4.11. The product of heterolytic cleavage could allow for rotation of the R_1 group to provide the other imine isomer.

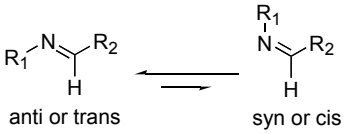

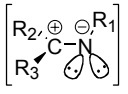

Scheme 4.11: *Cis-Trans* isomerization of imines by heterolytic cleavage of the π-bond.

Cis-trans isomerization of imines by a lateral shift mechanism proceeds by a shift of the substituent attached to nitrogen from one side to the other side. In order for this to occur, the nitrogen must adopt a linear *sp* hybridization and the π-bond remains intact with the lone pair occupying the perpendicular *p* orbital on nitrogen. It known that such inversions occur at sp^3 hybridized nitrogens, for example the pyramidal inversion of ammonia. Evidence supports that thermal *cis-trans* isomerizations of imines probably occurs by this lateral shift mechanism.[12] One very interesting thing to note is that in all cases when a heteroatom is directly bonded to the nitrogen of an imine, the configuration stability is much higher than *N*-alkyl and *N*-aryl imines.[11, 12]

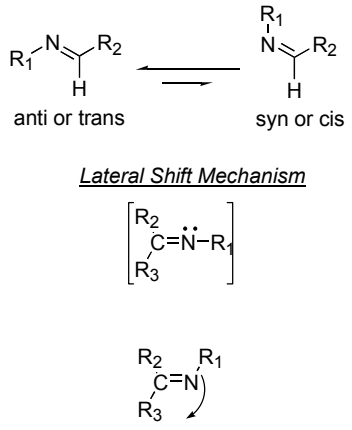

Scheme 4.12: *Cis-Trans* isomerization of imines by lateral shift mechanism.

4.3.3 REACTION OPTIMIZATION

The development of an intermolecular hydrogen-mediated reductive Mannich reaction began with the reductive coupling of methyl vinyl ketone and a *p*-methoxyphenyl-protected aldimine (Scheme 4.13). The aldimine **4.a** was easily prepared

according to known procedures[13] by combining ethylglyoxalate, *p*-anisidine, and dichloromethane in the presence of 4Å molecular sieves. The initial reaction conditions were those used in the *syn*-diastereoselective reductive aldol reaction discussed in Chapter 3. This transformation provided the Mannich base product **4.1** in 56% yield with a 1.3:1 syn:anti ratio (Table 4.1, entry 1). It is interesting to note that the basic additive had little effect on the reaction outcome (Table 4.1, entry 2). When the reaction was conducted in the absence of base the reaction proceeded in 42% yield with an identical 1.3:1 syn:anti ratio. The initial screenings with the PMP-protected aldimine derived from ethylglyoxalate were promising, but the aldimine did not have a long shelf life. Therefore, we synthesized an aldimine derived from *p*-nitrobenzaldehyde **4.b**.

Table 4.1: Optimization of the intermolecular hydrogen-mediated reductive Mannich reaction.

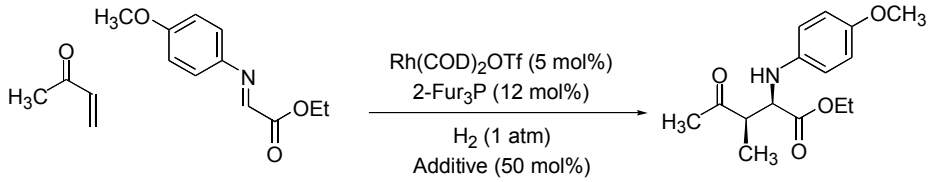

150 mol% **4.a** 100 mol% **4.1**

Entry	Additive	% Yield	dr
1	Li_2CO_3	56	1.3:1
2	No Additive	42	1.3:1

With the more stable aldimine **4.b** in hand, optimization of the intermolecular hydrogen-mediated reductive Mannich reaction began. Under identical conditions as

applied to imine **4.a**, the reductive coupling of MVK and imine **4.b** proceeded in 54% yield with a 1.4:1 syn:anti ratio to provide Mannich base **4.2** (Table 4.2, entry 1). Optimal yield was obtained by increasing the amount of MVK from 150 mol% to 300 mol% and eliminating the basic additive (Table 4.2, entry 4). This provided the product **4.2** in 91% yield with a 1.2:1 syn:anti ratio. Other ligands screened included the electron deficient benzofuran and the electron rich (p-MeOPh)$_3$P (Table 4.2 entries 5 & 6). The benzofuran ligated rhodium catalyst produced the Mannich product in poor yield and selectivity. When the electron rich (p-MeOPh)$_3$P was used no reaction occurred. Under optimized reaction conditions this transformation proceeds with excellent chemical yield, but the poor diastereoselectivity renders this transformation not synthetically useful.

Table 4.2: Optimization of the intermolecular hydrogen-mediated reductive Mannich reaction.

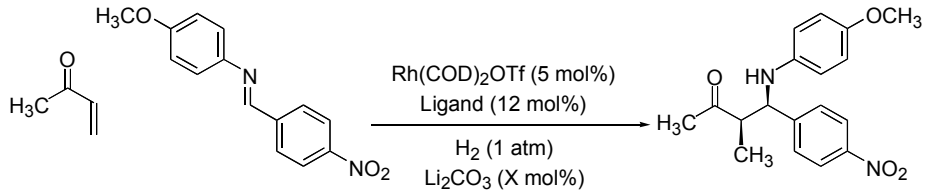

MVK (X mol%) | **4.b** (100 mol%) | **4.2**

entry	MVK	Ligand	Li_2CO_3	% Yield	dr	Reduced Imine
1	150 mol%	2-Fur$_3$P	50 mol%	54%	1.4:1	37%
2	150 mol%	2-Fur$_3$P	25 mol%	55%	1.4:1	37%
3	150 mol%	2-Fur$_3$P	No Additive	42%	1.4:1	53%
4	**300 mol%**	**2-Fur$_3$P**	**No Additive**	**91%**	**1.2:1**	**0%**
5	300 mol%	Benzofuran	No Additive	56%	1:1	0%
6	300 mol%	(p-MeOPh)$_3$P	No Additive	--	--	--

We decided to screen a variety of different nitrogen protecting groups in hope of developing a highly diastereoselective hydrogen-mediated Mannich reaction. Unfortunately, in every case the reductive Mannich product was obtained in poor diastereoselectivity (Table 4.3). We switched the *p*-methoxyphenyl protecting group for an *o*-methoxyphenyl protecting group to see if the *o*-methoxy group would provide a chelation controlled addition, but the diastereoselectivity was unaltered by this change. The reductive Mannich product **4.3** was obtained in 88% yield with 1:1 diastereoselectivity. Using an unsubstituted aniline as the nitrogen protecting group furnished the Mannich product **4.4** in excellent yield with poor diastereoselectivity. The reaction also proceeded with quantitative yield when a *p*-nitro substituted aniline was used as the nitrogen protecting group, but again the selectivity was poor (Table 4.3, **4.5**). An *o*-hydroxy aniline as the nitrogen protecting group provided the Mannich product **4.6** in 15% yield with 1:1 diastereoselectivity. Introducing steric bulk to the nitrogen protecting group did not produce an increase in selectivity, and as the size of the nitrogen protecting group increased the yield decreased (Table 4.3, **4.7** & **4.8**). The best diastereoselectivity (2:1) was obtained when a 2,6-dimethylaniline was used as the nitrogen protecting group (Table 4.3, **4.9**). Since, it appeared that the diastereoselectivity for the reductive Mannich reaction could not be improved by the steric or electron properties of the aniline-based nitrogen protecting group, we decided to screen other nitrogen protecting groups where the atom bonded to the imine nitrogen was not carbon. We hoped that this would impede the *cis-trans* isomerization of the imine and provide better diastereoselectivity for this transformation. Recall, that when a heteroatom is

directly bonded to the nitrogen of an imine the configuration stability is much higher than that of *N*-alkyl and *N*-aryl imines.[11, 12]

Table 4.3: Optimization of the intermolecular hydrogen-mediated reductive Mannich reaction – nitrogen protecting group screen.

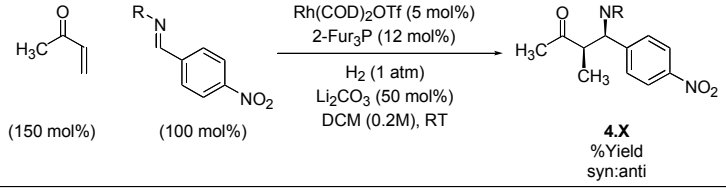

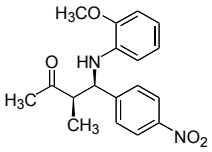 **4.3** 88% 1:1	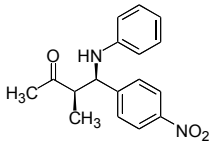 **4.4** 99% 1.5:1	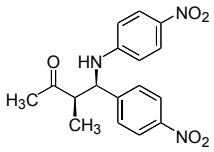 **4.5** quat. % 1.2:1
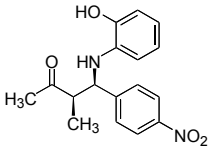 **4.6** 11% 1:1	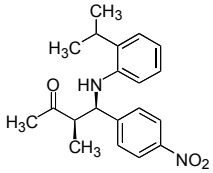 **4.7** 38% 1.6:1	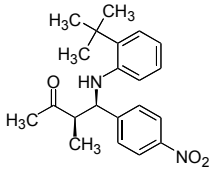 **4.8** trace --
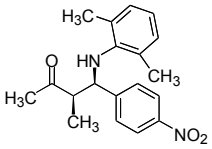 **4.9** 11% 2:1	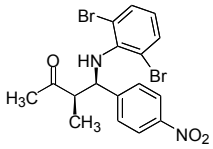 **4.10** No Rxn	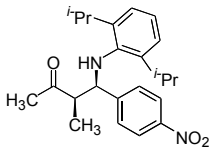 **4.11** No Rxn
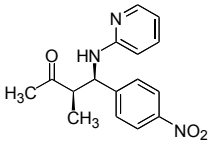 **4.12** No Rxn	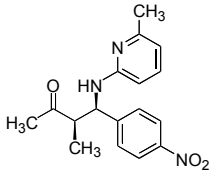 **4.13** No Rxn	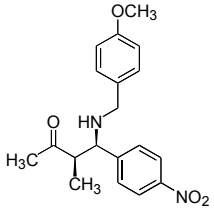 **4.14** No Rxn

Next, we focused our attention on a *N*-phosphinoylimine substrate. This substrate was easily prepared from a known literature procedure.[14] One very attractive feature of *N*-phosphinoylimines is that the nitrogen protecting group can effortlessly deprotected under mild acidic conditions to provide the amine. Unfortunately, the *N*-phosphinoylimine was not a suitable substrate. Under the reaction conditions *N*-phosphinoylimine was too unstable, and only trace product could be isolated (Table 4.4).

Table 4.4: Optimization of the intermolecular hydrogen-mediated reductive mannich reaction with *N*-phosphinoylimine substrates.

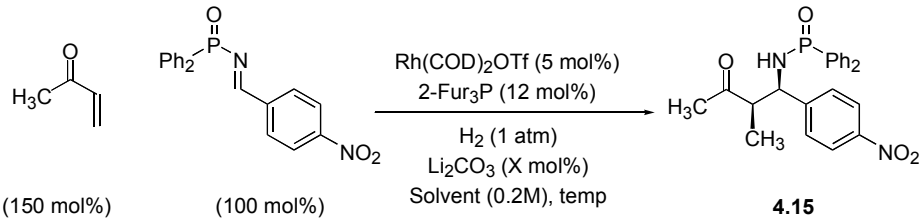

(150 mol%) (100 mol%) **4.15**

Entry	Li_2CO_3	Solvent	Temp	% Yield	dr
1	50 mol%	DCM	RT	--	--
2	No Additive	DCM	RT	--	--
3[a]	50 mol%	DCE	80 °C	5%	1:1

[a] Molecular sieves were added to the reaction mixture

Next, we turned our attention to the more robust *N*-sulfonylaldimines. The *N*-tosylaldimines were prepared without difficulty under neutral conditions according to a known literature procedure[15] by heating *p*-toluenesulfonamide and aldehyde in the presence of tetraethyl orthosilicate. The imine was then purified by trituration and

recrystallization. Gratifyingly, the *N*-tosylaldimine provided the Mannich product **4.16** in 71% yield and 20:1 syn:anti diastereoselectivity (Table 4.5, entry 1). Unfortunately, reproducibility was a major problem (Table 4.5, entry 2). The reproducibility issue couldstem from the low solubility of the *N*-toslyaldimine substrate. By decreasing the concentration of the reaction mixture from 0.2M to 0.1M, the *N*-toslyaldimine substrate was soluble but the yield dropped to 62% though 20:1 diastereoselectivity was preserved (Table 4.5, entry 3). Conducting the same reaction at room temperature resulted in a decrease in the chemical yield 40% (Table 4.5, entry 4). Changing the solvent to the more polar THF at 0.2M provided **4.16** in diminished yield and selectivity (Table 4.5, entry 5). Finally, attempting to push the reaction by using a higher boiling solvent, 1,2-dichloroethane, at 0.2M at 80 ºC furnished the product **4.16** in 27% yield with 4:1 diastereoselectivity. The structure of **4.16** was confirmed by the resonaces at δ 4.8 (d, 1H) and 3.1-3.2 (q, 1H) in the ^{1}H NMR spectrum corresponding to the methine proton adjacent to the tosyl-protected nitrogen and the methine at the α-position to the carbonyl group. HRMS data calculated [M + 1] for $C_{18}H_{21}N_2O_5S$: 377.1171 and found 377.1176 which also confirms the structure. A x-ray crystal structure was obtained for compound **4.16**, detailing the *syn* isomer was the preferred product (Figure 4.1).

Table 4.5: *N*-Toslyaldimine as substrates for the intermolecular hydrogen-mediated Mannich reaction.

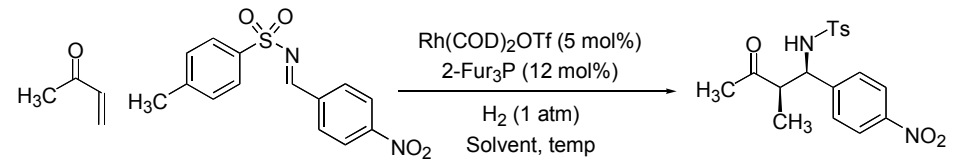

Entry	Solvent	Temp	% Yield	dr
1	DCM (0.2M)	35 °C	70%	20:1
2	DCM (0.2M)	35 °C	22%	18:1
3	DCM (0.1M)	35 °C	62%	20:1
4	DCM (0.1M)	RT	40%	20:1
5	THF (0.2M)	RT	22%	4:1
6	DCE (0.2M)	80 °C	27%	4:1

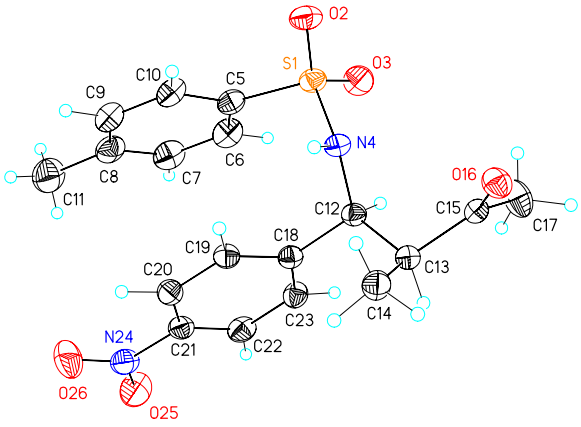

Figure 4.1: Single crystal x-ray diffraction analysis of **4.16.**

One possible explanation for the high levels of selectivity with the tosyl-protected aldimine could be that by placing a heteroatom directly on the nitrogen the energy barrier

for *cis-trans* isomerization is higher.[11, 12] Scheme 4.13 compares the reductive Mannich reaction with a tosyl-protected imine verses the same Mannich reaction with a *p*-methoxylphenyl-protected imine. In both reactions the Mannich product is obtained in reasonable yield, but the diastereoselectivities are drastically different (20:1 *vs* 1.2:1). For *N*-aryl imines the *cis-trans* isomerization is a facile process in solution and could account for the poor selectivity in this transformations.[11, 12]

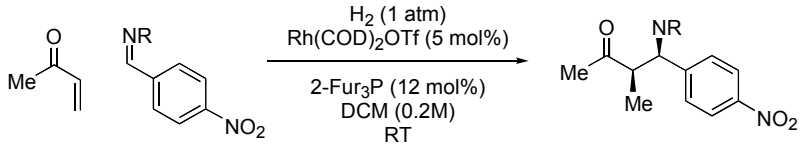

Scheme 4.13: Tosyl-protected imines verses *N*-aryl imines in the hydrogen-mediated Mannich reactions.

In order to improve the chemical yield and obtain reproducible results, variations of the tosyl-protected imine were screened. We envisioned that by making the nitrogen protecting group more electron deficient the imine would be a better electrophile for the hydrogen-mediated reductive Mannich reaction. An *o*-nitro-*N*-sulfonylaldimine **4.c** was synthesized. Employment of **4.c** in the hydrogen-mediated Mannich reaction produced the desired product **4.17** in a reproducible 78% yield with 7.5:1 diastereoselectivity (Scheme 4.14).

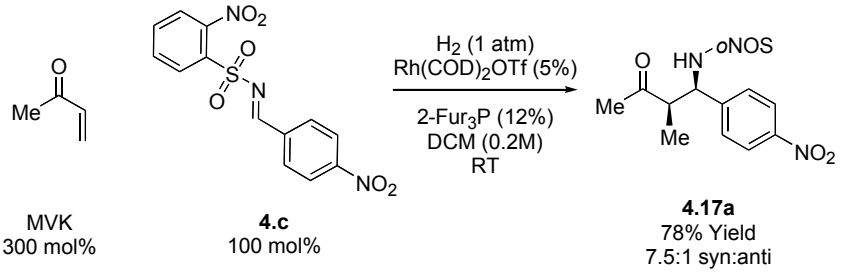

Scheme 4.14: *o*-Nitro-*N*-sulfonylaldimine as substrate for the hydrogen-mediated reductive Mannich reaction.

Attempting to apply these conditions to other *o*-nitro-*N*-sulfonylaldimines such as **4.d** proved to be disappointing, as the Mannich product **4.18** was obtained in only 23% yield with 13:1 diastereoselectivity (Table 4.6, entry 1). This led us to explore another reaction parameter, the catalyst counter ion. By changing the counter ion of the cationic rhodium metal from triflate to the less coordinating BF_4^- ion the yield increased to 46% with a 12:1 syn:anti ratio (Table 4.6, entry 2). The SbF_6^- ion provided **4.18** in 30% yield with a 10:1 diastereoselectivity (Table 4.6, entry 3). Lastly, when the large and uncoordinating $BARF^-$ ion is utilized as counter ion, the product is obtained in 17% yield. From this data BF_4^- appears to be the optimal counter ion for the cationic rhodium catalyst. This counter ion effect was confirmed using imine **4.c**, and this change increased the yield of the Mannich product **4.17** from 78% with triflate as the counter ion, to a 95% yield and 11:1 diastereoselectivity with BF_4^- as the counter ion. (Table 4.7).

Table 4.6: Catalyst counter ion effect on the hydrogen-mediated reductive Mannich reaction.

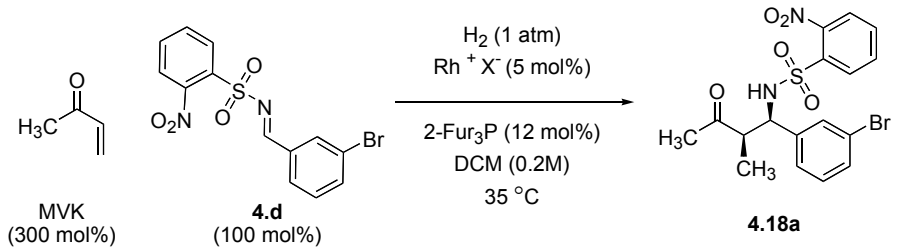

Entry	Rh^+X^-	% Yield	dr
1	$Rh(COD)_2$**OTf**	23%	13:1
2	$Rh(COD)_2$**BF_4**	46%	12:1
3	$Rh(COD)_2$**SbF_6**	30%	10:1
4	$Rh(COD)_2$**BARF**	17%	--

Table 4.7: Catalyst counter ion effect on the hydrogen-mediated reductive Mannich reaction.

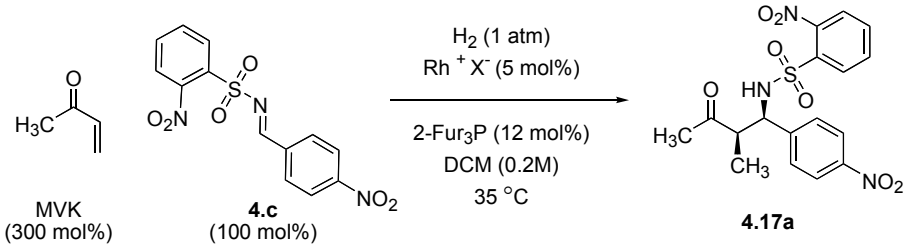

entry	Rh^+X^-	% Yield	dr
1	$Rh(COD)_2$**OTf**	78%	8:1
2	$Rh(COD)_2$**BF_4**	95%	11:1

In order to gain insight to the mechanism of this transformation, a reductive Mannich reaction was conducted under an atmosphere of deuterium gas. The result was the exclusive incorporation of a single deuterium atom at the former enone β-position (Scheme 4.15). This is consistent with irreversible enolization *via* enone hydrometallation. At this time it is not clear if this proceeds through a monohydride catalytic cycle (Scheme 4.16) or an enone-imine oxidative coupling mechanism (Scheme 4.17).

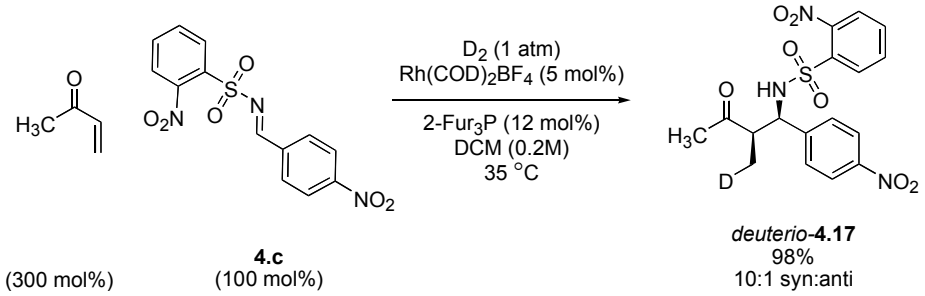

Scheme 4.15: Rhodium-catalyzed hydrogenative Mannich reaction under an atmosphere of deuterium.

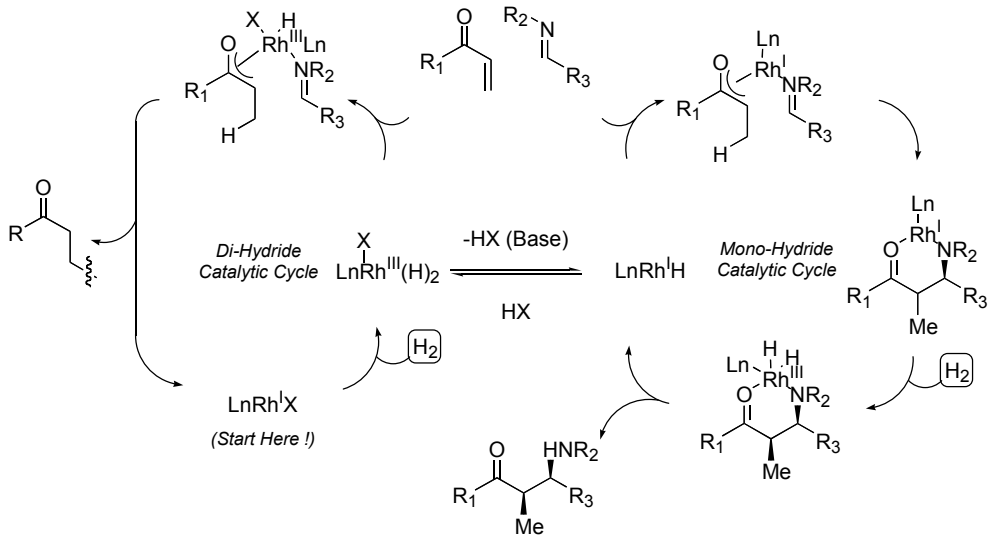

Scheme 4.16: Proposed monohydride catalytic cycle for hydrogen-mediated reductive Mannich reaction.

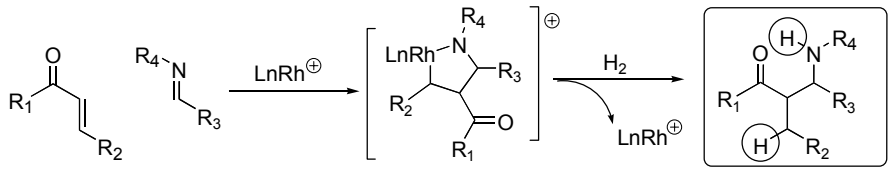

Scheme 4.17: Proposed oxidative coupling mechanism for hydrogen-mediated reductive Mannich reaction.

There are two possible transition states to consider in order to explain the high levels of syn-diastereoselectivity in the reductive Mannich reaction. Upon enone hydrometallation a *Z*(O)-enolate is stereospecifically generated *via* rhodium hydride addition to the *s*-cis conformer of the enone through a six-centered transition structure as depicted in Scheme 3.14. Then addition of the *Z*(O)-enolate to the *trans* imine can occur to the front or back side of the imine (Scheme 4.9). Both chair and boat-like transition

structures can predict the stereochemical outcome of the reaction (Scheme 4.18). At this time it is not clear which transition structure is preferred.

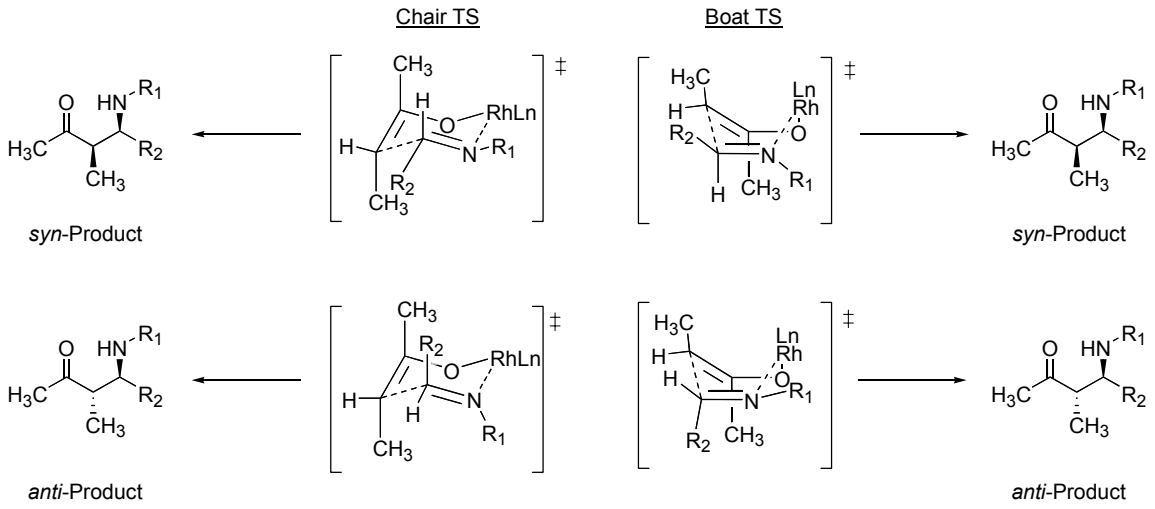

Scheme 4.18: Possible transition states for the hydrogen-mediated reductive Mannich reaction.

4.3.4 SUBSTRATE SCOPE

With optimized reactions conditions in hand, the substrate scope was explored. For the hydrogen-mediated reductive Mannich reaction only activated imines participated in the reaction. Table 4.8 shows the products obtained from the reductive coupling of MVK and activated imines. The best yield and selectivity was obtained from the *p*-nitrobenzaldehyde derived imine (Table 4.8, entry **4.17a**). This reaction proceeded at 5 mol% catalyst loading to provide the Mannich product **4.17a** in 92% yield with 13:1 syn:anti selectivity. For the remainder of the examples the catalyst loading had to be increased to 10 mol% and 200 mol% sodium sulfate was used in order to prevent imine

hydrolysis. For entries **4.18a**, **4.21a**, **4.22a**, and **4.23a** the reaction was conducted at 0.4M concentration with 500 mol% MVK, due to the fact that these imines are less eletrophilic. Table 4.9 demonstrates the reductive Mannich coupling of EVK and activated imines. The use of EVK dramatically slowed the reaction. With MVK the reaction was complete after 24 hours but EVK necessitated extending the reaction time to 48 hours. For the EVK examples 500 mol% of the reagent had to be used in order to achieve acceptable yields. The hydrogen-mediated reductive Mannich reaction proceeded with high levels of chemoselectivity, but the substrate scope is limited to activated imines. Electron rich imines do not participate in this transformation.

Table 4.8: Hydrogen-mediated intermolecular reductive Mannich reactions with MVK.

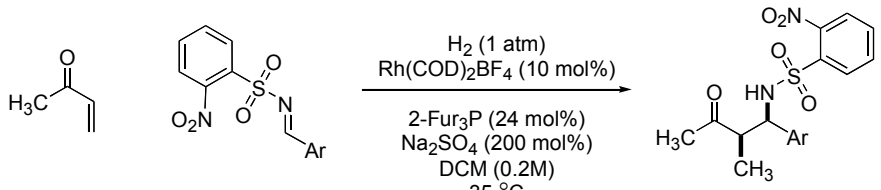

300 mol% | 100 mol% | **4.x** % Yield syn:anti

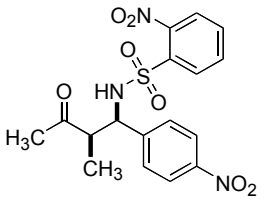

4.17a[b]
92 %Yield
13:1 dr

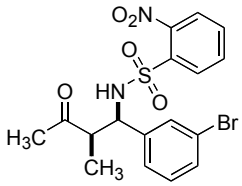

4.18a[c]
58 %Yield
9:1 dr

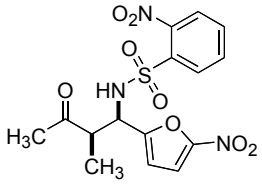

4.19a
87 %Yield
4:1 dr

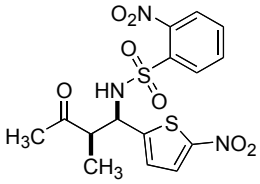

4.20a
90 %Yield
6:1 dr

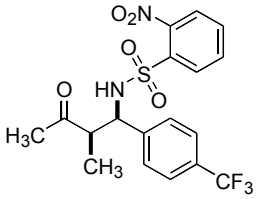

4.21a[c]
71 %Yield
6:1 dr

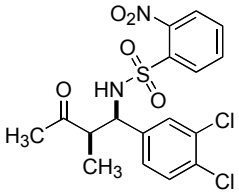

4.22a[c]
67 %Yield
9:1 dr

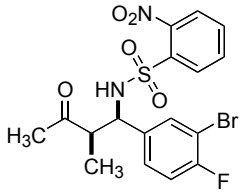

4.23a[c]
43%Yield
5:1 dr

[a]As product ratios were found to vary with surface to volume ratio of the reaction mixture, all transformations were conducted on 0.39 mmol scale in 13x100 mm test tube. [b] Reaction conducted at 5 mol% catalyst loading without Na_2SO_4 . [c] Reaction conducted with 500 mol% MVK at 0.4M DCM.

Table 4.9: Hydrogen-mediated intermolecular reductive Mannich reactions with EVK.

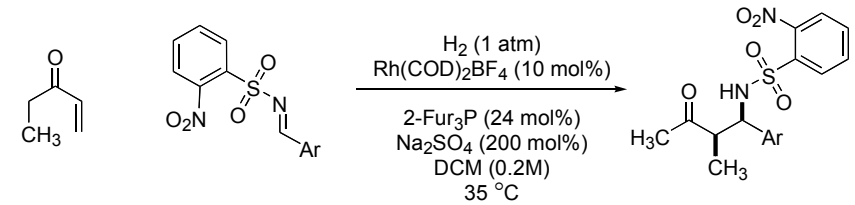

500 mol% | 100 mol% | **4.x** % Yield syn:anti

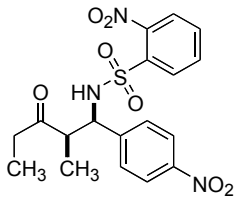

4.17b[b]
80 %Yield
7:1 dr

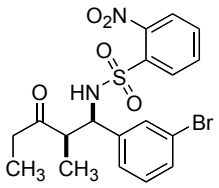

4.18b[c]
46 %Yield
6:1 dr

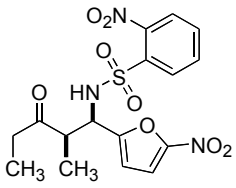

4.19b
83 %Yield
4:1 dr

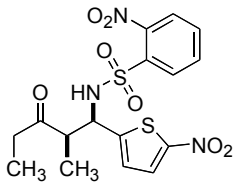

4.20b
55% Yield
5:1 dr

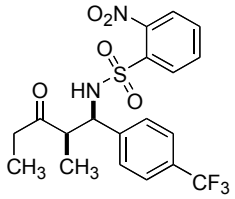

4.21b[c]
56 %Yield
6:1 dr

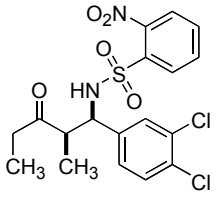

4.22b[c]
58 %Yield
7:1 dr

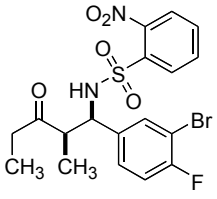

4.23b[c]
36%Yield
5.5:1 dr

[a]As product ratios were found to vary with surface to volume ratio of the reaction mixture, all transformations were conducted on 0.39 mmol scale in 13x100 mm test tube. [b] Reaction conducted at 5 mol% catalyst loading. [c] Reaction conducted at 0.4M DCM.

4.4 CONCLUSIONS

The developed hydrogen-mediated reductive Mannich methodology is a promising alternative to the classic Mannich reaction. The major limitation is the substrate scope. Only activated imines are viable electrophilic partners. There exists a fine line in which the imine needs to be activated towards addition, though with increased activation often comes problems in isolation and purification. Another issue is imine solubility; the *N*-sulfonylaldimines are not very soluble in organic media, which makes working with them difficult. Even with these limitations, this methodology has the promise of becoming a general method for the synthesis of Mannich bases. Future work includes the development of an enantioselective variant of the hydrogen-mediated reductive Mannich reaction would be a major advance.

4.5.1 EXPERIMENTAL SECTION

GENERAL

All reactions were run under an atmosphere of argon, unless otherwise indicated. Anhydrous solvents were transferred by an oven-dried syringe. Flasks were flame-dried and cooled under a stream of nitrogen. Dichloromethane (DCM) and 1,2-Dichloroethane (DCE) were distilled from calcium hydride. Tetrahydrofuran (THF) was purified by distillation from sodium-benzophenone/ketyl radical. Chemical reagents were purchased from Aldrich and Strem Chemicals. Commercially available aldehydes and enones were purified prior to usage. Deuterated solvents were used as received from Cambridge Isotope Laboratories. Analytical thin-layer chromatography (TLC) was carried out using 0.2-mm commercial silica gel plates (DC-Fertigplatten Kieselgel 60 F_{254}). Flash chromatography was performed on silica gel 60 (200-400 mesh) according to the method of Still.[16] Proton nuclear magnetic resonance (^{1}H NMR) spectra were recorded on a Varian Mercury 400, or Unity+ 300 spectrometer. ^{1}H NMR spectra were obtained at 400 MHz or 300 MHz, as indicated. Chemical Shifts are reported in delta (δ) units, parts per million (ppm) downfield from trimethylsilane for deuteriochloroform. In the case when deuterioacetone is used as a NMR solvent then the reference point is the center of the quintet at 2.05 ppm. Coupling constants are reported in Hertz (Hz). Carbon-13 nuclear magnetic resonance (^{13}C-NMR) spectra were recorded on a Varian Mercury 400, or Unity+ 300 spectrometer. ^{13}C-NMR spectra were obtained at either 100MHz or 75 MHz, as indicated. Chemical Shifts are reported in delta (δ) units, parts per million (ppm) relative to the center triplet at 77.0 ppm for deuteriochloroform. In the case when

deuterioacetone is used as a NMR solvent then the reference point is the center of the septet at 29.9 ppm. ^{13}C-NMR spectra were routinely run with broadband decoupling. High-resolution mass spectra (HRMS) were obtained on a Micromass ZAB-E spectrometer and are reported as m/z (relative intensity). Accurate masses are reported for the molecular ion (M+1) or a suitable fragment ion. FT-IR spectra were obtained using a Nicolet Impact 410 spectrometer. Melting points were obtained on a Thomas-Hoover Unimelt apparatus in open capillaries and are uncorrected.

4.5.2 General Procedure for the Synthesis of *N*-Nosylaldimines

N-Nosylaldimines were prepared according to the procedure established by Love for the synthesis of N-tosylaldimines.[15] To a round-bottomed flask charged with aldehyde (100 mol%) and 2-nitrobenzenesulfonamide (100 mol%) was added tetraethylorthosilicate (113 mol%). The round-bottomed flask was equipped with a still head and heated to 160 °C under an atmosphere of argon. The reaction was allowed to proceed for ~6 hours during which time ethanol collected in the receiving flask. The reaction was cooled to room temperature and then ethyl ether was added to the reaction mixture. The reaction mixture stirred with the ethyl ether for several hours and then it was filtered and washed with cold ethyl ether 3 times. The product was then recrystallized from the appropriate solvent.

4.5.3 General Procedure for the Intermolecular Hydrogen-Mediated Reductive Coupling of Methyl Vinyl Ketone and *N*-Nosylaldimines

To a 13 mm x 100 mm test-tube charged with Na_2SO_4 (0.78 mmol, 200 mol%) Fur_3P (0.094 mmol, 24 mol%), $Rh(COD)_2OTf$ (0.039 mmol, 10 mol%), and imine (0.39 mmol, 100 mol%) was added dichloromethane (0.2 M). Then the test-tube was sealed and the reaction system was purged with argon and then with hydrogen for 20 seconds each. The reaction was placed under one atmosphere of hydrogen using a balloon, and MVK (1.17 mmol, 300 mol%) was added to the reaction mixture and it was stirred for 24 hours. The products were separated by column chromatography. For entry **4.17a** the reaction was conducted at 5 mol% $Rh(COD)_2OTf$ without Na_2SO_4. For entries **4.18a, 4.21a, 4.22a, and 4.23a** the reaction was conducted using 500 mol% MVK at 0.4 M DCM.

4.5.4 General Procedure for the Intermolecular Hydrogen-Mediated Reductive Coupling of Ethyl Vinyl Ketone and *N*-Nosylaldimines

To a 13 mm x 100 mm test-tube charged with Na_2SO_4 (0.78 mmol, 200 mol%) Fur_3P (0.094 mmol, 24 mol%), $Rh(COD)_2OTf$ (0.039 mmol, 10 mol%), and imine (0.39 mmol, 100 mol%) was added dichloromethane (0.2 M). Then the test-tube was sealed and the reaction system was purged with argon and then with hydrogen for 20 seconds each. The reaction was placed under one atmosphere of hydrogen using a balloon, and EVK (1.95 mmol, 500 mol%) was added to the reaction mixture and it was stirred for 48 hours. The products were separated by column chromatography. For entry **4.17b** the

reaction was conducted at 5 mol% $Rh(COD)_2OTf$. For entries **4.18b, 4.21b, 4.22b, and 4.23b** the reaction was conducted using 500 mol% MVK at 0.4 M DCM.

4.6 SPECTROSCOPIC CHARACTERIZATION DATA

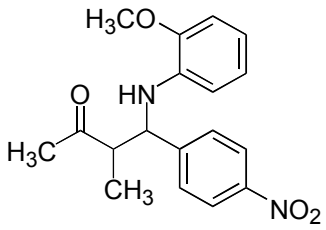

4.3
1:1(syn:anti)

4-(2-Methoxyphenylamino)-3-methyl-4-(4-nitrophenyl)-butan-2-one (4.3). This product was obtained as an inseparable mixture of syn:anti diastereomers. ^{1}H NMR (400 MHz, d6-DMSO): δ 0.82 (d, *J* = 7.2 Hz, 3H), 1.04 (d, *J* = 7.0 Hz, 3H), 2.04 (s, 3H), 2.16 (s, 3H), 3.17-3.31 (m, 2H), 3.78 (s, 3H), 3.80 (s, 3H), 4.76 (t, *J* = 9.5 Hz, 1H), 4.91 (t, *J* = 7.6 Hz, 1H), 4.91 (t, *J* = 7.6 Hz, 1H), 5.26 (d, *J* = 8.5 Hz, 1H), 5.68 (d, *J* = 9.8 Hz, 1H), 6.38 (dd, *J* = 6.3, 1.5 Hz, 1H), 6.44-6.56 (m, 2H), 6.58-6.63 (m, 2H), 6.75 (m, 1H), 6.78 (dd, *J* = 6.4, 1.4 Hz, 1H), 7.65 (d, *J* = 8.8 Hz, 2H), 7.76 (d, *J* = 8.8 Hz, 1H), 8.15 (d, *J* = 8.8 Hz, 3H). ^{13}C NMR (75 MHz, d6-DMSO): δ 11.9, 14.5, 28.9, 29.1, 50.9, 51.6, 55.4, 55.5, 57.0, 58.2, 60.4, 61.0, 110.0, 110.1, 110.5, 110.7, 116.5, 116.6, 120.8, 123.2, 123.3, 128.5, 128.8, 136.1, 136.2, 146.5, 146.6, 146.7, 150.4, 209.7, 211.0. HRMS: Calcd [M+1] for $C_{18}H_{21}N_2O_4$: 329.1501; Found: 329.1505. FTIR (film) 3420, 2255, 2129, 1659, 1518, 1348, 1024, 826, 764 cm^{-1}.

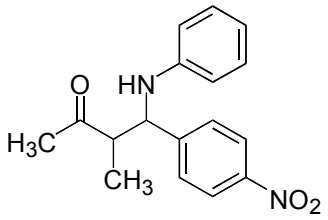

4.4
1.5:1 (syn:anti)

3-Methyl-4-(4-nitrophenyl)-4-phenylaminobutan-2-one (4.4). This product was obtained as an inseparable mixture of syn:anti diastereomers. ^{1}H NMR (400 MHz, d6-DMSO): δ 0.75 (d, *J* = 7.0 Hz, 3H), 1.06 (d, *J* = 7.0 Hz, 3H), 2.05 (s, 3H), 2.23 (s, 3H), 2.87-2.94 (m, 1H), 3.01-3.09 (quintet, *J* = 7.0 Hz, 1H), 4.75 (t, *J* = 10.1 Hz, 1H), 4.99 (t, *J* = 7.0 Hz, 1H), 6.14 (d, *J* = 9.1 Hz, 1H), 6.38 (d, *J* = 9.8 Hz, 1H), 6.44-6.50 (q, *J* = 7.7 Hz, 2H), 6.59 (t, *J* = 8.1 Hz, 3H), 6.93-7.00 (q, *J* = 8.2 Hz, 3H), 7.65 (d, *J* = 8.8 Hz, 2H), 7.76 (d, *J* = 8.8 Hz, 2H), 8.16 (dd, *J* = 6.3, 2.5 Hz, 3H). ^{13}C NMR (75 MHz, d6-DMSO): δ 11.6, 14.2, 28.5, 28.6, 51.8, 52.2, 57.0, 58.3, 113.0, 113.2, 116.5, 116.6, 123.3, 128.4, 128.7, 128.8, 146.4, 146.6, 147.2, 147.3, 150.4, 150.8, 209.0, 210.3. HRMS: Calcd [M+1] for $C_{17}H_{19}N_2O_3$: 299.1396; Found: 299.1401. FTIR (film) 3406, 1658, 1348, 1275, 1048, 1025. 996, 764 cm^{-1}.

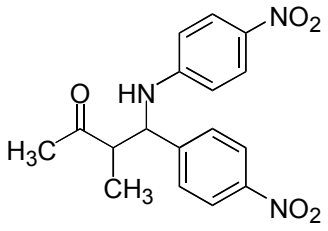

4.5
1.2:1 (syn:anti)

3-Methyl-4-(4-nitrophenyl)-4-(4-nitrophenylamino)-butan-2-one (4.5). This product was obtained as an inseparable mixture of syn:anti diastereomers. ^{1}H NMR (400 MHz, d6-DMSO): δ 0.80 (d, *J* = 7.2 Hz, 3H), 1.01 (d, *J* = 7.0 Hz, 3H), 2.05 (s, 3H), 2.24 (s, 3H), 2.99-3.08 (m, 1H), 3.11-3.18 (quintet, *J* = 7.0 Hz, 1H), 4.95 (t, *J* = 9.4 Hz, 1H), 5.14 (t, *J* = 7.9 Hz, 1H), 6.68 (d, *J* = 9.2 Hz, 1H), 6.74 (d, *J* = 9.0 Hz, 1H), 7.60 (d, *J* = 8.5 Hz, 1H), 7.64 (d, *J* = 8.8 Hz, 2H), 7.75 (d, *J* = 8.8 Hz, 2H), 7.82 (d, *J* = 8.8 Hz, 1H), 7.91 (t, *J* = 8.8 Hz, 3H), 8.20 (dd, *J* = 6.5, 2.3 Hz, 3H). ^{13}C NMR (75 MHz, d6-DMSO): δ 12.0, 14.2, 28.7, 29.6, 51.3, 51.9, 55.8, 56.8, 57.4, 68.5, 123.6, 125.9, 128.4, 128.8, 136.6, 136.7, 146.7, 146.8, 148.8, 149.2, 153.1, 153.4, 208.7, 209.8. HRMS: Calcd [M+1] for $C_{17}H_{18}N_3O_5$: 344.1246; Found: 344.1244. FTIR (film) 3418, 1658, 1309, 1026, 1004, 826, 764, 630 cm^{-1}.

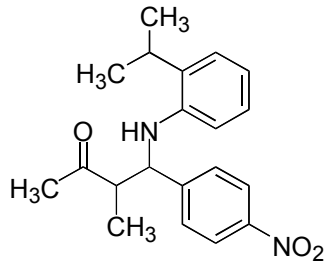

4.7
1.6:1 (syn:anti)

4-(2-Isoproylphenylamino)-3-methyl-4-(4-nitrophenyl)-butan-2-one (4.7). This product was obtained as an inseparable mixture of syn:anti diastereomers. ^{1}H NMR (400 MHz, d6-DMSO): δ 0.81 (d, *J* = 7.0 Hz, 3H), 1.09-1.20 (m, 15H), 2.01 (s, 3H), 2.19 (s, 3H), 3.08-3.19 (septet, *J* = 6.7 Hz, 2H), 3.21-3.30 (m, 1H), 4.75 (t, *J* = 9.5 Hz, 1H), 4.84 (t, *J* = 7.7 Hz, 1H), 5.18 (d, *J* = 8.1 Hz, 1H), 5.57 (d, *J* = 9.5 Hz, 1H), 6.35 (d, *J* = 7.5 Hz, 1H), 6.46 (d, *J* = 8.2 Hz, 1H), 6.49-6.56 (m, 2H), 6.82 (t, *J* = 7.7 Hz, 2H), 6.98 (dd, *J* = 6.0, 1.5 Hz, 1H), 7.02 (dd, *J* = 6.0, 1.5 Hz, 1H), 7.68 (d, *J* = 8.8, 2H), 7.81 (d, *J* = 8.8, 1H), 8.15 (m, 3H). ^{13}C NMR (75 MHz, d6-DMSO): δ 12.7, 14.6, 22.4, 22.5, 22.6, 25.9, 26.0, 29.2, 51.6, 52.5, 58.3, 59.5, 111.7, 117.6, 117.7, 124.1, 125.3, 125.4, 126.9, 129.3, 129.5, 130.7, 133.1, 133.2, 143.9, 144.0, 147.2, 147.3, 151.3, 151.5, 210.9, 212.0. HRMS: Calcd [M+1] for $C_{20}H_{25}N_2O_3$: 341.1865; Found: 341.1862. FTIR (film) 3406, 1656, 1275, 1025, 998, 826, 764, 631 cm^{-1}.

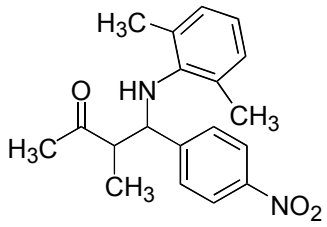

4.9
2:1 (syn:anti)

4-(2,6-Dimethylphenylamino)-3-methyl-4-(4-nitrophenyl)-butan-2-one (4.9). This product was obtained as an inseparable mixture of syn:anti diastereomers. ^{1}H NMR (400 MHz, d6-DMSO): δ 0.71 (d, *J* = 6.9 Hz, 3H), 1.36 (d, *J* = 6.9 Hz, 3H), 1.93 (s, 3H), 2.05, (s, 6H), 2.06 (s, 6H), 2.31 (s, 3H), 3.43-3.56 (m, 2H), 4.35-4.49 (m, 2H), 4.57 (d, *J* = 11.6 Hz, 2H), 6.56-6.81 (m, 2H), 6.75 (d, *J* = 7.5 Hz, 2H), 6.80 (d, *J* = 7.5 Hz, 1H), 7.48 (d, *J* = 8.8 Hz, 1H), 7.55 (d, *J* = 8.8 Hz, 2H), 8.05 (d, *J* = 8.8 Hz, 1H), 8.08 (d, *J* = 8.8 Hz, 2H). ^{13}C NMR (75 MHz, d6-DMSO): δ 15.3, 19.7, 31.9, 50.3, 63.3, 121.7, 123.7, 123.8, 129.3, 129.4, 129.5, 144.3, 144.5, 147.2, 151.0, 210.9, 212.3. HRMS: Calcd [M+1] for $C_{19}H_{23}N_2O_3$: 327.1709; Found: 327.1711. FTIR (film) 3406, 1656, 1275, 1025, 996, 827, 764 cm^{-1}.

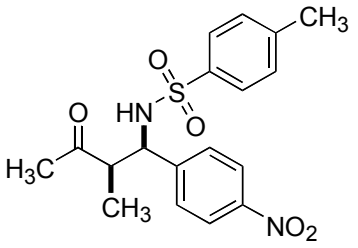

4.16

4-Methyl-*N*-[2-methyl-1-(4-nitrophenyl)-3-oxo-butyl]-benzenesulfonamide (4.16). ^{1}H NMR (400 MHz, d6-Acetone): δ 1.12 (d, *J* = 7.0 Hz, 3H), 1.97 (s, 3H), 2.26 (s, 3H), 3.17 (quintet, *J* = 7.4 Hz, 1H), 4.78 (d, *J* = 8.6 Hz, 1H), 7.11 (d, *J* = 8.3 Hz, 2H), 7.18 (bs, 1H), 7.40 (d, *J* = 8.4 Hz, 2H), 7.45 (d, *J* = 8.0 Hz, 2H), 7.93 (d, *J* = 8.0 Hz, 2H). ^{13}C NMR (75 MHz, d6-Acetone): δ 13.5, 21.2, 53.0, 59.7, 123.8, 127.7, 129.5, 130.0, 139.4, 143.7, 147.7, 148.5, 208.8. HRMS: Calcd [M+1] for $C_{18}H_{21}N_2O_5S$: 377.1171; Found: 377.1176. FTIR (film) 3278, 1710, 1598, 1520, 1443, 1347, 1160, 1089, 854, 664 cm^{-1}. MP = 159-161 °C.

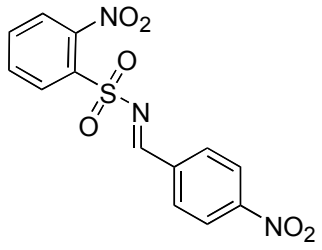

4.c

2-Nitro-*N*-(4-nitrobenzylidene)-benzenesulfonamide (4.c). ^{1}H NMR (400 MHz, $CDCl_3$): δ 7.84-7.89 (m, 3H), 8.20 (d, *J* = 9.9 Hz, 2H), 8.37 (d, *J* = 8.9 Hz, 2H), 8.43 (m, 1H), 9.18 (s, 1H). ^{13}C NMR (75 MHz, $CDCl_3$): δ 124.3, 125.0, 131.0, 132.3, 132.9, 135.2, 137.0, 148.6, 151.5, 171.2. HRMS: Calcd [M+1] for $C_{13}H_{10}N_3O_6S$:

336.0290; Found: 336.0296. FTIR (film) 1594, 1347, 1165, 1125, 1056, 839, 798, 748, 675, 590 cm^{-1}. MP = 186-187 °C.

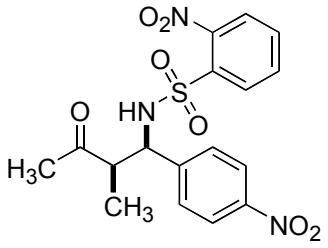

4.17a

***N*-[2-Methyl-1-(4-nitrophenyl)-3-oxo-butyl]-2-nitrobenzenesulfonamide**

(4.17a). ^{1}H NMR (400 MHz, d6-Acetone): δ 1.23 (d, *J* = 7.0 Hz, 3H), 1.93 (s, 3H), 3.29-3.44 (m, 1H), 4.86 (d, *J* = 9.2 Hz, 1H), 7.43 (bs, 1H), 7.56 (d, *J* = 8.8 Hz, 2H), 7.63 (t, *J* = 7.9 Hz, 1H), 7.72 (t, *J* = 6.9 Hz, 1H) 7.77 (m, 1H). 7.88 (dd, *J* = 6.5, 1.4 Hz, 1H), 7.96 (d, *J* = 8.8 Hz, 2H). ^{13}C NMR (75 MHz, d6-Acetone): δ 14.5, 52.6, 60.5, 123.9, 125.5, 129.7,131.3, 133.3, 134.3, 134.7, 147.9, 209.3. HRMS: Calcd [M+1] for $C_{17}H_{18}N_3O_7S$: 408.0865; Found: 408.0866. FTIR (film) 3324, 3099, 2938, 1712, 1607, 1540, 1441, 1349, 1268, 1167, 1124, 1060, 854, 741, 593 cm^{-1}. MP = 123-125 °C.

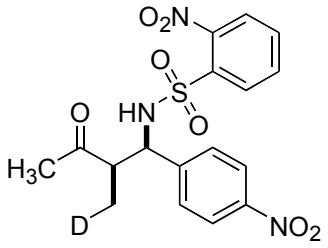

***deuterio*-4.17a**

Deuterio-*N*-[2-Methyl-1-(4-nitrophenyl)-3-oxo-butyl]-2-nitrobenzenesulfonamide (deuterio-4.17a). ^{1}H NMR (400 MHz, d6-Acetone): δ 1.22 (d, *J* = 6.8 Hz, 2H), 1.93 (s, 3H), 3.29-3.44 (m, 1H), 4.86 (d, *J* = 9.2 Hz, 1H), 7.43 (bd, *J* = 8.6 Hz, 1H), 7.57 (d, *J* = 8.8 Hz, 2H), 7.71 (t, *J* = 7.6 Hz, 1H), 7.72 (t, *J* = 6.9 Hz, 1H) 7.76-7.82 (m, 1H). 7.88 (dd, *J* = 6.7, 1.3 Hz, 1H), 7.97 (d, *J* = 9.0 Hz, 2H). ^{13}C NMR (75 MHz, d6-Acetone): δ 14.2 (t, *J* = 19.4 Hz), 29.7, 52.5, 60.5, 123.9, 125.5, 129.7, 131.4, 133.3, 134.3, 134.7, 147.9, 148.0, 148.2, 209.3. HRMS: Calcd [M+1] for $C_{17}H_{17}DN_3O_7S$: 409.0928; Found: 409.0926. FTIR (film) 3333, 3100, 1711, 1607, 1540, 1431, 1349, 1271, 1168, 1125, 1061, 855, 732, 593 cm^{-1}. MP = 126-127 °C.

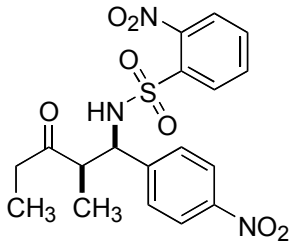

4.17b

***N*-[2-Methyl-1-(4-nitrophenyl)-3-oxo-pentyl]-2-nitrobenzenesulfonamide (4.17b).** ^{1}H NMR (400 MHz, d6-Acetone): δ 0.70 (t, *J* = 7.1 Hz, 3H), 1.23 (d, *J* = 6.8

Hz, 3H), 1.96-2.09 (m, 1H), 2.42-2.52 (m, 1H), 3.36-3.44 (m, 1H), 4.84 (d, J = 9.8 Hz, 1H), 7.46 (bs, 1H), 7.55 (d, J = 8.8 Hz, 2H), 7.64 (t, J = 7.6 Hz, 1H), 7.72 (t, J = 7.6 Hz, 1H) 7.78 (dd, dd, J = 6.7, 1.4 Hz, 1H) 7.90 (dd, J = 6.5, 1.4 Hz, 1H), 7.98 (d, J = 8.8 Hz, 2H). ^{13}C NMR (75 MHz, d6-Acetone): δ 6.5, 14.0, 35.4, 51.0, 60.0, 123.0, 124.6, 128.7, 130.5, 132.4, 133.4, 133.8, 147.0, 147.1, 147.3, 211.1. HRMS: Calcd [M+1] for $C_{18}H_{20}N_3O_7S$: 422.1022; Found: 422.1026. FTIR (film) 3324, 3099, 2978, 1711, 1606, 1540, 1500, 1443, 1349, 1169, 854, 593 cm^{-1}. MP = 141-142 °C.

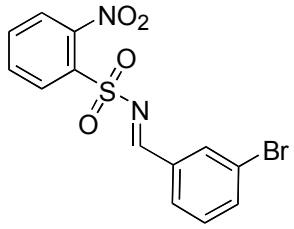

4.d

***N*-(3-Bromobenzylidene)-2-nitro-benzenesulfonamide (4.d).** ^{1}H NMR (400 MHz, $CDCl_3$): δ 7.42 (t, J = 7.9 Hz, 1H), 7.78 (m, 1H), 7.82 (m, 3H), 7.89 (d, J = 7.9 Hz, 1H), 8.16 (s, 1H), 8.40 (m, 1H), 9.03 (s, 1H). ^{13}C NMR (75 MHz, $CDCl_3$): δ 123.4, 124.8, 130.8, 131.3, 132.1, 132.7, 133.5, 133.8, 134.9, 138.2, 148.5, 172.1. HRMS: Calcd [M+1] for $C_{13}H_{10}N_2O_4SBr$: 368.9545; Found: 368.9551. FTIR (film) 1595, 1542, 1364, 1334, 1163, 1124, 808, 744, 587, 537 cm^{-1}. MP = 143-144 °C.

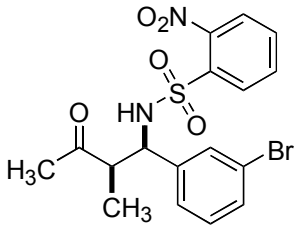

4.18a

***N*-[1-(3-Bromophenyl)-2-methyl-3-oxo-butyl]-2-nitrobenzenesulfonamide**

(4.18a). ^{1}H NMR (400 MHz, d6-Acetone): δ 1.22 (d, *J* = 6.8 Hz, 3H), 1.91 (s, 3H), 3.22-3.27 (m, 1H), 4.67 (d, *J* = 9.6 Hz, 1H), 7.05 (t, *J* = 7.9 Hz, 1H), 7.20-7.30 (m, 3H), 7.43 (s, 1H), 7.65 (t, *J* = 7.6 Hz, 1H), 7.72 (t, *J* = 7.7 Hz, 1H), 7.77 (m, 1H). 7.89 (dd, *J* = 6.8, 1.0 Hz, 1H), 7.86 (dd, *J* = 6.5, 1.4 Hz, 1H). ^{13}C NMR (75 MHz, d6-Acetone): δ 14.6, 52.6, 60.8, 122.5, 125.3, 127.3, 130.8, 131.2, 131.4, 133.2, 134.4, 134.7, 142.8, 148.2, 209.4. HRMS: Calcd [M+1] for $C_{17}H_{18}N_2O_5SBr$: 441.0120; Found: 441.0120. FTIR (film) 3323, 2977, 1710, 1540, 1441, 1356, 1260, 1167, 743, 590 cm^{-1}. MP = 86-87 °C.

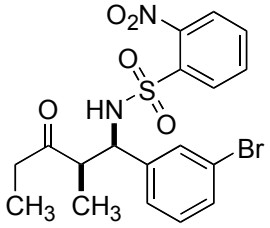

4.18b

***N*-[1-(3-Bromophenyl)-2-methyl-3-oxo-pentyl]-2-nitrobenzenesulfonamide**

(4.18b). ^{1}H NMR (400 MHz, d6-Acetone): δ 0.69 (t, *J* = 7.1 Hz, 3H), 1.20 (d, *J* = 6.8 Hz, 3H), 1.91-2.01 (m, 1H), 2.38-2.48 (m, 1H), 3.27-3.36 (m, 1H), 4.64 (d, *J* = 9.8 Hz, 1H), 7.05 (t, *J* = 7.8 Hz, 1H), 7.19-7.25 (m, 3H), 7.41 (t, *J* = 1.9 Hz, 1H), 7.63 (t, *J* = 7.2

Hz, 1H), 7.72 (t, *J* = 7.6 Hz, 1H), 7.77 (dd, *J* = 6.5, 1.4 Hz, 1H), 7.85 (dd, *J* = 3.2, 1.4 Hz, 1H). ^{13}C NMR (75 MHz, d6-Acetone): δ 7.14, 15.0, 36.5, 52.0, 61.2, 122.5, 125.3, 127.3, 130.8, 131.2, 131.3, 131.4, 133.2, 134.4, 134.6, 142.9, 148.2, 212.1. HRMS: Calcd [M+1] for $C_{18}H_{20}N_2O_5SBr$: 445.0276; Found: 455.0276. FTIR (film) 3321, 3098, 2977, 2938, 1711, 1540, 1442, 1358, 1168, 731, 590 cm^{-1}. MP = 99-101 °C.

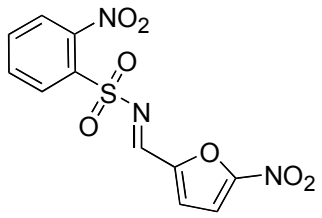

4.e

2-Nitro-*N*-(5-nitrofuran-2-ylmethylene)benzenesulfonamide (4.e). ^{1}H NMR (400 MHz, $CDCl_3$): δ 7.45 (d, *J* = 4.1 Hz, 1H), 7.53 (d, *J* = 4.1 Hz, 1H), 7.85 (m, 3H), 8.43 (m, 1H), 8.92 (s, 1H). ^{13}C NMR (75 MHz, Acetone): δ 113.6, 126.0, 127.8, 130.6, 133.0, 134.1, 137.0, 149.4, 159.7. HRMS: Calcd [M+1] for $C_{11}H_8N_3O_7S$: 326.0083; Found: 326.0087. FTIR (film) 3309, 3136, 1610, 1540, 1489, 1349, 1264, 1165, 1124, 1023, 966, 830, 769, 739, 591, 560 cm^{-1}. MP = 147-149 °C.

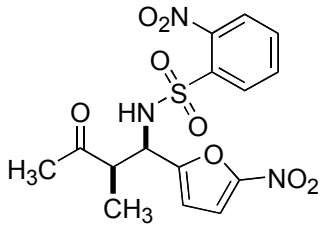

4.19a

***N*-[2-Methyl-1-(5-nitrofuran-2-yl)-3-oxo-butyl]-2-nitrobenzenesulfonamide**

(4.19a). ^{1}H NMR (400 MHz, d6-Acetone): δ 1.28 (d, *J* = 7.2 Hz, 3H), 2.16 (s, 3H), 3.44 (quintet, *J* = 7.2 Hz 1H), 4.95 (d, *J* = 9.2 Hz, 1H), 6.52 (d, *J* = 3.8 Hz, 1H), 7.20 (d, *J* = 3.8 Hz, 1H), 7.5 (bs, 1H), 7.74-7.91 (m, 3H), 8.06 (dd, *J* = 6.2, 1.4 Hz, 1H). ^{13}C NMR (75 MHz, d6-Acetone): δ 14.3, 50.2, 54.2, 112.3, 113.2, 125.7, 131.3, 133.6, 134.2, 135.0, 148.4, 157.1, 209.0. HRMS: Calcd [M+1] for $C_{15}H_{16}N_3O_8S$: 398.0658; Found: 398.0662. FTIR (film) 3318, 3135, 2981, 2882, 1711, 1590, 1540, 1498, 1356, 1248, 1170, 1022, 812, 784, 740, 593 cm^{-1}.

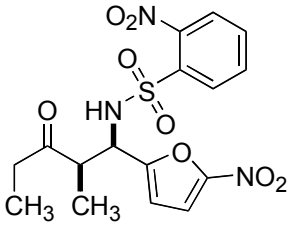

4.19b

***N*-[2-methyl-1-(5-nitrofuran-2-yl)-3-oxo-pentyl]-2-nitrobenzenesulfonamide**

(4.19b). ^{1}H NMR (400 MHz, d6-Acetone): δ 0.87 (t, *J* = 7.1 Hz, 3H), 1.25 (d, *J* = 7.0 Hz, 3H), 2.37-2.47 (m, 1H), 2.52-2.72 (m, 1H), 3.39-3.47 (m, 1H), 5.0 (t, *J* = 9.7 Hz, 1H), 6.49 (d, *J* = 3.7 Hz, 1H), 7.19 (d, *J* = 3.9 Hz, 1H), 7.49 (d, *J* = 10.0 Hz, 1H), 7.77-

7.92 (m, 3H), 8.07 (dd, J = 6.1, 1.6 Hz, 1H). ^{13}C NMR (75 MHz, d6-Acetone): δ 7.06, 14.7, 35.4, 48.6, 54.4, 112.3, 113.2, 125.7, 131.3, 133.6, 134.3, 135.0, 148.5, 157.2, 211.6. HRMS: Calcd [M+1] for $C_{16}H_{18}N_3O_8S$: 412.0815; Found: 412.0818. FTIR (film) 3323, 3135, 2979, 2939, 2882, 1711, 1541, 1498, 1356, 1247, 1170, 1022, 740, 593 cm^{-1}. MP = 128-130 °C.

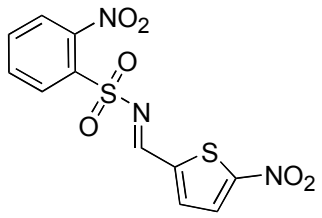

4.f

2-Nitro-*N*-(5-nitrothiophen-2-ylmethylene)benzenesulfonamide (4.f). ^{1}H NMR (400 MHz, d6-Acetone): δ 8.01-8.10 (m, 3H), 8.18 (d, J = 4.5 Hz, 1H), 7.53 (d, J = 4.3 Hz, 1H), 8.34 (m, 1H), 9.3 (s, 1H). ^{13}C NMR (75 MHz, d6-Acetone): δ 126.0, 130.3, 130.8, 132.8, 134.0, 136.9, 140.0, 142.8, 166.7. HRMS: Calcd [M+1] for $C_{11}H_8N_3O_6S_2$: 341.9855; Found: 341.9855. FTIR (film) 1585, 1539, 1511, 1343, 1275, 1166, 1118, 820, 750 cm^{-1}. MP = 195-196 °C.

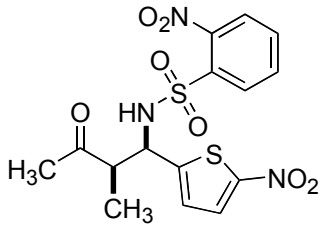

4.20a

***N*-[2-Methyl-1-(5-nitrothiophen-2-yl)-3-oxo-butyl]-2-nitrobenzenesulfonamide (4.20a).** ^{1}H NMR (400 MHz, d6-Acetone): δ 1.23 (d, *J* = 7.2 Hz, 3H), 2.08 (s, 3H), 3.44 (quintet, *J* = 7.5 Hz 1H), 5.05 (d, *J* = 9.1 Hz, 1H), 7.05 (d, *J* = 4.9 Hz, 1H), 7.52 (d, *J* = 9.8 Hz, 1H), 7.67 (d, *J* = 4.3 Hz, 1H), 7.75 (t, *J* = 7.6 Hz, 1H), 7.83 (t, *J* = 7.6 Hz, 1H), 7.88 (dd, *J* = 6.5, 1.5 Hz, 1H), 8.00 (dd, *J* = 6.5, 1.5 Hz, 1H). ^{13}C NMR (75 MHz, d6-Acetone): δ 14.7, 52.7, 56.7, 125.7, 127.5, 129.1, 131.3, 133.5, 134.3, 135.0, 148.4, 152.0, 209.9. HRMS: Calcd [M+1] for $C_{15}H_{16}N_3O_7S_2$: 414.0430; Found: 414.0430. FTIR (film) 3319, 3102, 2979, 1709, 1540, 1505, 1438, 1343, 1170, 1061, 734, 592 cm^{-1}.

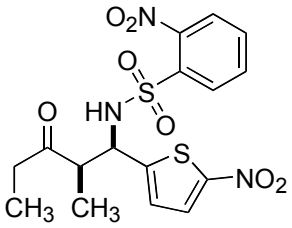

4.20b

***N*-[2-methyl-1-(5-nitrothiophen-2-yl)-3-oxo-pentyl]-2-nitrobenzenesulfonamide (4.20b).** ^{1}H NMR (400 MHz, d6-Acetone): δ 0.85 (t, *J* = 7.2 Hz, 3H), 1.21 (d, *J* = 7.2 Hz, 3H), 2.26-2.36 (m, 1H), 2.55-2.65 (m, 1H), 3.41 (quintet, *J*

= 7.2 Hz 1H), 5.04 (d, *J* = 8.9 Hz, 1H), 7.02 (d, *J* = 4.1 Hz, 1H), 7.56 (bs, 1H), 7.68 (d, *J* = 4.4 Hz, 1H), 7.76 (t, *J* = 7.6 Hz, 1H), 7.82 (t, *J* = 7.6 Hz, 1H), 7.88 (d, *J* = 7.5 Hz, 1H), 8.01 (d, *J* = 6.8 Hz, 1H). ^{13}C NMR (75 MHz, d6-Acetone): δ 7.6, 15.0, 35.7, 25.1, 56.9, 125.7, 127.4, 129.1, 131.3, 133.5, 134.3, 135.0, 148.3, 151.7, 152.2, 212.4. HRMS: Calcd [M+1] for $C_{16}H_{18}N_3O_7S_2$: 428.0586; Found: 428.0584. FTIR (film) 3323, 3103, 2979, 1710, 1540, 1506, 1437, 1341, 1169, 734, 591 cm^{-1}. MP = 155-156 °C.

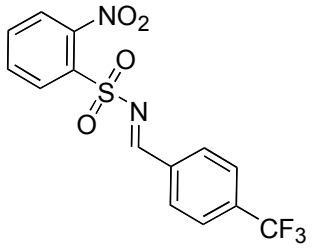

4.g

2-Nitro-*N*-(4-trifluoromethylbenzylidene)benzenesulfonamide (4.g). ^{1}H NMR (400 MHz, $CDCl_3$): δ 7.79 (m, 5H), 8.12 (d, *J* = 8.2 Hz, 2H), 8.42 (m, 1H), 9.14 (s, 1H). ^{13}C NMR (75 MHz, $CDCl_3$): δ 121.9, 124.9, 126.2 (q, *J* = 3.8 Hz), 129.9, 131.2, 131.8, 132.2, 132.8, 134.9, 135.0, 136.2, 148.5, 172.2. HRMS: Calcd [M+1] for $C_{14}H_{10}N_2O_4SF_3$: 359.0313; Found: 359.0311. FTIR (film) 1613, 1544, 1365, 1325, 1165, 1126, 1066, 803, 741, 586, 557 cm^{-1}. MP = 145-147 °C.

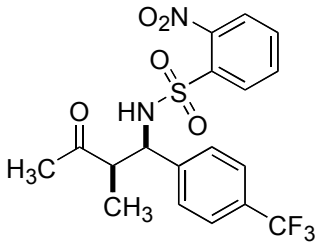

4.21a

***N*-[2-Methyl-3-oxo-1-(4-trifluoromethylphenyl)-butyl]-2-nitrobenzenesulfonamide (4.21a).** ^{1}H NMR (400 MHz, d6-Acetone): δ 1.23 (d, *J* = 7.0 Hz, 3H), 1.91 (s, 3H), 3.35 (m, 1H), 4.80 (d, *J* = 9.4 Hz, 1H), 7.36 (bs, 1H), 7.41 (d, *J* = 8.2 Hz, 2H), 7.49 (d, *J* = 8.2 Hz, 2H), 7.58 (t, *J* = 7.6 Hz, 1H), 7.70 (t, *J* = 7.6 Hz, 1H), 7.76 (dd, *J* = 6.8, 1.2 Hz, 1H), 7.82 (dd, *J* = 6.5, 1.2 Hz, 1H). ^{13}C NMR (75 MHz, d6-Acetone): δ 14.6, 52.6, 60.9, 125.4, 125.7 (q, *J* = 3.7 Hz), 129.2, 131.4, 133.2, 134.4, 134.5. 144.8, 148.2, 209.4. HRMS: Calcd [M+1] for $C_{18}H_{18}N_2O_5SF_3$: 431.0889; Found: 431.0886. FTIR (film) 3319, 1708, 1537, 1431, 1361, 1326, 1173, 1126, 1061, 585 cm^{-1}. MP = 105-106 °C.

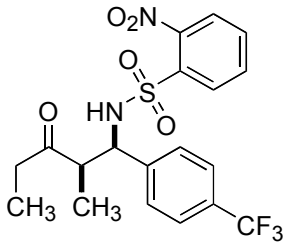

4.21b

***N*-[2-Methyl-3-oxo-1-(4-trifluoromethylphenyl)-pentyl]-2-nitrobenzenesulfonamide (4.21b).** ^{1}H NMR (400 MHz, d6-Acetone): δ 0.68 (t, *J* = 7.2 Hz, 3H), 1.22 (d, *J* = 6.8 Hz, 3H), 1.91-2.01 (m, 1H), 2.39-2.49 (m, 1H), 3.33-3.41 (m,

1H), 4.76 (d, J = 9.9 Hz, 1H), 7.36 (bs, 1H), 7.41 (d, J = 8.2 Hz, 2H), 7.46 (d, J = 8.5 Hz, 2H), 7.58 (t, J = 7.6 Hz, 1H), 7.70 (t, J = 7.6 Hz, 1H), 7.75 (dd, J = 6.5, 1.4 Hz, 1H), 7.81 (dd, J = 6.5, 1.4 Hz, 1H). ^{13}C NMR (75 MHz, d6-Acetone): δ 7.4, 15.0, 36.4, 51.9, 61.2, 125.3, 125.7 (q, J = 3.7 Hz), 129.2, 131.4, 133.2, 134.4, 134.5, 144.8, 148.2, 212.1. HRMS: Calcd [M+1] for $C_{19}H_{20}N_2O_5SF_3$: 445.1045; Found: 445.1048. FTIR (film) 3331, 2990, 1706, 1537, 1431, 1361, 1314, 1155, 1120, 750 cm^{-1}. MP = 138-139 °C.

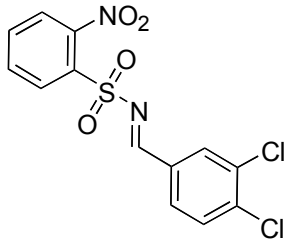

4.h

***N*-(3,4-Dichlorobenzylidene)-2-nitrobenzenesulfonamide (4.h).** ^{1}H NMR (400 MHz, $CDCl_3$): δ 7.63 (d, J = 8.5 Hz, 1H), 7.82 (m, 4H), 8.12 (d, J = 2.0 Hz, 1H), 8.42 (m, 1H), 9.01 (s, 1H). ^{13}C NMR (75 MHz, $CDCl_3$): δ 124.9, 130.6, 131.2, 131.4, 131.7, 132.2, 132.4, 132.7, 134.2, 134.9, 140.2, 148.5, 171.2. HRMS: Calcd [M+1] for $C_{13}H_9N_2O_4SCl_2$: 358.9660; Found: 358.9658. FTIR (film) 1590, 1543, 1361, 1331, 1267, 1161, 1120, 808, 750, 585 cm^{-1}. MP = 167-168 °C.

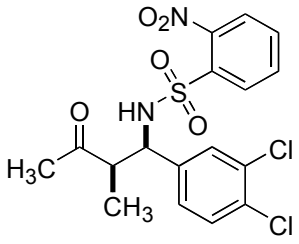

4.22a

***N*-[1-(3,4-Dichlorophenyl)-2-methyl-3-oxobutyl]-2-nitrobenzenesulfonamide (4.22a).** ^{1}H NMR (400 MHz, d6-Acetone): δ 1.23 (d, *J* = 7.0 Hz, 3H), 1.95 (s, 3H), 3.35 (m, 1H), 4.70 (d, *J* = 9.6 Hz, 1H), 7.23-7.34 (m, 3H), 7.44 (d, *J* = 2.0 Hz, 2H), 7.65 (t, *J* = 7.6 Hz, 1H), 7.75 (t, *J* = 7.6 Hz, 1H), 7.80 (dd, *J* = 6.3, 1.6 Hz, 1H), 7.88 (dd, *J* = 6.5, 1.4 Hz, 1H). ^{13}C NMR (75 MHz, d6-Acetone): δ 14.6, 52.5, 60.2, 125.3, 128.5, 130.6, 130.9, 131.5, 131.6, 132.2, 133.2, 134.3, 134.6, 141.4, 148.2, 209.4. HRMS: Calcd [M+1] for $C_{17}H_{17}N_2O_5SCl_2$: 431.0235; Found: 431.0237. FTIR (film) 3319, 3095, 2978, 1708, 1531, 1437, 1349, 1267, 1161, 738 cm^{-1}. MP = 169-170 °C.

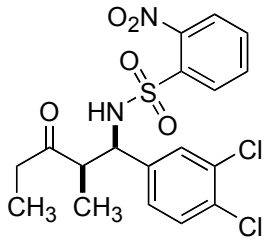

4.22b

***N*-[-[1-(3,4-Dichlorophenyl)-2-methyl-3-oxopentyl]-2-nitrobenzenesulfonamide (4.22b).** ^{1}H NMR (400 MHz, d6-Acetone): δ 0.73 (t, *J* = 7.1 Hz, 3H), 1.22 (d, *J* = 7.0 Hz, 3H), 1.97-2.10 (m, 1H), 2.43-2.61 (m, 1H), 3.31-3.38 (m, 1H), 4.68 (d, *J* = 9.8 Hz, 1H), 7.23 (dd, *J* = 6.5, 2.0 Hz, 1H), 7.30 (d, *J* = 8.4 Hz, 1H),

7.45 (d, *J* = 2.0 Hz, 1H), 7.65 (t, *J* = 7.6 Hz, 1H), 7.76 (t, *J* = 7.6, 1H), 7.80 (dd, *J* = 6.7, 1.4 Hz, 1H) 7.90 (dd, *J* = 6.7, 1.2 Hz, 1H). ^{13}C NMR (75 MHz, d6-Acetone): δ 7.4, 15.0, 36.3, 51.8, 60.5, 125.3, 128.5, 130.6, 130.9, 131.5, 131.6, 132.2, 133.2, 134.3, 134.6, 141.4, 148.2, 212.1. HRMS: Calcd [M+1] for $C_{18}H_{19}N_2O_5SCl_2$: 445.0392; Found: 445.0388. FTIR (film) 3319, 2978, 2884, 1708, 1537, 1437, 1350, 1260, 1169, 1031, 749 cm^{-1}. MP = 151-152 °C.

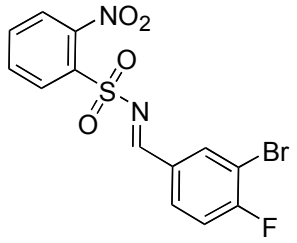

4.i

***N*-(3-Bromo-4-fluorobenzylidene)-2-nitrobenzenesulfonamide (4.i).** ^{1}H NMR (400 MHz, d6-Acetone): δ 7.54 (d, *J* = 4.3 Hz, 1H), 8.03 (m, 3H), 8.22 (m, 1H), 8.39 (m, 1H), 8.44 (m, 1H), 9.08 (s, 1H). ^{13}C NMR (75 MHz, $CDCl_3$): δ 110.8, 111.0, 117.4, 117.7, 124.9, 129.6, 129.7, 131.4, 132.2, 132.7, 133.2, 133.3, 134.9, 136.5, 148.5, 162.2, 164.7, 171.0. HRMS: Calcd [M+1] for $C_{13}H_9N_2O_4SBrF$: 386.9450; Found: 386.9454. FTIR (film) 1592, 1542, 1492, 1364, 1334, 1261, 1164, 1123, 821, 782 cm^{-1}. MP = 137-138 °C.

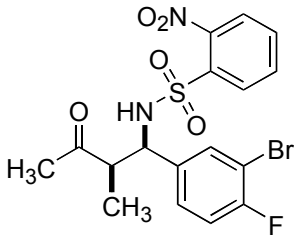

4.23a

***N*-[1-(3-Bromo-4-fluorophenyl)-2-methyl-3-oxobutyl]-2-nitrobenzenesulfonamide (4.23a).** ^{1}H NMR (400 MHz, d6-Acetone): δ 1.22 (d, *J* = 7.2 Hz, 3H), 1.94 (s, 3H), 3.34 (m, 1H), 4.68 (d, *J* = 9.6 Hz, 1H), 7.0 (t, *J* = 8.7 Hz, 1H), 7.27 (bs, 1H), 7.32 (m, 1H), 7.54 (dd, *J* = 4.4, 2.0 Hz, 1H), 7.67 (t, *J* = 7.6 Hz, 1H), 7.75 (t, *J* = 7.6 Hz, 1H), 7.80 (dd, *J* = 6.8, 1.0 Hz, 1H), 7.88 (dd, *J* = 6.8, 1.0 Hz, 1H). ^{13}C NMR (75 MHz, d6-Acetone): δ 14.7, 60.2, 52.7, 108.5, 108.7, 116.7, 117.0, 125.4, 129.6, 129.7, 131.5, 133.2, 133.7, 134.3, 134.7, 138.3, 138.4, 148.2, 157.5, 160.0, 209.5. HRMS: Calcd [M+1] for $C_{17}H_{17}N_2O_5SBrF$: 459.0026; Found: 459.0023. FTIR (film) 3319, 2935, 1710, 1541, 1496, 1442, 1359, 1248, 1169, 1126, 1060, 783, 731 cm^{-1}. MP = 124-126 °C.

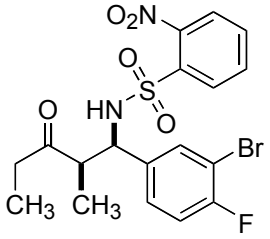

4.23b

***N*-[-[1-(3-Bromo-4-fluorophenyl)-2-methyl-3-oxopentyl]-2-nitrobenzenesulfonamide (4.23b).** ^{1}H NMR (400 MHz, d6-Acetone): δ 0.72 (t, *J* = 7.2 Hz, 3H), 1.22 (d, *J* = 7.2 Hz, 3H), 1.97-2.09 (m, 1H), 2.42-2.61 (m, 1H), 3.30-3.36 (m,

1H), 4.67 (d, *J* = 9.9 Hz, 1H), 7.01 (t, *J* = 8.5, Hz, 1H), 7.29 (m, 2H), 7.52 (dd, *J* = 4.4, 2.4 Hz, 1H), 7.67 (t, *J* = 7.6 Hz, 1H), 7.76 (t, *J* = 7.5, 1H), 7.80 (dd, *J* = 6.5, 1.4 Hz, 1H) 7.90 (dd, *J* = 6.5, 1.4 Hz, 1H). ^{13}C NMR (75 MHz, d6-Acetone): δ 7.4, 15.1, 36.4, 52.0, 60.5, 108.5, 108.7, 116.7, 117.0, 125.4, 129.6, 129.7, 131.5, 133.2, 133.6, 134.4, 134.7, 138.5, 138.5, 148.2, 157.5, 160.0, 212.2. HRMS: Calcd [M+1] for $C_{18}H_{19}N_2O_5SBrF$: 473.0182; Found: 473.0184. FTIR (film) 3321, 2977, 1710, 1540, 1495, 1426, 1352, 1247, 1170, 730 cm^{-1}. MP = 115-117 °C.

4.7 SPECTRA

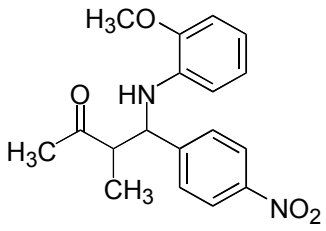

4.3
1:1(syn:anti)

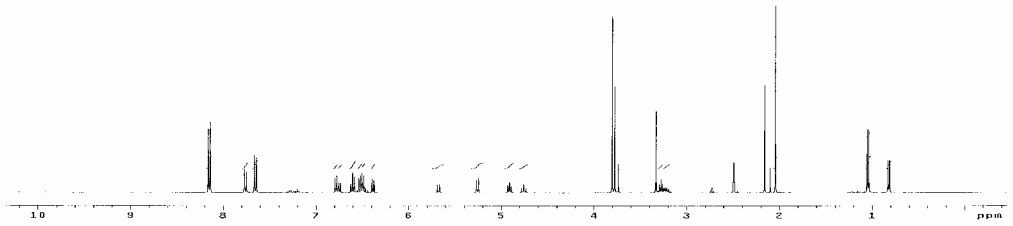

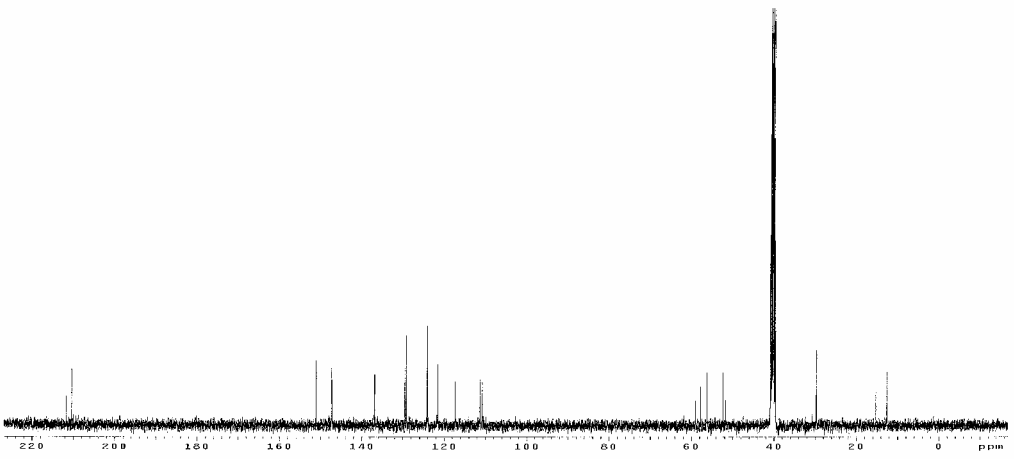

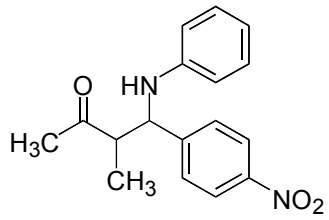

4.4
1.5:1 (syn:anti)

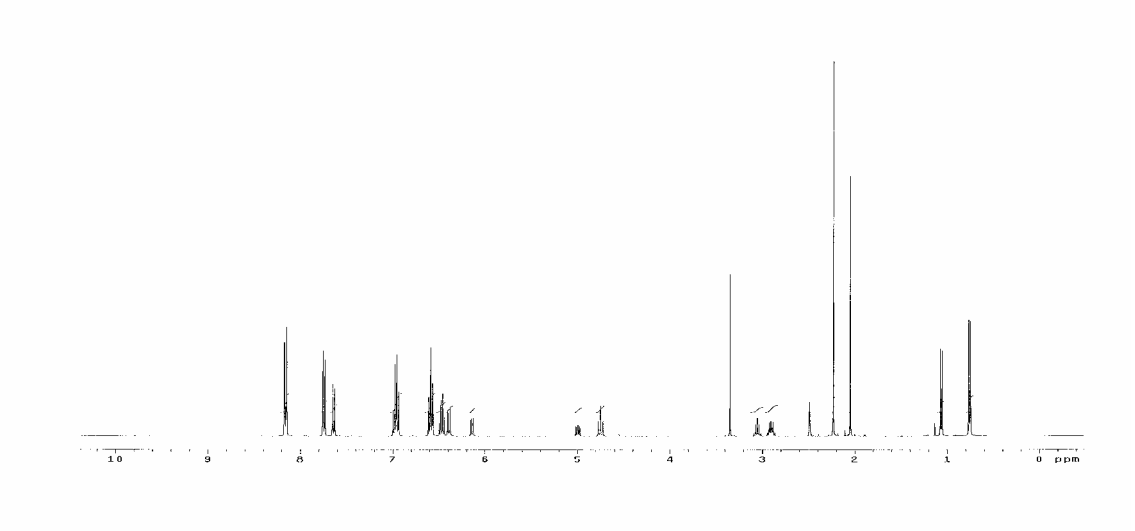

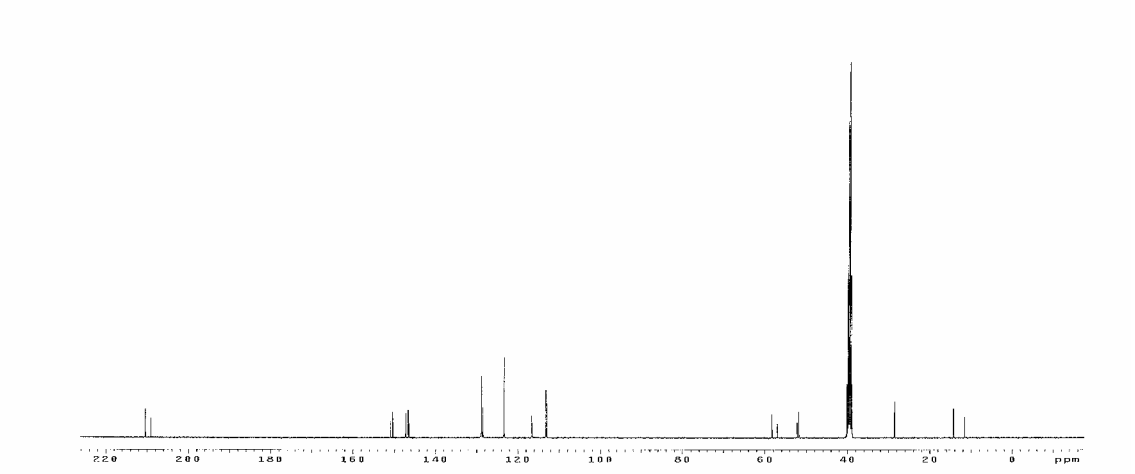

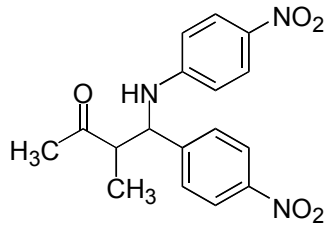

4.5
1.2:1 (syn:anti)

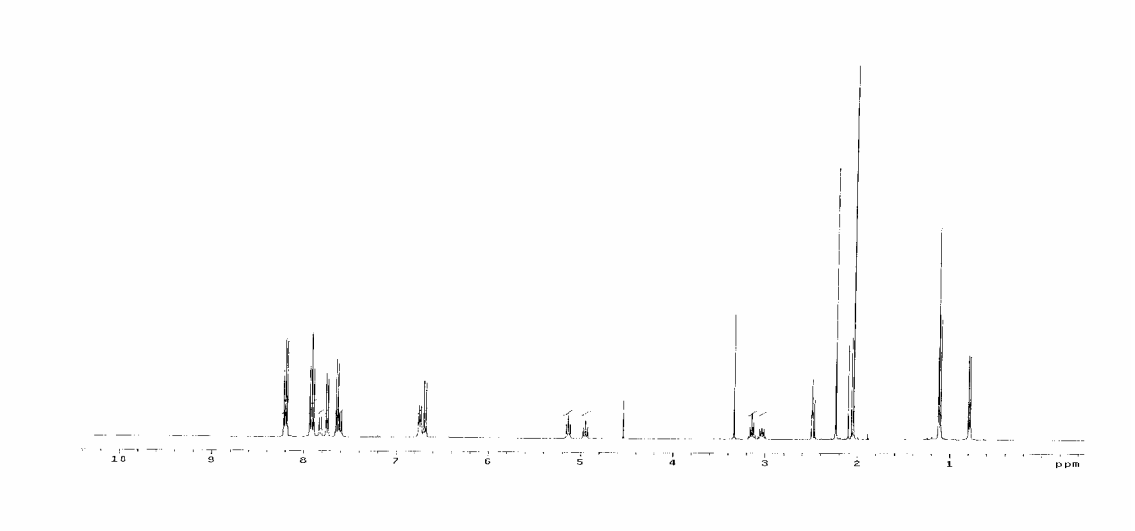

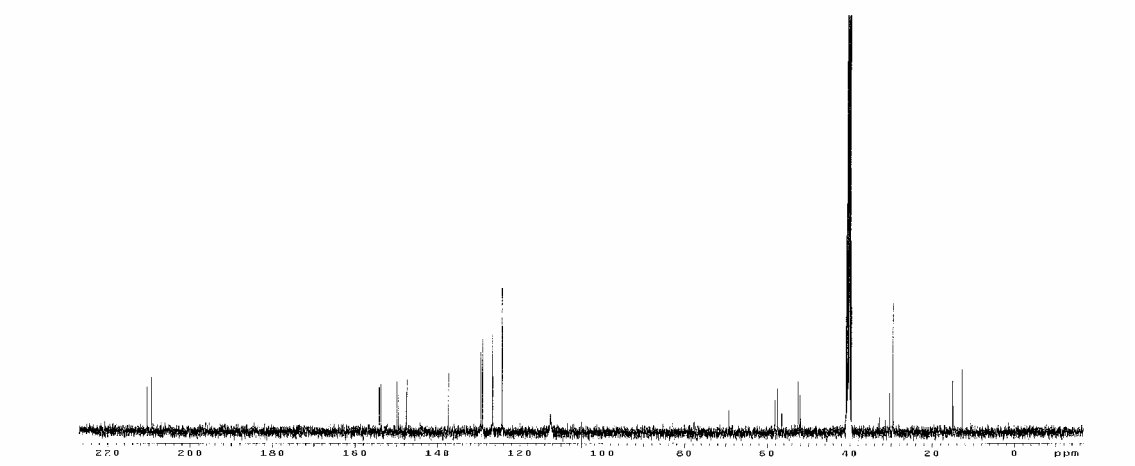

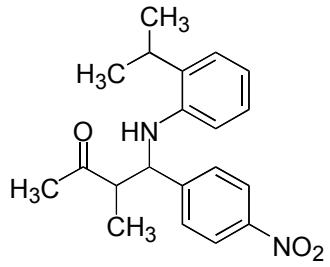

4.7
1.6:1 (syn:anti)

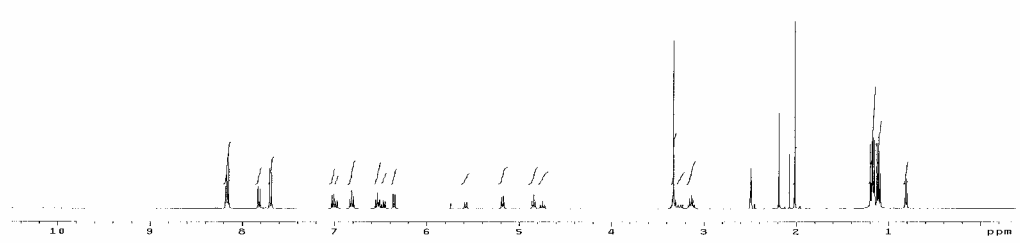

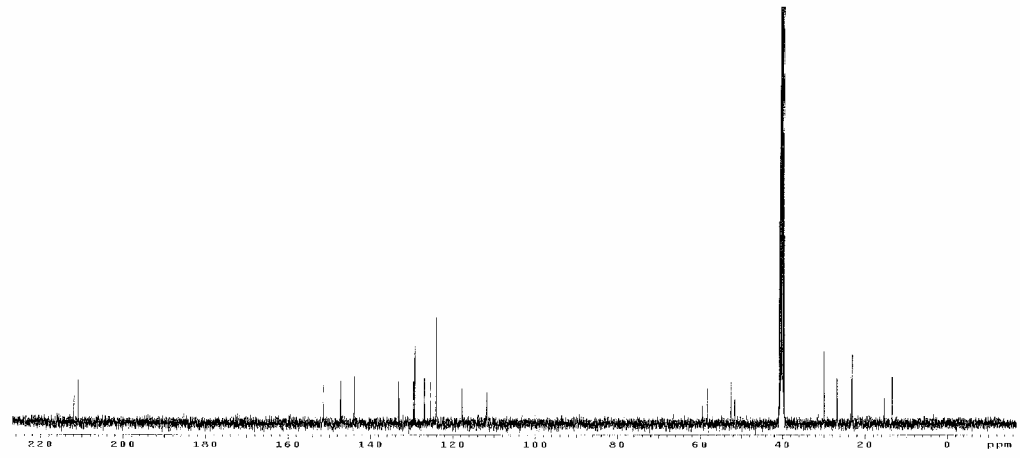

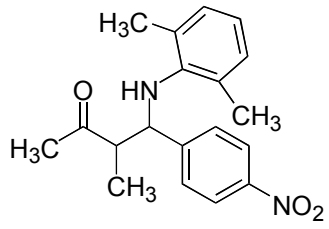

4.9
2:1 (syn:anti)

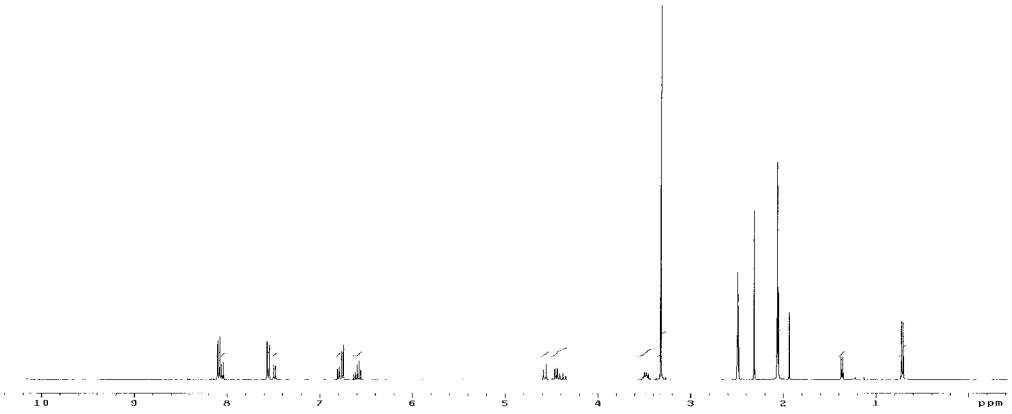

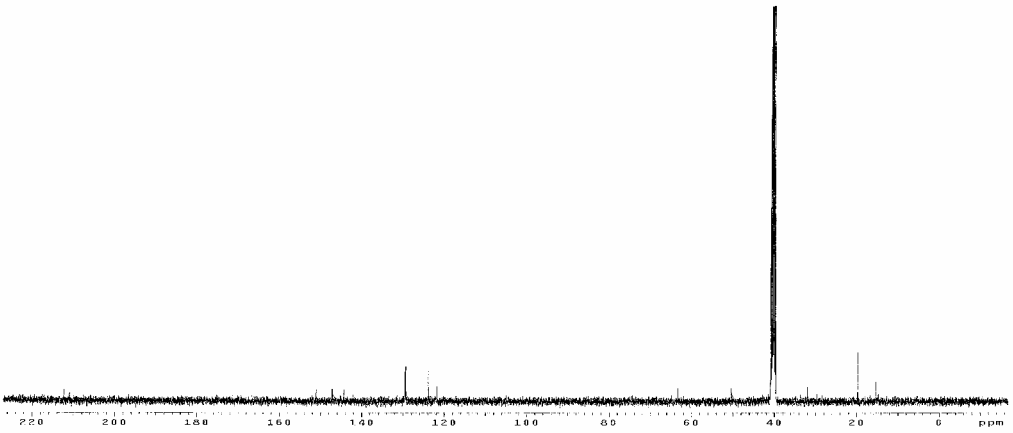

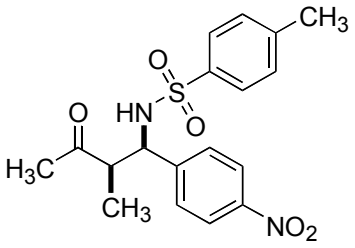
CH3
O
S
O
HN
O
H3C
CH3
NO2

4.16

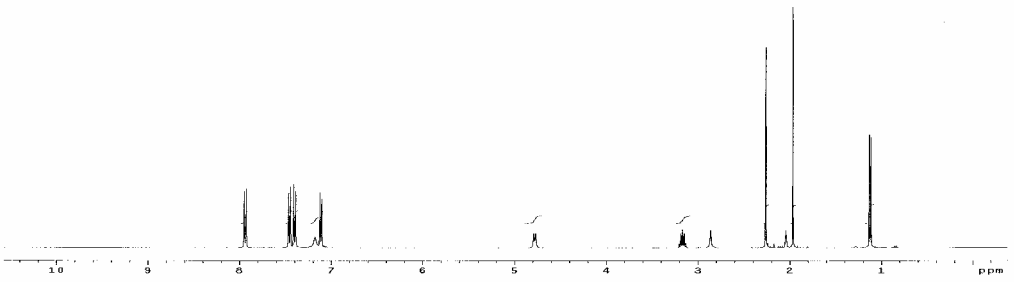
10
9
8
7
6
5
4
3
2
1
ppm

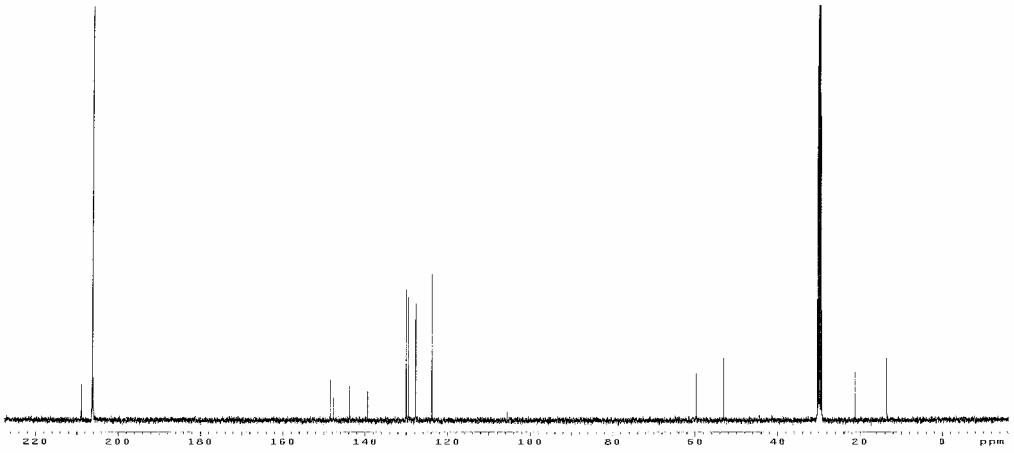
220
200
180
160
140
120
100
80
60
40
20
0
ppm

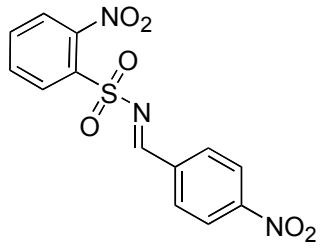
NO2
O
S
O
N
NO2

4.c

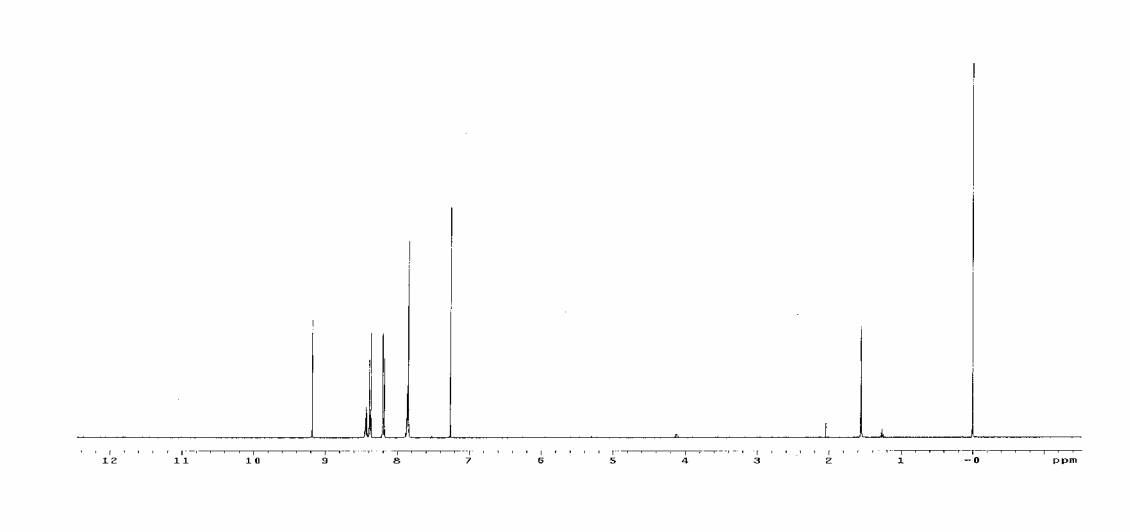
12
11
10
9
8
7
6
5
4
3
2
1
0
ppm

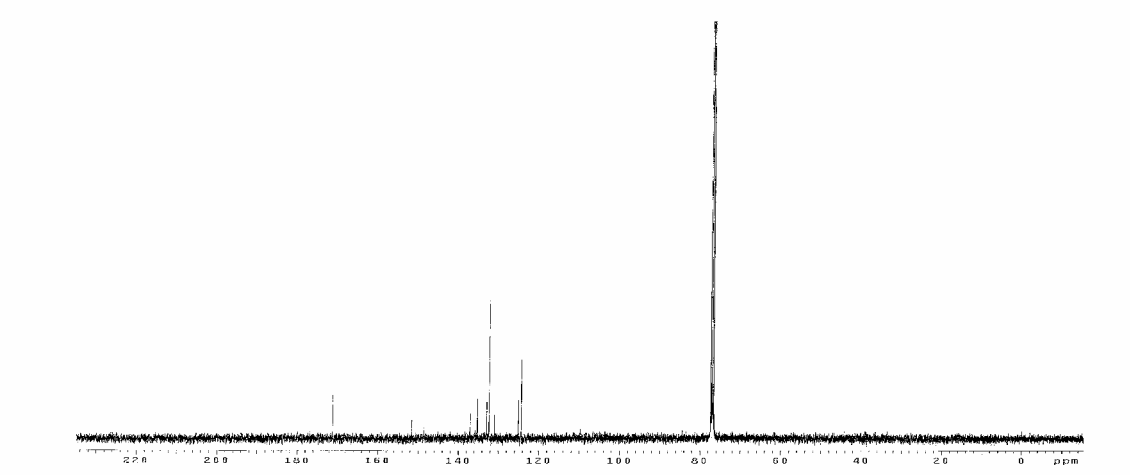
220
200
180
160
140
120
100
80
60
40
20
0
ppm

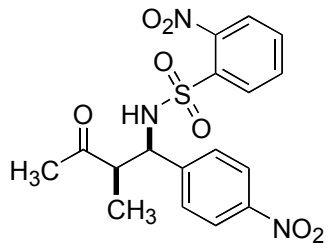
O2N
O
S
O
HN
O
H3C
CH3
NO2

4.17a

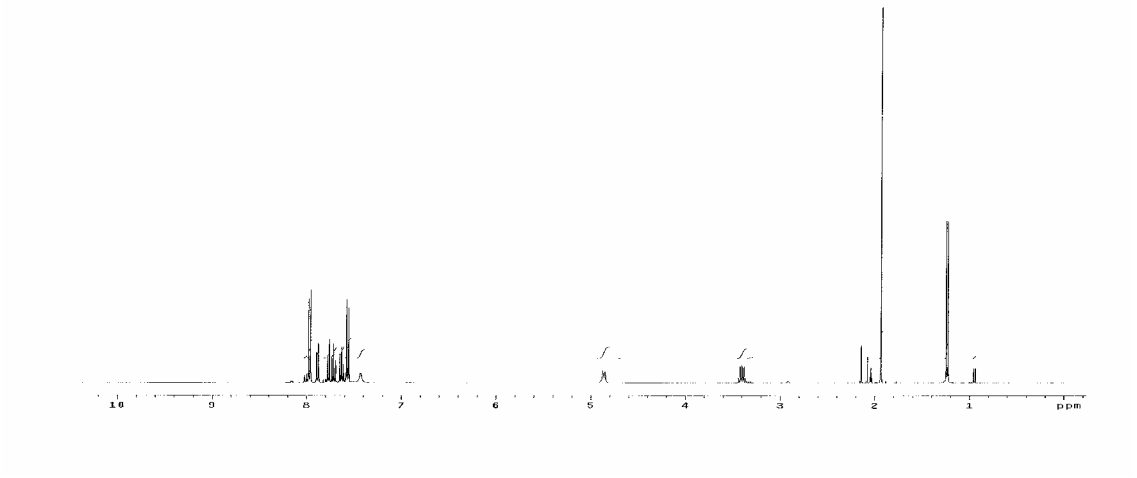
10
9
8
7
6
5
4
3
2
1
ppm

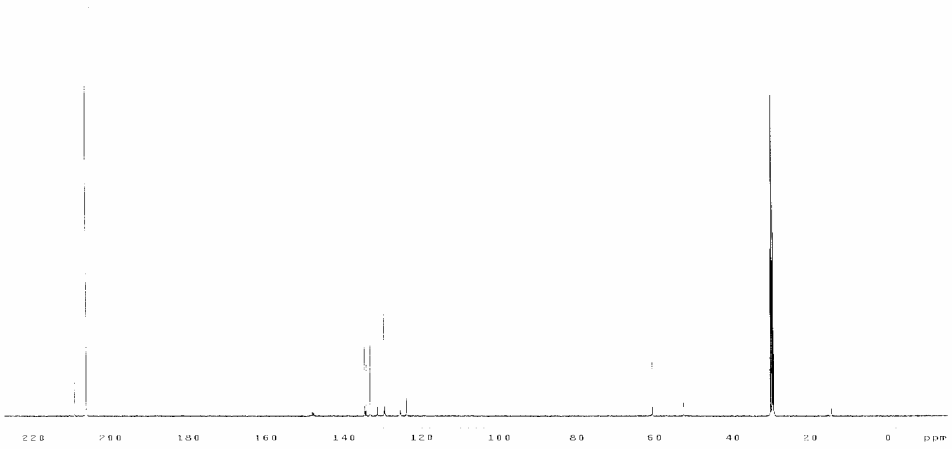
220
200
180
160
140
120
100
80
60
40
20
0
ppm

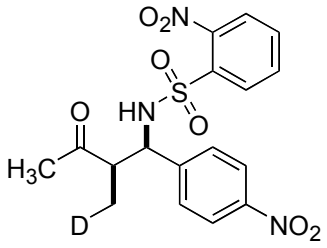

***deuterio*-4.17a**

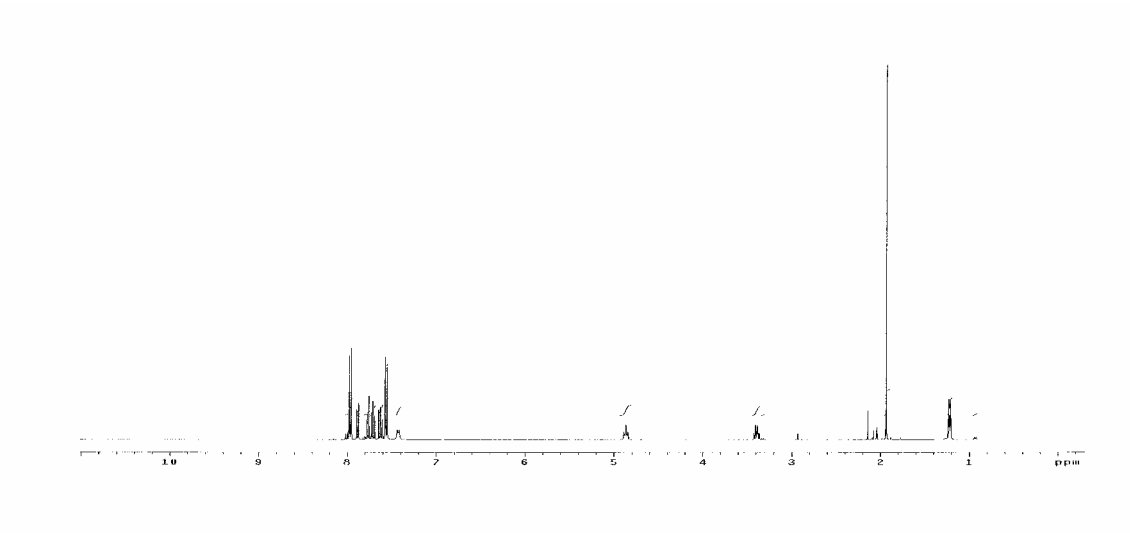

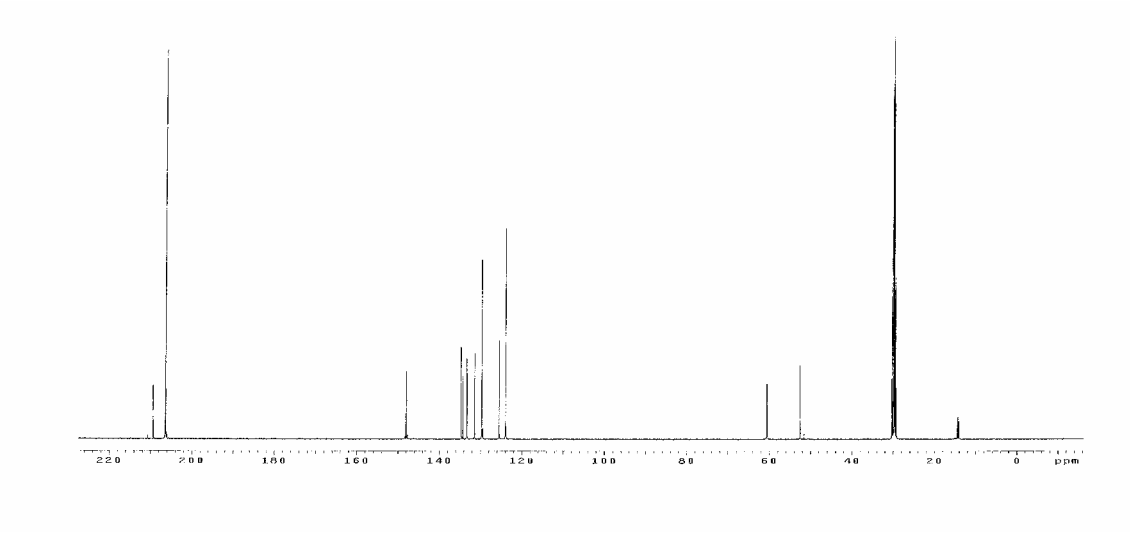

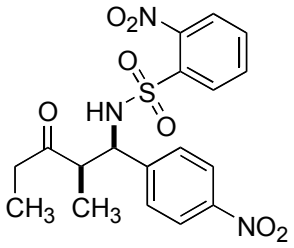
O2N
O
S
HN
O
O
CH3
CH3
NO2

4.17b

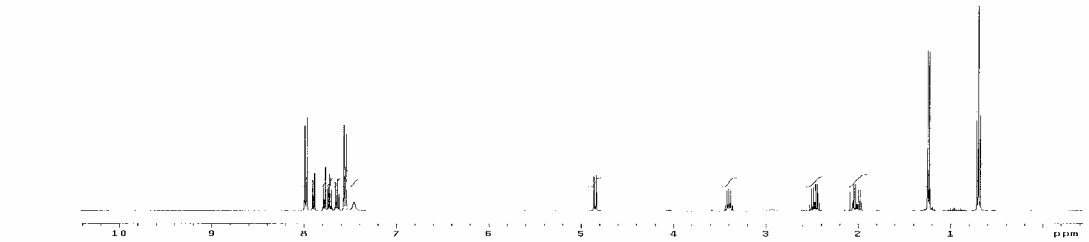
10
9
8
7
6
5
4
3
2
1
ppm

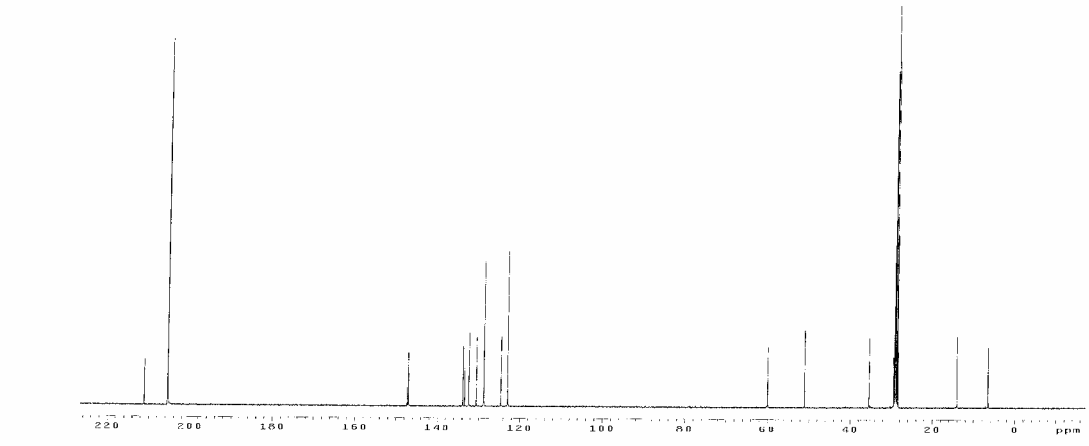
220
200
180
160
140
120
100
80
60
40
20
0
ppm

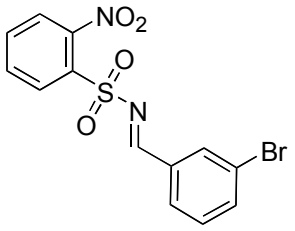
NO2
O
S
O
N
Br

4.d

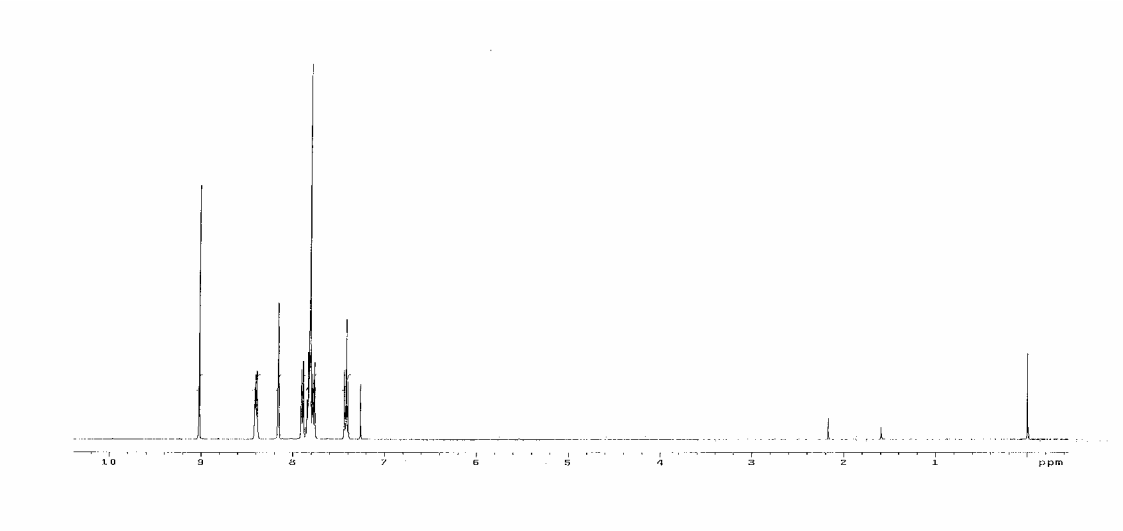
10
9
8
7
6
5
4
3
2
1
ppm

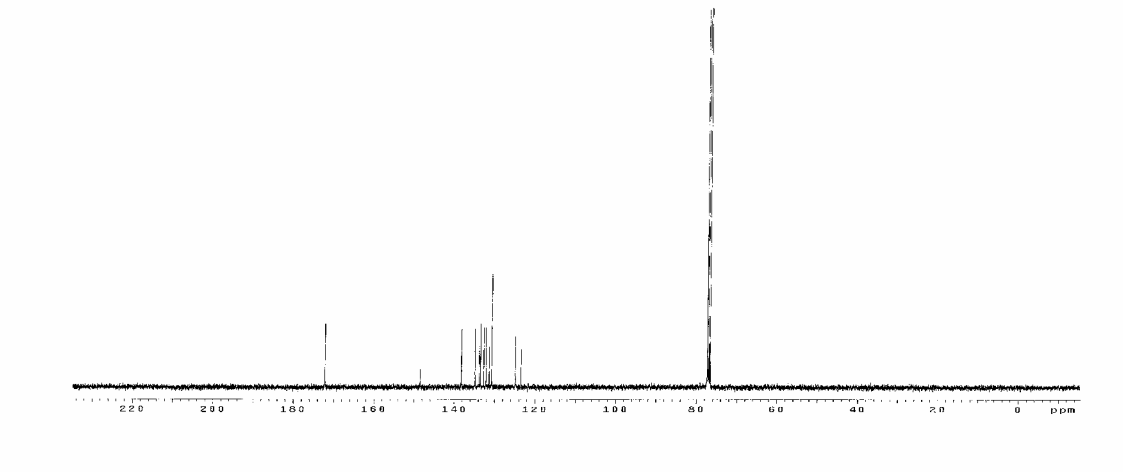
220
200
180
160
140
120
100
80
60
40
20
0
ppm

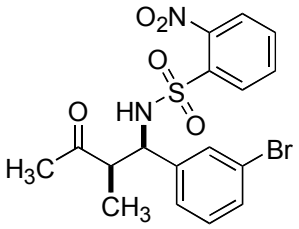

4.18a

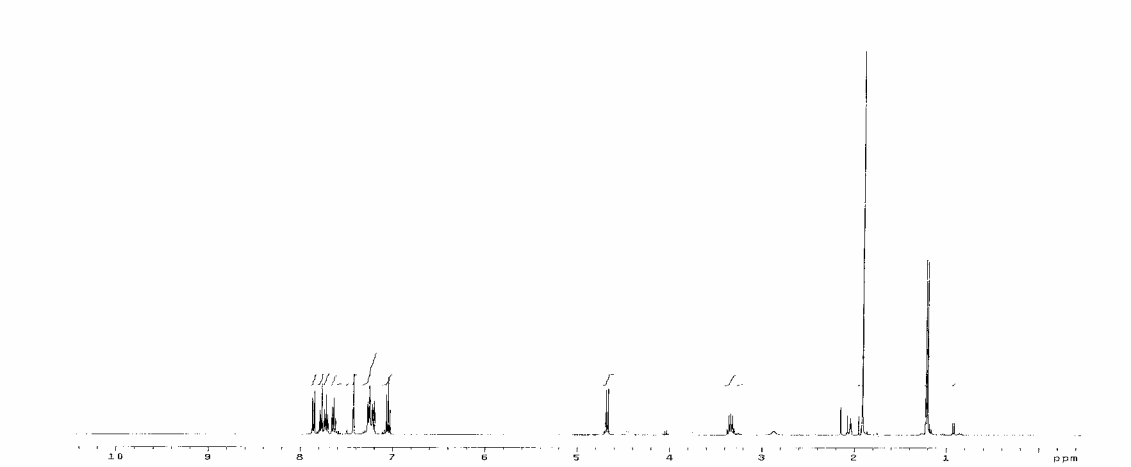

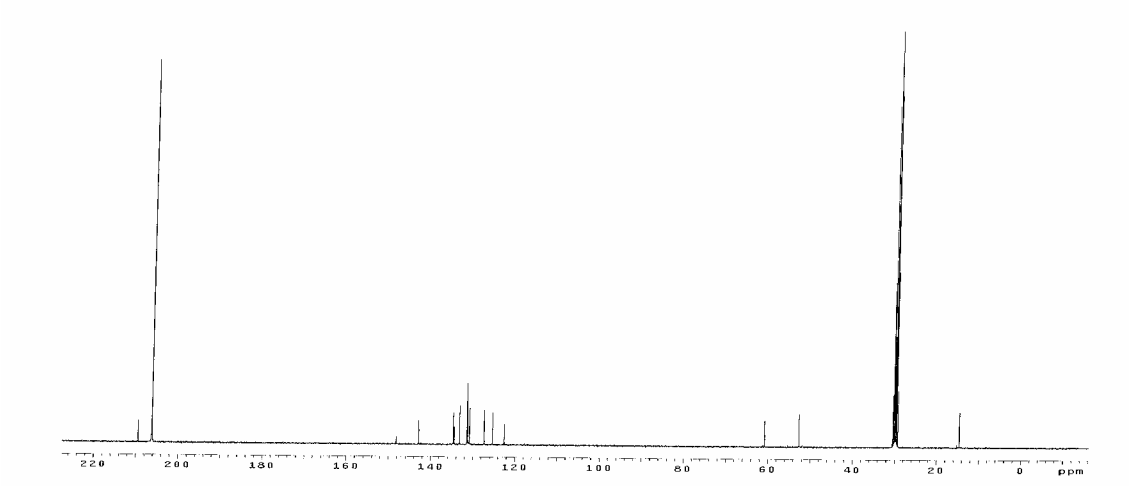

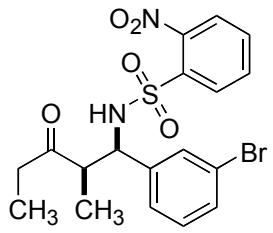

4.18b

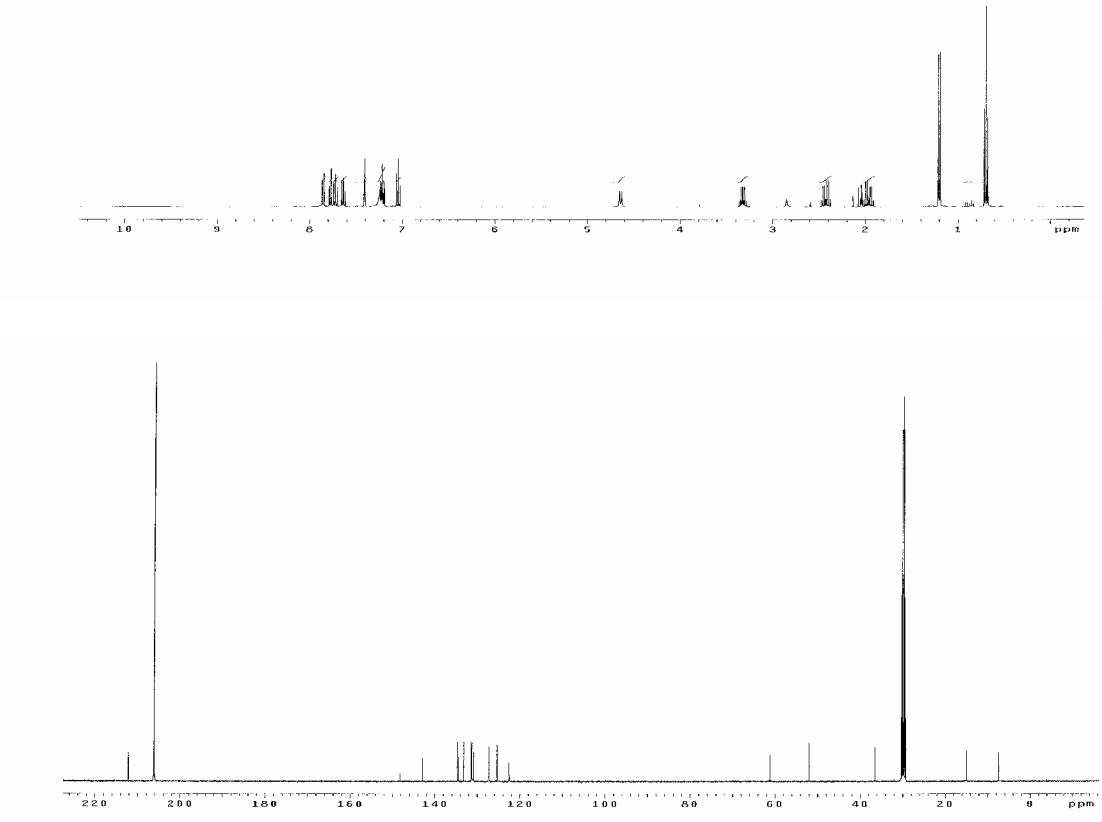

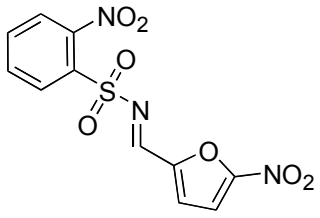

4.e

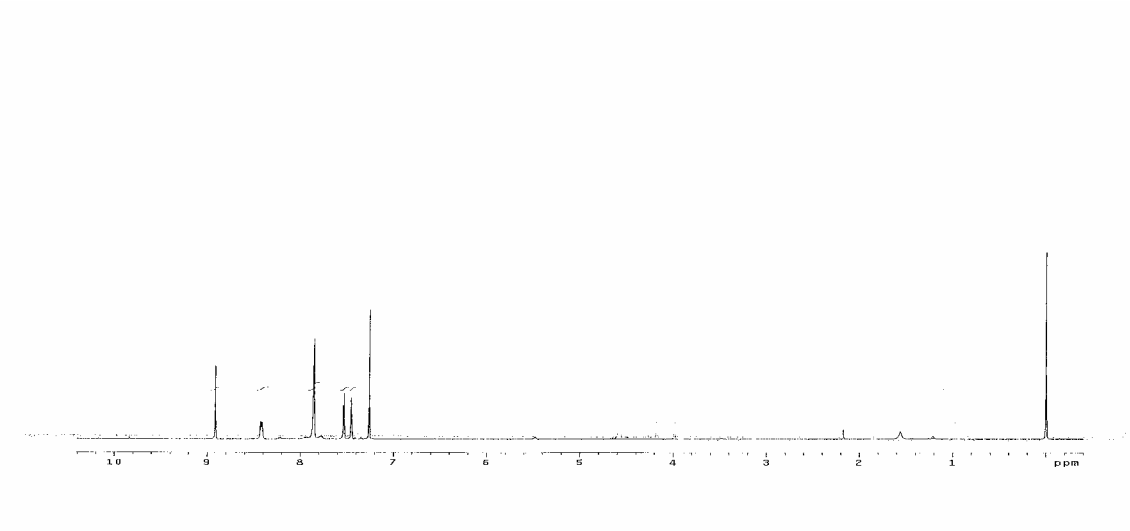

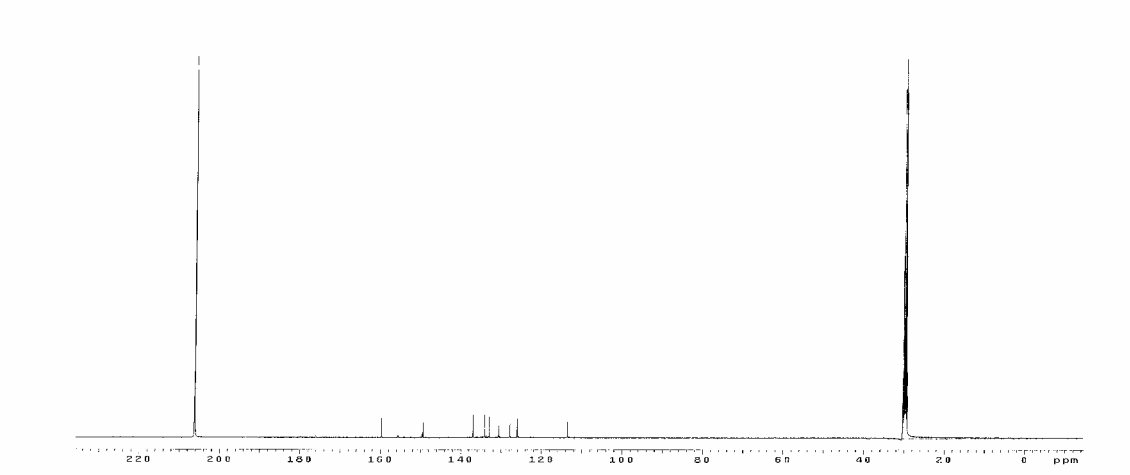

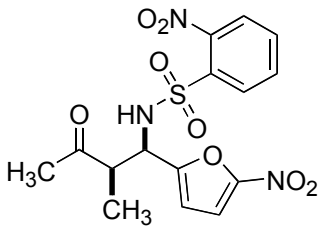

4.19a

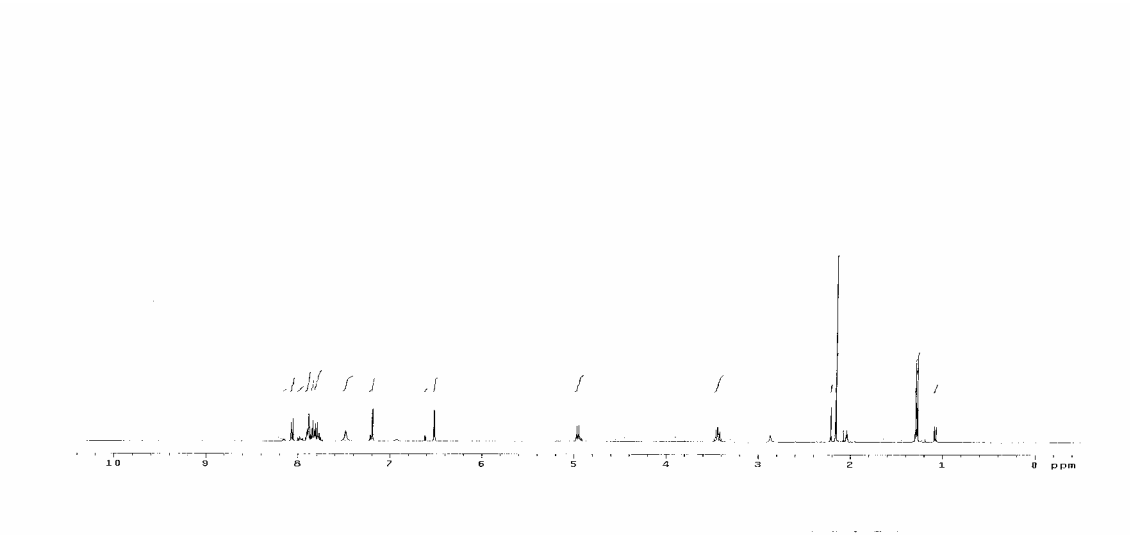

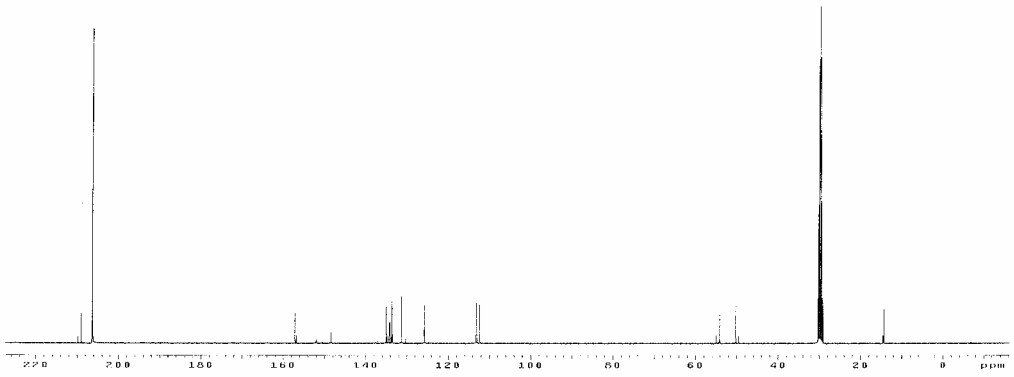

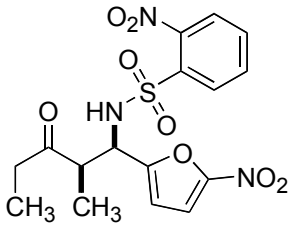

4.19b

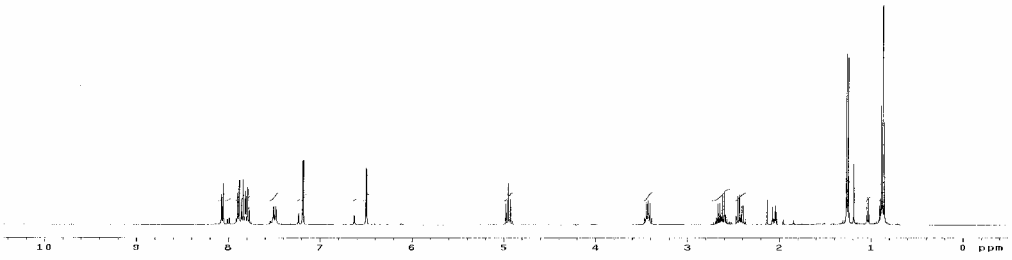

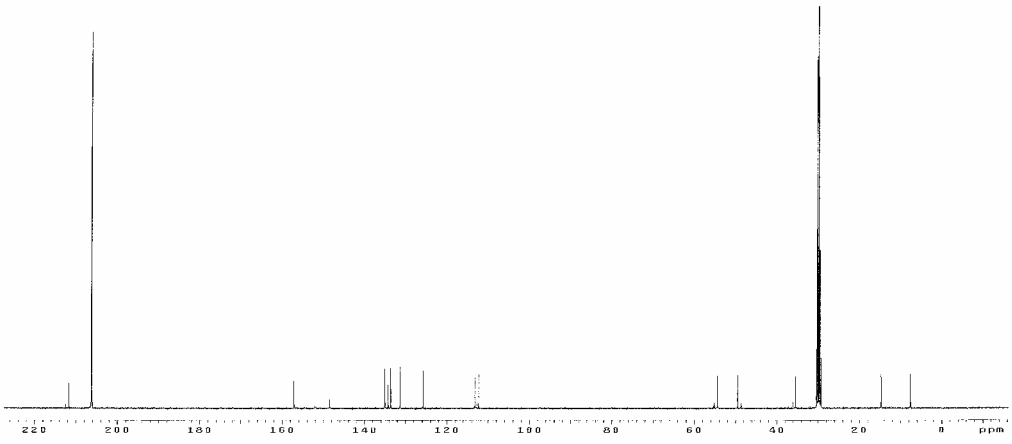

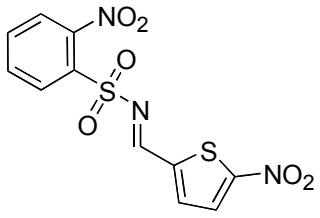
NO2
O
S
O
N
S
NO2

4.f

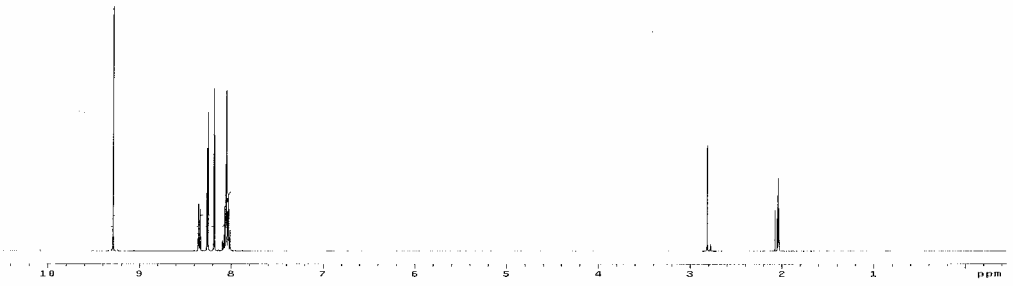
10
9
8
7
6
5
4
3
2
1
ppm

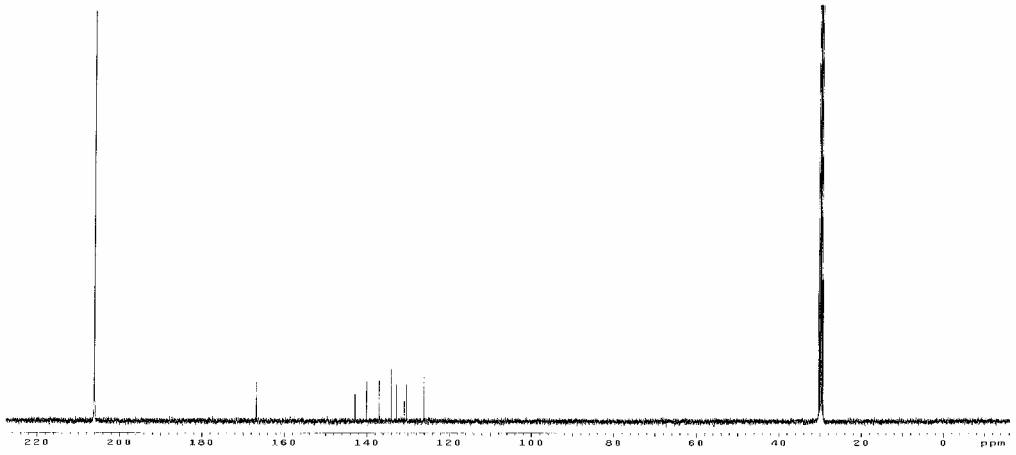
220
200
180
160
140
120
100
80
60
40
20
0
ppm

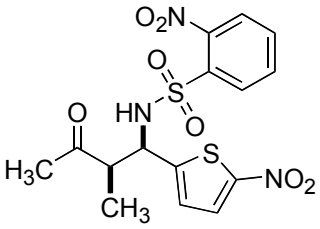

4.20a

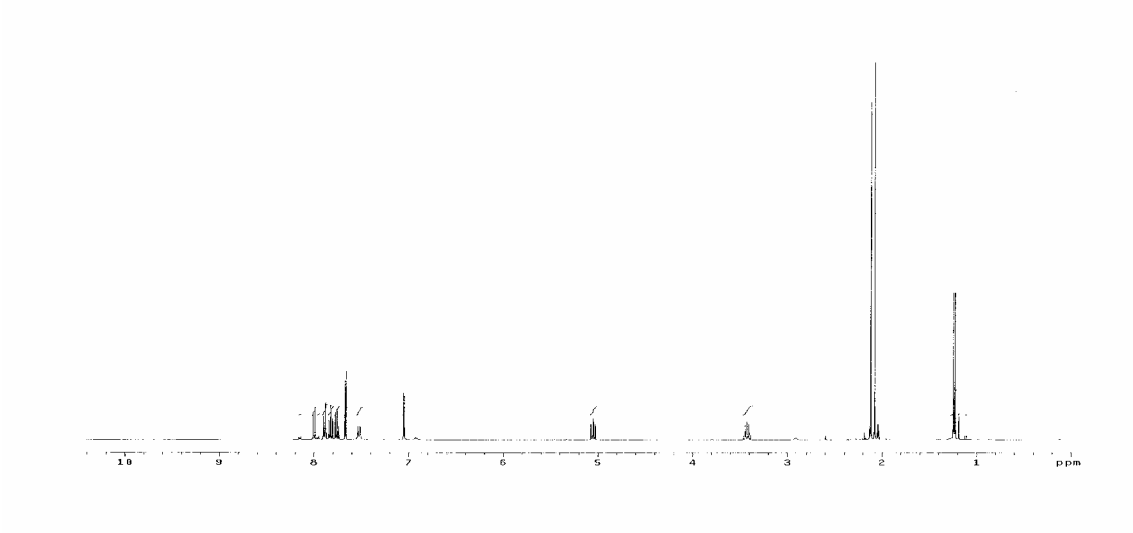

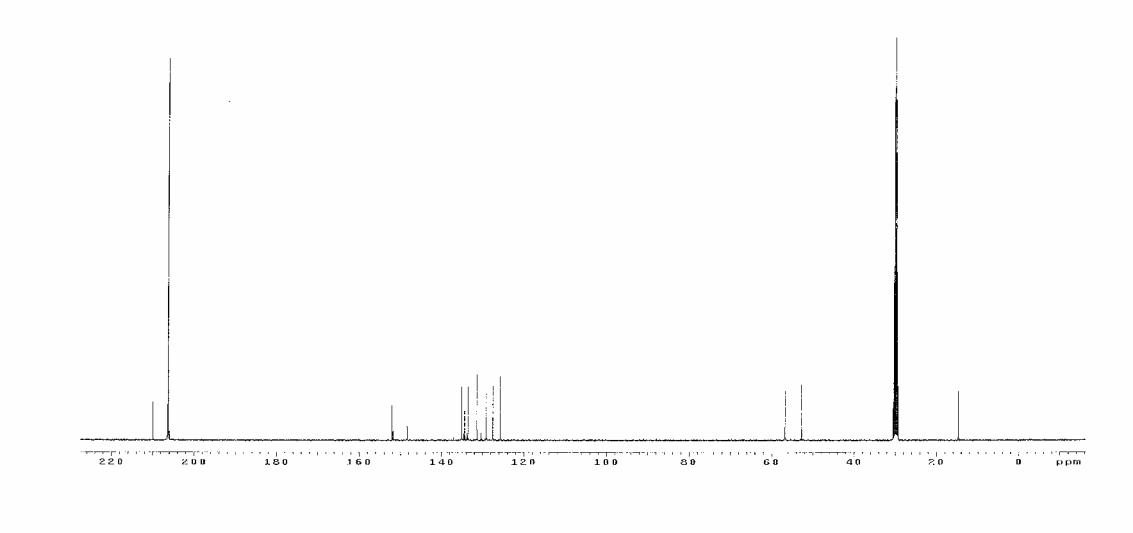

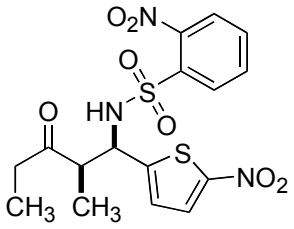

4.20b

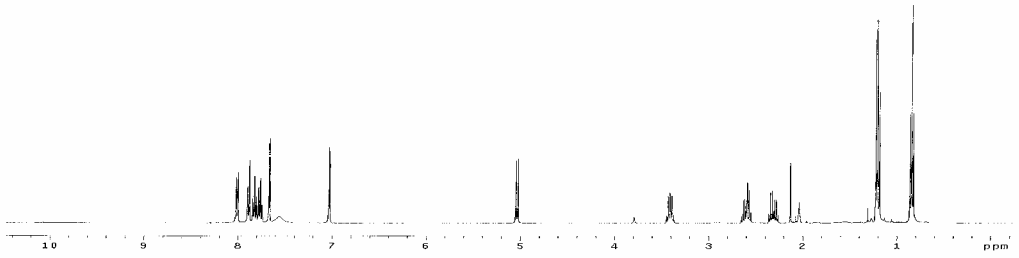

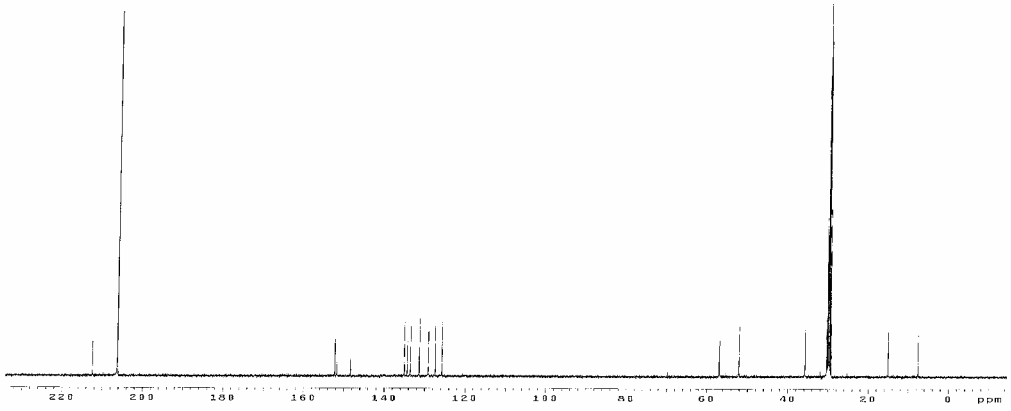

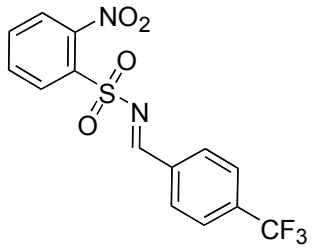
NO2
O
S
O
N
CF3

4.g

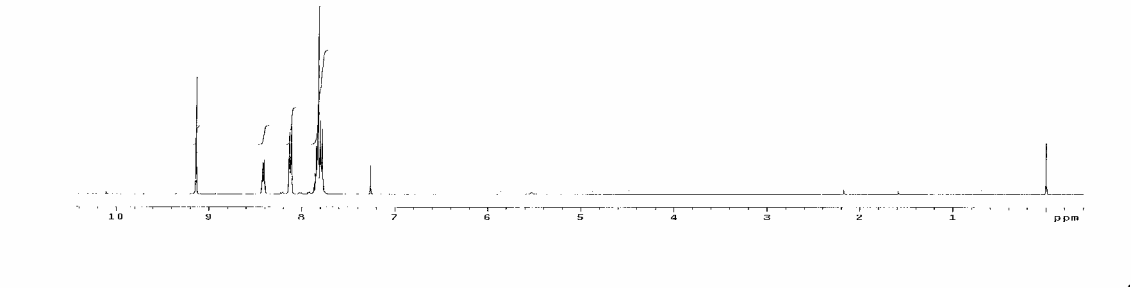
10
9
8
7
6
5
4
3
2
1
ppm

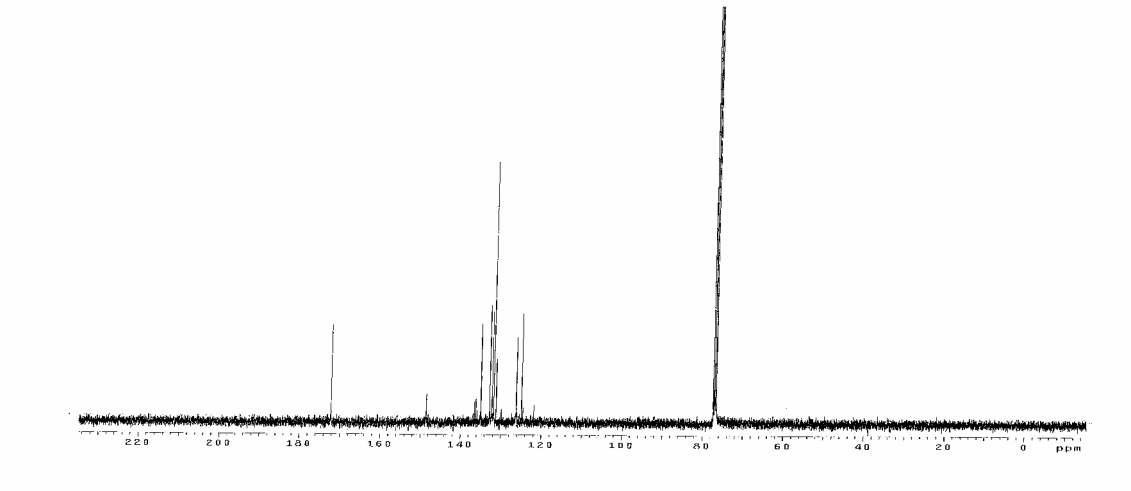
220
200
180
160
140
120
100
80
60
40
20
0
ppm

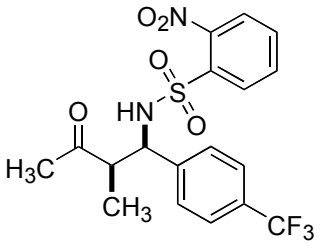
O2N
O
S
HN
O
O
H3C
CH3
CF3

4.21a

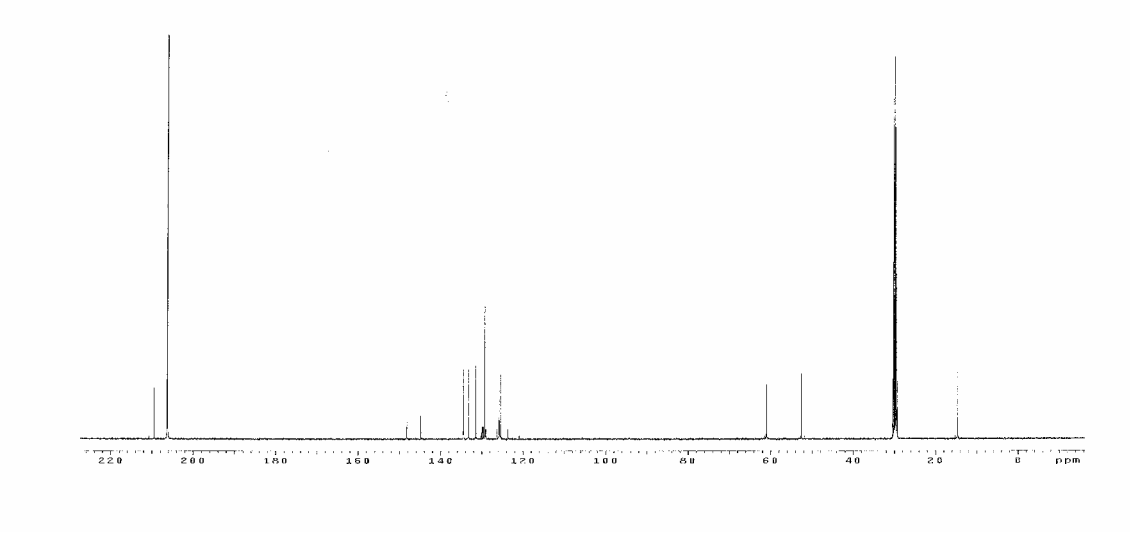
220
200
180
160
140
120
100
80
60
40
20
0
ppm

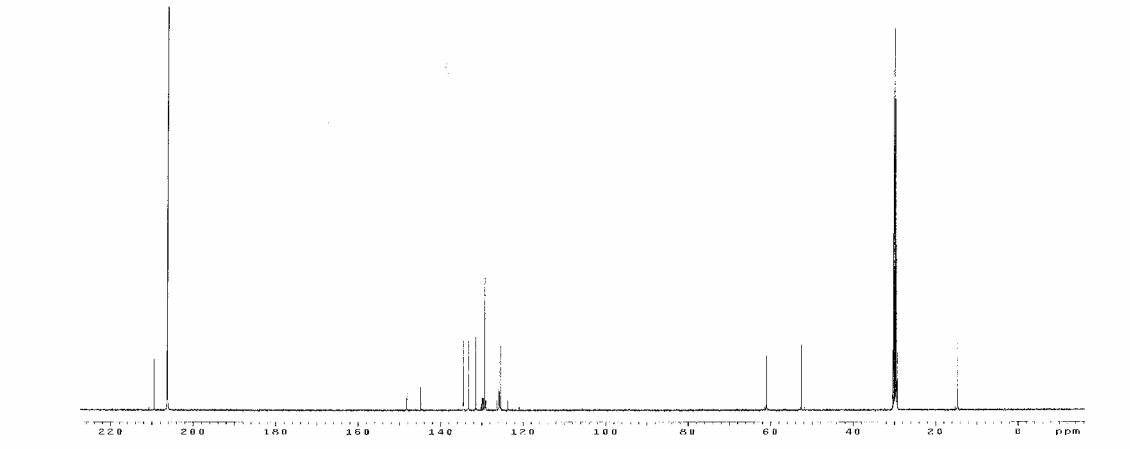
220
200
180
160
140
120
100
80
60
40
20
0
ppm

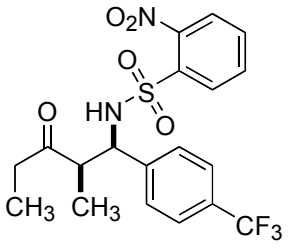
O2N
O
S
HN
O
O
CH3
CH3
CF3

4.21b

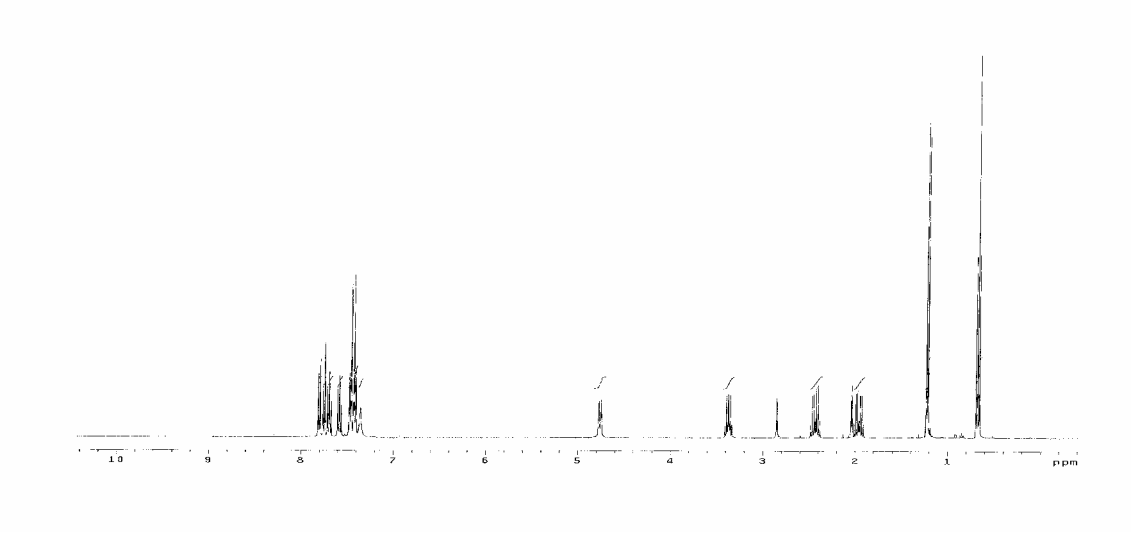
10
9
8
7
6
5
4
3
2
1
ppm

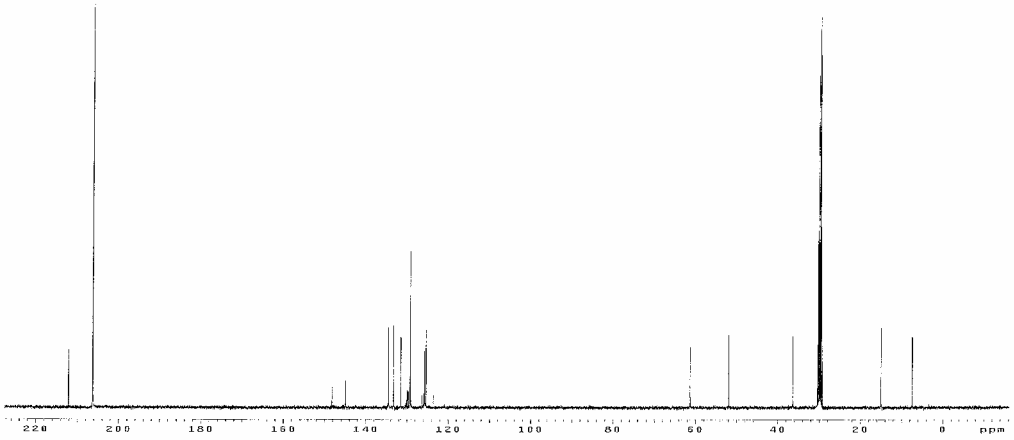
220
200
180
160
140
120
100
80
60
40
20
0
ppm

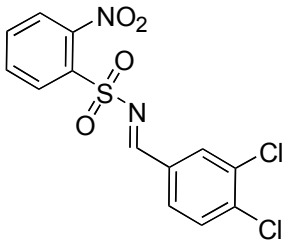
NO2
O
S
O
N
Cl
Cl

4.h

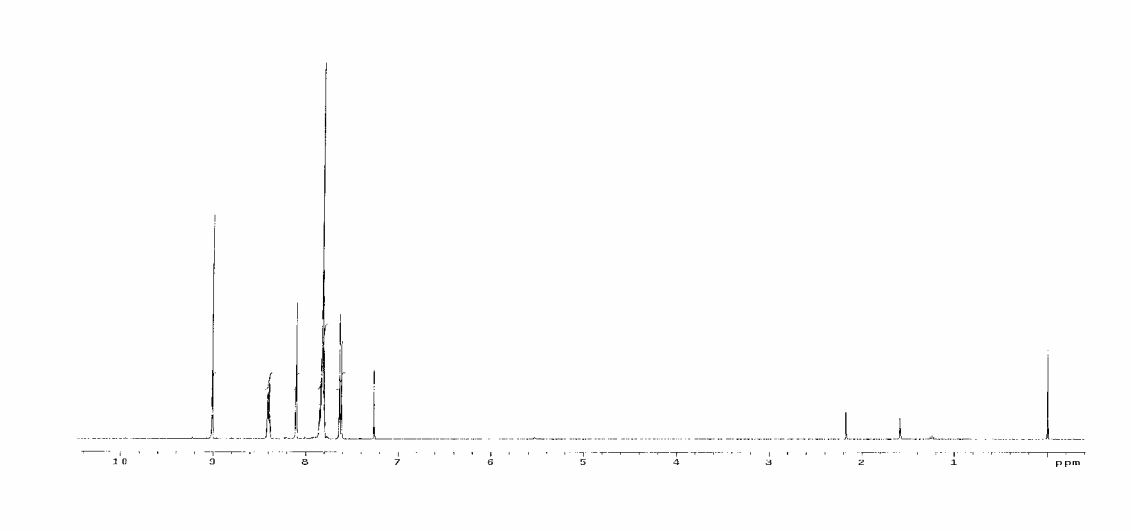
10
9
8
7
6
5
4
3
2
1
ppm

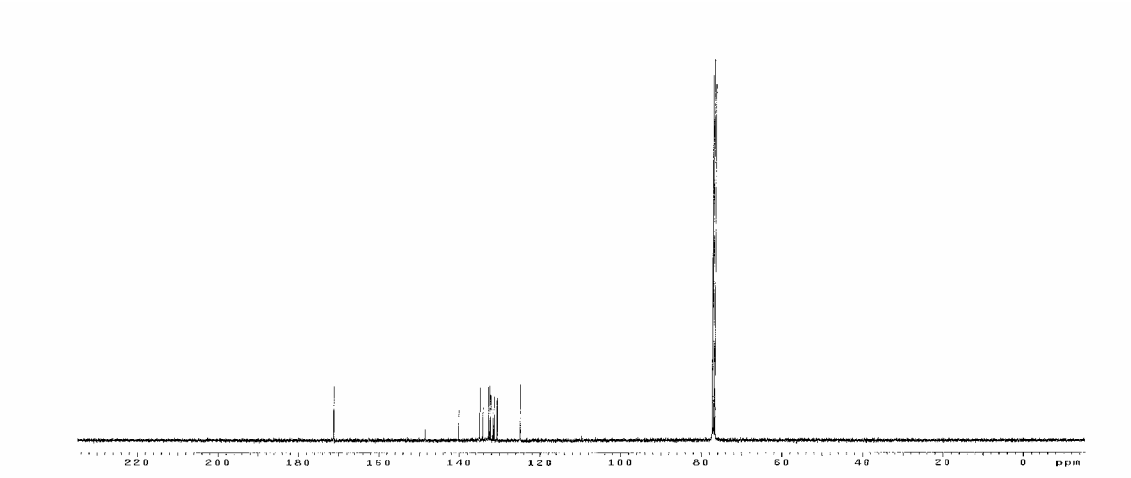
220
200
180
160
140
120
100
80
60
40
20
0
ppm

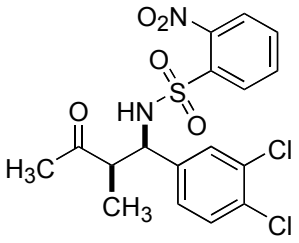

4.22a

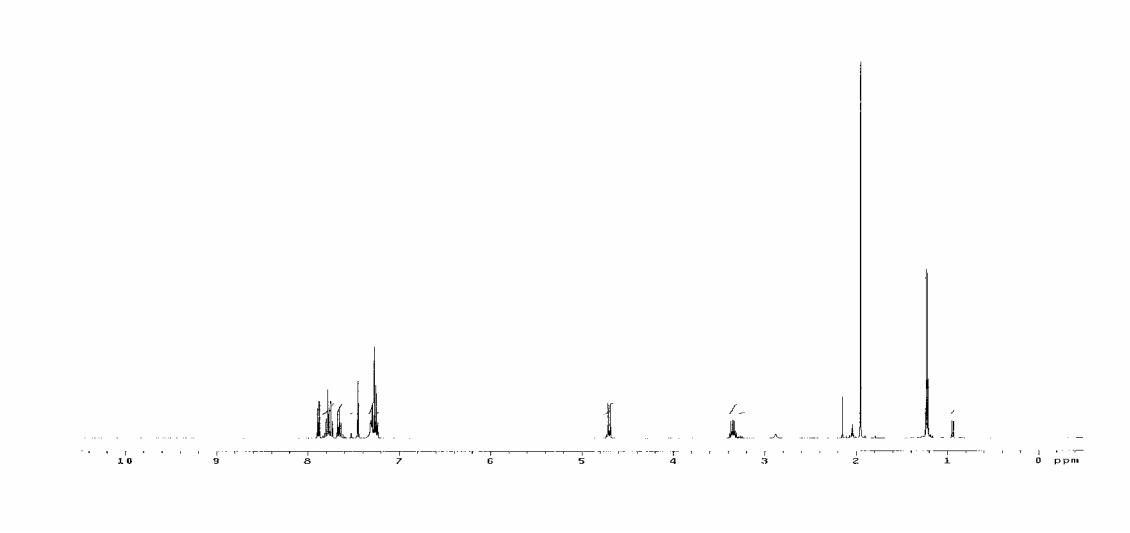

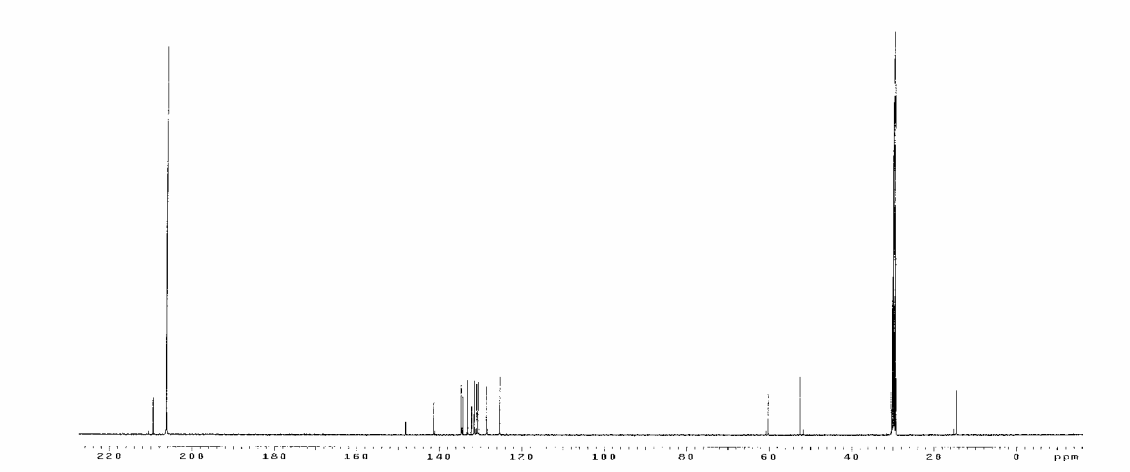

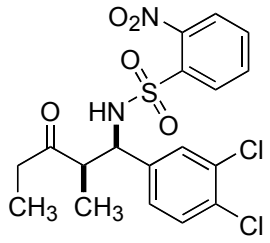
O2N
O
S
HN
O
O
Cl
Cl
CH3
CH3

4.22b

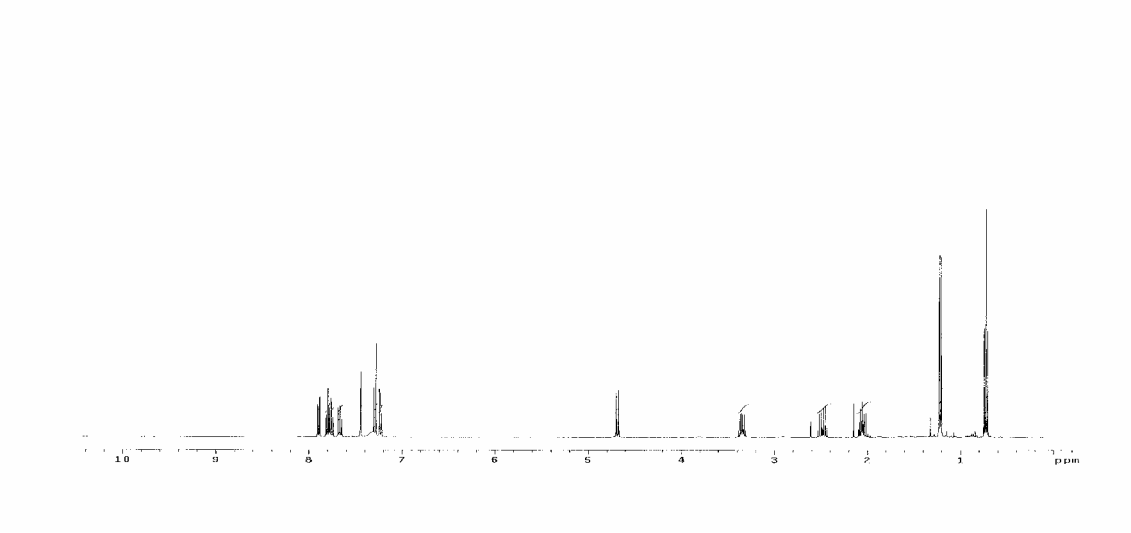
10
9
8
7
6
5
4
3
2
1
ppm

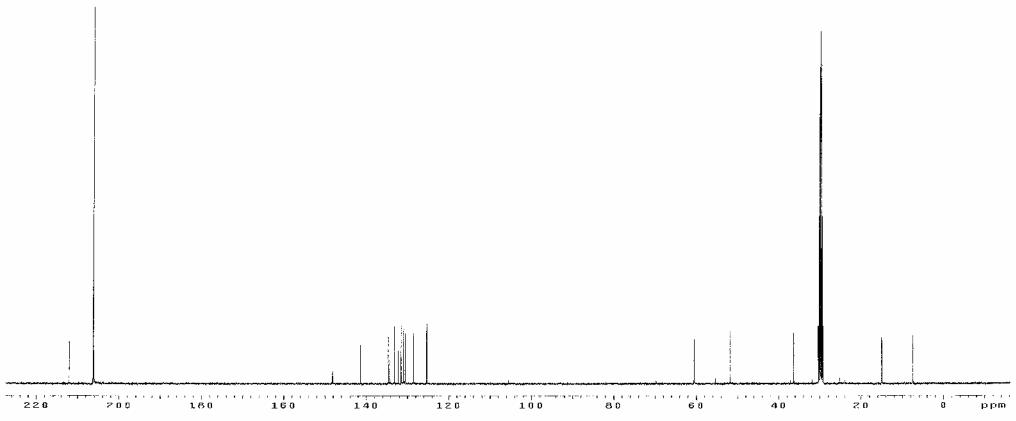
220
200
180
160
140
120
100
80
60
40
20
0
ppm

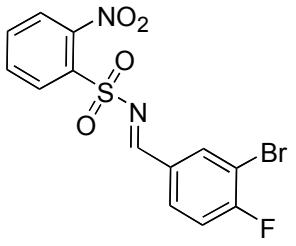
NO2
O
S
O
N
Br
F

4.i

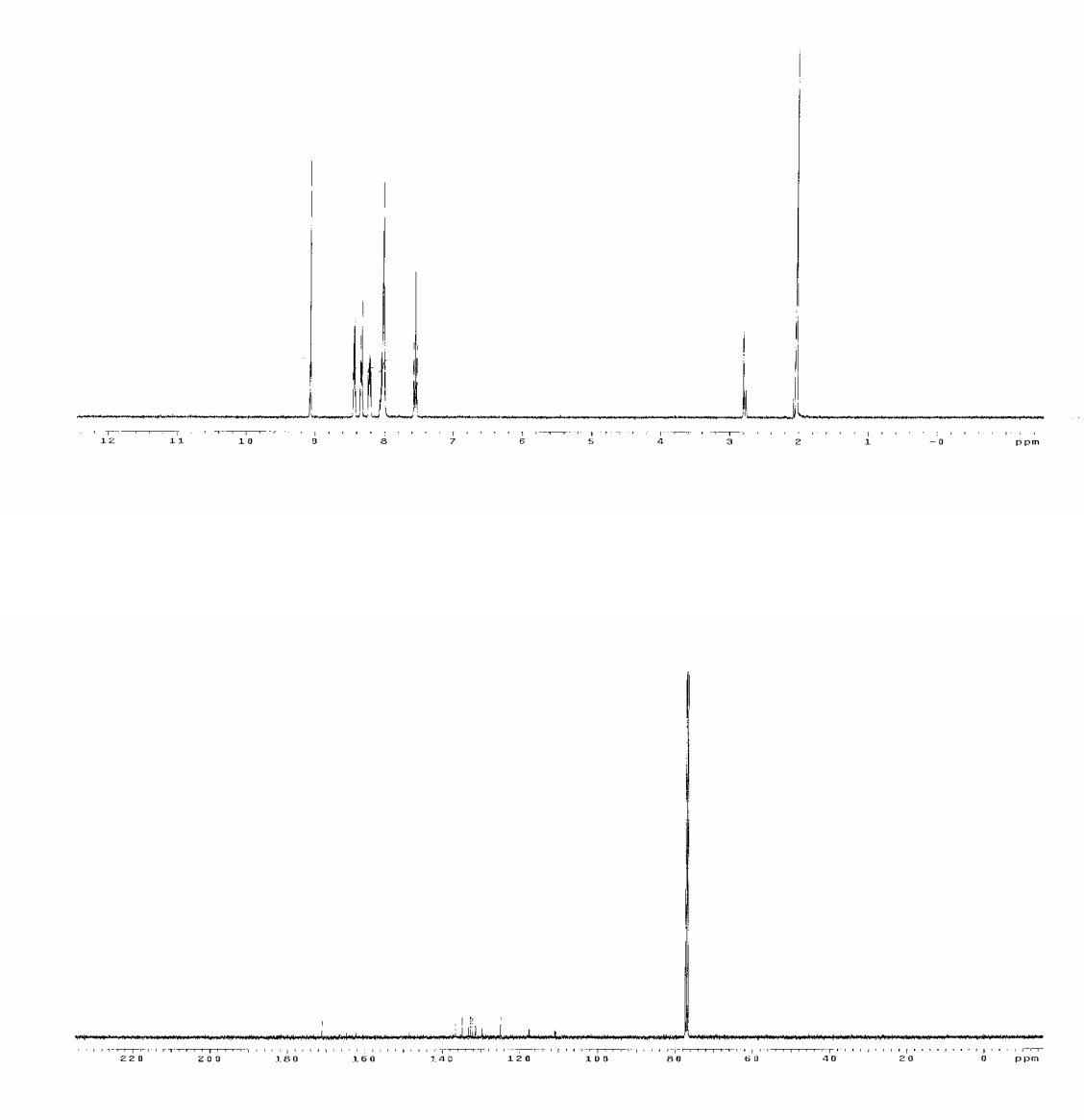
12
11
10
9
8
7
6
5
4
3
2
1
0
ppm
220
200
180
160
140
120
100
80
60
40
20
0
ppm

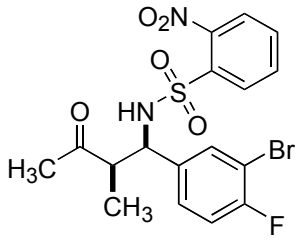
O2N
O
S
HN
O
O
H3C
CH3
Br
F

4.23a

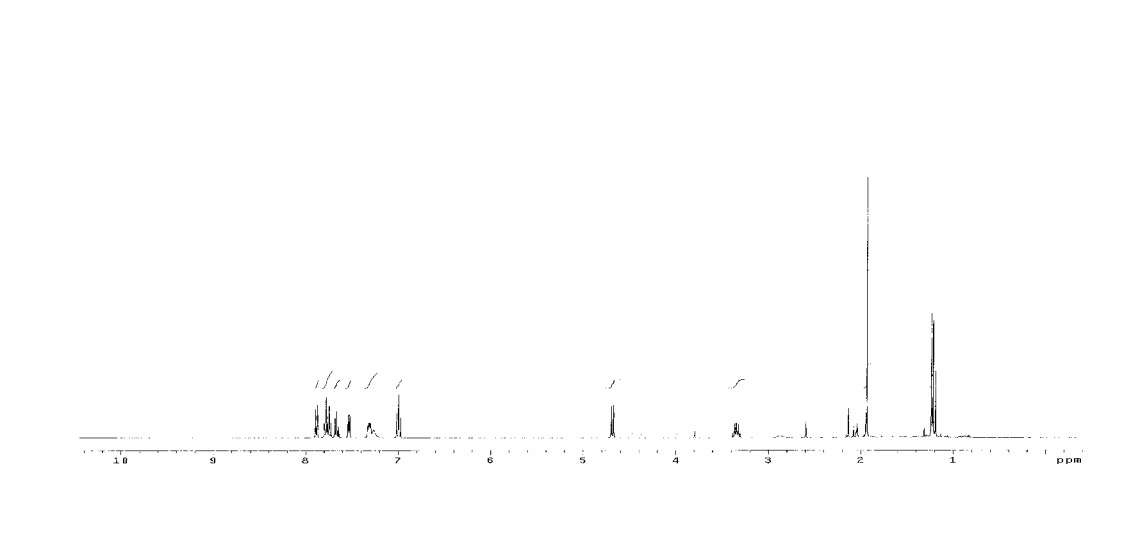
10
9
8
7
6
5
4
3
2
1
ppm

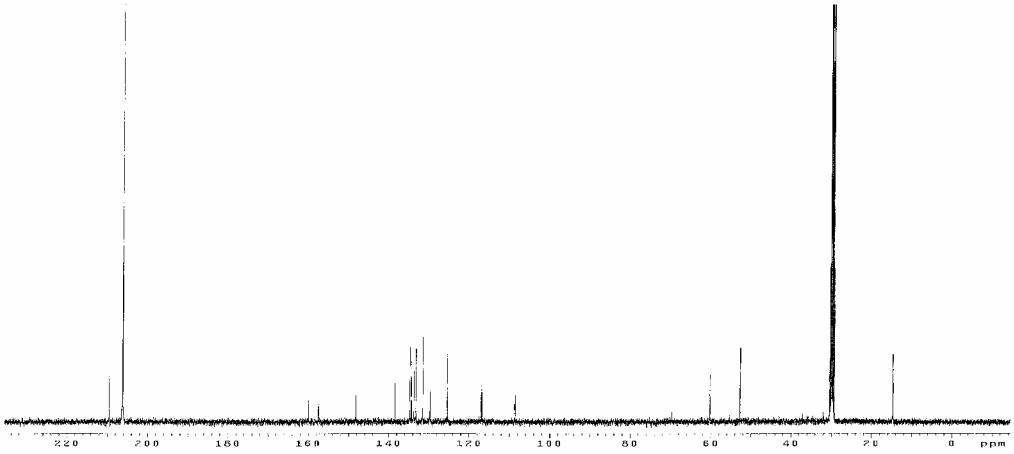
220
200
180
160
140
120
100
80
60
40
20
0
ppm

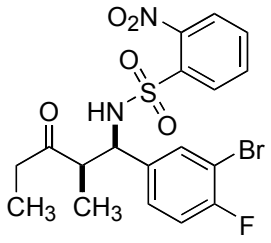
O2N
O
S
HN
O
O
Br
CH3
CH3
F

4.23b

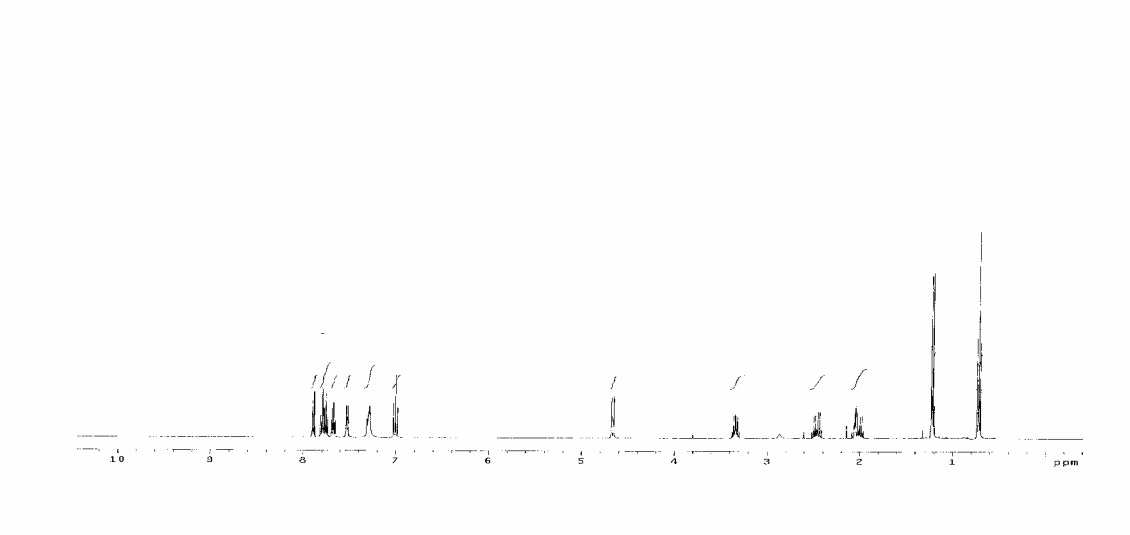
10
9
8
7
6
5
4
3
2
1
ppm

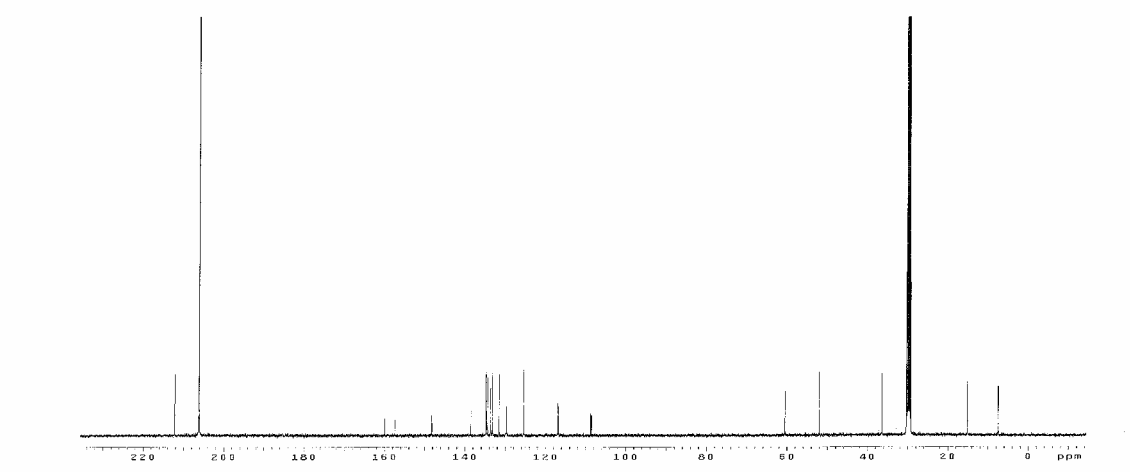
220
200
180
160
140
120
100
80
60
40
20
0
ppm

[1] Arend, M.; Westermann, B.; Risch, N. *Angew. Chem. Int. Ed*. **1998**, *37*, 1044.

[2] Tramontini, M.; Angiolini, L. *Mannich-Bases, Chemistry and Uses*, CRC, Boca Raton, FL, **1994**.

[3] (a) Traxler, P.; Trinks, U.; Buchdunger, E.; Mett, H.; Meyer, M.; Muller, M.; Regenass, U.; Rosel, J.; Lydon, N. *J. Med. Chem*. **1995**, *38*, 2441. (b) Dimmock, J. R.; Sidhu, K. K.; Chen, M.; Reid, R. S.; Allen, T. M.; Kao, G. Y.; Truitt, G. A. *Eur. J. Med. Chem*. **1993**, *28*, 313.

[4] Mannich, C.; Krosche, W. *Arch. Pharm*. **1912**, *250*, 647.

[5] Robinson, R. *J. Chem. Soc*. **1917**, *111*, 762.

[6] For reviews on the Mannich Reaction, see: (a) Kobayashi, S.; Ueno, M. *Mannich Reaction*, in *Comprehensive Asymmetric Catalysis II.* Jacobsen, E. N.; Pfaltz, A.; Yamamoto, H. Eds. Springer, **1999**, 143. (b) Uneo, M.; Kobayashi, S. Catalytic *Enantioselective Mannich Reactions*, in *Enantioselective Synthesis of β-Amino Acids*. Juaristi, E.; Soloshonok, V. Eds. Wiley, **2005**, 139.

[7] Ishitani, H.; Ueno, M.; Kobayashi, S. *J. Am. Chem. Soc*. **1997**, *119*, 7153.

[8] Notz, W.; Watanabe, S.; Chowdari, N. S.; Zhong, G.; Betancort, J. M.; Tanaka, F.; Barbas, C. F. *Adv. Synth. Catal*. **2004**, *346*, 1131.

[9] Kobayahi, S.; Ishitani, H. *Chem. Rev*. **1999**, *99*, 1069.

[10] Bjorgo, J.; Boyd, D. R.; Watson, C. G.; Jennings, W. B. *J. Chem. Soc. Perkin Trans II*. **1974**, 757.

[11] McCarty, C. G. *The Chemistry of the Carbon-Nitrogen Double Bond*. Patai, S. Ed. John Wiley & Sons: New York, **1970**, 363.

[12] Lehn, J. –M. *Chem. Eur. J.* **2006**, *12*, 5910.

[13] Manhas, M. S.; Ghosh, M.; Bose, A. K. *J. Org. Chem*. **1990**, *55*, 575.

[14] Yamada, K.; Harwood, S. J.; Gröger, H.; Shibasaki, M. *Angew. Chem. Int. Ed*. **1999**, *23*, 3504.

[15] Love, B. E.; Raje, P. S.; Williams, T. C. *Synlett.* **1994**, 493.

[16] Still, W. C.; Kahn, M.; Mitra, M. *J. Org. Chem*. **1978**, *43*, 2923.

CHAPTER 5. HYDROGEN-MEDIATED REDUCTIVE COUPLING OF DIENES AND GLYOXALS

5.1 INTRODUCTION

Even though alkene hydroformylation is the largest volume application of homogeneous metal catalysis in industry today very little has been done to expand this area beyond reductive coupling *via* carbon monoxide insertion. Upon successfully developing a hydrogen-mediated reductive coupling of enones and various electrophiles, this reaction manifold was extended to the reductive coupling of 1,3-dienes and glyoxals.[1] The development of this transformation is a positive step toward obtaining our ultimate goal of taking simple basic chemical feedstocks and coupling them in the presence of hydrogen gas and a rhodium catalyst to obtain more complex molecules.

5.2.1 BACKGROUND

Investigation of the reductive coupling of dienes and aldehydes began with the attempt to reductively couple *p*-nitrobenzaldehyde and 1,3-cyclohexadiene in the presence of the cationic rhodium (I) catalyst, $Rh(COD)_2OTf$. Unfortunately, none of the desired coupling product was obtained. Changing the electrophilic partner to a more reactive α-keto aldehyde (glyoxal) enabled the hydrogen-mediated C-C bond formation to occur (Table 5.1). Just as previously described, cationic rhodium catalysts are required in order for hydrogen-mediated carbon-carbon bond formation to occur. Attempting to couple 1,3-cyclohexadiene with phenyl glyoxal using the neutral Wilkinson's catalyst

provided none of the coupling product. (Table 5.1, entry 1), but the cationic rhodium (I) catalyst, $Rh(COD)_2OTf$ provided the desired product **5.1** in 61% yield (Table 5.1, entry 2). The choice of phosphine ligand had profound influence on the reaction outcome. When the electron deficient $(p\text{-}CF_3Ph)_3P$ was used as ligand in the reaction **5.1** was obtained in only 24% yield (Table 5.1, entry 3). On the other hand, switching to the electron rich $(p\text{-}CH_3OPh)_3P$ as ligand **5.1** was obtained in 77% yield (Table 5.1, entry 4). The final optimized reaction conditions were obtained by lowering the catalyst loading to 5 mol% $Rh(COD)_2OTf$ and using the electron rich $(p\text{-}CH_3OPh)_3P$ as ligand in 10 mol% to provide the desired reductive coupling product **5.1** in 76% yield (Table 5.1, entry 5).[1] The structure of **5.1** confirmed by the resonance at δ 5.59 (m, 2H) in the ^{1}HMR spectra corresponding to the olefin moiety on the cyclohexene ring. Also, HRMS data calculated [M +1] for $C_{18}H_{18}O_2$: 266.1307 and found 266.1306. The regiochemistry of the product was confirmed by a single crystal X-ray structure of **5.1** (Figure 5.1). [2]

Table 5.1: Hydrogen-mediated reductive coupling of 1,3-cyclohexadiene and phenyl glyoxal.[1]

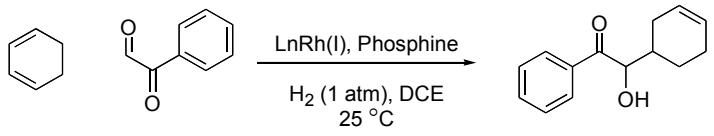

5.1

entry	Catalyst (mol%)	Ligand (mol %)	% Yield
1	$Rh(PPh_3)_3Cl$ (10 %)	---	---%
2	$Rh(COD)_2OTf$ (10 %)	Ph_3P (20 %)	61%
3	$Rh(COD)_2OTf$ (10 %)	$(p\text{-}CF_3Ph)_3P$ (20 %)	24%
4	$Rh(COD)_2OTf$ (10 %)	$(p\text{-}CH_3OPh)_3P$ (20 %)	77%
5	**$Rh(COD)_2OTf$ (5 %)**	**$(p\text{-}CH_3OPh)_3P$ (10 %)**	**76%**

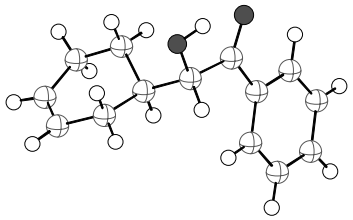

Figure 5.1: Single crystal x-ray structure of **5.1.**[2]

5.2.2 SUBSTRATE SCOPE

With optimized reaction conditions in hand the substrate scope for this reaction manifold was explored. Various glyoxal partners were screened and it was found that aryl, heteroaryl, and aliphatic glyoxals all participated in this transformation (Table 5.2). One limitation to this methodology is poor diastereoselectivity.

Table 5.2: Hydrogen-mediated reductive coupling of 1,3-cyclohexadiene and a variety of glyoxals.[1]

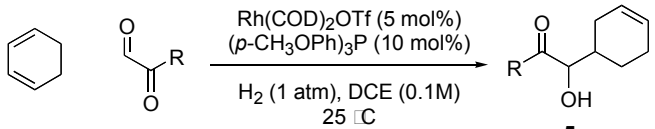

5.x
% Yield
dr

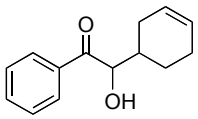

5.1
76 % Yield
1:1.6

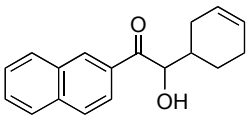

5.2
77 % Yield
1:1.5

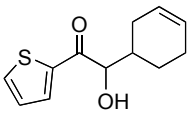

5.3
74% Yield
1:1.4

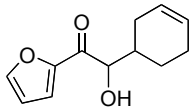

5.4
78% Yield
1:1.3

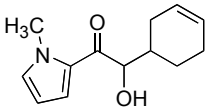

5.5
73% Yield
1:1.4

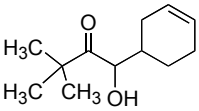

5.6
71% Yield
1:1.6

5.2.3 DEUTERIUM LABELING EXPERIMENT

In order to gain insight to the reaction mechanism a deuterium labeling experiment was conducted. The result revealed a mechanism very different from the proposed mechanism for the hydrogen-mediated reductive coupling of enones and aldehydes. The reductive coupling of 1,3-cyclohexadiene with 2-naphthyl glyoxal under an atmosphere of deuterium gas provided the reductive coupling product with precisely two deuterium atoms incorporated into the cyclohexene ring **5.7**. The product was obtained as a 1:1 mixture of 1,2- and 1,4-regioisomers (Scheme 5.1).[1] In order to simplify the ^{1}H NMR analysis, the product was modified *via* oxidation to eliminate the

diastereomeric mixture and **5.8** was obtained in 89% yield. This study revealed two mechanistic possibilities a hydrometallative mechanism and an oxidative coupling mechanism.

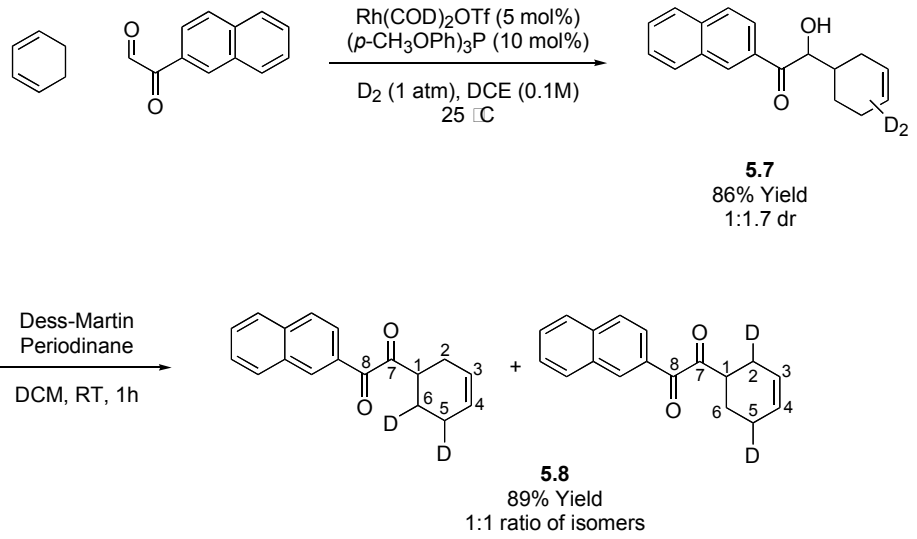

Scheme 5.1: Catalytic reductive coupling of 1,3-cyclohexadiene and 2-naphthyl glyoxal under an atmosphere of deuterium gas.[1]

The hydrometallative mechanism would begin by the heterolytic activation of molecular hydrogen to provide the starting rhodium (I) deuteride complex (Scheme 5.2). Deuteriometalation of the diene gives the homoallyl rhodium complex **5.a**, which adds to 2-naphthyl glyoxal to afford the rhodium alkoxide **5.b**.[3] Intermediate **5.c** is formed by allylic C-H insertion to provide the rhodium π-allyl. The next step is O-H reductive elimination to provide **5.d**. Then oxidative addition of deuterium to the rhodium center gives intermediate **5.e**. C-H Reductive elimination provides the deuterated product **5.7**.

The formation of the rhodium π-allyl accounts for the formation of the two dideuterated isomers.

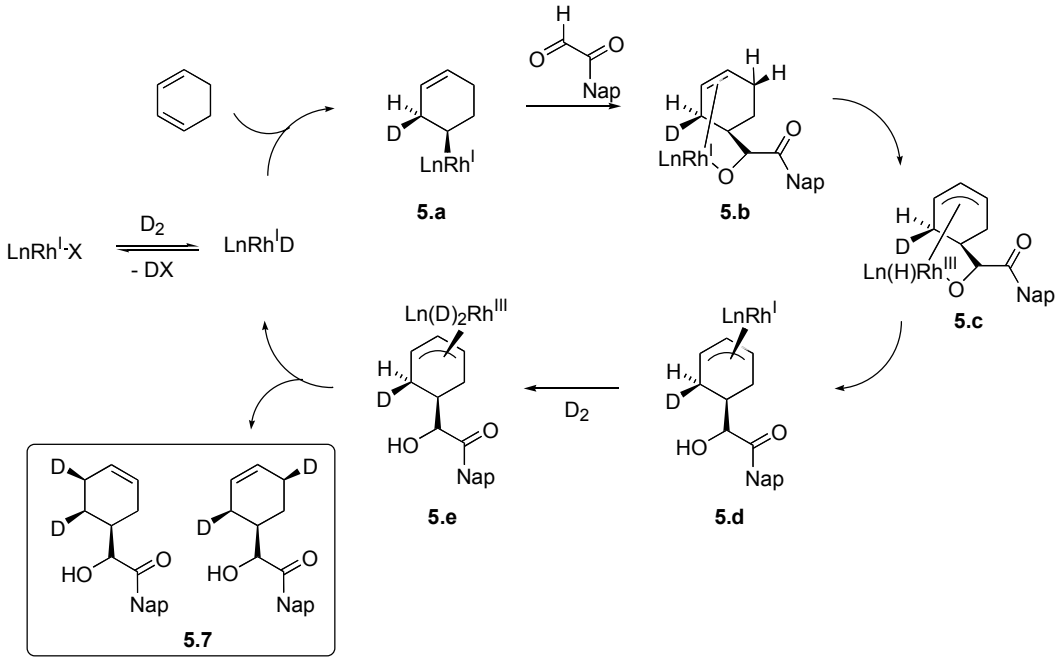

Scheme 5.2: Hydrometallative mechanism for the reductive coupling of 1,3-cyclohexadiene and 2-naphthyl glyoxal.

An alternative mechanism is an oxidative coupling mechanism where rhodium couples the 1,3-cyclohexadiene and the 2-naphthyl glyoxal prior to hydrogen activation (Scheme 5.3). This mechanism begins with the complexation of 1,3-cyclohexadiene by the rhodium (I) catalyst **5.f**, which is supported by the Dewar-Chatt-Duncanson model for alkene coordination.[4] It is well known that for early transition metals such as titanium back-bonding is driven by the stabilization gained by achieving a d^0-electronic configuration, but for late transition metal complexes like rhodium a d^0-electronic

configuration can not be obtained *via* this coordination. This is the reason why electron deficient carbonyl compounds are required before coupling can occur. Oxidative coupling of the diene and the glyoxal provides intermediate **5.g**. The next step is probably sigma-bond metathesis between **5.g** and deuterium to give intermediate **5.h**. Next, allylic C-H insertion provides the rhodium π-allyl complex. Reductive elimination provides the deuterated product **5.7**. The formation of the rhodium π-allyl accounts for the formation of the two dideuterated products. At this point two questions remain to be answered. (1) Which mechanism is operating, the hydrometallative or the oxidative coupling mechanism? (2) What is the relative stereochemistry of the dideuterated products?

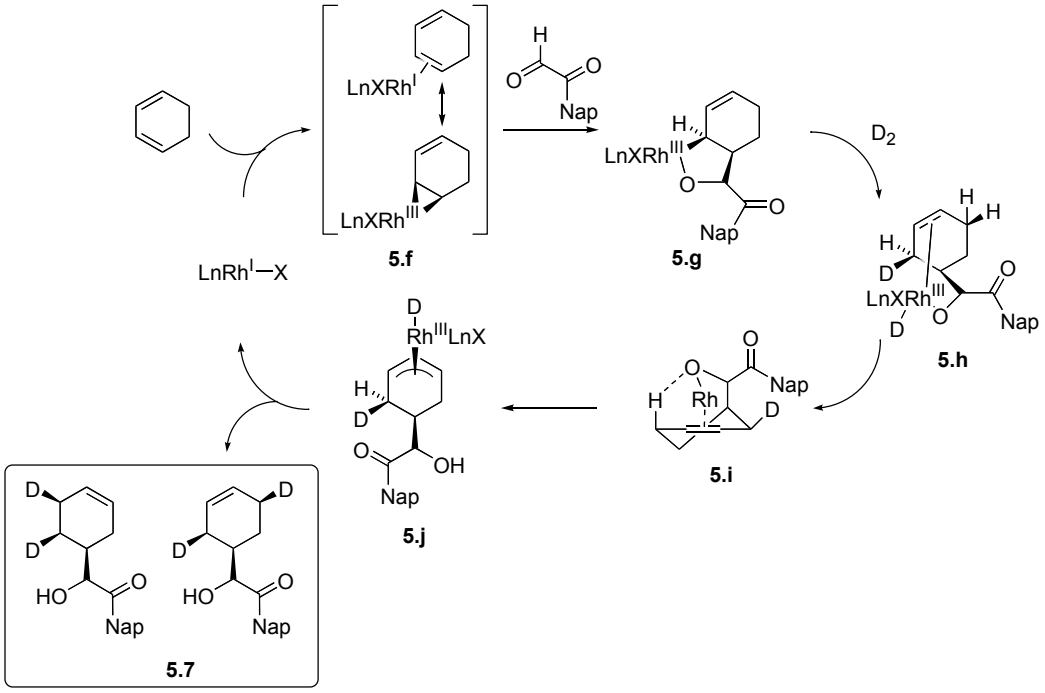

Scheme 5.3: Oxidative coupling mechanism for the reductive coupling of 1,3-cyclohexadiene and 2-naphthyl glyoxal.

5.3 H-D EXPERIMENT

In order to determine which mechanism is operating in this reaction manifold an experiment was conducted under an atmosphere of H-D gas (Scheme 5.4). It was found that the coupling product **5.9** of this reaction incorporated a single deuterium atom. The single deuterium atom was distributed over the same three carbons atoms (2, 5, and 6) as found with the D_2 experiment (Scheme 5.1). The structure of **5.9** was confirmed by ^{1}H and ^{13}C NMR. Also, HRMS data calculated [M + 1] for $C_{18}H_{18}DO_2$: 268.1448 and found 268.1452. Compound **5.9** was modified by oxidation with Dess Martin periodinane in order to eliminate the diastereomeric mixture. A DEPT experiment on

5.10 clearly indicates three isomers all with single deuterium incorporation at carbons 2, 5, and 6 (Figure 5.1). An INADEQUATE experiment also was conducted in order to establish the exact location of the deuterium atoms. The result of the deuterium hydride labeling experiment supports the oxidative coupling mechanism shown in Scheme 5.3 and disqualifies the hydrometallative mechanism in Scheme 5.2. If the hydrometallative mechanism was operative then the product would be a mixture of di-deuterated, mono-deuterated, and undeuterated compounds and this is not observed.

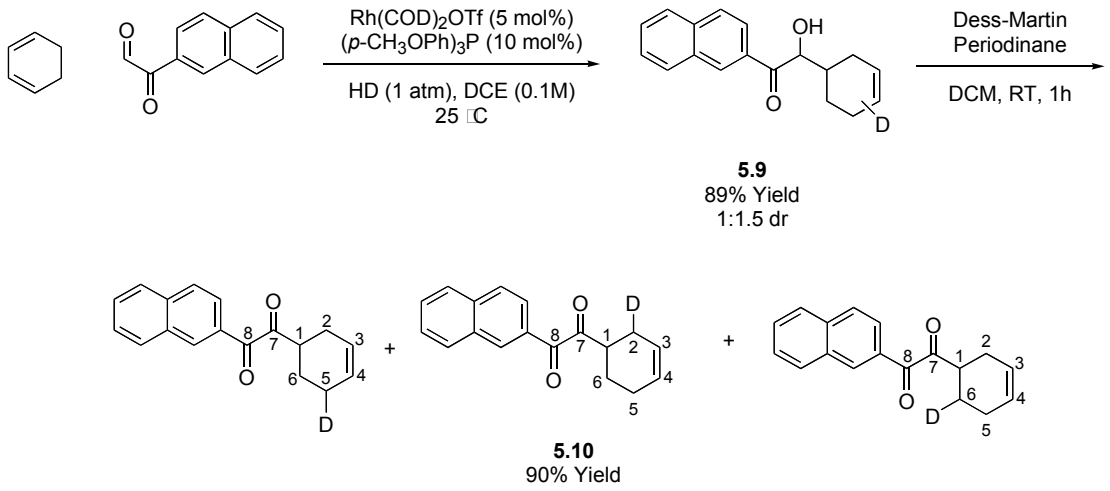

Scheme 5.4: Catalytic reductive coupling of 1,3-cyclohexadiene and 2-naphthyl glyoxal under an atmosphere of deuterium hydride gas.

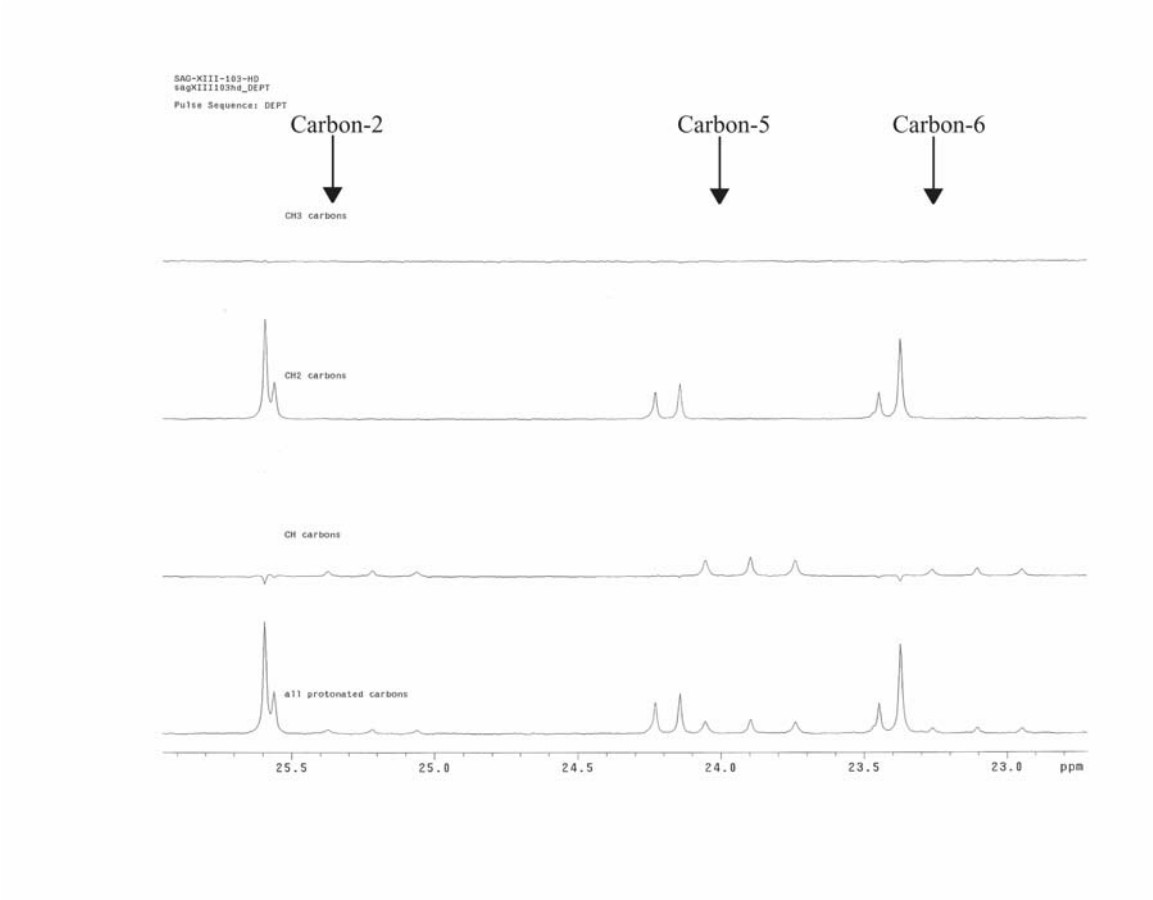

Figure 5.2: DEPT experiment of **5.10.**

5.4 RELATIVE STEREOCHEMISTRY

The next question to be answered is relative stereochemistry of the dideuterated regioisomers **5.8**. This information would provide important insight into the precise details of the catalytic mechanism. Unfortunately, NMR experiments could not determine the relative stereochemistry. Various NMR experiments were conducted in order to determine the relative stereochemistry, but the aliphatic region of the cyclohexene ring is too complicated. X-Ray crystallography cannot be utilized to solve

this problem because hydrogen and deuterium are electronically equivalent, but neutron diffraction analysis would give definitive evidence for the relative stereochemistry. Collaboration with Arthur Schultz at Argonne National Laboratory was formed in order to use their Single Crystal Diffractometer (SCD). The crystal of **5.7** (Scheme 5.1) was submitted to Argonne National Laboratory, but regrettably the crystal gave a weak signal and no data was collected from the experiment.

With the failure of the neutron diffraction experiment we focused our attention on modifying **5.7** in order to simplify the ^{1}H NMR spectra. We envisioned that performing a bromoetherification of the alkene of **5.7** would generate a strained ring system and the ^{1}H NMR spectrum would be easier to interpret (Scheme 5.5). Unfortunately, this method was unsuccessful in simplifying the problem. The isolated product is believed to be an inseparable mixture of the bicyclo[2.2.2] and the bicyclo[3.2.1] ring systems. At this time it appears that the only method of determining the relative stereochemistry is by growing a larger crystal and resubmitting it to neutron diffraction analysis.

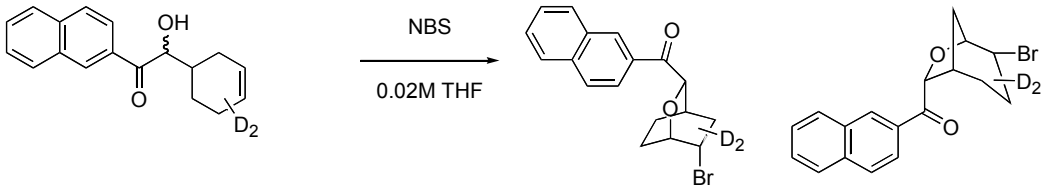

5.7 **5.11a** **5.11b**

Scheme 5.5: Bromoetherification of **5.7.**

5.5 CONCLUSION

This reaction methodology is the first report of coupling of simple π-unsaturated precursors *via* catalytic hydrogenation without the use of carbon monoxide insertion. At the current time the scope of the transformation is limited but more work is being conducted in order to expand the substrate scope. During the development of this reaction an unusual catalytic mechanism involving σ-bond metathesis of a rhodium alkoxide with an allylic C-H bond was discovered. Future directions include determining the relative stereochemistry and improving the substrate scope and diastereoselectivity.

5.6 EXPERIMENTAL SECTION

GENERAL

All reactions were run under an atmosphere of argon, unless otherwise indicated. Anhydrous solvents were transferred by an oven-dried syringe. Flasks were flame-dried and cooled under a stream of nitrogen. Dichloromethane (DCM) and 1,2-Dichloroethane (DCE) were distilled from calcium hydride. Tetrahydrofuran (THF) was purified by distillation from sodium-benzophenone/ketyl radical. Chemical reagents were purchased from Aldrich and Strem Chemicals. Commercially available aldehydes and enones were purified prior to usage. Deuterated solvents were used as received from Cambridge Isotope Laboratories. Analytical thin-layer chromatography (TLC) was carried out using 0.2-mm commercial silica gel plates (DC-Fertigplatten Kieselgel 60 F_{254}). Flash chromatography was performed on silica gel 60 (200-400 mesh) according to the method of Still.[16] Proton nuclear magnetic resonance (^{1}H NMR) spectra were recorded on a Varian Mercury 400, or Unity+ 300 spectrometer. ^{1}H NMR spectra were obtained at 400 MHz or 300 MHz, as indicated. Chemical Shifts are reported in delta (δ) units, parts per million (ppm) downfield from trimethylsilane for deuteriochloroform. In the case when deuterioacetone is used as a NMR solvent then the reference point is the center of the quintet at 2.05 ppm. Coupling constants are reported in Hertz (Hz). Carbon-13 nuclear magnetic resonance (^{13}C-NMR) spectra were recorded on a Varian Mercury 400, or Unity+ 300 spectrometer. ^{13}C-NMR spectra were obtained at either 100MHz or 75 MHz, as indicated. Chemical Shifts are reported in delta (δ) units, parts per million (ppm) relative to the center triplet at 77.0 ppm for deuteriochloroform. ^{13}C-NMR spectra were

routinely run with broadband decoupling. High-resolution mass spectra (HRMS) were obtained on a Micromass ZAB-E spectrometer and are reported as m/z (relative intensity). Accurate masses are reported for the molecular ion (M+1) or a suitable fragment ion. FT-IR spectra were obtained using a Nicolet Impact 410 spectrometer. Melting points were obtained on a Thomas-Hoover Unimelt apparatus in open capillaries and are uncorrected.

5.6.2 General Procedure for the Reductive Coupling of Dienes and Glyoxals[1,2]

To a solution of glyoxal (1.0 mmol, 100 mol%) and 1,3-cyclohexadiene (5.0 mmol, 500 mol%) in DCE at ambient temperature was added $Rh(COD)_2OTf$ (0.05 mmol, 5 mol%) and (p-$CH_3OPh)_3P$ (0.1 mmol, 10 mol%). The system was purged with hydrogen gas and the reaction was allowed to stir at 25 °C under 1 atm of hydrogen until consumption of substrate at which point the reaction mixture was evaporated onto silica gel. Isolation and purification of the product was carried out *via* silica gel chromatography.

5.6.3 Procedure for the Oxidation of 5.9

To a solution of **5.9** (0.56 mmol, 100 mol%) in dry DCM (0.1M) Dess Martin Periodinane (0.84 mmol, 150 mol%) was added. The reaction mixture stirred at ambient temperature under an atmosphere of argon for 1 hour. Upon completion ethyl ether (50 mL) was added. The reaction mixture was poured slowly into (50 mL) 1M NaOH. The

mixture was stirred until homogeneous. Then the reaction mixture was extracted with ethyl ether. The combined organic layers were washed with NaOH, brine, and dried ($MgSO_4$). The mixture was concentrated and then purified *via* silica gel chromatography.

5.6.4 PROCEDURE FOR THE BROMOETHERIFICATION OF 5.7[5]

To a stirred solution of **5.7** in THF was added *N*-bromosuccinimide and the reaction mixture stirred at ambient temperature under an atmosphere of argon until deemed complete *via* TLC analysis. The mixture was passed through a short pad of silica gel with hexanes:ethylacetate (5:1) as eluent. The mixture was concentrated and then purification *via* silica gel chromatography.

5.7 SPECTROSCOPIC CHARACTERIZATION DATA

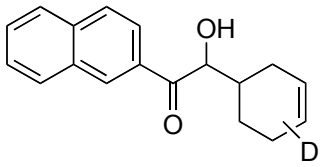

5.9
1:1.5 dr

***Deuterio*-2-cyclohex-3-enyl-2-hydroxy-1-naphthalen-2-yl-ethanone (5.9).** ^{1}H NMR ($CDCl_3$, 500 MHz): δ 1.3 (m, 1H), 1.43 (m, 1H), 1.80 (m, 2H), 1.98-2.23 (m, 5H), 2.40 (m, 1H), 3.70 (d, *J* = 6.8, Hz, 1H), 3.79 (d, *J* = 6.2, Hz, 1H), 5.17 (dd, *J* = 4.0, 2.8 Hz 1H), 5.21 (dd, *J* = 3.2, 2.8 Hz 1H), 5.50 (m, 1H), 5.65 (m, 2H), 5.69 (m,1H), 7.58 (m, 2H), 7.94 (m, 4H), 8.41 (s, 2H). ^{13}C NMR ($CDCl_3$, 125 MHz): δ 20.8, 20.9, 21.1, 21.2, 23.0, 23.2, 23.3, 23.5, 24.4, 24.6, 24.7, 24.8, 24.9, 25.0, 25.2, 25.3, 25.5, 26.1, 26.2, 28.7,

38.5, 38.6, 38.7, 38.8, 76.2, 123.7, 123.8, 125.7, 125.8, 126.1, 126.2, 126.5, 126.6, 126.6, 127.0, 127.8, 128.7, 128.8, 128.9, 129.6, 129.6, 130.1,130.2,131.4, 131.4, 132.3, 135.9, 201.7, 201.8. HRMS calcd [M + 1] for $C_{18}H_{18}DO_2$: 268.1448; Found: 268.1452. FTIR (film): 3470, 2906, 1674, 1626, 1281, 1105, 804, 474 cm^{-1}. MP = 102-103 °C.

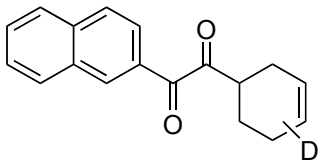

5.10

***Deuterio*-1-cyclohex-3-enyl-2-naphthalen-2-yl-ethane-1,2-dione (5.10).** ^1H NMR ($CDCl_3$, 500 MHz): δ 1.73 (m, 1H), 2.15 (m, 3H), 2.36 (m, 2H), 3.42 (m, 1H), 5.72 (m, 2H), 7.54 (t, *J* = 7.6 Hz, 1H), 7.61 (t, *J* = 7.6 Hz, 1H), 7.84 (d, *J* = 8.1 Hz, 1H), 7.92 (m, 2H), 7.84 (dd, *J* = 6.9, 1.7 Hz, 2H), 8.44 (s, 1H). ^{13}C NMR ($CDCl_3$, 125 MHz): δ 23.1 (t, *J* = 19.6 Hz), 23.3, 23.4, 23.9 (t, *J* = 19.8 Hz), 24.1, 24.2, 25.1, 25.2 (t, *J* = 19.6 Hz), 42.0, 42.1, 124.0, 124.8, 124.9, 126.8, 126.9, 126.9, 127.1, 127.9, 129.0, 129.4, 129.8, 130.0, 132.3, 133.3, 136.2, 193.8, 205.7. HRMS calcd [M + 1] for $C_{18}H_{15}DO_2$: 265.1213; Found: 265.1208. FTIR (film): 3026, 2925, 1703, 1665, 1626, 1283, 751 cm^{-1}.

5.8 SPECTRA

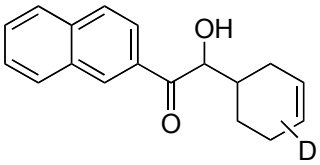

5.9
1:1.5 dr

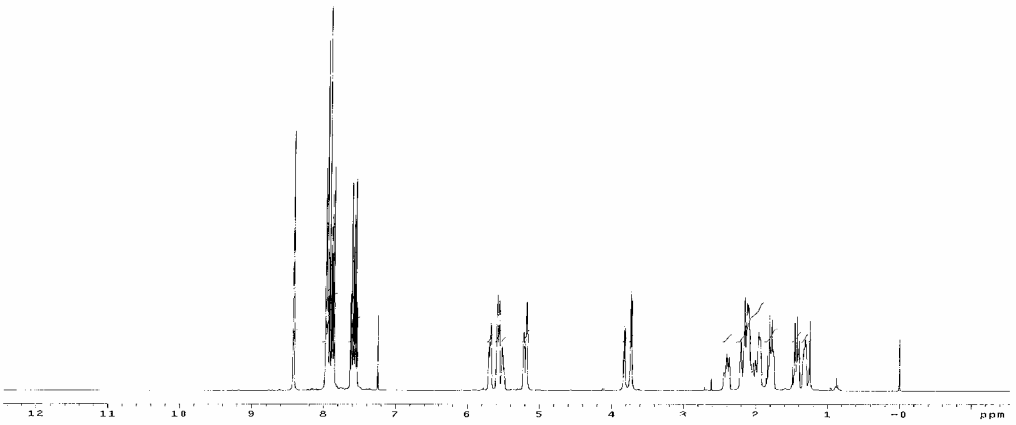

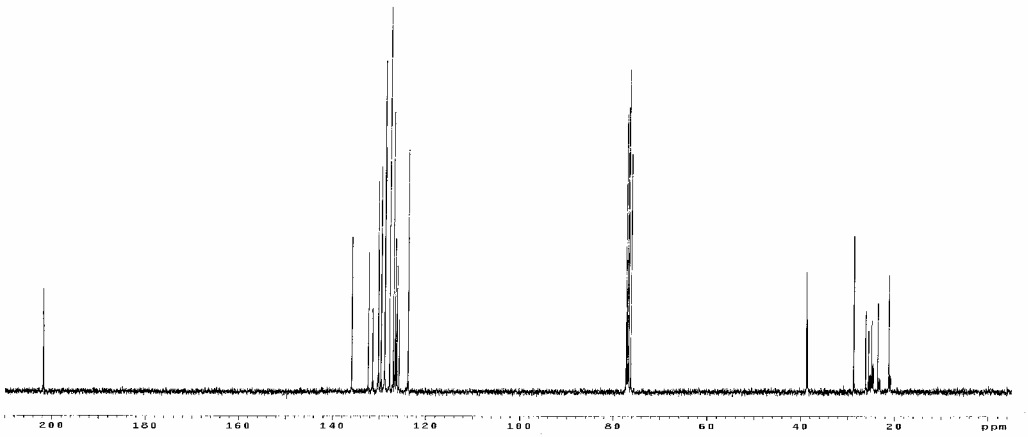

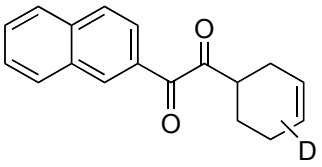

5.10

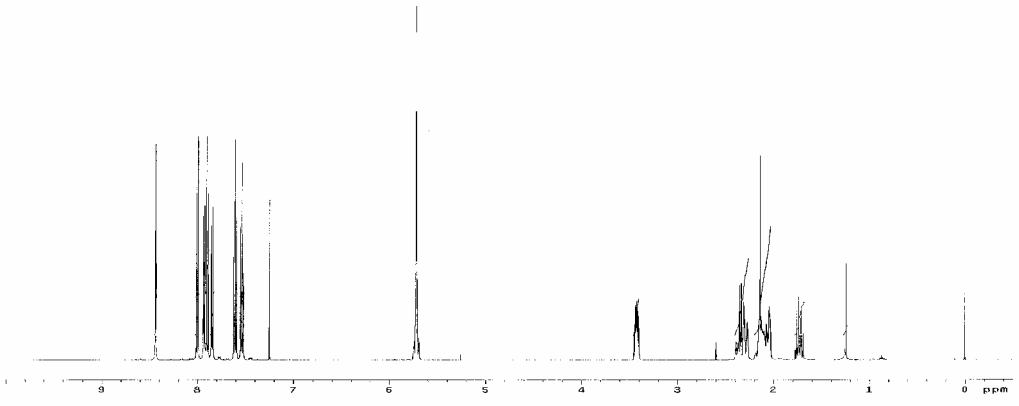

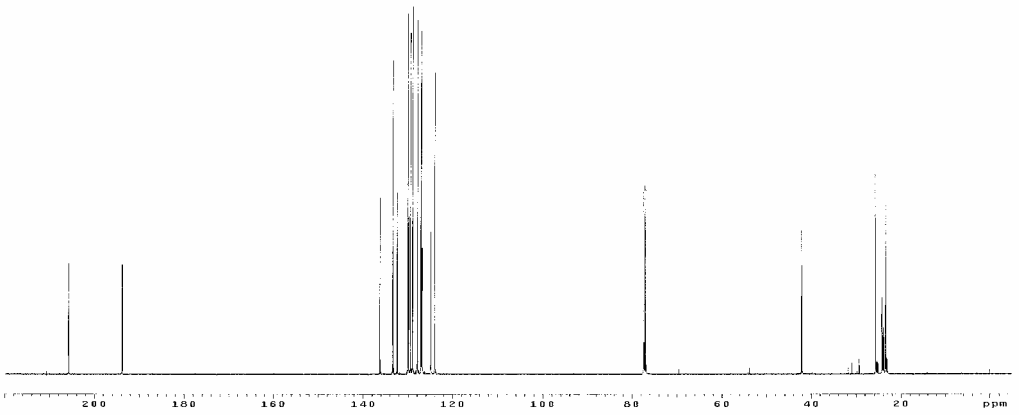

[1] Jang, H. –Y.; Huddleston, R. R.; Krische, M. J. *Angew. Chem. Int. Ed*. **2003**, *42*, 4074.

[2] Jang, H. –Y. **2005**. *Development of Hydrogen-Mediated Carbon-Carbon Bond Formations*, PhD-thesis, The University of Texas at Austin.

[3] The same regiochemistry is observed by Loh in a nickel catalyzed reductive coupling of 1,3-cyclohexadine and aldehydes. Loh, T. –P; Song, H. –Y.; Zhou, Y. *Org. Lett*. **2002**, *4*, 2715.

[4] (a) Dewar, M. J. S. *Bull. Soc. Chim. Fr*. **1951**, *18*, C71-C79. (b) Chatt, J.; Duncanson, L. A. *J. Chem. Soc*. **1953**, 2939.

[5] White, J. D.; Choi, Y. *Org. Lett*. **2000**, *2*, 2373.

CHAPTER 6. CONCLUSION

Catalytic hydrogenation has a long history, starting over a century ago with Sabatier's hydrogenation of benzene to cyclohexane. In this dissertation one can see how we have added a new family of carbon-carbon bond forming reactions *via* catalytic hydrogenation. This new methodology offers great improvements over classical methods.

In this dissertation the reductive aldol and Mannich reactions were studied. The result is a promising alternative to classical methods. This chemistry is catalytic and provides regio- and chemoselectivity. Also, the terminal reductant, hydrogen gas, is the cleanest and most cost-effective reductant available to mankind. Scheme 6.1 demonstrates an entire family of hydrogen-mediated carbon-carbon bond forming reactions. This reaction manifold has been expanded to include the reductive couplings of π-unsaturated systems with aldehydes and (*N*-sulfinyl)iminoacetates. Also, the reductive cyclization of 1,6-diynes and 1,6-enynes has been explored. This field of research has expanded extensively over the past six years, but the full synthetic potential has yet to be realized.

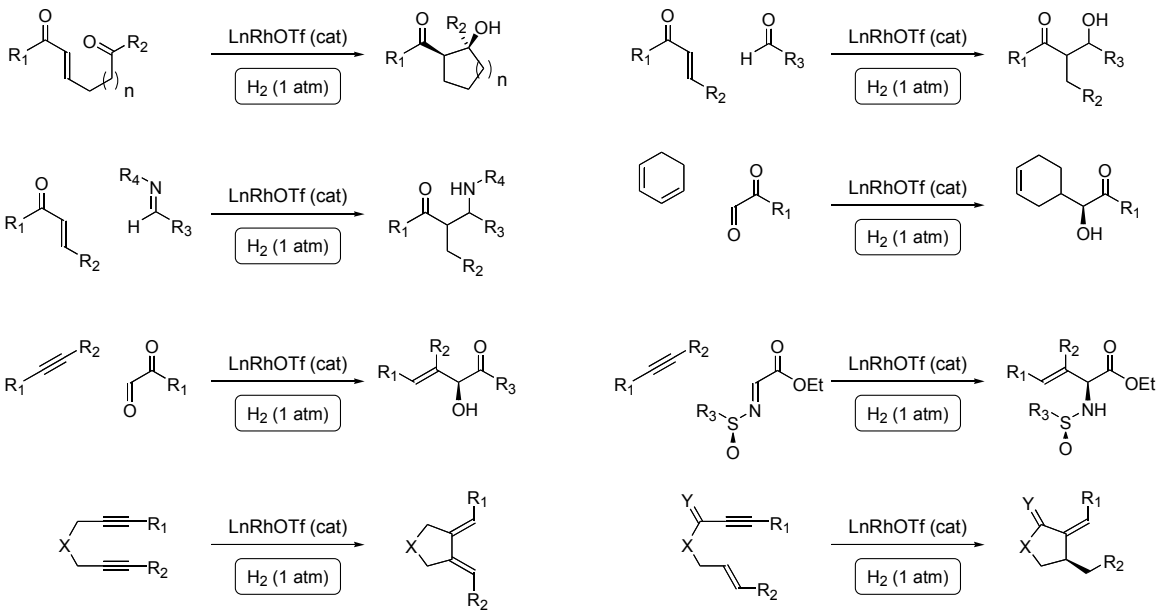

Scheme 6.1: A family of hydrogen-mediated carbon-carbon bond forming reactions.

Vita

Susan Amy Garner was born in Newnan, Georgia on March 18, 1980, the daughter of Jeffery Alan Hughes and Bertha Mae Hughes. After graduating from Flint River Academy, Woodbury, Georgia in May 1998, she began working her Bachelor of Science degree in chemistry at State University of West Georgia in Carrollton, Georgia. She received her degree in May 2002, and enrolled in the graduate chemistry program at the University of Texas at Austin in August 2002.

Permanent Address: 4707 Saint Michaels Court, Sugar Land, TX 77479

This dissertation was typed by the author.